PROCEEDINGS

OF THE

AMERICAN SOCIETY OF CIVIL ENGINEERS

VOL. 69 NOVEMBER, 1943 No. 9

TECHNICAL PAPERS

AND

DISCUSSIONS

Published monthly, except July and August, at Prince and Lemon Streets, Lancaster, Pa., by the American Society of Civil Engineers. Editorial and General Offices at 33 West Thirty-ninth Street, New York, N. Y. Reprints from this publication may be made on condition that the full title of Paper, name of Author, page reference, and date of publication by the Society, are given.

Entered as Second-Class Matter, September 23, 1937, at the Post Office at Lancaster, Pa., under the Act of March 3, 1879. Acceptance for mailing at special rate of postage provided for in Section 1103, Act of October 3, 1917, authorized on July 5, 1918.

Subscription (if entered before January 1) $8.00 per annum. Price $1.00 per copy

Copyright, 1943, *by the* AMERICAN SOCIETY OF CIVIL ENGINEERS

Printed in the United States of America

CURRENT PAPERS AND DISCUSSIONS

		Discussion closes
The Hydraulic Jump in Sloping Channels. *Carl E. Kindsvater*	Nov., 1942	
Discussion	Feb., May, June, Sept., 1943	Closed*
Application of Soil Mechanics in Designing Building Foundations. *A. Casagrande and R. E. Fadum*	Nov., 1942	
Discussion	Mar., June, Sept., 1943	Closed*
Flow Characteristics at Rectangular Open-Channel Junctions. *Edward H. Taylor*	Nov., 1942	
Discussion	June, Sept., Oct., 1943	Closed*
Relation of Undisturbed Sampling to Laboratory Testing. *P. C. Rutledge*	Nov., 1942	
Discussion	Dec., 1942, Mar., Apr., June, Sept., 1943	Closed*
Concrete Reservoirs of the Vertical-Beam Type. *C. Maxwell Stanley*	Dec., 1942	
Discussion	Mar., Apr., May, 1943	Closed*
Illinois Water Litigation, 1940–1941. *Langdon Pearse*	Dec., 1942	
Discussion	May, June, 1943	Closed*
Physical Properties that Affect the Behavior of Structural Members. *Wilbur M. Wilson*	Dec., 1942	
Discussion	Mar., May, June, Sept., Oct., 1943	Closed*
Organizing and Financing Sewage Treatment Projects. *Samuel A. Greeley*	Dec., 1942	
Discussion	Dec., 1942, Apr., May, Sept., 1943	Closed*
Seismic Subsurface Exploration on the St. Lawrence River Project. *E. R. Shepard and Reuben M. Haines*	Dec., 1942	
Discussion	Apr., June, 1943	Closed*
Pendleton Levee Failure. *Kenneth E. Fields and William L. Wells*	Dec., 1942	
Discussion	Dec., 1942, June, 1943	Closed*
Aeration of Spillways. *G. H. Hickox*	Dec., 1942	
Discussion	Mar., May, June, Nov., 1943	Closed
Riveted and Pin-Connected Joints of Steel and Aluminum Alloys. *Leon S. Moisseiff, E. C. Hartmann, and R. L. Moore*	Jan., 1943	
Discussion	Apr., Nov., 1943	Closed
Dewatering, Incineration, and Use of Sewage Sludge: A Symposium	Jan., 1943	
Discussion	Feb., June, Sept., 1943	Closed*
Primary Rôle of Meteorology in Flood Flow Estimating. *Merrill Bernard*	Jan., 1943	
Discussion	Mar., Apr., June, Oct., Nov., 1943	Closed*
Strains, Stresses, and Shear in Engineering Problems. *Silas H. Woodard*	Feb., 1943	
Discussion	Apr., June, Sept., Nov., 1943	Closed*
Determination of Kutter's *n* for Sewers Partly Filled. *C. Frank Johnson*	Feb., 1943	
Discussion	Apr., Sept., 1943	Closed*
Characteristics of Heavy Rainfall in New Mexico and Arizona. *Luna B. Leopold*	Feb., 1943	
Discussion	Apr., June, Nov., 1943	Dec. 1, 1943
Effect of Turbulence on Sedimentation. *William E. Dobbins*	Feb., 1943	
Discussion	Apr., May, June, Oct., 1943	Dec. 1, 1943
Flow Around Bends in Stable Channels. *C. A. Mockmore*	Mar., 1943	
Discussion	Sept., Oct., 1943	Dec. 1, 1943
The Queens Midtown Tunnel. *Ole Singstad*	Mar., 1943	
Discussion	May, June, Sept., Nov., 1943	Dec. 1, 1943
Water Supply Engineering: Report of the Committee of the Sanitary Engineering Division for the Three Years Ending December, 31, 1942	Mar., 1943	
A Method of Computing Urban Runoff. *W. I. Hicks*	Apr., 1943	Dec. 1, 1943
Highway Engineering Education: Progress Report of the Committee of the Highway Division	Apr., 1943	
Simplified Analysis of Skewed Reinforced Concrete Frames and Arches. *Richard M. Hodges*	May, 1943	
Discussion	Sept., Nov., 1943	Dec. 1, 1943
Rôle of the Land During Flood Periods. *W. W. Horner*	May, 1943	
Discussion	June, Sept., Oct., 1943	Dec. 1, 1943
A Symmetrically Loaded Base Slab on an Elastic Foundation. *Stanley U. Benscoter*	May, 1943	
Discussion	Sept., Nov., 1943	Dec. 1, 1943
Sedimentation in Reservoirs. *Berard J. Witzig*	June, 1943	
Discussion	Sept., Oct., Nov., 1943	Jan. 1, 1944
Development of the Chicago Type Bascule Bridge. *Donald N. Becker*	Feb., 1943	
Discussion	June, Sept., 1943	Jan. 1, 1944
Strength of Slender Beams. *George Winter*	June, 1943	
Discussion	Sept., 1943	Jan. 1, 1944
Sludge Drying Developments at Chicago, Ill. *Lloyd M. Johnson*	Sept., 1943	
Discussion	Sept., Oct., 1943	Feb. 1, 1944
Rainbow Arch Bridge Over Niagara Gorge: A Symposium	Oct., 1943	Mar. 1, 1944

NOTE.—The closing dates herein published are final except when names of prospective discussers are registered for special extension of time.

* Publication of closing discussion pending.

CONTENTS FOR NOVEMBER, 1943

PAPERS

PAGE

Storage and the Unit Hydrograph.
By C. O. Clark 1333

Rigidity and Aerodynamic Stability of Suspension Bridges.
By D. B. Steinman 1361

Unusual Cutoff Problems—Dams of the Tennessee Valley Authority: A Symposium 1399

Shear Effect on the Strength of Struts.
By S. Sergev 1447

DISCUSSIONS

Aeration of Spillways.
By G. H. Hickox 1461

Riveted and Pin-Connected Joints of Steel and Aluminum Alloys.
By Leon S. Moisseiff, E. C. Hartmann, and R. L. Moore 1463

Simplified Analysis of Skewed Reinforced Concrete Frames and Arches.
By Bernard L. Weiner, and Alfred L. Parmé 1465

Primary Rôle of Meteorology in Flood Flow Estimating.
By L. Standish Hall 1480

The Queens Midtown Tunnel.
By Orrin L. Brodie 1483

Sedimentation in Reservoirs.
By Carl B. Brown, and C. S. Jarvis 1493

CONTENTS FOR NOVEMBER, 1943 (*Continued*)

PAGE

Strains, Stresses, and Shear in Engineering Problems.
By A. A. Eremin 1501

A Symmetrically Loaded Base Slab on an Elastic Foundation.
By Alfred L. Parmé 1503

Characteristics of Heavy Rainfall in New Mexico and Arizona.
By Clarence S. Jarvis 1505

For Index to all Papers, the discussion of which is current in PROCEEDINGS, *see page 2*

The Society is not responsible for any statement made or opinion expressed in its publications

AMERICAN SOCIETY OF CIVIL ENGINEERS

Founded November 5, 1852

PAPERS

STORAGE AND THE UNIT HYDROGRAPH

BY C. O. CLARK,[1] JUN. AM. SOC. C. E.

SYNOPSIS

During the period since 1930, study of the flow records of many and various types of streams by the engineers of the United States has resulted in an improved concept and understanding of the physical factors which influence runoff and the flood-producing capacity of streams. Two fundamental tools have emerged from these studies, the unit hydrograph and methods of flood routing (means of modifying a hydrograph by the effects of valley storage), both of which have been the subject of many papers.

The purpose of this paper is to clarify the inherent relationship between these fundamental tools and to show how this relationship may be used to derive accurate unit hydrographs for very short periods of initial runoff which accurately reflect the influence of shape of drainage area upon the shape of the hydrograph, allow the segregation of elements of the hydrograph attributable to particular components of the drainage area, and permit the definition of the calculation procedure to a degree which reduces the dependence of accurate stream flow calculations on intangible factors of personal judgment.

After showing that the constant time units characteristic of unit hydrographs are the characteristics induced by storage capacity of the streams and that storage capacity and discharge capacity are each a limiting factor on the other, the paper illustrates the incorporation of these characteristics in hydrograph calculations.

DEFINITIONS

Throughout this paper, the terms "unit hydrograph" and "unitgraph" are used interchangeably to mean a regimen of stream flow for a unit quantity of uniformly distributed runoff originating at a uniform rate during a specified unit period of time. The time elements of the regimen are independent of the

NOTE.—Written comments are invited for immediate publication; to insure publication the last discussion should be submitted by April 1, 1944.

[1] Hydr. Engr., U. S. Engr. Office, Winchester, Va.

quantity of runoff and the discharge quantities are directly proportional to the quantity of runoff. Included are both the unit hydrograph of L. K. Sherman,[2] M. Am. Soc. C. E., and the distribution graph of Merrill Bernard,[3] M. Am. Soc. C. E. The terms "storage" and "valley storage" are applied to the entire volume of water stored between any two designated points along a river and include both the volume in the channel and on the flood plain. The same terms, expressed in time units, are used to designate the average ratio of storage volume to discharge capacity of the river reach.

The following definition of accuracy will apply to the writer's use of the term in subsequent paragraphs, and at the same time will illustrate some of the problems and aims of incorporating accuracy in stream flow calculations:

> An engineer should learn early to distinguish between the forms of accuracy which sometimes are called absolute, real, and relative. Absolute accuracy is the mathematical precision of correctly manipulated numbers, as used by engineers in computing payments to the cent from earthwork surveys by cross sections or soundings. Real accuracy is an evaluation of the closeness with which a measurement or computation approximates the truth, a quality inherent in the meaning of the engineering term "precision." Relative accuracy is an evaluation of the closeness with which a measurement or computation approximates another measurement or computation, preferably where both determinations are comparable, and frequently is expressed as a ratio or the difference between them, without necessarily giving an absolute value of either. The elevation of one bench mark with respect to another is a value that may have great relative accuracy without any absolute accuracy. The terms with which others designate these qualities of accuracy may differ, but the essential difference between them is acknowledged widely.

In the fields of evaluation and planning of river developments, relative accuracy is attainable at low cost, usually by thoroughly planned systematic analysis; and it is sufficient in the selection of the better of alternative plans. Real accuracy, as in the evaluation of the selected plan of construction, high-order surveys, or field observation and measurement of natural phenomena, such as river stage and discharge, is an elusive value pursued at great cost, with each additional fraction of attainment sometimes costing more than all prior to it. Absolute accuracy in most engineering offices is the product of a calculating machine, useful as a tool in attainment of relative accuracy regarding influences of small variables, but a source of colossal waste of time if confused with real or relative accuracy. One cannot start with an hypothesis having a real accuracy of 80% and develop therefrom conclusions of 95% real accuracy.

By any unmodified references to accuracy which may be made in the body of the paper which follows, the writer means only relative accuracy and the degree to which a computational determination by simplified procedure approximates the result of more laborious, accepted means of computation. No claims of unusual real accuracy are intended.

Investigators entering the field of flood flow analysis will do well to maintain

[2] "Stream Flow from Rainfall by the Unit Hydrograph Method," by Leroy K. Sherman, *Engineering News-Record*, Vol. 108, 1932, pp. 501–505.

[3] "An Approach to Determinate Stream Flow," by Merrill Bernard, *Transactions*, Am. Soc. C. E., Vol. 100 (1935), p. 347.

an open mind on the subject of real accuracy, since the difficulties of field observation and measurement under severe flood conditions make it necessary to concede the possibility of errors as large as 20% (or more) in some items of published data. Such possibilities are indicated in many published records by the discussion preceding the tabulations, and in others by subsequent revisions when more reliable data are obtained.

The attainment of a high order of relative accuracy in computation is expedited by concise, precise definition of procedure and the desired result. As an aid to the more rapid attainment of relative accuracy in the computation of flood hydrographs, the paper seeks to define the determination of the unit hydrograph of surface and subsurface runoff in terms of two, large, basic factors —the shape of the watershed from which runoff must come and the storage through which it must come.

The writer does not claim that the determinations will exceed in real accuracy the many excellent ones which have been obtained by trial and error, tried, tested, modified, and retried until they reproduce, well, the hydrographs of record. He does believe that the first determination of the unit hydrographs will prove satisfactory for use without modification in more cases than those determined by any of several other methods with which he is familiar.

Introduction

Rapid advances in the understanding of floodtime stream flow date from the Report of the Committee on Floods of the Boston Society of Civil Engineers in which it was recognized that, for storms of equal duration, the period of flood runoff was a constant not dependent upon the total volume of runoff and that the maximum rate of discharge was, therefore, a direct function of the total runoff. "For an instantaneous storm, the peak flow will vary directly with the maximum width of the drainage area, all other conditions remaining the same * * * unit peak flows will vary directly with the velocity of flow, all other conditions remaining the same" and "pondage tends to reduce the peak flow in the direct ratio that the volume of pondage bears to the total flood run-off." In these conclusions[4] lie the bases for many current concepts of the unit hydrograph, time-area concentration curves, and valley storage modification of flood flow.

A refinement of theory by Mr. Sherman[2] confirms the conclusion that the flood period is a constant and that the peak flow is proportional to the total volume of runoff, and extends the theory to show that, for a given unit quantity of runoff, uniform over the drainage area, originating in a small unit interval of time, the length of the hydrograph is a constant; that all ordinates will be proportional to the total runoff; and that, by the application of this so-called "unit hydrograph" to successive short periods of uniform runoff throughout the flood-producing storm period, the resulting hydrograph of stream flow could be reproduced with reasonable accuracy. This theory combines sufficient verification in many watersheds with convenience of use to a degree which has

[4] Report of the Committee on Floods of the Boston Society of Civil Engineers, *Journal*, Boston Soc. of Civ. Engrs., September, 1930.

made it acceptable to many in the engineering profession and deserving of the status of an original contribution to fundamental hydrologic theory.

By the limitation of its definition, as pointed out by Mr. Sherman, the unit hydrograph is correct and applicable only to areas from which the runoff for a given period of time is uniform and therefore to drainage areas for which the rainfall is essentially uniform over the entire basin. The extension of the theory to the areas of such size that this condition is not strictly true is a matter of practical expediency, but one which introduces fundamental discrepancies between theory and fact which are not a fault of the theory but of its application. In its original conception and application, the unit period was taken as one day, and the agreement of computed and observed discharges within that period of time was considered to be confirmation of the theory. The accuracy of the determination of the unit hydrograph was limited by the practical requirement of finding an isolated flood hydrograph resulting from a uniform unit rainfall. This latter requirement, while not a serious limitation on the use of the method for periods of one day, provides an almost insurmountable obstacle to the derivation of the unitgraph for very small drainage areas and very short unit periods of time.

A number of writers[5,6] have shown that the theory is equally applicable to very small drainage areas when the unit period used is sufficiently short to be in proper proportion to the total hydrograph.

In determinations of unit hydrographs for short periods of time, practical difficulties of finding uniform, short-period rainfall, which produced large enough stream flow to be analyzed accurately, make it necessary to determine unitgraphs from multiple periods of runoff. However, such a procedure is indeterminate, as there are always more equations than unknowns and a multiple of possible solutions.[7] For example, in determining a seven-period unitgraph from a flood resulting from three periods of runoff, it is possible to determine thirty-six unit hydrographs which, applied to the three items of runoff, will reproduce the composite hydrograph exactly. The approximate solutions are even more numerous. Consequently, the range of possible solutions by independent investigators is too large—far greater than the range of inaccuracy of stream discharge records. Most methods, graphical and mathematical, of selection of the most probable of these unitgraphs underestimate the capacity of a stream to reach a high instantaneous peak from short, intense rainfall and ignore tendencies toward double peaks which some streams exhibit following intense, short-period rainfall.

The range of possible unitgraph determinations can be reduced by correlating recognized discharge concepts with the physical limitations of valley storage and with the time elements which necessarily result from storage and discharge relations. The correlation can be utilized to develop, from time-area concentration curves of specific drainage areas, unit hydrographs with a small

[5] "Relation between Rainfall and Run-off from Small Urban Areas," by W. W. Horner and F. L. Flynt, *Transactions*, Am. Soc. C. E., Vol. 101 (1936), p. 140.

[6] "The Unit Hydrograph Principle Applied to Small Water-Sheds," by E. F. Brater, *ibid.*, Vol. 105 (1940), p. 1154.

[7] "Engineering Procedure as Applied to Flood Control Reservoirs with Reference to the Muskingum Flood Control Project, Appendix IV," The Engineer School, Fort Belvoir, Va., 1936.

range of determination variability, independent of assumptions regarding run-off distribution in the flood-producing storm and reflecting influences of drainage area shape and stream pattern. The streams of Virginia and North Carolina, with a wide range of basin shapes, stream slopes, and patterns, present admirable opportunities to prove or disprove some of the theories advanced.

In some respects, the degree of proof or disproof is limited by the quality of records and the means of their interpretation. Although recording stream gages have been installed on many of the streams, few of them are rated to a discharge more than one half of the maximum stage of automatic record. For the very flashy streams it is almost impossible for measuring parties to reach the streams before they have fallen well below peak stage. The greatest limitations on the check of accuracy of the theories, however, are the lack of recording rainfall gages and contour maps. Because of rainfall data limitations, determinations of the time of precipitation without a possible error of 3 to 6 hours were seldom possible. If the reproduced hydrographs agreed with the observed within these limits of time, the theories were regarded as confirmed. In all but a few cases, the agreement was much closer than the allowable error.

The constant time elements which have been indicated as essential to the theory of the unit hydrograph are dictated by valley storage relationships. For that reason, some of the vital elements of valley storage concepts are reviewed.

Valley Storage

One of the principal characteristics of the passage of a flood wave down an open channel is the time elapsing between passage at one point and at some downstream point—frequently referred to as the time of travel. The concept of this time of travel as a function of the velocity of the water and therefore influenced by the slope of the river, channel friction, and other items which influence the velocity of flow in the river, is deeply rooted in the hydrology of streams. However, time of travel is more closely related to the variable storage capacity of the open channel; dimensionally, time is the ratio of storage to discharge. Flow in pipes is influenced by all the elements of slope, friction factor, etc., which influence velocity of water in an open channel; but there is no time of travel in a closed pipe, which is full at the beginning of the passage of the wave, where an increase in the velocity and discharge at the upstream end is accompanied almost simultaneously by an increase in velocity and a duplication of the waves at the exit end of the pipe. Time of travel is almost nonexistent in rigid pipes, such as cast iron and concrete, and becomes increasingly apparent in pipes which are elastic enough to have some variable capacity for storage, such as rubber hose and the arteries of the human body.

Most methods of taking account of the storage in a river valley involve the solution, either graphically or mathematically, of the storage equation:

$$\frac{I_1 + I_2}{2} t - \frac{O_1 + O_2}{2} t = S_2 - S_1 \quad \ldots\ldots\ldots\ldots\ldots\ldots (1)$$

in which I is the total inflow rate and O the outflow rate, both in cubic feet per second; S is the total volume in storage in the reach in (cubic feet per second)-hours (12 (cu ft per sec)-hr = 1 acre-ft); and the subscripts 1 and 2 refer to the beginning and the end of the period respectively.[8] This is the arithmetic expression of the storage equation. The calculus equation for the same condition is:

$$dS = (I - O)\, dt \quad \ldots\ldots (2a)$$

or

$$\frac{dS}{dt} = I - O \quad \ldots\ldots (2b)$$

which is merely a mathematical way of saying that the rate of change of storage is equal to the difference between the inflow and the outflow rates. In Eqs. 2, t is the length of a period of time, in hours.

In general, the quantity of water stored in a short open channel increases with an increase in the flow in the channel, or:

$$S = C\, Q^n \quad \ldots\ldots (3)$$

in which Q is the flow in the channel, n is a positive exponent, and C is a constant for the particular channel. Thus the storage in a river is a function of the flow and varies directly with some power of it.

In a short reach of river it may make little difference whether storage is considered as a function of inflow discharge or outflow discharge since there is little difference between them. In long reaches of the length considered practical for flood routing studies or of the length over which appreciable backwater effects may extend in floodtime, there is a great difference.

Methods of accounting for the influence of storage on discharge originally were used in analyzing flood reduction effects of reservoirs, where storage was a function of outflow. The accounting of storage between successive level pool surfaces whose elevation was controlled at the dam was a satisfactory approximation of the total storage. The amount of storage above the slack-water pool level and under the backwater curve was ignored as truly of small consequence.

The backwater storage, however small, existed because of the concurrent existence of inflow to the reservoir. Reduction of the inflow rate necessarily would be accompanied by a decrease in storage and an increase of outflow rate. Rapid inflow shutdown necessarily would be accompanied by a release of the backwater storage and a consequent increase in the slack-water storage or in the outflow discharge or in both. The released volume of water would be free to roll, as a pressure wave, to the lower end of the reservoir. Others have compared the movement to the rotation of saturated soil in a landslide. In either case, the lower end of the reservoir would have to rise slightly and the outflow discharge would have to increase.

The extension of concepts of storage modification to sloping channels and natural streams extended the practise of correlating storage with outflow. In

[8] "Flood Routing," by Edward J. Rutter, Quinton B. Graves, and Franklin F. Snyder, *Transactions*, Am. Soc. C. E., Vol. 104 (1939), p. 278.

some river reaches, the correlation with inflow is as close as the correlation with outflow. Some current concepts of the action of valley storage in reducing flood peak discharge are faulty because they are in terms of the original, limited theory. The storage which may be treated as a function of outflow reduces flood peak outflow discharge, but the portion which is a function of inflow increases outflow, so that the net decrease or increase of peak discharge depends on which storage portion is the greater.

The idea that there is some valley storage which does not decrease flood peaks is rather new. The nature of the actions is illustrated in Fig. 1, which

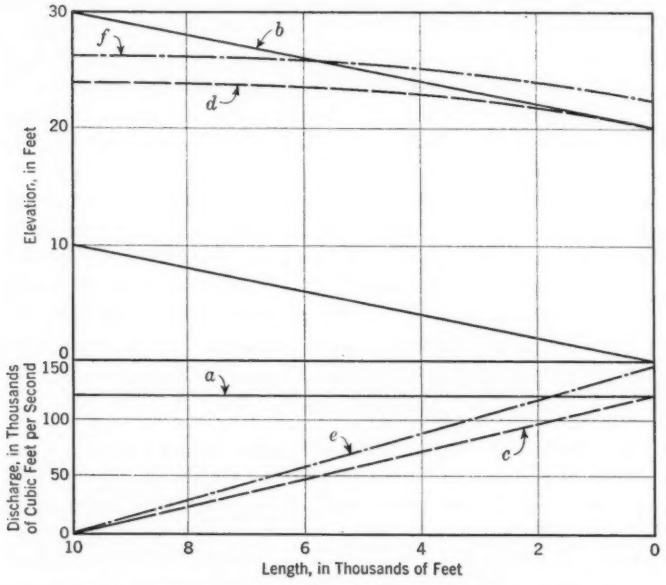

FIG. 1.—EFFECT OF DECREASING INFLOW ON FLOOD PROFILE

shows water-surface profiles for a uniform, rectangular channel 500 ft wide, 20 ft deep, and with a fall of 10 ft in its length of 10,000 ft. Line b shows the profile for steady flow of 116,000 cu ft per sec throughout the channel length. Assume that the steady flow into the channel at the upper end is reduced quickly as by the closure of gates on a reservoir or the crevassing of a levee. With discharge reduced at the upper end of the reach and maintained at the lower end by storage release, the distribution of discharge in the reach would be similar to line c to which profile d would apply. The change from profile b to profile d involves the release from storage of 260 acre-ft during the period of inflow reduction and requires the outflow discharge to increase to accommodate such a release. However, as the outflow increases, the discharge distribution in the channel approaches profile e and the water-surface profile approaches that indicated by line f. Storage under profile f is the same as under profile b.

A shift of water-surface profile from lines b to f takes place in a natural channel by mass rotation transmitted by means of pressure waves of small

amplitude which surge back and forth through the reach, ceasing when the stable profile for the new discharge distribution has been attained. In natural channels under normal flow conditions, the reductions of inflow rates are gradual with the greater changes of discharge distribution occurring near peak stage. The surge of small amplitude transition waves is clearly apparent as a broad trace in many autographic records of stage. Following discharge change, the profile transition takes place in a very short time. The writer has a record of a natural flow reduction, caused by the crevassing of a large levee, in which the effect of the break in transforming the water-surface profile was transmitted 17 miles in as many minutes, whereas a normal flood wave transit of the same distance requires about 15 hours.

In the example of Fig. 1, if the water-surface elevation at the lower end is held constant by opening the gates of a dam, a material increase of outflow rate would be required. To prevent any increase in outflow discharge, a rise of about 3 ft would be required to store the initial volume as it shifted to the lower end of the reservoir.

In an unregulated reservoir of large capacity compared with the inflow to it, the storage may be solely a function of the outflow. In a long and uniform channel, the storage may be almost equally a function of the inflow and the outflow. All during the early stage of rapid increase in discharge in dry channels, such as occurs naturally in the arroyos of the Southwest, the storage is solely a function of the inflow. Thus, Q in Eq. 3 is to be considered as a weighted average value of the inflow and the outflow:

$$Q = x\,I + (1 - x)\,O \quad \ldots\ldots\ldots\ldots\ldots\ldots\ldots\ldots (4$$

in which x is a coefficient with a value between 0.0 and 1.0.

According to Eq. 3, storage tends to increase with some power of the stream flow. There seems to be no theoretical reason why the power could not be either greater or less than unity. If it were less than unity, the peaks of large floods would occur earlier than those of small floods; if the power were greater than unity, the reverse would be true. If the power is unity, storage and discharge are in constant direct proportion, and time elements are constant regardless of flood magnitude.

Storage in a river channel does not necessarily increase directly with the discharge, but studies of the variation in a large number of streams indicate that this is the case for most smaller streams and is a condition closely approximated over large ranges of discharge in many large streams. That is, the exponent is 1.0 for small streams, and for many rivers of as much as 10,000 sq miles of drainage area it is less than 1.3. Even for the latter streams, over a large range the true storage may be closely approximated by storage directly proportional to discharge.

Storage which is directly proportional to discharge does not interfere with the accuracy of the unit hydrograph theory, as its characteristically constant time elements are compatible with, and necessary to, the similarly constant time elements of the unit hydrograph. Wherever the unitgraph theory is applicable, or wherever the time elements of flood passage are essentially constant, the storage is proportional to discharge.

There are a great many mathematical and graphical solutions for the storage equations, both for conditions where the storage is considered to vary directly with the discharge and where it is considered to vary directly with some exponential power of the discharge. All but a few of these solutions are for the special case in which the storage is a function of the outflow only and, therefore, are applicable only to routing floods through a very large reservoir. Use of these special solutions for natural channels, or for small reservoirs in which backwater storage is appreciable, leads to undesirable optimism regarding reductions of discharge by storage use.

The scope of this paper is limited to the general conditions in which the storage is considered to vary directly as the discharge, but where the discharge is a weighted value of the inflow and the outflow. Mathematically, these statements resolve to the three equations previously given:

$$dS = (I - O)\,dt \quad \ldots\ldots (2a)$$

$$Q = x\,I + (1 - x)\,O \quad \ldots\ldots (4)$$

$$S = K\,Q \quad \ldots\ldots (5)$$

from which it is evident that:

$$K = \frac{dS}{dQ} = \frac{(I - O)\,dt}{x\,dI + (1 - x)\,dO} \quad \ldots\ldots (6a)$$

and

$$O = I - K\,x\,\frac{dI}{dt} - K\,(1 - x)\,\frac{dO}{dt} \quad \ldots\ldots (6b)$$

Eq. 5*b* can be solved arithmetically for successive short periods of time, T in length, by designating the flows at the beginning of the short period as O_1 and I_1 and those at the end by O_2 and I_2, thus:

$$\frac{O_1 + O_2}{2} = \frac{I_1 + I_2}{2} - K\,x\,\frac{I_2 - I_1}{T} - K\,(1 - x)\,\frac{O_2 - O_1}{T} \quad \ldots\ldots (6c)$$

from which the following simple equation evolves:

$$O_2 = C_0\,I_2 + C_1\,I_1 + C_2\,O_1 \quad \ldots\ldots (6d)$$

In Eqs. 6:

$$C_0 = -\frac{K\,x - 0.5\,T}{K - K\,x + 0.5\,T} \quad \ldots\ldots (7a)$$

$$C_1 = +\frac{K\,x + 0.5\,T}{K - K\,x + 0.5\,T} \quad \ldots\ldots (7b)$$

$$C_2 = \frac{K - K\,x - 0.5\,T}{K - K\,x + 0.5\,T} \quad \ldots\ldots (7c)$$

and

$$C_0 + C_1 + C_2 = 1.00 \quad \ldots\ldots (7d)$$

This is the Muskingum method of flood routing developed by T. S. Burns and F. B. Harkness, Members, Am. Soc. C. E., and G. T. McCarthy,[7] Assoc. M. Am. Soc. C. E.

To illustrate the action of linear storage upon wave forms, two mathematical curves have been routed through various quantities of storage by the Muskingum method. Fig. 2 illustrates the modification of a cosine-type curve by storage represented by a value of K of four time units, with various values

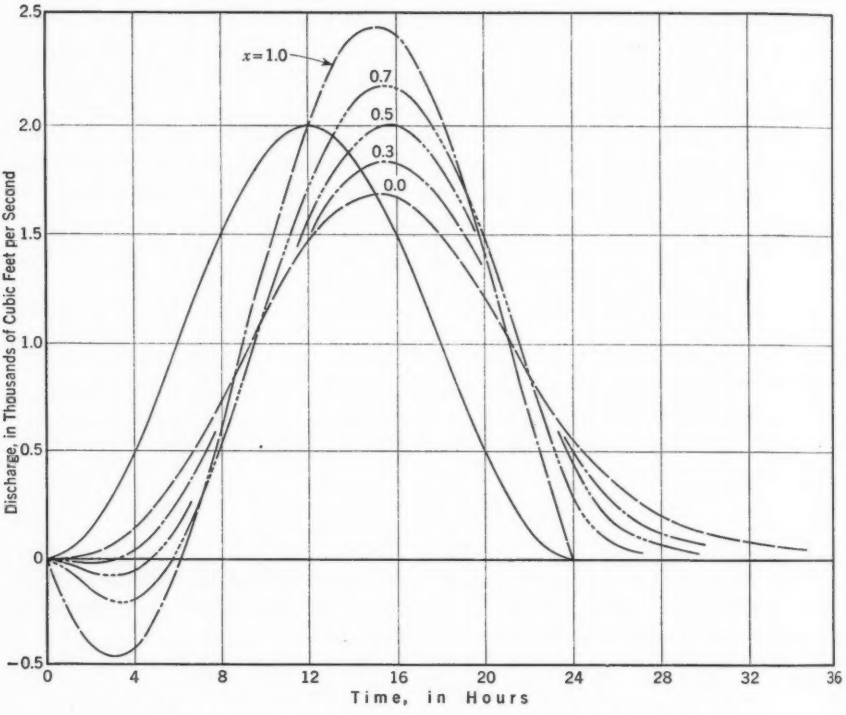

FIG. 2.—MODIFICATION OF COSINE TYPE OF WAVE BY STORAGE

of x from 0.0 to 1.0. For this well-rounded initial wave form, the fundamental effect of the storage modification is to translate the entire wave approximately four time units, and to change the magnitude of the peak. The change of magnitude seems to be more a function of the value of x than of K, because when $x = 0.5$, the modified wave appears to be a close duplication of the initial wave, except for the parts of the curve before initial outflow and after final inflow.

It may be desirable to explain the unorthodox appearance of the modified wave forms (Fig. 2) between the initial inflow and initial outflow. The indicated negative values are partly erroneous and partly correct. A slight error arises in the theory assumption that the average discharge in the reach of river is indicated by a weighted value of the discharge at the ends and, therefore, that the storage prism between successive positions of the rising water surface may be approximated by two wedges of storage extending the length of the reach, one a function of inflow and the other a function of outflow. Consider-

ing the real bulbous shape of an advancing wave front in a near-dry channel, the true storage in the reach is less than the full-length wedge during the first part of the initial inflow. During this period, the actual outflow discharge is more than computed. At the instant the wave front reaches the lower end, the actual storage in the reach is somewhat more than that of a full-length wedge. At this time and for a short time after, the actual discharge at the lower end of the reach is less than indicated by the theory and the actual rise is later than that calculated. The inequalities between the theory and fact of wedge storage approximation are ironed out by the time the rates of flow increase at both ends are equal. Since the discharge at the lower end is closely indicated at this time, the true rise at the downstream end is more rapid than computed. The maximum total storage volume in the reach, represented by the area between the inflow and outflow hydrographs, is the same at this time for actual and computed modifications.

In the case of a wave passing into a partly full channel, into which flow is also coming from local streams, much less of the indicated negative discharge is to be regarded as error. The negative values indicate the capacity of the advancing wave not only to store its own waters, but to force the storage of the incoming local flows through the induced backwater effect. Only when the algebraic sum of all components of flow (including the negative values of the routed inflow wave) is less than the flow prior to the flood can the sum be discounted as error. Even then, the appearance of large negative values is an indication of a period of hydraulic instability which in extreme cases results in the formation of a hydraulic bore.

The negative values play an important part in the accuracy of the general storage theory and are to be discounted judiciously. The writer follows the practise of retaining the computed negative values, discounting them only in the drawing of the final hydrograph.

Fig. 3(*a*) shows the effect of storage that is equally a function of inflow and outflow; that is, $x = 0.5$ on a wave form with an initially very sharp peak. The first wave has been routed through 2 hours of storage in each of five successive reaches. In this case as in the case of the cosine curve, the translation effected by storage is approximately equal to the value of K; but some reduction of peak discharge is effected. However, the reductive influence of the storage decreases as the initial wave approximates the stable, well-rounded form.

The actual progressive modification by storage which is almost equally a function of inflow and outflow rates, illustrated in Fig. 3(*a*), has about the same effect as the bodily transposition of the initial wave form combined with a final modification of the transposed wave by a small amount of reservoir storage. The difference between the progressive calculation of storage effect, which is probably closer to truth, and the more easily computed transposition and single storage modification calculation is illustrated in Fig. 3(*b*), in which the wave form (a) has been progressively modified by passage through five reaches, each having 2 hours of storage (2 (cu ft per sec)-hr per cu ft per sec of discharge) to become wave form (b). The approximation wave form (c) was derived by bodily transposition of wave form (a) by 9 hours and routing it through reser-

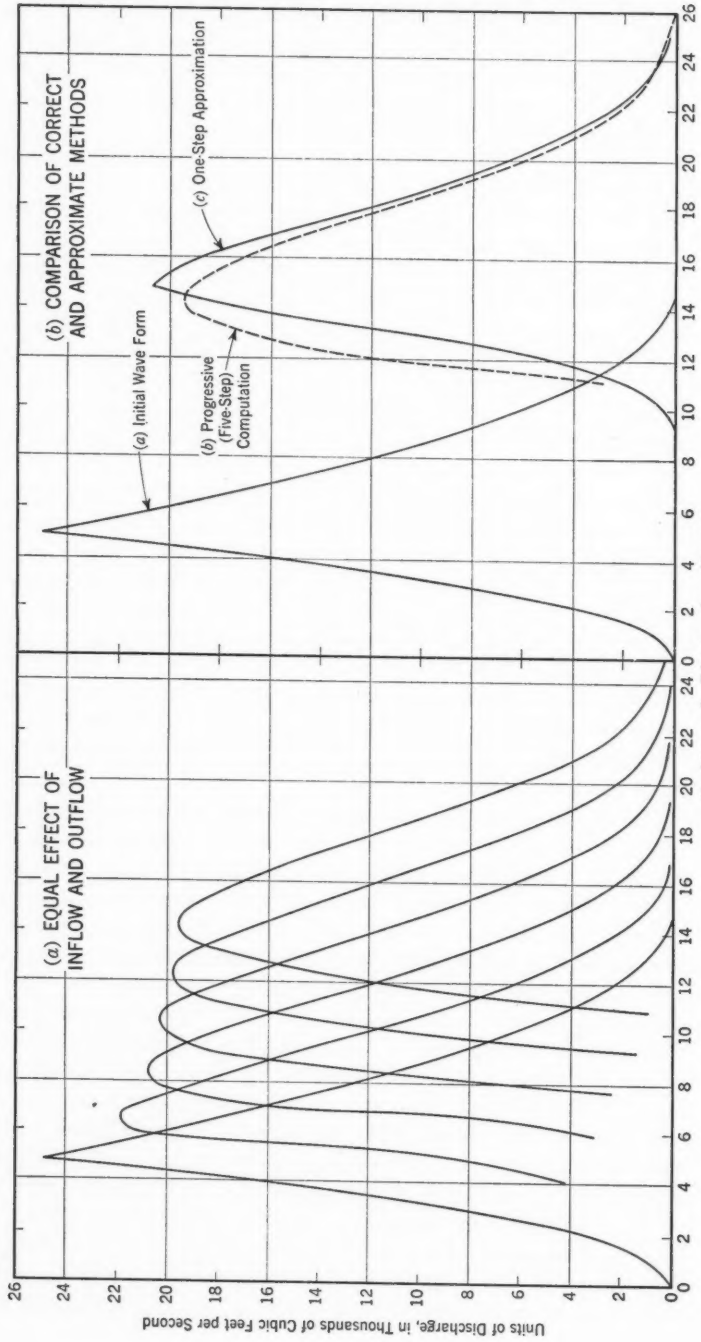
(a) EQUAL EFFECT OF INFLOW AND OUTFLOW
(b) COMPARISON OF CORRECT AND APPROXIMATE METHODS
(a) Initial Wave Form
(b) Progressive (Five-Step) Computation
(c) One-Step Approximation
Units of Time, in Hours
Units of Discharge, in Thousands of Cubic Feet per Second

FIG. 3.—MODIFICATION OF A SHARP-CRESTED WAVE BY STORAGE

voir-type storage ($x = 0.0$) of 1 hour. The agreement between curves (b) and (c), far from perfect, is within the degree of accuracy usually attainable in runoff calculations.

This approximate form of storage calculation is used subsequently in the derivation of unit hydrographs; a time-area concentration curve of the drainage area (a composite of all of the transposed, unmodified wave elements of the watershed) is modified by a small amount of storage to form the basic unit-graph. The procedure will be explained in detail.

For many natural streams, the value of x, in Eq. 4, varies from 0.4 to 0.5, but the presence of a large flood plain carrying little flow near the lower end of a reach will cause the storage to be more of a function of outflow than inflow, and will reduce the relative influence of inflow, x, to 0.3 or lower. The back-water effect of a large incoming tributary may act in a similar manner. Conversely, if the large storage is near the upper end of the reach, the value of x may exceed 0.5 and result in an increase of crest discharge rather than the usually assumed decrease (the hydrographs in Fig. 12, introduced subsequently, indicate such an influence).

An understanding of the mechanical process of flow of water through a reach of river or a reservoir in light of the Muskingum routing theory will provide a clearer concept of what can and cannot be accomplished by valley storage. It also will show that, contrary to popular concept:

(*a*) Valley storage does not always decrease flood peaks; and

(*b*) The reservoir pool above a dam may not reduce flood discharges. In fact, if the pool level at the dam is held constant by gate control, the storage becomes the function of inflow solely, and the peak outflow may be larger than the peak inflow. Furthermore, such control, by reducing the effective storage, may decrease the time of travel through the reservoir to almost nothing, with a beneficial or detrimental effect as the case may be.

Significant Storage Relationships

The fundamental storage equation for storage which varies directly with a weighted average of the inflow and the outflow is (see Eq. 5*b*):

$$O + (1 - x)\, K \frac{dO}{dt} = I - K\, x \frac{dI}{dt} \quad \ldots\ldots\ldots\ldots\ldots\ldots (8)$$

Although the Muskingum equations are easier to use in routing procedure, a knowledge of the following relationships which exist at certain points in the hydrographs of inflow and outflow is of great value in determining the quality and quantity of the storage effect in the reach. The symbols, $\frac{dI}{dt}$ and $\frac{dO}{dt}$, are used to represent the slope of the inflow and outflow hydrographs. When the slope of inflow and outflow hydrographs is equal:

$$\frac{dI}{dt} = \frac{dO}{dt} \quad \ldots\ldots\ldots\ldots\ldots\ldots\ldots\ldots\ldots\ldots (9a)$$

and

$$I - O = K \frac{dO}{dt} \quad \ldots\ldots\ldots\ldots\ldots\ldots\ldots\ldots\ldots\ldots (9b)$$

When inflow and outflow are equal:

$$I = O \quad \ldots\ldots (10a)$$

and

$$\frac{dO}{dt} = -K\frac{x}{1-x}\frac{dI}{dt} \quad \ldots\ldots (10b)$$

At peak inflow:

$$O = I - K\frac{dO}{dt}(1-x) \quad \ldots\ldots (11a)$$

At peak outflow:

$$O = I - Kx\frac{dI}{dt} \quad \ldots\ldots (11b)$$

When inflow has ceased:

$$O = -\frac{K\,dO}{dt}(1-x) \quad \ldots\ldots (12a)$$

and

$$K = -\frac{O}{\frac{dO}{dt}(1-x)} \quad \ldots\ldots (12b)$$

Volume of runoff remaining in storage is

$$KO = -\frac{O^2}{\frac{dO}{dt}(1-x)} \quad \ldots\ldots (13)$$

Valley Storage and the Unit Hydrograph

A few years ago, the unit hydrograph was thought to be inapplicable to streams having a great amount of valley storage. However, when valley storage is defined as "all of the volume displaced by water during the passage of a flood wave, including the volume in the river channel," it is evident that no flood wave is unaffected by valley storage.

From a different point of view, the nature of the effect is clear. The essential difference between nonsteady flow in open channels and in pipes is in the time that elapses in the former only between the change of inflow rate and the change of outflow rate. The essential difference between an open channel and a pipe is the variable capacity of the former for storage as compared with the constant capacity of the latter. The time element and the storage capacity are related, for the ratio of storage capacity to discharge capacity is time; that is, $\frac{S}{Q} = T$.

The unit hydrograph theory assumes that the ordinates of any flood hydrograph originating from uniform runoff in the unit period of time will be directly proportional to the quantity of runoff, but that the abscissas, or time elements, will be constant and, therefore, unaffected by magnitude of discharge. Since the time elements are a function of the ratio of storage to discharge but not of discharge alone, it follows that the ratio of storage to discharge must be a constant throughout the entire range of discharge to which the unit hydrograph is to be applied. In other words, the storage-discharge curve for all reaches of river above the point to which the unit hydrograph is to be used must be

straight lines when plotted on rectangular coordinate graph paper. This is the simplest of the storage discharge relationships for which methods of solution have been devised—the basis of the Muskingum method outlined by Mr. McCarthy.[9] An understanding of the manner in which it is possible for this type of storage to modify a flood wave will provide an understanding of several significant relationships which must exist in any actual unit hydrograph if the theory is applicable to the drainage area being studied.

The Hydrograph as an Index of Storage

Any flood hydrograph is the resultant of all of the factors that have created it. Although no exact determination of the effect of any factor is possible without the segregation of the results of other influences, it is possible to determine the effect between certain limits. The accuracy of the determination will depend on the degree to which other influences can be segregated or discounted as insignificant.

The analysis of the hydrograph, as an index of previous storage effect, is based on the hypothesis that, after inflow to the channel has ceased, all water which will eventually become runoff, but which has not yet passed the gage, is in storage (axiomatic), and that such storage varies directly with the discharge (approximate, approaching truth in very small impervious watersheds). After such a time, the ratio of rate of change of discharge to total discharge reaches its greatest negative value, and remains constant thereafter:

$$\frac{\frac{dO}{dt}}{O} = -\frac{1}{K(1-x)} \quad \ldots\ldots\ldots\ldots\ldots\ldots\ldots\ldots (14)$$

If all storage in a stream above a gage has been equally a function of inflow and outflow (that is, if $x = 0.5$), the greatest ratio of decrease of discharge to total discharge will correspond closely to a K-value of the time elapsing since the cessation of inflow. For the same amount of total storage, entirely a function of outflow, the ratio would have only half as large a magnitude, indicating a lesser slope of the depletion curve.

The falling legs of a large number of hydrographs of flood discharge for streams in major drainage basins from New Hampshire to North Carolina exhibit a ratio of decrease of discharge to total discharge which, for a value $x = 0.5$, indicates a value of K closely approximating the time elapsing between termination of runoff producing rainfall and the point of most rapid relative decrease in discharge. The fact that the hydrographs fall so rapidly is highly indicative that the storage affecting the hydrographs is of the balanced variety, and, therefore, chiefly effective in the translation of waves.

The writer has indicated that the effect of such storage may be approximated by (*a*) the bodily transposition of the runoff wave element from its source to the gage, and (*b*) the routing of the element through some amount of storage less than the total with a value of $x = 0$. The summation of all of the transposed elements for an entire drainage area is the same as a time-area concentration

[9] "The Unit Hydrograph and Flood Routing," by Gerald T. McCarthy, unpublished manuscript presented at the Conference of the North Atlantic Div., Corps of Engrs., U. S. Army, New London, Conn., June 24, 1938; printed by the U. S. Engr. Office, Providence, R. I.

curve whose base length is the time between cessation of runoff and the time of most rapid relative decrease in discharge. The value of K selected for the routing of the time-area concentration curve is one corresponding to the ratio of discharge decrease to total discharge for an observed hydrograph (Eq. 12*b* with $x = 0.0$).

The application of this method to a theoretical drainage area of rectangular shape with uniform instantaneous rainfall over the entire drainage basin is shown in Fig. 4(*a*). If the rainfall were to remain constant for a unit period

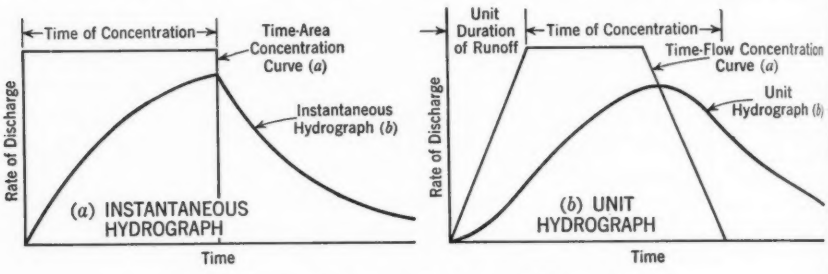

FIG. 4.—HYDROGRAPHS FOR A RECTANGULAR DRAINAGE AREA

of time, as is predicated in the theory of unit hydrographs, the flow concentration curve which was the time-area diagram (curve (a), Fig. 4(*a*)) is modified to become the time-flow diagram (curve (a), Fig. 4(*b*)) which, routed through the same storage, becomes curve (b), Fig. 4(*b*). The advantage of an instantaneous hydrograph is that it can be derived from the fundamental characteristics of the basin and then used with any length of unit period to determine the unit hydrograph, in which any ordinate of discharge is the average ordinate of the instantaneous hydrograph for the unit time period previous to time desired. Where the curvature of the instantaneous hydrograph is not excessive, the ordinate can be determined by averaging ordinates of that graph separated by the unit time period desired.

DETERMINATION OF THE INSTANTANEOUS HYDROGRAPH FROM STREAM FLOW RECORDS

Where adequate planimetric maps of a stream are provided in which recorder rainfall and discharge records are available, the elements to be determined are the base length of the time-area concentration curve, or the time of concentration, the time-area curve, and the magnitude of the unbalanced storage effect or the amount of valley storage (solely a function of discharge) by which the time-area curve is to be modified.

Referring to Eq. 12*b*, it will be seen that, when the inflow to the storage reach has ceased, the ratio of decrease of discharge to total discharge is a constant; or, as the Muskingum flood routing equation expresses it, the outflow at the end of any period of time bears a constant ratio, C_2, to the outflow at the beginning of the period of time.

Plotting the value of K which is indicated by the rate of decrease of discharge throughout the falling hydrograph, the indicated value should decrease

to a minimum at the time that inflow ceased and remain constant thereafter. The time between cessation of runoff-producing rainfall and the minimum indicated value of K is the writer's concept of time of concentration and is so used in the remainder of this paper.

Taking the time of concentration derived in this manner as the time base length, a time-area concentration curve for the drainage area above the gage is prepared. This curve is used as the inflow to the river channel and is routed through an amount of storage represented by the indicated minimum K-value and an x-value of zero.

Extension of Storage Theory to Ground-Water Flow

In practise, the indicated value of K does not remain constant after reaching its minimum value. The inflow from ground water continues and does not

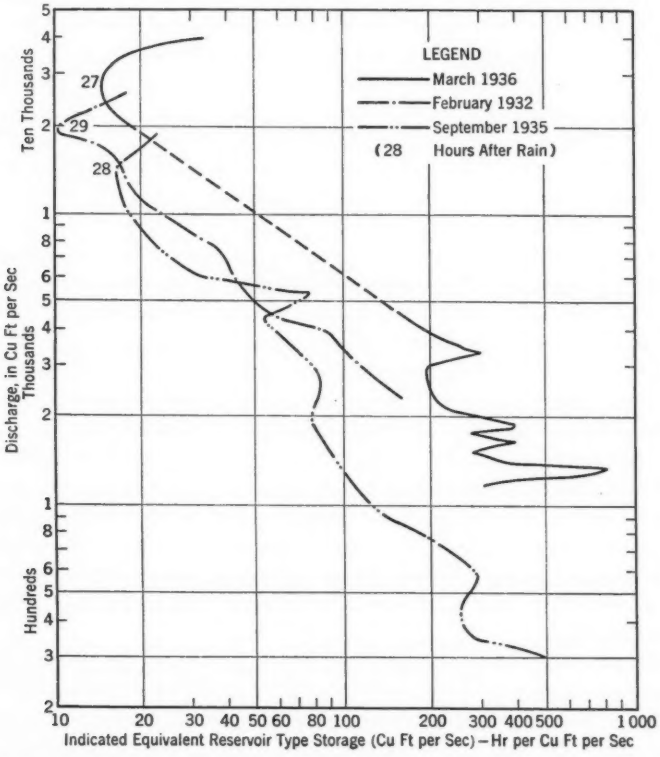

Fig. 5.—Determination of Effective Storage from Recessional Hydrograph; James River at Lick Run

decrease as rapidly as the storage-controlled surface runoff. Therefore, it becomes an increasingly larger percentage of the total discharge and increases the indicated value of K.

Actual curves of the indicated value of K are plotted in Fig. 5 against the

discharge rate for the major part of the falling leg of several hydrographs at a stream gaging station at Lick Run, Va., on the James River (drainage area = 1,369 sq miles). The indicated value of K decreases to a certain minimum value which is essentially constant for all hydrographs and then increases from that point as the discharge decreases, becoming very large as the discharge becomes very small.

Application of this theory of runoff would imply a definition of surface runoff as being that quantity of total runoff which, after the cessation of inflow, is discharged in direct proportion to the amount of flow remaining to run off. Ground-water flow would include all other flow.

Since ground water is detained by storage also, it would be convenient for hydrologists if that storage were found to be in direct proportion to the rate of discharge. In analyzing the discharge hydrograph of any stream, it is rare to find one which, after reaching an abnormally high peak, continues to fall without further rainfall until it has reached an abnormally low flow. However, this was the case following the flood of September, 1935, on the James River. In that hydrograph, the discharge at Lick Run increased from 271 cu ft per sec to 19,400 cu ft per sec and then fell steadily to 258 cu ft per sec, the lowest discharge of the year. During the falling period, the rainfall was so small and scattered that it is doubtful if it contributed in any way to the stream flow. The indicated K-curve for this hydrograph is among those shown in Fig. 5.

After studying a large number of hydrographs extending into periods of low flow, both for this station and for several other stations in the James River basin, an approximate value of K of 200 hours was selected as an average representation of the ground-water storage effect in that watershed. For this station and for three others of good record, five hydrographs for each station were separated into the two volumes which could be represented by the channel storage modification outlined and the subsurface (ground-water) flow released from storage of 200 hours. No hydrographs were found in which the subsurface part was less than 30% of the total runoff, and there were no major flood hydrographs in which it exceeded 42%. Using a value of K of 200 hours and of $x = 0.0$, another unitgraph for subsurface flow was derived. Combination of 70% of the surface unitgraph and 30% of the subsurface unitgraph provided an excellent practical unitgraph for this drainage area, which included both surface and subsurface flow.

Thus in the derivation of a unitgraph for instantaneous origin of runoff, by the method proposed by the writer, a unitgraph of surface runoff, derived by routing the time-area concentration curve through an amount of unbalanced storage as outlined herein, is combined with a unitgraph of subsurface runoff determined by routing the same histogram through an appropriate amount of subsurface storage. What the ratio of these components will be in the final hydrograph will depend on the pertinent fact of how much of the water comes from surface runoff and how much from subsurface runoff in the particular watershed. For the streams analyzed along the eastern Appalachian slope, a 70 : 30 ratio seemed quite satisfactory. (If the additional work is justified,

separate unitgraphs of surface and subsurface runoff may be utilized. With such use, no assumption of a fixed ratio is necessary.)

Although such a division is arbitrary, it is not as unsatisfactory as the current practise of attributing to ground-water discharge all flow beneath a straight line drawn from a point before the rise to an arbitrary and undefinable point on the descending hydrograph. The volume of flow so neglected frequently contains more than 20% of the total runoff. Any determination of runoff from subsequent storms, to be used in a unitgraph so derived, must be made in the light of such a derivation, with the result that, in times of great floods, the runoff percentage used for the flood-producing precipitation may be less than the average percentage runoff for the month corrected for prior and subsequent ground water.

Derivation of the Instantaneous and Unit Hydrographs

For the purpose of illustrating the method of derivation of unitgraphs, the Appomattox River at Petersburg, Va., was selected. There are several reasons why the drainage basin is not a good location for the application of the unit-

TABLE 1.—Derivation of Instantaneous Hydrograph and 12-Hr Unitgraph on Appomattox River Near Petersburg

Time, in days	Time-area curve (%)	Routing Calculation[a]			Surface flow = 0.70 × Col. 5	Subsurface flow 0.30[b]	Instantaneous Hydrograph		12-hr unit hydrograph (cu ft per sec[c])
		$C_0 I_2 + C_1 I_1$ = 0.56 × Col. 2	$C_2 O_1$ = 0.44 × Col. 5	Routed time-area curve = Col. 3 + Col. 4			% per 12 hr[c]	Cu ft per sec[c]	
(1)	(2)	(3)	(4)	(5)	(6)	(7)	(8)	(9)	(10)
0.0	0.0	0.0	0.0	0.0	0.0	0.0	0.0	....	....
0.5	1.8	1.01	0.0	1.01	0.70	0.03	0.73	500	250
1.0	3.8	2.13	0.44	2.57	1.80	0.10	1.90	1,300	900
1.5	6.9	3.86	1.13	4.99	3.50	0.22	3.72	2,550	1,920
2.0	10.8	6.05	2.19	8.24	5.75	0.40	6.15	4,220	3,380
2.5	19.1	10.70	3.63	14.33	10.00	0.72	10.72	7,360	5,790
3.0	7.6	4.25	6.32	10.57	7.40	0.81	8.21	5,630	6,490
3.5	6.5	3.64	4.64	8.28	5.80	0.88	6.68	4,580	5,100
4.0	5.5	3.08	3.64	6.72	4.70	0.93	5.63	3,870	4,230
4.5	9.0	5.04	2.96	8.00	5.60	1.03	6.63	4,550	4,210
5.0	14.0	7.83	3.52	11.35	7.80	1.22	9.02	6,180	5,360
5.5	9.5	5.32	4.98	10.30	7.20	1.32	8.52	5,850	6,010
6.0	5.5	3.08	4.53	7.61	5.33	1.34	6.67	4,580	5,210
6.5	....	....	3.35	3.35	2.35	1.25	3.60	2,470	3,520
7.0	....	....	1.47	1.47	1.03	1.18	2.21	1,510	1,990
7.5	....	....	0.65	0.65	0.46	1.11	1.57	1,110	1,310
8.0	....	....	0.29	0.29	0.20	1.04	1.24	850	980
8.5	....	....	0.13	0.13	0.09	0.98	1.07	735	800
9.0	....	....	0.06	0.06	0.04	0.92	0.96	660	700
9.5	....	....	0.03	0.03	0.02	0.86	0.88	600	630
10.00	....	....	....	....	....	0.81	0.81	560	580[d]

[a] Cols. 3, 4, and 5 are routing of Col. 2 with K = 15 hr, x = 0.0. [b] Col. 7 equals 0.30 × Col. 2 routed with K = 200 hr, x = 0.0. [c] Instantaneous rate of discharge. [d] 116,000 (cu ft per sec)-hr, or 13%, remaining to run off. Successive values of unitgraph hereafter are 0.942 × preceding value.

graph principle; but, because of its peculiar shape, it is particularly adapted to the illustration of the benefits inherent in the method of unitgraph derivation proposed. Because it was not used in any way in the derivation of any of the data or principles on which this method is predicated and because the writer

had done no work on this stream previous to the present calculation, this basin was used. The calculations in Table 1 show the first computations made and neither the original data, the first interpretations of these data, the calculations, nor the plotting, have been changed or altered in any way to make the computed hydrograph agree more closely with the observed hydrograph. (Only a

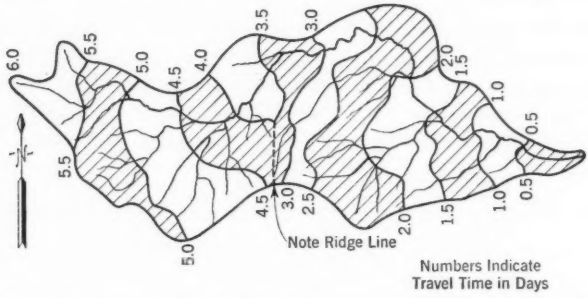

FIG. 6.—DRAINAGE AREA OF THE APPOMATTOX RIVER ABOVE PETERSBURG

slight change in estimated time distribution of runoff is necessary to improve the agreement.) This stream has a flatter slope and a longer time of concentration than any other stream of comparable drainage area in its immediate vicinity and therefore is adapted to illustrating some of the faults as well as the good points of the application. Fig. 6 shows the drainage area of the Appomattox River above Petersburg and the manner in which it was divided to provide the data for the time-area concentration curve; Fig. 7 is the profile

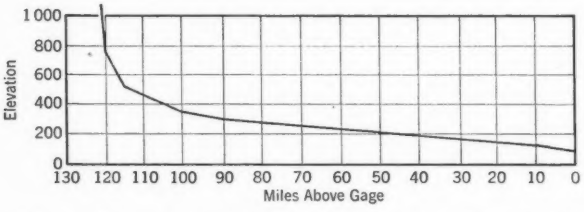

FIG. 7.—PROFILE OF THE APPOMATTOX RIVER ABOVE PETERSBURG

of the river above the gaging station as taken from the best available U. S. Geological Survey topographic sheets; and Fig. 8, curve (a), shows, in bar diagram form, the time-area concentration curve; and curves (b) and (c) show the time-area curve after routing through 9 hours and 200 hours, respectively, of storage. A combination of 70% of curve (b) and 30% of curve (c) is the instantaneous hydrograph, curve (d), for the Appomattox River at Petersburg. Fig. 9 shows the application of the 12-hr unitgraph derived from the instantaneous hydrograph to the flood of April, 1937. This is the second largest flood for which there is any available record at Petersburg and one of the largest floods that has occurred in the past 100 years. (The largest flood, August, 1940, caused by protracted rainfall, did not exhibit a double peak but is equally well reproduced with the same unitgraph.)

The following statements of fact must be taken into consideration in judging the degree of accuracy with which the computed record follows the observed record:

1. The area is too large for the proper application of a single unitgraph (drainage area, 1,335 sq miles). Because of the direction of the stream in comparison with the general east and west travel of storm fronts in this vicinity and because of the long time of concentration, a difference in rainfall both in the

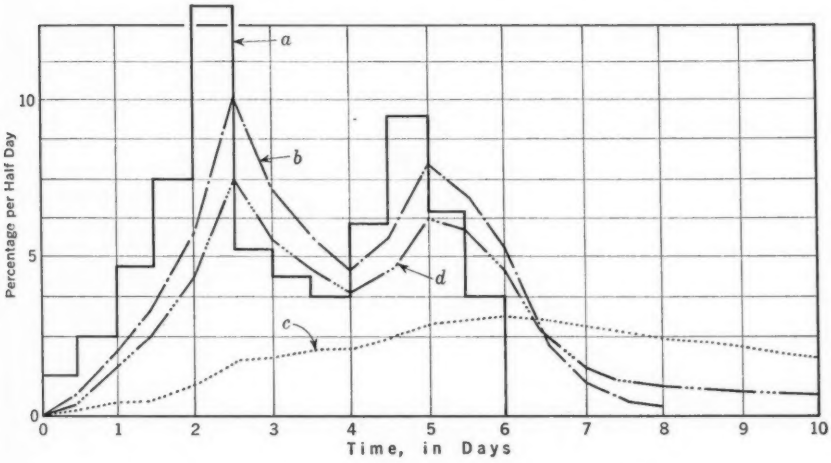

FIG. 8.—TIME-AREA CONCENTRATION CURVE, APPOMATTOX RIVER

quantity and in time on the east part and west part of the drainage area may be considerable as it was in this case. Much better results could be obtained by using separate unitgraphs at the same gaging point for the upper and the lower drainage areas.

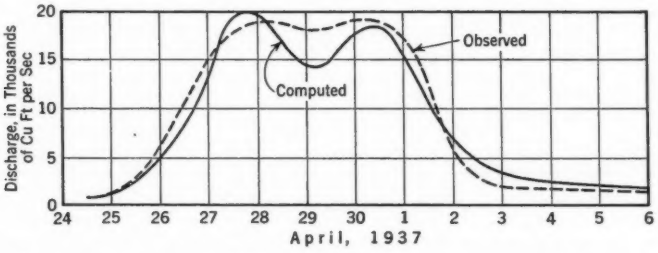

FIG. 9.—APPLICATION OF THE 12-HR UNITGRAPH, DERIVED FROM THE INSTANTANEOUS HYDROGRAPH, TO THE FLOOD OF APRIL, 1937

2. A more than usual degree of doubt as to the actual quantity of total precipitation is present in view of the small number of gaging stations (only one in the drainage basin), the nearest recording rainfall stations being some miles outside. The station in the center of the upper drainage area recorded 5.18 in.

of rain as compared with 2.58 in. recorded at Hopewell, Va., a station several miles east of Petersburg.

3. Observed discharges are from a single-stage discharge curve without slope correction. The gage is on a very flat stream and only 2.5 miles above a power dam. Although the gage is reported to be out of the backwater area in times of low water, the control for high water is thought to be the dam, in which case there is probably a large slope correction to discharges at this gage. If so, the observed stage hydrograph could not reflect the marked discharge decrease on April 29. At peak stage, 1 ft on the stage discharge curve is 3,000 cu ft per sec. This, and other features of the reported record, are sufficiently in doubt to cover the variation between observed and computed hydrographs.

4. On the other hand, the method may be no more accurate than is indicated by the agreement of the curves.

A comparison between the instantaneous unitgraph for the Appomattox River near Petersburg (drainage area, 1,335 sq miles; average slope of the river profile, 2.9 ft per mile; length above gage, 122 miles; and concentration time,

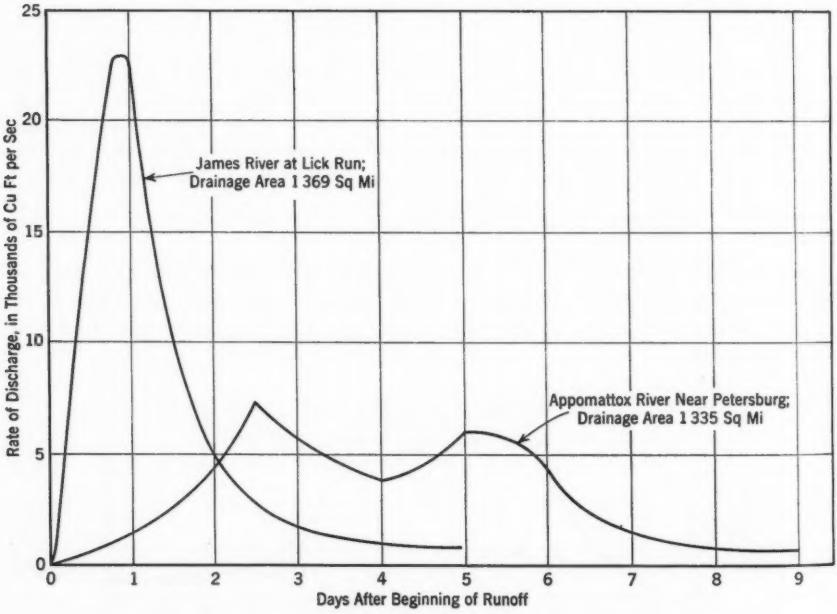

FIG. 10.—INSTANTANEOUS HYDROGRAPHS, APPOMATTOX RIVER NEAR PETERSBURG AND JAMES RIVER AT LICK RUN

144 hours) and for the James River at Lick Run (drainage area, 1,369 sq miles; average slope 17.3 ft per mile; length, 78 miles; and concentration time, 28 hours) is shown in Fig. 10. Fig. 11(*a*) shows a similar comparison between the instantaneous hydrographs of the Smith River at Bassetts, Va. (drainage area, 265 sq miles; average slope, 16.6 ft per mile; length, 37 miles; and concentration

time, 7 hours) and for the Meherrin River at Emporia, Va. (drainage area, 750 sq miles; average slope, 2.4 ft per mile; length, 86 miles; and concentration time, 78 hours). Fig. 11(*b*) shows a comparison of observed and computed flood hydrographs at Bassetts for the flood of August 18, 1939, and a similar comparison at Emporia for the flood of March 6, 1932.

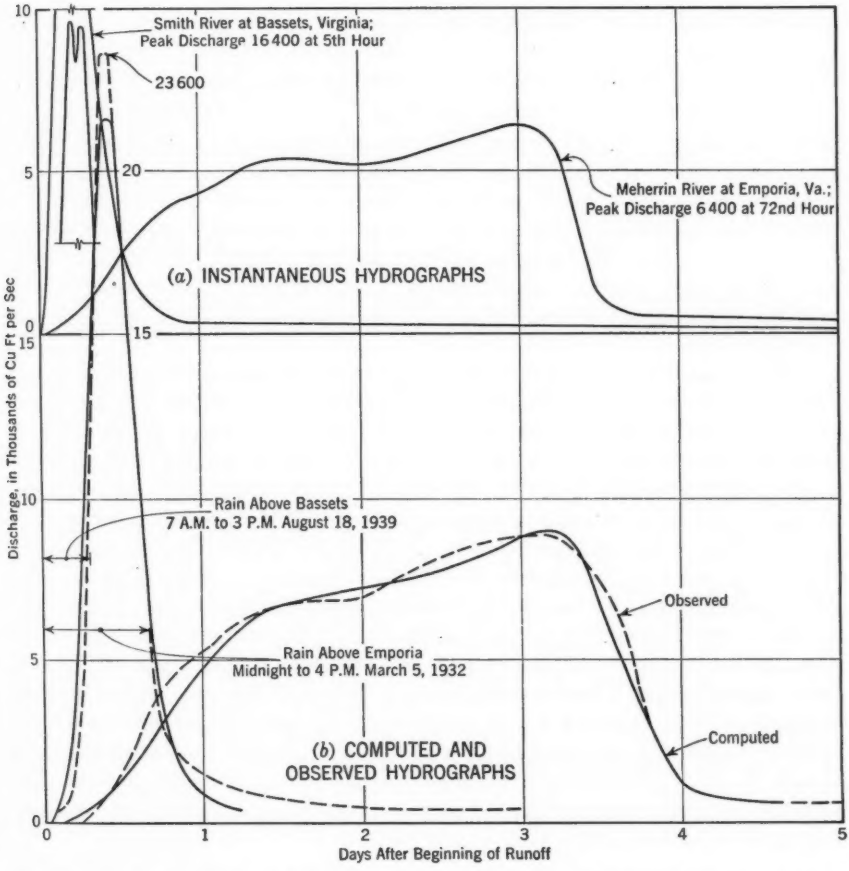

FIG. 11.—HYDROGRAPHS FOR THE SMITH RIVER AT BASSETTS AND THE MEHERRIN RIVER AT EMPORIA

DETERMINATION OF THE INSTANTANEOUS HYDROGRAPH FOR STREAMS WITHOUT FLOW RECORDS

The determination of any kind of unit hydrograph for a stream without records is a hazardous task. In most cases, it will be possible to install river stage recorders temporarily, obtain a record of rise and fall, compute a rating curve, and determine the elements of time of concentration, K and x, with a fair degree of accuracy. Since the record is utilized chiefly to determine the time of concentration, the proposed derivation of a unit hydrograph from a

record of a small flood is not subject to the errors incurred by use of similar records in unit hydrograph derivations as originally proposed by Mr. Sherman. However, it is necessary occasionally to approximate the flow characteristics of a stream without records. For such attempts, a correlation of time of concentration or storage capacity with river slope would be adequate.

Attempting to correlate the storage per mile of river expressed as hours per mile (the reciprocal of velocity) with average slope of the stream above the gage, the writer found, as would be expected, that this item increased with the decrease of slope. The average storage in hours per mile was found to be numerically equal to the reciprocal of the square root of the slope in feet per mile from source to gage, when the slope is taken as that of a straight-line profile with the same area below it as the actual profile. For some streams the variation from the average value was large—sometimes as much as 100%. The storage was larger for streams in alluvial beds than for those in rock gorges, although the range in slope for which studies were made overlapped. The average storage above two or more gages on the same stream, although varying with the slope, was more nearly constant than indicated by the aforementioned average criterion.

How much of the variation in storage is to be attributed to the natural causes and how much to limits of data cannot be ascertained. Most of the stream profiles were determined from U. S. Geological Survey sheets of 100-ft contour interval, although some of the flatter streams crossed only two such contours in their entire length. For steeper streams, crossing enough contours to reduce the possible error in slope determination, the time of concentration became so small that the possible error of 6 hours in time of precipitation was a large percentage of the total time. Perhaps someone working in an area for which good maps were available and which contain recording rainfall gages may be able to find a more precise relationship. Also, the writer was unable to find a usable definition of average river slope that could evaluate the influence of local concentration of extreme slope as a truly small influence on flow-time of the entire stream, compared with well distributed fall of the same amount.

The amount of the storage by which the time-area concentration curve should be modified will approximate 10% to 25% of the time of concentration, with the smaller values being used with the longer times of concentration and extremely narrow drainage areas.

Unit Hydrographs for Large Drainage Areas

By definition the application of the unit hydrograph is limited to areas over which the amount of runoff originating in any unit period may be considered as uniform within the required accuracy of the solution. For the flashy streams of the South Atlantic Coast, this is a drastic limitation, because they drain areas whose principal dimension is west to east, whereas the usual rainfall isohyets run north to south, and complete coverage of a major drainage basin by any storm is the exception rather than the rule. Because the streams are flashy, 6-hr unit periods are too long for component drainage areas, but the

shortest practical period for entire principal river systems. Under such conditions, the difference between the theory and fact of uniform origin of runoff may be large even for drainage areas of 500 sq miles or less.

For these streams, the storage-discharge relationship in all reaches of many of the rivers may be approximated closely by a straight line throughout the range of flood discharge. This being the case, the Muskingum method of flood routing is applicable to the translation and storage modification of flood waves. Where the Muskingum method is applicable, the unit hydrograph theory may be used, by deriving the unit hydrograph for the component drain-

TABLE 2.—UNIT HYDROGRAPH OF JAMES RIVER AT RICHMOND IN 1,000 CU FT PER SEC PER 1-IN. UNIFORM RUNOFF IN 6 HOURS

Time, in days[a]	James River at Lick Run, Va.	Craig Creek at Parr, Va.	Catawba Creek at Fincastle, Va.	Local at Buchanan, Va.	North River at Buena Vista, Va.	Local at Holcombs Rock, Va.	Local at Bent Creek, Va.	Buffalo River at mouth	Rockfish River at mouth	Local at Scottsville, Va.	Hardware River at mouth	Slate River near Arvonia, Va.	Rivanna River at Palmyra, Va.	Willis River at Flanagan Mills, Va.	Local at Cartersville, Va.	Local at Richmond, Va.	James River at Richmond, Va.	Time, in days[a]
Area[b]	1,369	331	104	280	660	506	421	417	245	238	135	235	675	247	379	515	6,757	Area[b]
.25	0	0	0	0	0	0	0	0	0	0	0	0	0	0	0	0.82	0.82	0.25
.50	0	0	0	0	0	0	0	0	0	0	0	0	0	0	0	5.94	5.94	0.50
.75	0	0	0	0	0	0	0	0	0	0	0	0	0	0	3.65	13.12	16.77	0.75
1.00	0	0	0	0	0	0	0	0	0	2.24	0	0	0	0	8.92	11.06	22.22	1.00
1.25	0	0	0	0	0	0	0	0	0	4.42	0	0	0	0	8.12	5.43	17.97	1.25
1.50	0	0	0	0	0	0	4.73	3.30	0	4.57	0.39	0.44	0	0.34	5.62	2.50	21.89	1.50
1.75	0	0	0	0	0	0.89	7.16	6.54	2.01	3.88	1.59	1.78	2.58	0.73	3.53	1.23	31.92	1.75
2.00	0	0	0	1.75	0	4.56	7.30	7.24	3.58	2.94	2.34	3.34	8.26	1.17	2.18	0.72	45.38	2.00
2.25	0	0	0.37	3.47	3.55	6.96	6.22	6.53	3.91	2.07	2.21	3.89	10.38	1.55	1.36	0.51	52.98	2.25
2.50	1.58	0	1.18	4.14	7.19	7.48	4.78	5.18	3.46	1.41	1.70	3.36	9.74	1.61	0.90	0.44	54.15	2.50
2.75	6.89	1.97	1.63	3.95	9.03	6.75	3.45	3.82	2.72	0.96	1.21	2.51	8.00	1.63	0.61	0.38	55.51	2.75
3.00	11.83	3.56	1.68	3.30	8.87	5.44	2.40	2.70	1.98	0.68	0.81	1.74	6.07	1.88	0.46	0.37	53.77	3.00
3.25	14.64	4.37	1.49	2.56	7.86	4.12	1.64	1.88	1.41	0.49	0.53	1.15	4.40	2.14	0.38	0.35	49.41	3.25
3.50	15.29	4.37	1.19	1.89	6.44	3.02	1.13	1.30	0.98	0.37	0.36	0.77	3.11	2.22	0.33	0.35	43.12	3.50
3.75	14.25	3.87	0.90	1.37	4.97	2.18	0.81	0.93	0.67	0.29	0.25	0.43	2.21	2.06	0.30	0.33	35.82	3.75
4.00	12.39	3.13	0.64	0.97	3.71	1.55	0.60	0.69	0.47	0.25	0.18	0.32	1.60	1.69	0.28	0.32	28.79	4.00
4.25	10.24	2.39	0.56	0.69	2.69	1.12	0.44	0.53	0.35	0.21	0.14	0.26	1.18	1.25	0.27	0.31	22.63	4.25
4.50	8.19	1.78	0.38	0.51	1.98	0.84	0.37	0.44	0.28	0.19	0.12	0.21	0.90	0.88	0.26	0.30	17.63	4.50
4.75	6.30	1.32	0.26	0.38	1.45	0.65	0.33	0.37	0.24	0.17	0.10	0.19	0.71	0.62	0.24	0.29	13.62	4.75
5.00	5.00	0.99	0.20	0.31	1.12	0.52	0.30	0.33	0.22	0.16	0.09	0.17	0.59	0.45	0.24	0.29	10.98	5.00
5.25	3.96	0.75	0.16	0.27	0.90	0.45	0.27	0.31	0.20	0.15	0.09	0.16	0.52	0.34	0.23	0.28	9.04	5.25
5.50	3.09	0.57	0.12	0.25	0.75	0.40	0.27	0.29	0.18	0.14	0.09	0.16	0.47	0.26	0.22	0.27	7.53	5.50
5.75	2.40	0.48	0.08	0.22	0.66	0.38	0.26	0.28	0.17	0.14	0.09	0.16	0.44	0.22	0.21	0.26	6.45	5.75
6.00[c]	1.88	0.41	0.06	0.21	0.59	0.35	0.25	0.26	0.15	0.14	0.09	0.16	0.42	0.19	0.21	0.25	5.62	6.00[c]

[a] After beginning of runoff. [b] Drainage area above station in square miles. [c] Values beyond 6 days omitted.

age areas of such size as to approximate the uniformity criterion and by routing the unit hydrographs themselves to the point for which a composite unit hydrograph is desired. The use of the proper amount and distribution of runoff with each routed component unitgraph will reproduce the component of runoff from the drainage area in question, and the sum of all components will be the desired composite flood wave. The degree of accuracy will be the same as though flood hydrographs had been computed for all tributary gages and then routed to the point for which the hydrograph is desired. In flood control work, the advantage of being able to identify individual components of a hydrograph is obvious.

For forecast work, it is desirable not only to have a complete breakdown of the drainage area into small parts but also to have a table of summations of these component unit hydrographs in various applicable combinations. If, for any particular storm pattern, practical uniformity of runoff origin over several component drainage areas exists, considerable time may be saved by using the combination graphs rather than the separate components.

Table 2 is a typical arrangement of component unit hydrographs prepared for the James River at Richmond, Va. Illustrating the nonuniformity of occurrence of runoff typical of South Atlantic rivers, the largest known flood (May, 1771) at this city is reported to have occurred without sufficient rain in the city to settle the dust.

Determination of Approximate Routing Constants

There are several ways of determining the storage constants for use in the routing of the unitgraph components. If the inflow between the tributary gage and the outflow is small or if it can be determined with enough accuracy to give proper weight to its influence, the amount of storage effective between the tributary gage and the desired outflow point can be determined from the relationships of Eqs. 9 to 12; or, where the hydrographs are of similar shape,

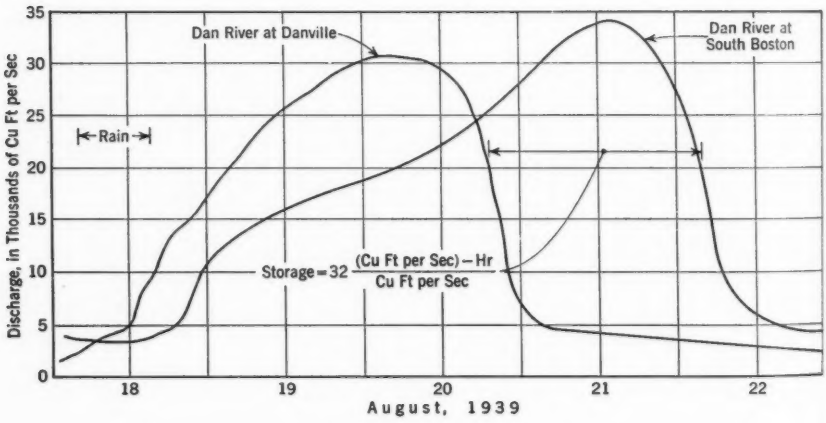

Fig. 12.—Approximate Determination of Storage from Hydrographs

as is frequently the case, by measuring the displacement between the falling leg of the inflow and outflow hydrographs. Thus, in Fig. 12, the storage effect between Danville, Va., and South Boston, Va., on the Dan River, is 32 hours. Although there are 680 sq miles of intervening drainage area, the discharge from that area had decreased to insignificant proportions prior to the time which is used as a criterion.

The most accurate method of determining the storage-discharge relation is still from the accumulated differential between inflow and outflow, as outlined by Mr. McCarthy.[9]

Summary

The paper has attempted to show that:

1. The constant time elements essential to the theory of the unit hydrograph, and common in many streams, are attributable to fundamental characteristics of the watersheds which maintain the storage capacities of the stream channels in constant direct proportion to the flows in them.

2. Such a relationship between storage capacity and discharge capacity produces certain characteristics in the rates of rise and fall of the hydrograph which are calculable by a simple established method.

3. These characteristics can be incorporated in a unit hydrograph, without the necessity of making or utilizing any quantitative determination of runoff distribution, in a few steps defined as follows:

(*a*) From a record of flood discharge, determine the time at which the rate of discharge decrease is greatest in relation to the prevailing discharge;
(*b*) The time elapsed between the end of runoff-producing rainfall and the time so determined is the base length (time) of a time-area concentration curve derived by dividing the watershed a long its water courses;
(*c*) The time-area concentration curve is routed as if through a reservoir with storage equal to K times the outflow when K is the time indicated by Eq. 12*b* at the time determined as in step (*a*) when $x = 0.0$;
(*d*) The result expressed in cubic feet per second per inch of runoff depth on the watershed at unit intervals of time is the instantaneous hydrograph; and
(*e*) The instantaneous hydrograph is converted to a unit hydrograph for any desired period of time by subdividing the instantaneous graph into periods of the desired unit length and averaging the ordinates over the preceding periods of time. Thus, in a 6-hr unit hydrograph, the rates of discharge at the end of 6, 12, and 18 hours, respectively, are the average ordinates to the instantaneous hydrograph in the 6-hr periods preceding the sixth, twelfth, and eighteenth hours.

4. A similar procedure may be applied to the determination of a unit hydrograph of subsurface flow, and the two unitgraphs may be combined in the average proportion applicable to the watershed, or used separately if desired.

5. The derivation of the unit hydrograph in this manner has some advantages:

(*a*) The procedure is definable so that all hydrographs derived by different individuals will be identical;
(*b*) The determination is independent of any knowledge of runoff distribution, except the time of ending, and therefore not subject to the errors due to indeterminability of runoff distribution which are factors in other methods known to the author;
(*c*) The influences of shape of drainage area and the capacity to produce large peak flows from concentrated runoff—both factors which are obscured by protracted runoff in other methods of derivation—are well indicated. The method also can be used to indicate the change in hydrograph form which is likely if a natural reach of river is replaced by a reservoir pool; and
(*d*) The unit hydrograph quantities are instantaneous rates of discharge at the time specified, not average values during the preceding unit period as in Mr. Sherman's original method, and the resulting hydro-

graph is properly drawn through all computed points, rather than as a bar diagram, and peaking of the hydrograph is no longer a matter of personal judgment. Hydrographs computed from the same distribution of runoff with 6-hr unitgraphs will agree with those by 1-hr graphs.

6. The derivation of the unit hydrograph in this manner has some disadvantages:

(*a*) Hydrographs are likely to fall a little too low on the receding leg between the point of maximum recession rate and the point where subsurface flow becomes predominant;

(*b*) When applied to too large drainage areas, the hydrograph may have too slow a rise and too rapid a fall, as a result of using the same storage factor for near and remote elements. This fault is corrected easily by subdividing the drainage area and computing separate unitgraphs for the components and combining them in the manner indicated in Table 2;

(*c*) Although this method reflects influence of shape of drainage area and capacity to produce high peaks well—better than any other one known to the author—it is possible that such influences are exaggerated slightly.

AMERICAN SOCIETY OF CIVIL ENGINEERS

Founded November 5, 1852

PAPERS

RIGIDITY AND AERODYNAMIC STABILITY OF SUSPENSION BRIDGES

By D. B. Steinman,[1] M. Am. Soc. C. E.

Synopsis

Coefficients of rigidity, natural oscillation periods, excitation and amplification of vertical and torsional oscillations, aerodynamic forces and moments, lift and torque graphs, velocity relations, energy relations, positive and negative damping effects, critical wind velocities, rates of amplification, limiting amplitudes, effects of phase difference, and methods of predicting, testing, checking, and preventing aerodynamic instability—all of these factors are treated herein, as they affect the design of suspension bridges against aerodynamic effects.

New basic formulas for computing the various modes of oscillation are presented, which are believed to be simpler and more complete, at the same time being of equal or greater accuracy, than those hitherto available to the profession.

The physical relations affecting analysis and design are expressed in working formulas of a form convenient for direct application by bridge engineers. New graphic solutions that broaden scope and clarify conception supplement the analysis. The formulas derived from fundamental theory and those deduced empirically from available data are illustrated and checked by numerical examples applied to known structures.

Introduction

Investigation and analysis have been concentrated in the recent past on the related problems of the rigidity and aerodynamic stability of suspension bridges.

The analysis presented herein has been found useful in explaining past experiences and in predicting new results. By such verification, the mathematical and physical relations developed and coordinated appear to have high

Note.—Written comments are invited for immediate publication; to insure publication the last discussion should be submitted by **April 1, 1944.**

[1] Cons. Engr. (Robinson & Steinman), New York, N. Y.

consistency and validity—both as a diagnosis and as a guide for correction and prevention. At the same time the writer recognizes the gaps that still remain to be filled by further experimental investigation and the empirical deductions that need to be made more accurate.

Notation.—The letter symbols used in this paper follow customary notation as far as practicable, and are assembled in the Appendix for convenience of reference.

PART 1.—OSCILLATIONS OF SUSPENSION BRIDGES AND MEASURE OF RIGIDITY

The Spring Constant (K).—The "spring constant" K of any span is a measure of the elastic resistance of the structure to deformations or oscillations. It is used in the formula for natural period P or frequency of oscillations N:

$$P = \frac{1}{N} = 2\pi\sqrt{\frac{m}{K}} \quad \ldots\ldots\ldots\ldots\ldots\ldots\ldots\ldots (1)$$

in which K is defined as the mean effective ratio of the distributed force of restitution or "loading increment" Δw to displacement η, m = mass of the span per unit length, and N = natural frequency of vertical oscillations. The equation of kinetic and potential energy in a simple harmonic cycle yields the general formula

$$K = \frac{\int_0^l \eta\, \Delta w\, dx}{\int_0^l \eta^2\, dx} \quad \ldots\ldots\ldots\ldots\ldots\ldots\ldots\ldots (2)$$

in which x = abscissa of any point of the span, measured from one end.

Application to Suspension Bridges.—For a suspension span, by simply substituting the fundamental equilibrium equation

$$\Delta w = -\frac{d^2}{dx^2}(H\eta + y\,\Delta H) + \frac{d^2}{dx^2}\left(E\,I\,\frac{d^2\eta}{dx^2}\right) \quad \ldots\ldots\ldots\ldots (3)$$

in Eq. 2, the general formula—

$$K = \frac{-\int_0^l \eta\,\frac{d^2}{dx^2}(H\eta + y\,\Delta H)\,dx + \int_0^l \eta\,\frac{d^2}{dx^2}\left(E\,I\,\frac{d^2\eta}{dx^2}\right)dx}{\int_0^l \eta^2\,dx} \quad \ldots\ldots (4)$$

—is obtained. In Eqs. 3 and 4: H = horizontal component of tension in one cable; E = modulus of elasticity of the stiffening girders; I = moment of inertia of the section of one stiffening girder; and y = coordinate of any point of the cable, measured from the cable chord. This yields K per cable.

The Sine Wave Curve.—In any span l vibrating in n equal segments, if the displacements follow a sine curve,

$$\eta = a_m \sin\frac{\pi n}{l}x \times \sin 2\pi N t \quad \ldots\ldots\ldots\ldots\ldots\ldots (5)$$

in which a_m is the vertical amplitude at the middle of a segment. In this case the elastic increments of loading Δw and their resulting bending moments M are proportional to the displacements η, and follow proportionate sine curves with the same nodes, period, and phase.

For any case in which $\Delta H = 0$, Eq. 3 then yields

$$K = \frac{\Delta w}{\eta} = \frac{\pi^2 n^2}{l^2} H + \frac{\pi^4 n^4}{l^4} E I \ldots\ldots\ldots\ldots\ldots\ldots (6)$$

For an unstiffened suspension bridge, the H-term alone remains. For an unsuspended span, or for a self-anchored suspension span, the EI-term alone remains.

If n is a multiple of 4, also for other even values of n if the midpoint of the cable is free to move horizontally, Eq. 6 is complete, since the condition of inextensibility of the cable ($\Delta l_c = 0$) then is satisfied without involving the adjoining spans and without requiring elastic stretch of the cable.

Other Deflection Curves.—Corresponding expressions for K for other assumed curves of displacement η may be written directly from Eq. 4.

For displacements following, in each segment, the elastic curve of a uniformly loaded beam of constant cross section,

$$K = \frac{306}{31} \frac{n^2}{l^2} H + \frac{3{,}024}{31} \frac{n^4}{l^4} E I \ldots\ldots\ldots\ldots\ldots\ldots (7)$$

which is almost identical numerically with Eq. 6.

For displacements following parabolic curves between nodes,

$$K = 10 \frac{n^2}{l^2} H + 96 \frac{n^4}{l^4} E I \ldots\ldots\ldots\ldots\ldots\ldots (8)$$

in which I is the mean effective value of the variable moment of inertia. This value of K varies less than 1.6% from the value by Eq. 6.

K for Odd Number of Segments.—If $n > 1$ is odd, the governing requirement $\Delta l_c = 0$ may be satisfied, without involving the adjoining spans, by superimposing a single-segment oscillation of relative amplitude $\frac{1}{n}$, yielding

$$\eta = a_m \sin \frac{\pi n x}{l} - \frac{a_m}{n} \sin \frac{\pi x}{l} \ldots\ldots\ldots\ldots\ldots\ldots (9)$$

Substituting in Eq. 4,

$$K = \frac{\pi^2}{l^2} \left(\frac{n^4 + 1}{n^2 + 1} \right) H + \frac{\pi^4}{l^4} \left(\frac{n^6 + 1}{n^2 + 1} \right) E I \ldots\ldots\ldots (10a)$$

(Compare Eqs. 9 and 10*a* with the solution offered by H. M. Westergaard,[2] M. Am. Soc. C. E.)

Eq. 10*a* may be generalized for any case of superimposed undulations of different values of n (including even values of n). If the same relation is maintained—namely, that the respective amplitudes of the component har-

[2] "On the Method of Complementary Energy," by H. M. Westergaard, *Transactions*, Am. Soc. C. E., Vol. 107 (1942), pp. 786–793.

monics are proportional to their values of n—the generalized form reduces to

$$K = \frac{\pi^2}{l^2}\frac{\Sigma n^4}{\Sigma n^2} H + \frac{\pi^4}{l^4}\frac{\Sigma n^6}{\Sigma n^2} E I \quad \ldots\ldots\ldots\ldots\ldots\ldots (10b)$$

The resulting value of Δl_c or Δl will be the algebraic sum of the component values.

Three Spans Coupled.—The main and side spans may oscillate in unison, with a single segment or any odd number of segments (n and n_1, respectively) in each span. If the bridge is symmetrical, the relative amplitudes are determined by balancing $\Delta l/2$ with Δl_1 at each tower top. If K_0 and K_1 are the values by Eq. 6 for the respective spans, the energy equation yields, for the three spans coupled:

$$K = \frac{K_0 + q\,K_1}{1 + q} \quad \ldots\ldots\ldots\ldots\ldots\ldots\ldots\ldots (11a)$$

or

$$K = \frac{\pi^2\left[\frac{n^2}{l^2} + q\frac{(n_1)^2}{(l_1)^2}\right] H + \pi^4\left[\frac{n^4}{l^4} + q\frac{(n_1)^4}{(l_1)^4}\right] E I}{1 + q} \quad \ldots\ldots\ldots (11b)$$

in which the coupling factor q is given by

$$q = \frac{(n_1)^2\, l}{2\, n^2\, l_1}\sec^4\gamma_1 \quad \ldots\ldots\ldots\ldots\ldots\ldots\ldots (11c)$$

in which γ_1 is the slope of the cable chord in the side span. Eqs. 11 also may be written by extending the integrations in Eqs. 2 and 4 over all three spans. If $l_1/n_1 = l/n$, the main and side spans are in resonance and $K = K_0 = K_1$.

If $n = 2, 6, 10, \cdots$, $\Sigma\Delta(l/n)$ is zero for the full span but is not zero for the half span. If the midpoint of the cable is not free to take the longitudinal motion $\Delta(l/2)$, as when effectively anchored by center stays, the lengthening and shortening of the respective half spans will tend to be taken up by side-span participation to produce $\Delta l_1 = \Delta(l/2)$ at each tower top. Eqs. 11*a* and 11*b* then will apply, with

$$q = \frac{2\,(n_1)^2\, l}{n^2\, l_1} \quad \ldots\ldots\ldots\ldots\ldots\ldots\ldots\ldots (12)$$

Oscillations with Longitudinal Motion of Span.—If $n = 2, 6, 10, \cdots$, without participation of the side spans, the longitudinal motion $\Delta(l/2)$ of the midpoint of the cable (Fig. 1) may be imparted to the suspended span through any physical coupling at midspan, as when center stays are provided. The energy equation then yields

$$K = \frac{K_0}{1 + 2\left(\frac{16}{3}\frac{f}{n\,l}\right)^2} \quad \ldots\ldots\ldots\ldots\ldots\ldots (13)$$

in which f = the vertical sag of the cable. If the two side spans oscillate in opposite phase, with the main span free of vertical oscillation, the parallel and synchronous movement Δl_1 of the two tower tops produces longitudinal

motion of the main span equal to Δl_1. For this case the energy equation yields

$$K = \frac{K_1}{1 + \frac{l}{l_1}\left(\frac{16}{3\,n_1}\frac{f_1}{l_1}\cos^2\gamma_1\right)^2} \quad \ldots\ldots\ldots\ldots\ldots\ldots (14)$$

Eqs. 13 and 14 express an apparent reduction in K as the equivalent of an increase in the effective value of the oscillating mass m in Eq. 1.

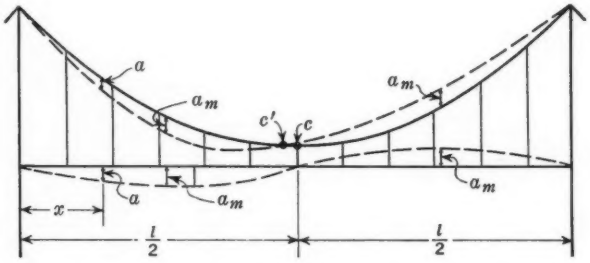

FIG. 1.—SPAN OSCILLATING IN TWO SEGMENTS ($n = 2$) SHOWING CENTER OF CABLE DISPLACED TOWARD THE DEPRESSED SEGMENT

Single Span with Straight Backstays.—For this case, for any odd number of segments including $n = 1$, the necessary increment Δl_c of the cable curve is provided by an increment of cable tension, ΔH, to produce an equal elastic elongation Δl_c of the cable between anchorages. Eq. 4 then yields:

$$K = \frac{\pi^2\,n^2}{l^2}\left[H + \frac{1}{n}\frac{E_c\,A_c}{1 + \frac{3\,l}{16\,f^2}(l + 2\,l_1\sec^2\gamma_1)}\right] + \frac{\pi^4\,n^4}{l^4}E\,I \quad \ldots\ldots (15)$$

in which E_c = modulus of elasticity of the cables and A_c = the section area of the cable.

Example 1: Numerical Application of Formulas for K.—In Table 1 the pertinent formulas for K are applied to the recorded modes of vertical oscillation of the bridge across Tacoma Narrows in the State of Washington (1940). Remarkably consistent agreement between the corresponding calculated and observed frequencies is indicated, within the range of variations of observed and assumed data.

(The accuracy of the foregoing formulas for the various modes of oscillation is attested by the exceptionally close agreement noted in Table 1. Compare the results with those from formulas by W. D. Rannie[3] and others. For this comparison, the same assumed value of $I = 1{,}000$ has been used.)

For the bridge engineer, it is useful to note that, for $n > 1$, the values of K and N are given with sufficient accuracy for all practical purposes by simply using Eq. 6 without further correction. In fact, for values of n from 2 to 8,

[3] "The Failure of the Tacoma Narrows Bridge," a report to the Hon. John M. Carmody, Administrator of the Federal Works Agency, Washington, D. C., March 28, 1941, by a board of engineers consisting of O. H. Ammann, Theodor von Kármán, and Glenn B. Woodruff, Appendix VI, p. 19.

inclusive, the values of K given by Eq. 6, without correction, appear to check the observed frequencies of oscillation even more closely than do the values of K calculated more scientifically (except when the effect of center stays in forcing side-span participation needs to be considered).

TABLE 1.—APPLICATION OF FORMULAS FOR K AND N TO THE OBSERVED MODES OF OSCILLATION OF THE TACOMA NARROWS BRIDGE

Mode Type	n	n_1	Equation No.	K_0	K_1	K	Frequency N per Minute	
							Calculated	Observed
1	1	1	11*a*	15	100	65	8.2	8
2	2	0	6	62	....	62	8.0	8.7
		1	12	62	100	83[a]	9.3	
4	0	1	14	....	100	94	9.8	....
5	3	1	11*a*	140	100	135	11.8	11.9
6	1, 3	0	10*a*	128	....	128	11.5	....
7	4	....	6	254	....	254	16.2	16.5
8	5	1	11*a*	408	100	392	20.1	20.8
9	6	1, 2	10*b*, 12	605	359	575	24.4	24.6
10	7	1	11*a*	853	100	832	29.3	....
		1, 2	10*b*, 11*a*	853	359	839	29.4	
11	8	....	6	1,159	....	1,159	34.6	34
12	9	3	11*a*	1,530	1,042	1,466	38.3	38

[a] Note effect of center stays, by forcing side-span participation, to raise K from 62 to 83 (if fully effective).

Use of K for Estimating Deflections.—The deflection at the quarter point of a span produced by applied load p covering that half span is given approximately by the formula

$$\eta \approx \frac{p}{K} \quad \ldots\ldots\ldots\ldots\ldots\ldots\ldots\ldots\ldots\ldots (16)$$

using K as given by Eq. 6 for $n = 2$. When the applied load p is large relative to the dead load, K needs to be recomputed for the increased H before use in Eq. 16.

As a rule, the greatest deflections of a suspension bridge occur under half-span loading, and the comparative rigidity of suspension bridges is gaged by such deflections. The value of K as defined, simply calculated and conveniently applied, may therefore, appropriately, be used as the "coefficient of rigidity" of a suspension span.

Example 2: Use of K for Estimating Deflections.—For the Tacoma main span, for $p = 100$ and $K = 62$, Eq. 16 yields a quarter-point deflection $\eta \approx 1.61$ ft, as compared with a computed value of 1.59 ft by the deflection theory. For $p = 750$, K is increased to 69, and Eq. 16 yields $\eta \approx 10.9$ ft (as against 10.9 ft by the deflection theory).

Values of K for Various Suspension Bridges.—Numerical values of the coefficient of rigidity K per cable (or per group of cables), calculated by Eq. 6 for $n = 2$, for various suspension bridges, are recorded in Table 2. For equal applied loads per square foot (live load or aerodynamic pressure), the significant value is K per foot of width (b), or $2\,K/b$. In Table 2, the values of K per foot range from 32.40 to 2.56. The physical meaning of $2\,K/b$ is the loading

increment or vertical pressure in pounds per square foot required to produce 1-ft deflection.

It is a significant fact that all of the plate-girder suspension bridges with K per foot less than 15, and all of the open-truss suspension bridges with K per ft less than 6, have been subject to undesirable or dangerous aerodynamic oscillations. (The George Washington Bridge is considered as belonging in neither category.) Both of these indicated critical values happen to coincide with the normal design values for suspension bridges with a vertical slenderness ratio (l/d) of 100 (see Fig. 2).[3a] For assured safety at high wind velocities, considerably higher values of K per foot are indicated (see Parts 2 and 3).

TABLE 2.—VALUES OF K FOR VARIOUS SUSPENSION BRIDGES
(K BY EQ. 6, FOR $n = 2$)

Date	Bridge	K per cable	K per foot	PERCENTAGE DUE TO:	
				Cable	Girder (R)
1903	Williamsburg	1,082	32.40	22	78
1939	Wabash River[a]	327	26.20	0	100
1931	Maumee River[a]	648	22.00	51	49
1926	Philadelphia	735	16.52	44	56
1931	Waldo-Hancock	212	15.14	56	44
1929	Grand Mère	188	14.48	34	66
1909	Manhattan	618	12.88	31	69
1930	Mid-Hudson	262	12.50	56	44
1929	Mount Hope	201	11.82	54	46
1936	Triborough	547	11.18	66	34
1936	Transbay	324	9.81	62	38
1931	St. Johns	252	9.70	65	35
1938	Thousand Islands[a]	141	9.25	74	26
1938	Thousand Islands[a]	127	8.30	78	22
1929	Detroit	212	7.13	71	29
1939	Deer Isle[a]	69	5.85	80	20
1938	Vancouver	112	5.62	67	33
1931	George Washington	244	4.60	100	0
1939	Bronx-Whitestone[a]	141	3.81	97	3
1940	Tacoma[a]	62	3.16	98.5	1.5
1937	Golden Gate	116	2.56	95	5

[a] Denotes construction with solid-web stiffening girders.

The last two columns in Table 2 record the percentage contributions of the cables and the stiffening girders, respectively, to the coefficient of rigidity K. The proportionate contribution of the stiffening girders or trusses, designated by the ratio R, ranges from 100% in a self-anchored suspension bridge and 78% in the Williamsburg Bridge to 1.5% in the Tacoma span and practically to zero in the George Washington Bridge. Girder or truss suspension bridges with values of R less than 0.25 are peculiarly sensitive to aerodynamic oscillations.

Approximate Formulas for K and N.—Using the cable term alone, the foregoing formulas yield the convenient approximate relations:

$$K \approx 1.234\, n^2 \frac{w}{f} \qquad (17a)$$

and

$$P = \frac{1}{N} \approx \frac{1}{n} \sqrt{f} \qquad (17b)$$

in which f is simply the sag of the cable. These simplified formulas may be used for estimating the coefficient of rigidity and the natural period or frequency of an unstiffened suspension bridge or of one with negligible stiffening system, for all values of $n > 1$.

[3a] Correction for *Transactions:* In Fig. 2, the sensitive area for truss bridges extends between ordinates 0 and 6.

Similarly, using the girder term alone:

$$K \approx 1.27\, n^4 \frac{w}{\eta_w} \quad \ldots\ldots\ldots\ldots\ldots\ldots\ldots\ldots\ldots\ldots (18a)$$

and

$$P = \frac{1}{N} \approx \frac{1}{n^2} \sqrt{\eta_w} \quad \ldots\ldots\ldots\ldots\ldots\ldots\ldots\ldots\ldots\ldots (18b)$$

in which η_w is the central deflection theoretically producible (with E constant) by the dead load w acting on the span as a simple beam. Eqs. 18 may be used for simple spans and for self-anchored suspension spans, for all values of n.

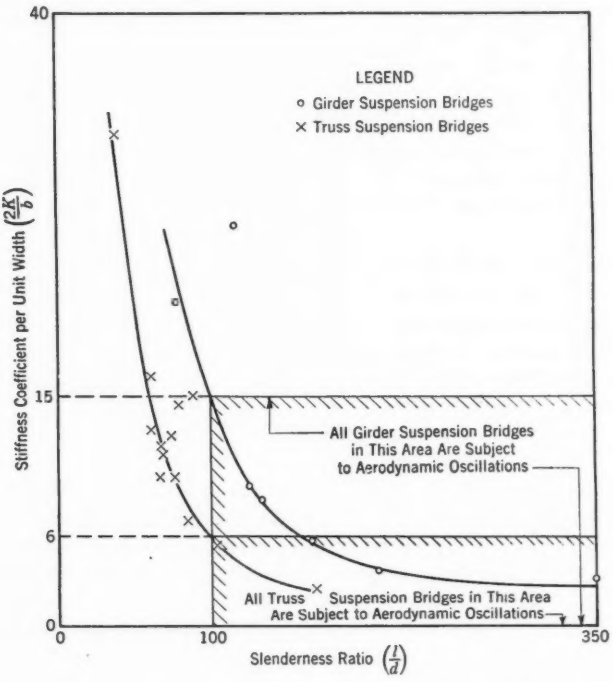

FIG. 2.—CORRELATION OF STIFFNESS COEFFICIENTS (2 K/b) WITH SLENDERNESS RATIOS (l/d) OF VARIOUS BRIDGES, SHOWING RANGE OF BRIDGES SUBJECT TO AERODYNAMIC OSCILLATIONS

For a stiffened suspension bridge (except the self-anchored type), the composite rigidity K is the sum of the respective contributions (Eqs. 17*a* and 18*a*) of cable and stiffening girder. Hence

$$\frac{1}{P} = N \approx \sqrt{\frac{n^2}{f} + \frac{n^4}{\eta_w}} \quad \ldots\ldots\ldots\ldots\ldots\ldots\ldots\ldots\ldots\ldots (19)$$

Example 2a: Calculation of Rigidities and Frequencies by Simple Approximate Formulas.—For the Tacoma main span, for $n = 2$, with $f = 232$ ft and

η_w = 61,400 ft:

By Eq. 17*b*, the natural frequency of cable = 7.9 cycles per min.
By Eq. 18*b*, the natural frequency of girder = 1.0 cycle per min.
By Eq. 19, the natural frequency of combination = 7.96 cycles per min.
Also, by Eqs. 17*a* and 18*a*, $K = 60.6 + 0.98 = 61.58$.

The foregoing results are almost identical with those given by Eqs. 1 and 6.

Fundamental Equations for Torsional Oscillations.—The general equation of torsional oscillations of a span is

$$\theta = \frac{2\,a_m}{b} \sin \frac{\pi\,n}{l}\,x \times \sin 2\,\pi\,N_t\,t \ldots\ldots\ldots\ldots\ldots\ldots (20)$$

in which θ is the instantaneous angular displacement of any section x at time t, N_t is frequency of torsional oscillations, and a_m is the maximum vertical displacement of cable or girder at the middle of each segment, since torsional oscillation may be treated simply as out-of-phase vertical oscillation of the two cables.

The values of K and N determined for vertical oscillations, multiplied by simple dimensional constants, yield with sufficient accuracy the corresponding values for torsional oscillations. The spring constant of the span in torsion, or the coefficient of torsional rigidity, will be

$$K_t = \frac{b^2}{2} K \ldots\ldots\ldots\ldots\ldots\ldots\ldots\ldots (21a)$$

and the natural frequency will be

$$N_t = \frac{b}{2\,r} N \ldots\ldots\ldots\ldots\ldots\ldots\ldots\ldots (21b)$$

in which r is the polar radius of gyration of the mass of the cross section of the span. It is important to note that, for torsional resistance of a suspension bridge, the polar moment of inertia ($r^2\,m$) pertains, not to a localized built-up cross section at the panel points, but to the average cross section throughout, including the long ranges between panel points. For the usual proportions, $b/(2\,r)$ = 1.3 to 1.5.

Example 3: Calculation of Natural Frequency of Torsional Oscillations.—For the Tacoma Narrows Bridge, for n = 2, Table 1 gives two values: N = 9.3 (per min) with center stays forcing side-span participation, and N = 8 (per min) without center stays. Applying Eq. 21*b* to these frequencies, and using an indicated effective value of $b/(2\,r)$ = 1.5, one obtains N_t = 14 and 12 (per min), respectively, which are identical with the two successive frequencies recorded at the time of the failure. The higher frequency was observed at the commencement of the torsional oscillations and corresponds to the functioning of the center stays to force side-span participation. Hold-down stays in the side spans prevented their normal participation beyond a limited amplitude. After failure of the center stays, the torsional oscillations, released from their initial coupling restraint, assumed the lower natural frequency of N_t = 12 cycles per min.

Use of K_t for Estimating Torsional Deflections.—When the applied torsional loading is relatively small, the angular deflection θ at the quarter point of a span, produced by applied uniform torsional loading T covering that half of the span, is given approximately by the formula

$$\theta \approx \frac{T}{K_t} \quad \ldots\ldots\ldots\ldots\ldots\ldots\ldots\ldots\ldots\ldots (22)$$

in which K_t is the coefficient of torsional rigidity of the span (calculated for $n = 2$).

Example 4: Use of K_t for Estimating Torsional Deflections.—For the Tacoma main span, for $T = 10{,}000$ ft-lb per lin ft and $K_t = 47{,}000$, Eq. 22 yields $\theta \approx 0.213$ radians, as compared with a computed value of $\theta = 0.209$ by the deflection theory.

PART 2.—AERODYNAMIC EXCITATION OF VERTICAL OSCILLATIONS

Initiation of Oscillations.—Small vertical oscillations of a span may be initiated by traffic, by wind gusts, or by the longitudinal component of the wind acting on the cambered span as an aerofoil. The importance of the last cause is confirmed by the fact that the recently built spans that have given trouble all had been provided with steep camber (for reasons of economy), and by the further fact that the oscillations usually have started with a quartering wind. The longitudinal component of the wind initiates the oscillations and the transverse component then rapidly amplifies them in a logarithmic ratio.

Effect of Vertical Oscillations Upon Aerodynamic Lift.—The instantaneous vertical velocity of any point in the span is

$$v = \frac{d\eta}{dt} = 2\,\pi\,N\,a\cos(2\,\pi\,N\,t) \quad \ldots\ldots\ldots\ldots\ldots\ldots (23a)$$

in which a, the local amplitude, is ordinarily defined by

$$a = a_m \sin\frac{\pi\,n}{l}\,x \quad \ldots\ldots\ldots\ldots\ldots\ldots\ldots\ldots (23b)$$

Composition of the wind velocity V and its relative vertical velocity, $-v$, yields a resultant change in effective angle of attack (α):

$$\Delta\alpha = -\frac{v}{V} \quad \ldots\ldots\ldots\ldots\ldots\ldots\ldots\ldots\ldots\ldots (23c)$$

Downward velocity of the section will thus produce or augment an upward angle of attack. In an "aerodynamically unstable section," such upward angle of attack tends to produce a downward resultant pressure, in the direction of the motion.

In the following basic analysis (Eqs. 24 to 36, inclusive), high relative wind velocity V is assumed; the effect of phase difference across the section is introduced subsequently.

The change $\Delta\alpha$ in the effective angle of attack will change the instantaneous lift force on a unit length of the span by an amount

$$\Delta L = -s'\left(\frac{\rho}{2}V^2 b\right)\Delta\alpha = -s'\frac{\rho}{2}v\,V\,b \quad \ldots\ldots\ldots\ldots (24)$$

in which ρ is the mass density of air and s' is the corrected slope of the lift graph:

$$s' = s + C_D \quad \ldots\ldots\ldots\ldots\ldots\ldots\ldots\ldots (25)$$

This correction is necessary because L, the vertical lift force, and D, the horizontal drag force, in the wind tunnel are measured perpendicular and parallel to the wind whereas ΔL in Eq. 24 is measured vertically. The correction represented by Eq. 25 may be made directly upon the lift graph (Fig. 3) by simply augmenting each ordinate (C_L) by the vertical component $C_D\,\alpha$.

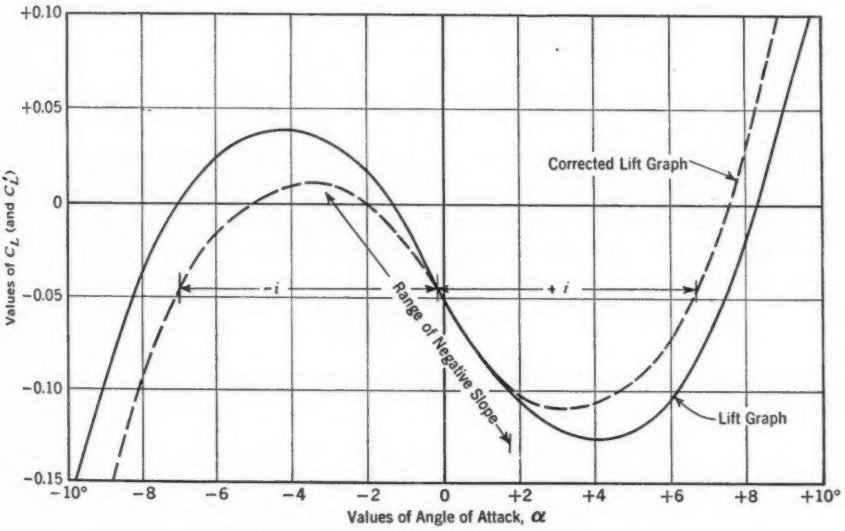

FIG. 3.—LIFT GRAPH (AND CORRECTED LIFT GRAPH)

If the slope s of the lift graph is negative and numerically exceeds the drag coefficient C_D, then s' will be negative and, by Eq. 24, ΔL will be positive when v is positive, and negative when v is negative. This will produce amplification of vertical oscillations. Such a condition constitutes aerodynamic vertical instability.

From the foregoing relations, the maximum value, in a cycle, of the amplifying force ΔL acting on a unit length of the span will be

$$\Delta L(\max) = -\pi\,s'\,N\,\rho\,b\,V\,a \quad \ldots\ldots\ldots\ldots\ldots\ldots (26)$$

Self-Excited Amplification of Vertical Oscillations.—Since the increment of lift ΔL is automatically resonant with the harmonic motion of the vertical

oscillations and, moreover, is 90° out of phase with that harmonic motion, it will produce an increment of energy in each cycle. This increment of energy, per unit length, will be

$$\Delta W = \pi \, \Delta L(\max) \, a = - \pi^2 \, s' \, \rho \, a^2 \, b \, N \, V \quad \ldots\ldots (27a)$$

and, over the span l,

$$\Delta W(\text{total}) = - \frac{\pi^2}{2} \, s' \, \rho \, (a_m)^2 \, b \, N \, V \, l \quad \ldots\ldots (27b)$$

The maximum kinetic (or potential) energy W in a cycle, per unit length, is

$$W = K \, a^2 \quad \ldots\ldots (28a)$$

Hence, over the entire span,

$$W(\text{total}) = \tfrac{1}{2} \, K \, l \, (a_m)^2 \quad \ldots\ldots (28b)$$

The relative increase per cycle in the amplitude, or the logarithmic increment per cycle, is denoted by δ:

$$\delta = \frac{\Delta a_m}{a_m} = \frac{\Delta a}{a} = \frac{\Delta W}{2 \, W} = - \frac{\pi^2}{2} \, s' \, \rho \, \frac{b}{K} \, N \, V \quad \ldots\ldots (29a)$$

If s' is negative, δ will be positive, representing a self-excited amplification of oscillations. By Eq. 29*a*, the amplification ratio δ increases with the width b, or inversely with the coefficient of rigidity per foot of width, $2 \, K/b$ (see Table 2 and Fig. 2). Substituting numerical values for ρ and g, Eq. 29*a* may be written:

$$\delta = - 0.0096 \, \frac{s' \, b \, V}{w \, N} \quad \ldots\ldots (29b)$$

The negative damping coefficient, or the logarithmic increment per second, is denoted by λ:

$$\lambda = (1 + \delta)^N - 1 \approx N \, \delta = - 0.0096 \, \frac{s' \, b \, V}{w} \quad \ldots\ldots (30)$$

Limiting Amplitude of Vertical Oscillations.—The amplitudes of self-excited vertical oscillations, under aerodynamic negative damping, are limited. As the amplitudes increase, they will cause the resultant values of α, by Eq. 23*c*, to extend more and more beyond the range of negative slope of the lift graph, until the positive contribution of ΔW from the range of negative slope is balanced by the tapering negative contributions of ΔW from the flanking ranges of positive slope.

To take into account the variation of slope s', Eq. 27*a* is replaced by the more general equation

$$\Delta W = \oint L' \, d\eta \quad \ldots\ldots (31a)$$

in which $\oint$ denotes integration over the cycle and in which $L' = L + D \, \alpha$, corresponding to the corrected lift graph. This expression for energy input may also be written

$$\Delta W = \oint \eta \, dL' \quad \ldots\ldots (31b)$$

The condition $\Delta W = 0$ will define a limiting local amplitude a_o; and the condition,

$$\int_0^l \Delta W \, dx = 0 \quad \ldots\ldots\ldots\ldots\ldots\ldots\ldots\ldots (32)$$

will define the limiting segment amplitude a_{om}.

If the lift graph is not readily expressible as a mathematical function, graphic or tabular methods are best adapted for the solution of Eqs. 31 and 32. A graphic solution of Eq. 31a is shown in Fig. 4. The variation of ΔW with

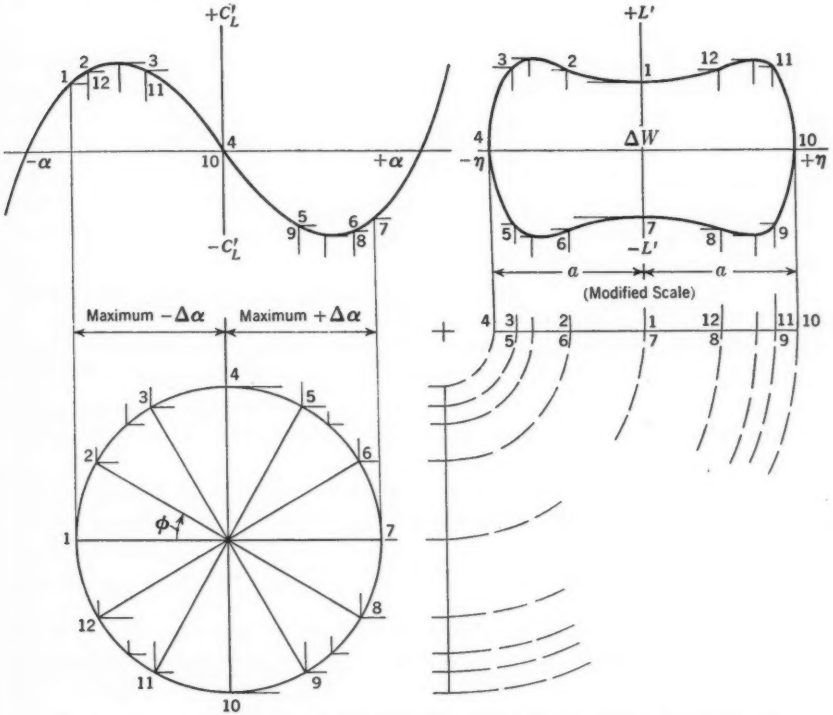

FIG. 4.—GRAPHIC DETERMINATION OF ENERGY INPUT (ΔW) FOR A GIVEN AMPLITUDE (a) OF VERTICAL OSCILLATIONS

amplitude a is first found by any of these methods, and is then plotted for the sine-curve amplitudes a over a span segment, using trial values of a_m at mid-segment, until the limiting value a_{om} satisfying Eq. 32 is found.

If the lift graph is of the typical form shown in Fig. 3, identified with aerodynamic instability, it may be represented by a cubic equation:

$$(C_L)' = s' \alpha \left(1 - \frac{\alpha^2}{i^2} \right) \quad \ldots\ldots\ldots\ldots\ldots\ldots (33)$$

in which $-i$, 0, and $+i$ are the intercepts on the horizontal axis. (The curve is assumed centered through the origin. This merely changes the

inclination datum from which α is measured, and otherwise does not affect the final results.) When used in Eqs. 31 and 32, this yields

$$a_o = \sqrt{\frac{4}{3}}\, i \left(\frac{V}{2\,\pi\,N} \right) \quad \ldots\ldots\ldots\ldots\ldots\ldots (34a)$$

and

$$a_{om} = \frac{4}{3}\, i \left(\frac{V}{2\,\pi\,N} \right) \quad \ldots\ldots\ldots\ldots\ldots\ldots (34b)$$

in which a_{om} is the limiting segment amplitude without structural damping.

Structural Damping.—Accurate information on the structural damping of suspension bridges is lacking. For oscillations of flexible suspension spans, the structural damping is represented by a varying logarithmic decrement δ_s of the indicated order of magnitude of 0.002 to 0.130. It is essentially a function of R (the proportion of K due to the stiffening girder), since the principal contribution is from the energy dissipated in deformations of the stiffening system whereas the gravitational resistance to deformation of cable curve (without increment of cable stress) contributes little to damping. Moreover, the energy in the structure (compare Eq. 28*b*) is proportional to $(a_m)^2$, whereas the energy loss due to structural hysteresis is proportional to a fractionally higher power of a_m—$(a_m)^{2.3}$ according to some recorded tests[4]; hence δ_s is a function of a fractional power of a_m (multiplied by $n^2\,d/l^2$ in order to translate a_m into a function of strain). If other losses by dissipation of energy are included, such as those caused by secondary vibrations, roadway deformations, atmospheric damping, joint and bearing frictions, and cable hysteresis, the expression for the structural damping decrement will include terms independent of R and a_m.

In the light of the limited data thus far available, the following semiempirical expression for the logarithmic decrement δ_s is indicated:

$$\delta_s = (0.001 + 0.06\,R) \left(1 + 1{,}700\,\frac{n}{l}\,\sqrt{a_m\,d} \right) \quad \ldots\ldots\ldots (35)$$

An indicated increase with increasing amplitudes is provided by the second factor in the formula. The coefficients and exponents in this formula are written to fit available data and are subject to future revision. A higher value of δ_s is indicated when trusses are used instead of girders.

The critical wind velocity at which aerodynamic amplification of vertical oscillations can commence, defined by the condition $\delta - \delta_s = 0$, will then be, by Eq. 29*b*,

$$V_c = -\,104\,\frac{w\,N}{b\,s'}\,\delta_s \quad \ldots\ldots\ldots\ldots\ldots\ldots (36a)$$

in which δ_s is calculated for zero amplitude. At any wind velocity lower than V_c, the aerodynamic negative damping factor is insufficient to overcome the structural damping. Eq. 36*a* may be written in the significant form,

$$V_c = -\,\frac{1 + 60\,R}{15\,s'}\,\sqrt{\frac{w}{b}}\,\sqrt{\frac{2\,K}{b}} \quad \ldots\ldots\ldots\ldots\ldots (36b)$$

[4] "Mechanical Vibrations," by J. P. Den Hartog, McGraw-Hill Book Co., Inc., New York, N. Y., 2d Ed., 1940, pp. 253–254.

in which $2\,K/b$ is the coefficient of rigidity per foot of width. Correcting for structural damping, the net energy input per cycle will be, by Eqs. 28*b* and 29*a*,

$$\Delta W = K\,l\,(\delta - \delta_s)\,(a_m)^2 \ldots\ldots\ldots\ldots\ldots\ldots (37)$$

Limiting Amplitude Corrected for Structural Damping.—At some limiting amplitude below a_{om}, the increasing value of δ_s will become equal to the diminishing value of δ, terminating further self-excited amplification. For the typical lift graph with reversals of slope (Eq. 33 and Fig. 3), the diminished δ will be

$$\delta = \delta_0 \left[\, 1 - \frac{(a_m)^2}{(a_{om})^2} \,\right] \ldots\ldots\ldots\ldots\ldots\ldots (38)$$

in which δ_0 is the value at zero amplitude (or maximum effective s'). The limiting amplitude corrected for structural damping then will be given by the relation:

$$a_r = a_{om} \sqrt{1 - \frac{\delta_s}{\delta_0}} \ldots\ldots\ldots\ldots\ldots\ldots (39)$$

in which a_r is the limiting vertical amplitude reduced by structural damping. This yields for the Tacoma span a maximum limiting amplitude of 1.5 ft (for any mode), which checks the recorded observations.

The Effect of Phase Difference on Vertical Oscillations.—The following relations, whereby aerodynamic instability at low wind velocities may be created by the phase difference across the width of the section, hitherto have been unsuspected and unexplored.

The aerodynamic disturbance traveling across the width of the vertically oscillating section, especially at low wind velocities, encounters a progressive phase difference, with both relative displacements and relative velocities of the different points along the width when referred to the respective instants of successive impingement. The total phase difference across the section, in cycles, is represented approximately by $N\,b/V$. To correct for the effect of this phase difference, a correction factor β needs to be inserted in the formulas based on the lift graph of a stationary model in order to obtain the relations for an oscillating section, similar to the corresponding correction factor subsequently used in the formulas for torsional oscillations in Part 3.

In the case of vertical oscillations, the indicated critical wind velocity due to phase difference is $V_p \approx 2\,N\,b$, corresponding to a total phase difference of one half of a cycle; and a corresponding indicated expression for the correction factor (assuming a single $-\beta$-range below V_p) is of the form,

$$\beta \approx \frac{V^2 - (V_p)^2}{V^2 + (V_p)^2 \left(0.2 + 0.45\,\dfrac{V_p}{V} \right)} \ldots\ldots\ldots\ldots\ldots\ldots (40)$$

asymptotic to unity at higher velocities. This yields $\beta = 0$ at $V = V_p$, and β negative in the low-velocity range from $V = 0$ to $V = V_p$. This negative value of β means a reversal of stability or instability in this range. If the section is aerodynamically stable as previously defined (s' positive), the application of the negative value of β in the formulas for ΔL, ΔW, and δ,

will reverse the stability and create a condition of aerodynamic instability in the low-velocity range. The wider the bridge, the greater will be the range of wind velocity to which the normally stable section will be aerodynamically sensitive.

Analytical Derivation of β for Vertical Oscillations.—The physical concept underlying the correction factor β may be visualized as an initiated pressure impulse traversing the width of the section in the time dimension (measured in cycles or fractions of a cycle). If $V \leqq 4\,N\,b$, the action extends through one fourth of a cycle or less, so that the traversing pressure impulse does not encounter any reversal of phase; hence β remains positive. If $V = 2\,N\,b$, the action extends through one half of a cycle, and therefore enters a reversal of phase (direction of motion) at the midpoint of this range and if the pressure impulse traverses the section with undiminished intensity, the integrated effect will be zero ($\beta = 0$ at $V_p = 2\,N\,b$). If $V = 4\,N\,b/3$, the action extends through three fourths of a cycle; the pressure impulse traverses the first third of the width in assumed phase with the direction of motion and the remaining two thirds with the motion in reversed or opposed phase, so that the integrated effect will be negative ($\beta = -$). This concept may be expressed mathematically in simple form:

$$\beta = \frac{\int_0^{\phi'} \cos\phi\, d\phi}{\int_0^{\phi'} d\phi} = \frac{\sin\phi'}{\phi'} \qquad (41)$$

in which the numerator represents the integration of the action traversing the oscillating section and the denominator represents the corresponding integration (over the same assumed transit time) across the stationary section. Here $\phi = 2\,\pi\,N\,t$ is the relative phase angle at any instant of the action, and ϕ' is the total effective phase difference across the width of the oscillating section. Assuming unmodified V and undiminished effectiveness of the traveling pressure impulse throughout the range,

$$\phi' = 2\,\pi\,\frac{N\,b}{V} \qquad (42)$$

Eq. 41 yields:

Velocity V	Correction factor β	Velocity V	Correction factor β
∞	$+1$	$\frac{4}{5}\,N\,b$	$+\frac{2}{5\,\pi}$
$4\,N\,b$	$+\frac{2}{\pi}$	$\frac{4}{6}\,N\,b$	0
$\frac{4}{2}\,N\,b$	0	$\frac{4}{7}\,N\,b$	$-\frac{2}{7\,\pi}$
$\frac{4}{3}\,N\,b$	$-\frac{2}{3\,\pi}$	$\frac{4}{8}\,N\,b$	0
$\frac{4}{4}\,N\,b$	0	...	...

thus making $V_p = 2\,N\,b$. In the low-velocity range below V_p, the resulting values of β (or $V\,\beta$) follow an oscillating curve converging toward the origin. This yields a series of critical ranges for vertical oscillations at low wind velocities. The Tacoma Narrows Bridge likewise showed a series of critical ranges for oscillations at low wind velocities (see Table 3). The actual correspondence (covering all of the observed modes) is too striking to be accidental. Table 3 is the distribution for an aerodynamically stable section—one for which

TABLE 3.—Comparison of Theoretical and Observed Ranges of Vertical Oscillations

Values of $V/(N\,b)$	First Critical Range	Intermediate Range	Second Critical Range	Intermediate Range	Third Critical Range	Intermediate Range	Fourth Critical Range
	$\beta = -$	$\beta = +$	$\beta = -$	$\beta = +$	$\beta = -$	$\beta = +$	$\beta = -$
By Eq. 41	2.00–1.00	....	0.67–0.50	....	0.40–0.33	....	0.29–0.25
Observed	2.35–0.93	....	0.89–0.53	....	0.43–0.37	....	0.30–0.26
Number of observations	79	0	56	0	4	0	3

s' is positive. The vertical oscillations are limited to the ranges in which β is negative. For an aerodynamically unstable section (s' negative), the distribution would have been reversed.

Eq. 41 may be improved toward perfect correspondence with the observed critical ranges by advancing the integration limits by the amount of the phase lag between any instant of incidence of wind pressure on the outside of the section and the actual traverse of the interior width by the consequent vertical pressure reaction. Assume that the mean path of the deflected air flow is lengthened from b to $d + b$, and that, in partial compensation, the linear velocity of the deflected air flow is speeded up in the proportion of b to $b + 0.4\,d$. For the Tacoma section, the following integration limits are thus obtained:

$$\beta = \frac{\int_{0.19\phi'}^{1.11\phi'} \cos\phi\, d\phi}{\int_{0.19\phi'}^{1.11\phi'} d\phi} = \frac{\sin 1.11\,\phi' - \sin 0.19\,\phi'}{0.92\,\phi'} \quad \ldots\ldots\ldots (43)$$

This yields, for the critical ranges, $V/(N\,b) = 2.60$–0.92, 0.87–0.52, 0.46–0.37, 0.31–0.29, etc., or a practically perfect correspondence with the ranges of the observed oscillations.

Eq. 43 also yields striking agreement with the preliminary empirical formula, Eq. 40, from $V = \infty$ to V at the middle of the first critical range (see Table 4). Below V_p, Eq. 40 approximately envelopes the oscillating graph representing the critical ranges.

By advancing the integration limits as in Eq. 43, the major critical ranges are widened, and tend to coalesce. Only the widths and ordinates above or below a secant line representing δ_s will be critical. The recorded observations of oscillations in the third and fourth critical ranges (and one in the fifth) show that, in the Tacoma span, the structural damping was almost negligible.

Conclusions Relative to Vertical Aerodynamic Oscillations.—The foregoing results confirm the significance and validity of the β-concept and its suggested

TABLE 4.—AGREEMENT BETWEEN VALUES OF β COMPUTED BY EQS. 40 AND 43

Equation No.	VALUES OF $V/(N\,b)$								
	∞	8	6	4	2.6	2	1.85	1.7	0
40	1	0.86	0.75	0.48	0	−0.31	−0.38	−0.43	0
43	1	0.86	0.75	0.48	0	−0.30	−0.38	−0.43	0

analytical evaluation. Moreover, there now appears to be a conclusive and completely consistent diagnosis of the action of the Tacoma span:

(*a*) For vertical oscillations, the section was aerodynamically stable. The span was therefore aerodynamically unstable at low wind velocities (below V_p) and stable at high wind velocities (above V_p).

(*b*) For torsional oscillations (as will be developed in Part 3) the entire picture was exactly reversed, since the torque graph, unlike the lift graph, had a range of negative slope.

The validity of the series of lift graphs obtained in the wind-tunnel tests at the California Institute of Technology at Pasadena also is confirmed. These point to a critical ratio of girder depth to section width for vertical oscillations: If $d/b > 1/4$, with solid girders, aerodynamically unstable sections are indicated, and such bridges (if K and R are inadequate) may be expected to show vertical aerodynamic instability in the high-velocity range (above V_p) and possibly, to a limited extent, in the low-velocity range (below V_p). If $d/b < 1/4$ (or a higher ratio with open trusses), the section is aerodynamically stable, and any self-amplified vertical oscillations will be limited to the low-velocity range. The Tacoma span belonged to the latter category.

Critical Velocities Calculated with β.—Eq. 29*b*, with β inserted, may be written

$$\delta = -0.025\,\beta\,s'\,\frac{b^2}{w}\,\frac{V}{V_p} \qquad (44a)$$

in which $V_p = 2.6\,N\,b$. All critical velocities, defined by $\delta - \delta_s = 0$, will then be given by

$$\frac{V_c}{V_p} = -40\,\frac{w}{b^2}\,\frac{\delta_s}{\beta\,s'} \qquad (44b)$$

From Eq. 40 or 43, a simplified expression for β may be written, sufficiently accurate in the useful range from $V/V_p = 0.8$ to 4:

$$\beta = 1.3\,\frac{V - V_p}{V} \qquad (45a)$$

(Compare Eq. 58*b* introduced subsequently.) Eq. 44*b* then yields

$$\frac{V_c}{V_p} = 1 - 31\,\frac{w}{b^2}\,\frac{\delta_s}{s'} \qquad (45b)$$

At very low wind velocities (up to $V/V_p = 0.2$), Eq. 40 yields, with sufficient accuracy,

$$\beta = -2\frac{V}{V_p} \qquad (46a)$$

Hence, by Eq. 44*b*,

$$\left(\frac{V_c}{V_p}\right)^2 = 20\,\frac{w}{b^2}\,\frac{\delta_s}{s'} \qquad (46b)$$

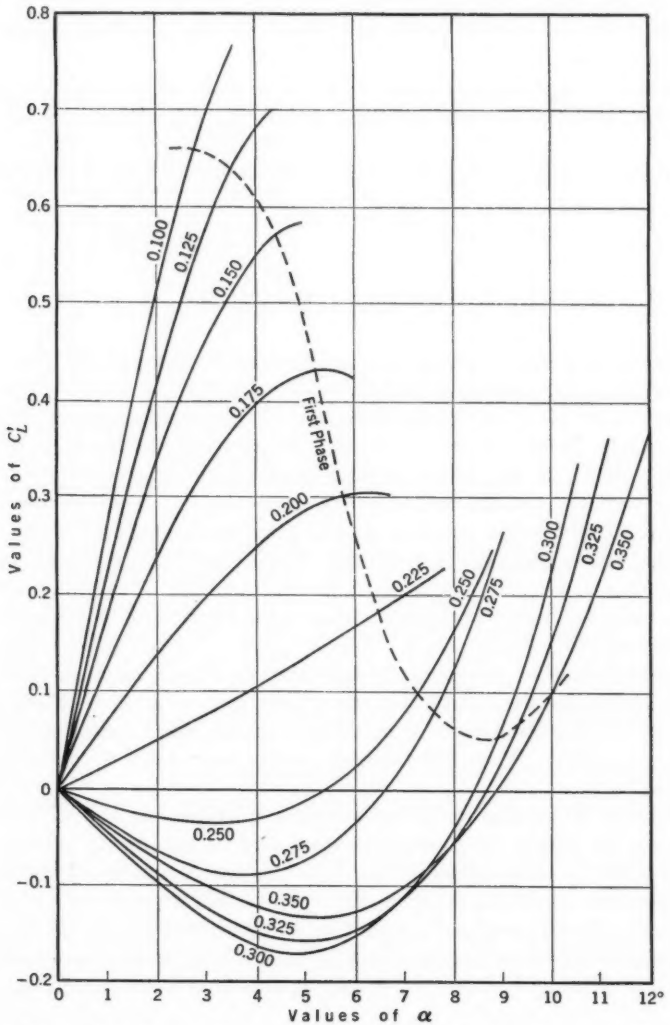

FIG. 5.—LIFT GRAPHS (CORRECTED FOR DRAG) FOR VARIOUS VALUES OF d/b

Example 5: Critical Velocities Calculated with β.—For the Tacoma Narrows Bridge (with $s' = +3.50$, $\delta_s = 0.002$, $b^2/w = 0.53$), Eq. 45*b* yields a maximum

critical velocity of $V_c = 2.51\,N\,b$, or 42 miles per hr for $n = 9$, as compared with 40 miles per hr reported, and Eq. 46*b* yields a minimum critical velocity of $V_c = 0.38\,N\,b$, or 1.3 miles per hr for $n = 1$ or 2, as compared with a minimum reported velocity of 1 mile per hr for observed oscillations.

For the Deer Isle Bridge (without stays), with $s' = -2.52$, $\delta_s = 0.013$, and $b^2/w = 0.46$, Eq. 45*b* yields a minimum critical velocity of $V_c = 3.50\,N\,b$, or 12.2 miles per hr for $n = 1$ or 2, which agrees with observations. For the Toledo Bridge, with $s' = +7.3$, $b^2/w = 0.535$, and $\delta_s = 0.030$, Eqs. 44 yield $\delta < \delta_s$ and $V_c > V$ for all values of V, representing aerodynamic stability at all wind velocities.

Method of Predicting Lift Graphs.—From a study of recorded lift graphs of bridge cross sections, the parameters s' and i (or s'/i^2) of these graphs may be written as functions of the ratio d/b of the H-section. Accordingly, referring to Eq. 33, a single formula is obtained for this entire family of lift graphs:

$$(C_L)' = \frac{28 - 118\frac{d}{b} + 0.024\frac{b}{d}}{1 + 21{,}500\left(\frac{d}{b}\right)^8 + 0.012\frac{b}{d}}\alpha - \frac{1{,}300 - 5{,}900\frac{d}{b}}{1 + 33{,}000\left(\frac{d}{b}\right)^8 + 0.005\frac{b}{d}}\alpha^3 \ldots (47)$$

This is plotted in Fig. 5, giving the lift graphs for values of d/b from 0.100 to 0.350. (The antisymmetrical half for $-\alpha$ is omitted.)

As the angle of attack increases from $\alpha = 0$, the aerodynamic action is in its first phase (bridge floor completely screened by the front girder) up to $\alpha = d/2\,b$, which is the angle of attack at which air-stream lines, if they continued straight, would first impinge upon the horizontal member of the H-section. Beyond this value of α, the lift graph changes in form, usually with a point of inflection. Eq. 47 and Fig. 5 give the lift graphs (corrected for drag) with sufficient accuracy up to $\alpha = 0.6\,d/b$. The range of Eq. 47 may be extended to cover higher values of α by including terms of higher power (α^5 and α^7).

It is significant to note that, as indicated in Fig. 5, all negative lifts and negative slopes are limited to the first phase, $\alpha < d/(2\,b)$. If the horizontal member of the H-section is not at midheight, the lift graphs will not be centered through the origin. More wind-tunnel results are needed to determine such variations.

All known lift graphs for girder suspension bridges fit Eq. 47 and Fig. 5. The known lift graphs for truss suspension bridges also fit Eq. 47 and Fig. 5, provided 0.50 *d* is used instead of *d*. This relation is significant and warrants further tests for confirmation or modification of this truss factor.

Following the same general procedure as illustrated by Eq. 47 and Fig. 5, torque graphs for all values of d/b may be similarly formulated and plotted for use in predicting, reducing, or avoiding torsional aerodynamic instability.

PART 3.—AERODYNAMIC EXCITATION OF TORSIONAL OSCILLATIONS

Self-Excited Amplification of Torsional Oscillations.—It is primarily and principally the frontal angle of attack at the leading edge that determines the deflection and disturbance of the air stream, including any eddies produced. The instantaneous vertical velocity v of the leading edge of the cross section (the front girder), combined with the horizontal velocity of the wind V, will change the effective frontal angle of attack by an amount $\Delta\alpha$, given by Eq. 23*c*. Downward velocity of the leading edge thus will produce or augment an upward angle of attack. On an aerodynamically unstable section, such upward angle of attack produces a torque in the direction of the motion. (As the angle of attack increases—due to increasing amplitude—the negative lift increases to a maximum, and then diminishes and reverses; but the negative torque continues to increase through an additional range.)

The change $\Delta\alpha$ in the effective angle of attack will change the instantaneous torque acting on a unit length of the span by an amount

$$\Delta T = -\beta s_t \left(\frac{\rho}{2} V^2 b^2\right) \frac{v}{V} \quad \ldots\ldots\ldots\ldots\ldots\ldots (48)$$

in which s_t is the slope of the wind-tunnel torque graph, and β is a correction factor from the stationary model in the wind tunnel to the oscillating structure.

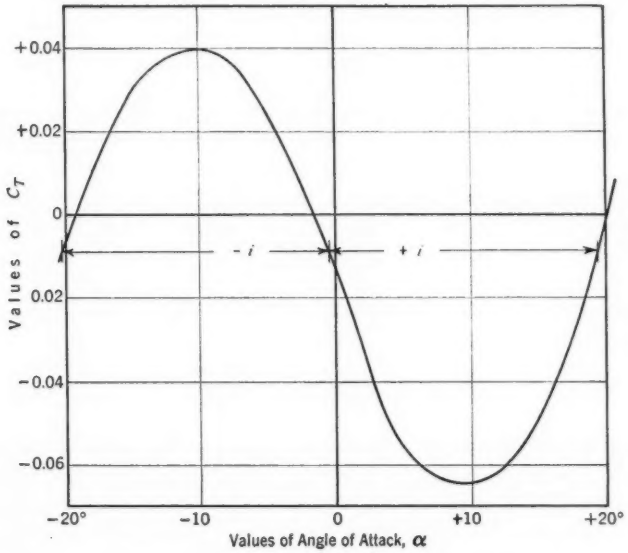

FIG. 6.—TORQUE GRAPH

Consideration of the effect of phase difference indicates that the relative vertical motion across the section will modify and actually may augment the aerodynamic torque effect produced by $\Delta\alpha$ at the leading edge, and wind-tunnel tests on oscillating models confirm this conclusion.

If the slope s_t of the torque graph (Fig. 6), when multiplied by β, is negative in the range of oscillation, ΔT by Eq. 48 will be positive (clockwise) when v is positive (upward at the left or leading edge) and negative when v is negative. This will produce self-excited amplification of torsional oscillations. Such condition constitutes aerodynamic torsional instability.

The maximum value, in a cycle, of the amplifying torque ΔT on a unit length of the span will be

$$\Delta T(\max) = -\pi \beta s_t N_t \rho b^2 V a \ldots\ldots\ldots\ldots\ldots (49)$$

Since the increment of torque ΔT is automatically resonant with the harmonic motion of the torsional oscillations and is, moreover, 90° out of phase with that harmonic motion, it will produce an increment of energy in each cycle:

$$\Delta W = \pi \Delta T(\max) \frac{2a}{b} = -2\pi^2 \beta s_t \rho b a^2 N_t V \ldots\ldots\ldots (50a)$$

and, over the span l,

$$\Delta W(\text{total}) = -\pi^2 \beta s_t \rho b (a_m)^2 N_t V l \ldots\ldots\ldots\ldots (50b)$$

The total kinetic plus potential energy in torsional oscillation, per unit length and over the span, will be given by Eqs. 28.

The relative increase, per cycle, in the amplitude of oscillation, or the logarithmic increment per cycle, then will be

$$\delta = \frac{\Delta a}{a} = \frac{\Delta a_m}{a_m} = \frac{\Delta W}{2W} = -\pi^2 \frac{b}{K} \beta s_t \rho N_t V \ldots\ldots\ldots (51a)$$

If βs_t is negative, δ will be positive, representing a self-excited amplification of torsional oscillations. By Eq. 51*a*, the torsional amplification ratio δ increases with the width b, or inversely with K/b.

Substituting numerical values for ρ and g, Eq. 51*a* reduces to

$$\delta = -0.0048 \frac{\beta s_t b^3 V}{r^2 w N_t} \ldots\ldots\ldots\ldots\ldots\ldots (51b)$$

and the negative damping coefficient (λ), or the logarithmic increment per second, then will be

$$\lambda \approx -0.0048 \beta \frac{s_t b^3 V}{r^2 w} \ldots\ldots\ldots\ldots\ldots\ldots (52)$$

Limiting Amplitudes of Torsional Oscillations.—The self-excited amplification of oscillations will continue until the positive contribution of ΔW from the range of negative slope of the torque graph is balanced by the tapering negative contribution from the flanking ranges of positive slope (see Fig. 7). The limiting local amplitude (θ_o or a_o) then is defined by the condition $\Delta W = 0$, in which

$$\Delta W = \oint T \, d\theta \ldots\ldots\ldots\ldots\ldots\ldots (53a)$$

which also may be written

$$\Delta W = \oint \theta \, dT \ldots\ldots\ldots\ldots\ldots\ldots (53b)$$

The limiting segment amplitude (θ_{om} or a_{om}) then is defined by Eq. 32. A graphic solution of Eqs. 53 is shown in Fig. 7.

If the torque graph is of the typical form (Fig. 6) represented by a cubic equation similar to Eq. 33, with intercepts $-i$, 0, and $+i$, then

$$\theta_o = \sqrt{\frac{4}{3}}\, i \qquad (54a)$$

and

$$\theta_{om} = \frac{4}{3}\, i \qquad (54b)$$

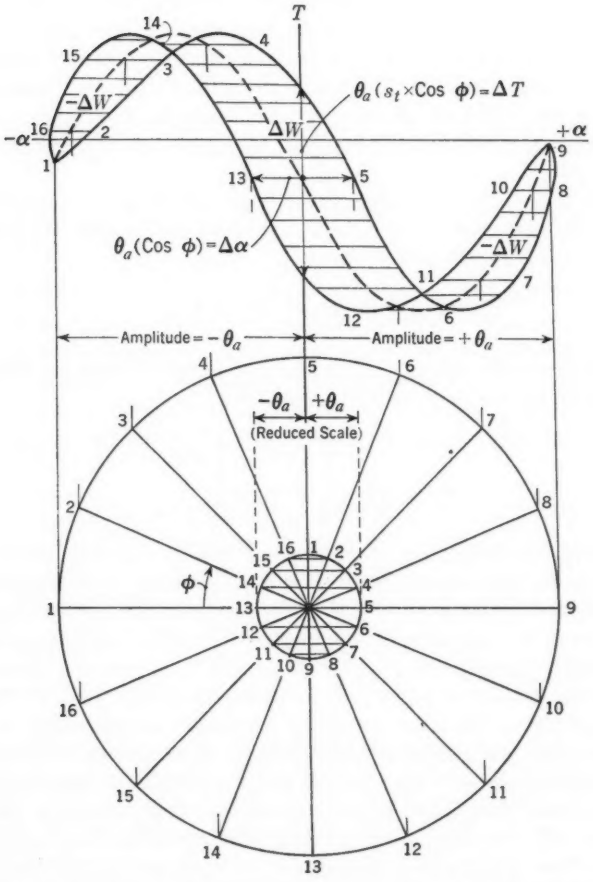

FIG. 7.—GRAPHIC DETERMINATION OF ENERGY INPUT (ΔW) FOR A GIVEN TORSIONAL AMPLITUDE (θ_a)

The limiting angular amplitudes (θ_o at any point, and θ_{om} at midsegment) thus are independent of wind velocity, span length and rigidity, and modes of oscillation, but depend only on the form of the torque graph. Wind-tunnel

tests yield similar torque graphs for all sections having torsional aerodynamic instability, with $i = 21°$ to $36°$, and therefore $\theta_{om} = 28°$ to $48°$. (The value of i appears to be a function of d/b.) The corresponding vertical amplitudes of torsional oscillations then will be

$$a_o = \frac{b}{2} \sin \theta_o \ldots\ldots\ldots\ldots\ldots\ldots\ldots\ldots (55a)$$

and

$$a_{om} = \frac{b}{2} \sin \theta_{om} \ldots\ldots\ldots\ldots\ldots\ldots\ldots\ldots (55b)$$

in which a_{om} is the limiting amplitude before correction for structural damping.

The torque graph obtained (1943) for the Tacoma cross section by Harold A. Thomas, M. Am. Soc. C. E., at the Carnegie Institute of Technology in Pittsburgh, Pa., has $i = 34°$. Hence, by Eq. 54*b*, the limiting torsional amplitude would be 45°, which checks the reported value for the Tacoma bridge and which also checks the oscillating-model test results obtained by Professor Thomas.

Change of Period by Forced Vibrations.—In any range of constant or mean effective s_t, the aerodynamic torque T varies in phase with the angular displacement θ:

$$T = \left(s_t \frac{\rho}{2} b^2 V^2 \right) \theta + T_{\theta=0} \ldots\ldots\ldots\ldots\ldots\ldots\ldots (56a)$$

This will not affect the energy or amplitude, but will change the frequency N_t from natural frequency to a "forced" frequency:

$$N_t = \frac{1}{2\pi} \sqrt{\frac{K_t - s_t \frac{\rho}{2} b^2 V^2}{2 r^2 m}} \ldots\ldots\ldots\ldots\ldots\ldots\ldots (56b)$$

If s_t is negative, the frequency N_t thus is increased. At high wind velocities, this increase in N_t may amount to 2% or 3%; normally it is negligible.

As a suggested explanation of self-excited amplification, this effect may be eliminated, since the amplitudes are unaffected. The work diagram follows the torque graph through the angular range and then retraces the same path, and is therefore reduced to a line of zero area. It is only the ΔT-effect, represented in Eqs. 48 to 53, that produces a relative displacement of the two tracings of the path along the torque graph (Fig. 7), similar to the displacements in a "hysteresis diagram." In one half of the cycle the torques are $T + \Delta T$, in the other half, $T - \Delta T$. The resulting intercepts through the angular range produce ΔW, the increment of energy that amplifies the oscillations.

Effect of Phase Difference.—Aerodynamic torsional instability associated with a negative slope of the torque graph does not occur at low wind velocities. Wind-tunnel tests on oscillating models, with the effect of structural damping eliminated by subtraction, show that there is a minimum wind velocity at which aerodynamic amplification (negative damping) appears. This critical velocity V_p is explained by the relative phase difference (represented by

$N_t\, b/V$) of aerodynamic disturbance and torsional oscillation between the two sides of the cross section.[5] The theory of aerodynamic damping further indicates that the "density-mass ratio" $\rho\, b^2/(2\, m)$ of the structure has some influence on V_p, and this is confirmed by the model tests. The recorded values of $V_p/(N_t\, b)$ actually ranged from 3.3 to 5.1 for different values of the density-mass ratio. The limited test results thus far available yield, approximately,

$$V_p = N_t\, b \left(4.8 - 82 \frac{\rho\, b^2}{2\, m} \right) \ldots\ldots\ldots\ldots\ldots\ldots (57a)$$

On substitution of numerical values for ρ and g, this reduces to

$$V_p = 1.41 \frac{b}{r} \frac{b}{\sqrt{w}} \left(1.53 - \frac{b^2}{w} \right) \sqrt{K} \ldots\ldots\ldots\ldots\ldots\ldots (57b)$$

(For the Tacoma span, for $N_t = 12$ cycles per min, Eq. 57*a* or 57*b* gives $V_p = 16.6$ miles per hr. With omission of the correction for density-mass ratio in Eq. 57*a*, or its reduced form b^2/w in Eq. 57*b*, either formula gives $V_p = 25.4$ miles per hr. This significant correction has been overlooked by other investigators.)

The correction factor β in the negative damping formulas for the oscillating structure is also a function of the phase difference across the section; hence it is a function of V_p/V. A qualitative analysis of the aerodynamic action, as confirmed and supplemented by the test results, indicates that β is negative for $V < V_p$; is zero at $V = V_p$; then increases to a maximum greater than unity; and finally diminishes toward unity as a limit at high wind velocities. This variation is represented by the following empirical formula (which fits the test results):

$$\beta = \frac{5.5 \left(\frac{V}{V_p} - 1 \right) + 0.005 \left(\frac{V}{V_p} - 1 \right)^2}{\frac{V}{V_p} + \frac{V_p}{V} + 0.005 \left(\frac{V}{V_p} - 1 \right)^2} \ldots\ldots\ldots\ldots (58a)$$

or, with close accuracy from $V = 0.8\, V_p$ to $V = 4\, V_p$,

$$\beta = 5 \frac{V - V_p}{V} \ldots\ldots\ldots\ldots\ldots\ldots\ldots\ldots (58b)$$

For various cross sections of the Tacoma type, the wind-tunnel torque graphs are almost identical in their middle parts of negative slope, with $s_t \approx -0.50$, very closely. Substituting this value of s_t, and the value of β from Eq. 58*b*, Eq. 51*b* may be written

$$\delta = 0.012 \frac{b^3}{r^2\, w\, N_t} (V - V_p) \ldots\ldots\ldots\ldots\ldots\ldots (59)$$

This is identical with the plotted results obtained in wind-tunnel tests on oscillating models.

[5] "The Failure of the Tacoma Narrows Bridge," Appendix VIII of official report, analysis by Louis G. Dunn.

Analytical Derivation of β for Torsional Oscillations.—Analogous to Eq. 43 for vertical oscillations and representing a similar physical interpretation, a tentative analytical derivation of β may be written for torsional oscillations:

$$\beta = \frac{\int_{0.19\phi'}^{1.11\phi'} (1 - u\,\phi^3)\,(0.65\,\phi' - \phi)\cos\phi\,d\phi}{\int_{0.19\phi'}^{1.11\phi'} (1 - u\,\phi^3)\,(0.65\,\phi' - \phi)\,d\phi} \quad \ldots\ldots\ldots (60a)$$

In this case a factor of the indicated form $(1 - u\,\phi^3)$ is included to represent a variation of the intensity or effectiveness of the vertical pressure impulse as it traverses the section; and the factor $(0.65\,\phi' - \phi)$ must be included to represent the varying lever arm about the center of the section. Values of β as computed by Eq. 60*a* are given in Table 5. In conformity with the test

TABLE 5.—ANALYTICAL DERIVATION OF β FOR TORSIONAL OSCILLATIONS ($u = 1/3$)

Equation No.	VALUES OF $V/(N_t\,b)$						
	12	8	4	3	2.5	2.0	1.5
60*a*	3.7	2.8	0.7	−0.1	−0.6	−0.9	−0.6
60*b*	3.7	2.5	0.8	−0.02	−0.5	−0.8	−0.5

results, values of β exceeding unity are obtained. Varying values of $V_p/(N_t\,b)$ are also obtained, as follows:

u	$\frac{V_p}{N_t\,b}$
1/7	2.57
1/5	2.80
1/3	3.13
1	3.66
∞	5.34

The value of $V_p/(N_t\,b) = 3.13$ (and therefore $u = 1/3$) corresponds to the Tacoma section.

Each integrand in Eq. 60*a* consists of two modified triangular influence areas, concentrated toward the outer edges of the section. By considering these influence areas as concentrated at their respective centroids, an approximate equivalent formula is obtained as a welcome short cut:

$$\beta = \frac{\cos 0.3\,\phi' - [1 - 0.9\,u\,(\phi')^3]\cos\phi'}{0.9\,u\,(\phi')^3} \quad \ldots\ldots\ldots\ldots (60b)$$

for which the computed values are given in Table 5. The denominator is the algebraic sum of two resultant pressure forces acting near the outer edges of the section, and the numerator is the algebraic sum of the same two resultants corrected for phase difference by their respective cosine factors.

The several theoretical and empirical formulas for β yield remarkably consistent results. Any further refinement of the values in Table 6 would not be warranted by the present available data.

TABLE 6.—COMPARISON OF THEORETICAL AND EMPIRICAL FORMULAS FOR β

Equation No.	Values of V/V_p							
	∞	5	4	3	2	1	0.5	0
60*a*	1	3.9	3.8	3.2	2.1	0	−0.6	0
60*b*	1	4.4	3.8	2.9	1.8	0	−0.5	0
58*a*	1	4.2	3.8	3.3	2.2	0	−1.1	0
58*b*	....	4	3.8	3.3	2.5	0	....	....

The coefficient u, introduced in Eq. 60*a* to represent a rate of progressive reduction or modification in pressure reaction by transfer of energy as the air disturbance traverses the section, is related to the density-mass ratio $\rho\, b^2/(2\, m)$, and therefore to the critical dimensional ratio b^2/w. The indicated relation (based on the comparison for the known data of the Tacoma section) is

$$\frac{1}{u} = 355{,}000 \left(\frac{\rho\, b^2}{2\, m}\right)^3 = 20 \left(\frac{b^2}{w}\right)^3 \quad \ldots\ldots\ldots\ldots\ldots (61a)$$

In the useful range, the derived variation of V_p with u, as recorded under Eq. 60*a*, is given very closely by

$$\frac{V_p}{N_t\, b} = 4.8 - 1.16 \sqrt[3]{\frac{1}{u}} \quad \ldots\ldots\ldots\ldots\ldots\ldots (61b)$$

With the correlation recorded in Eq. 61*a*, Eq. 61*b*, independently derived, proves to be identical with the empirical Eqs. 57 previously written from the wind-tunnel tests on oscillating models.

The development of the concepts and relationships introduced herein offers many interesting possibilities and will repay further exploration by both experiment and analysis.

Determination of Required K for any Specified Critical Velocity V_p.—Eqs. 57 enable the required design value of K to be determined for any specified value of V_p (the critical velocity before correction for structural damping). From Eq. 57*b*

$$K = \frac{r^2}{2\, b^2} \frac{w/b^2}{(1.53 - b^2/w)^2} (V_p)^2 \quad \ldots\ldots\ldots\ldots\ldots\ldots (62a)$$

As a rule, for the suspension bridges under consideration, w/b^2 ranges from 1.67 to 2.50; and, for this range, the function of w/b^2 and b^2/w in Eq. 62*a* remains practically constant (between 1.88 and 1.93) and may be taken as approximately equal to 1.90. Using this value, and $r^2/b^2 \approx 0.125$, Eq. 62*a* yields

$$K = 0.12\, (V_p)^2 \quad \ldots\ldots\ldots\ldots\ldots\ldots\ldots\ldots (62b)$$

Hence, for $V_p = 50$ miles per hr, the required K is 645.

Wider bridges (unless made heavier per square foot) fall outside of the values of w/b^2 assumed herein, and require a higher K. (For the Bronx-Whitestone Bridge, the required K by Eq. 62*a* is 80% higher than that given by Eq. 62*b*, or $K = 1{,}170$ for $V_p = 50$ miles per hr.)

Critically Dangerous Value of b^2/w.—Eq. 62*a* indicates that there is a critical value of b^2/w for aerodynamically unstable bridges, namely $b^2/w = 1.53$ (equivalent to $\rho\, b^2/(2\, m) = 0.0585$). For bridges having this dimensional ratio, V_p will be zero for all values of K. As b^2/w approaches the critical value of 1.53, sensitiveness to torsional aerodynamic instability increases and becomes more difficult to cure. (The structure that comes nearest to this critical ratio is the Bronx-Whitestone Bridge, with the abnormally high value of $b^2/w = 1$. The prevailing values of b^2/w for other suspension bridges of this type are close to the optimum value of 0.51, for which the required K is a minimum, as given by Eq. 62*b*.) The observed high aerodynamic sensitiveness of certain suspension bridges during erection, with floor forms in place and before pouring the concrete, is also explained by the critical value of b^2/w in that stage.

Structural Damping.—Until more adequate experimental data are available, the tentative indicated expression for δ_s, Eq. 35, previously written for vertical oscillations, also may be used for torsional oscillations of flexible suspension bridges.

The critical velocity due to structural damping, defined by the condition $\delta - \delta_s = 0$, then will be given by

$$V_c - V_p = \frac{r^2\, w\, N_t}{0.012\, b^3}\, \delta_s \qquad (63a)$$

where δ_s is calculated for zero amplitude, and the limiting amplitude corrected for structural damping will be given by

$$a_r = a_{om} \sqrt{1 - \frac{V_c - V_p}{V - V_p}\left(1 + 1{,}700\, \frac{n}{l}\, \sqrt{a_r\, d}\right)} \qquad (63b)$$

This yields for the Tacoma span, at $V = 40$ miles per hr, with $i = 34°$, a maximum limiting torsional amplitude of 13.1 ft, compared with 14 ft estimated as observed.

Corrected for structural damping, the net energy gain per cycle will be given by Eq. 37.

Determination of Required K for Any Specified Critical Velocity V_c.—From Eqs. 57*b* and 63*a*,

$$\sqrt{K} = \frac{V_c}{1.41\, \frac{b}{r}\, \frac{b}{\sqrt{w}} \left(1.53 - \frac{b^2}{w}\right) + 37.7\, \frac{r}{b}\, \frac{\sqrt{w}}{b}\, (0.001 + 0.06\, R)} \qquad (64a)$$

For the prevailing values of $b^2/w = 0.45$ to 0.55, and $r/b \approx 0.354$, Eq. 64*a* reduces to

$$\sqrt{K} = \frac{V_c}{2.93 + 1.13\, R} \qquad (64b)$$

Hence, for $R = 0$,

$$K = 0.116\ (V_c)^2 \quad \ldots\ldots\ldots\ldots\ldots\ldots\ldots\ldots (64c)$$

and, for $R = 1$,

$$K = 0.061\ (V_c)^2 \quad \ldots\ldots\ldots\ldots\ldots\ldots\ldots\ldots (64d)$$

or a reduction of 3% to 49% in the required value of K, as given by Eq. 62*b*, when structural damping is taken into account. To make $V_c = 50$ miles per hr, the required value of K ranges from 626 for $R = 0$, down to 328 for $R = 1$.

With abnormally high values of b^2/w, higher values of K will be required. At the critical value of $b^2/w = 1.53$, to make $V_c = 50$ miles per hr (which then will be due to structural damping alone), the required value of K ranges from 12,500 for $R = 1$, to 46,500,000 for $R = 0$. The obvious measure is to increase R and w or to eliminate the cause of the aerodynamic instability.

PART 4.—METHODS OF SECURING RIGIDITY AND AERODYNAMIC STABILITY

Anticipating Aerodynamic Instability.—The phenomena of aerodynamic instability, both vertical and torsional, are a combined function of flexibility of the span and disposition of the cross section.

The conventional H-type of cross section, with solid floor between vertical stiffening girders, tends to produce the effects of aerodynamic instability. Modification of the section by moving the floor slab to the top or to the bottom of the cross section may reduce the effect, but will not necessarily eliminate it.

Wind-tunnel tests on a scale model of the cross section will yield characteristic curves, useful in analysis, and offer a method of testing or predicting aerodynamic instability of the section. If the graph of aerodynamic lift for varying angles of attack has a range of negative slope, aerodynamic vertical instability of the section may be anticipated. Similarly, if the graph of aerodynamic torque for varying angles of attack has a range of negative slope, aerodynamic torsional instability of the section may be anticipated. In addition, an aerodynamically stable section may develop aerodynamic oscillations (limited to a range of low wind velocities) if the structure has a low value of R. For a complete investigation, wind-tunnel tests on oscillating models are desirable.

The use of open trusses instead of solid-web girders for the stiffening construction reduces, but does not necessarily eliminate, susceptibility to aerodynamic instability.

Influence of Rigidity.—Susceptibility to the effects of aerodynamic instability is obviously reduced by increasing the rigidity of the structure—primarily the rigidity of the main span. Rigidity of the side spans and towers is helpful in the lowest mode ($n = 1$), and may be helpful in some higher modes ($n = 2, 6, \cdots$) if center stays are provided.

For resistance to these aerodynamic effects, the most significant single factor is the coefficient of rigidity, K, or the coefficient of rigidity per foot, $2K/b$.

In a bridge with solid-web stiffening girders, the numerical value of K should be kept well above 300, and the numerical value of $2K/b$ should be

kept well above 15 (lb per ft^3), unless aerodynamic stability is otherwise assured (see Eqs. 36, 62, 63, and 64, and the related text).

In a bridge with open-web stiffening trusses, the numerical value of K should be kept well above 120, and the numerical value of $2\,K/b$ should be kept well above 6 (lb per ft^3), unless aerodynamic stability is otherwise assured (see Table 2 and Fig. 2).

Another significant factor is R, the ratio of the rigidity contributed by the stiffening construction to the total rigidity. Higher values of R, by increasing the structural damping, raise the critical wind velocity, restrict the maximum amplitudes, and prevent development of oscillations at low wind velocities. The value of R should preferably be kept well above 0.25, unless aerodynamic stability is otherwise assured. With low values of R, the required values of K and $2\,K/b$ may be two or more times the foregoing values (see Eqs. 64).

The depth of the stiffening truss or girder, in proportion to the span, is also directly effective in augmenting structural damping and thereby restricting amplitudes (see Eq. 35). Experience to date indicates the hazard of making the depth of the stiffening truss or girder less than 1/100 of the span, unless the cross section is aerodynamically stable or unless other means of resisting oscillations or assuring aerodynamic stability are provided (see Fig. 2).

Lateral flexibility of the span does not appear to be a factor in aerodynamic instability. A suspension span is inherently stable against lateral displacement.

Use of Center Stays.—In amplitudes attainable and magnitude of kinetic energy accumulated, two-segment (single node) torsional oscillations are generally the most dangerous potential manifestation of aerodynamic instability.

A highly effective method of preventing or resisting such two-segment torsional oscillations is the provision of adequately proportioned center stays or other equivalent means of preventing relative longitudinal motion of cable and suspended structure at midspan.

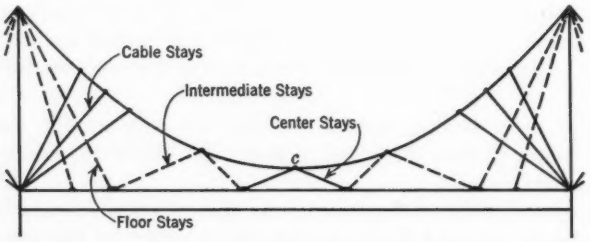

FIG. 8.—VARIOUS SYSTEMS OF LONGITUDINAL STAYS FOR STIFFENING SUSPENSION BRIDGES TO INCREASE THEIR AERODYNAMIC STABILITY

Without such center stays or their equivalent, two-segment ($n = 2$) oscillations of a main span cable involve longitudinal displacement of its midpoint (see Fig. 1). If both cables are in phase, as in vertical oscillations of the span, the longitudinal displacements of their midpoints will be in phase, tending to produce corresponding longitudinal oscillation of the suspended

span. If the two cables are out of phase, as in torsional oscillations of the span, the longitudinal displacements of their midpoints will be out of phase, tending to move in opposite directions. Such relative longitudinal movements of the midpoints of the two cables in opposite directions are prevented by anchoring the two midpoints to the suspended span (Fig. 8). When such midspan anchorage of the cables is provided, by center stays or their equivalent, two-segment torsional oscillation is resisted. It cannot then take place without the concurrence of substantial increments of cable tension (such increments being of opposite sign in the two halves of the span), synchronous related torsional distortions of the towers, and synchronous related torsional deformations of the side spans.

The resisting force to be provided by the center stays can be calculated, and they should be proportioned accordingly.

Apparently no substantial two-segment aerodynamic torsional oscillations have developed in any span equipped with center stays as long as such stays and their connections have remained firm and intact.

Use of Longitudinal Diagonal Stays.—An economical method of providing concentrated, localized resistance to vertical or torsional oscillations is the use of longitudinal diagonal stays, inclined in either direction, in the planes of the cables (Fig. 8). Such stays may be located either above or below the roadway and may have their attachment to points of the cable or to points of the stiffening girder, or to both.

If such longitudinal diagonal stays run from the main tower ends of the span upward to the quarter points or other intermediate points of the cable, they are equivalent to stays running in the same direction under the roadway from shore or piers to corresponding points of the stiffening girders. The effect will be a direct resistance to upward displacement or upward swing of the points of attachment and an indirect and lesser resistance to downward displacement or downward swing of the same points of attachment, by virtue of any symmetrically disposed stays in opposing segments or in adjacent spans. Also there is a direct resistance to downward swing, by virtue of any initial tension in the stays, since a member under tension is elastically equivalent to a compression member (until it becomes slack).

If the longitudinal diagonal stays run downward from the tops of the towers to the quarter points or other intermediate points of the stiffening girders, their effect will be a direct resistance to downward deflection or downward swing of the points of attachment, and indirect and direct resistance to upward deflection or upward swing of the same points of attachment, for the same reasons as the foregoing.

In either case, the effect of the longitudinal diagonal stays will be equivalent to a substantial increase in the coefficient of rigidity K during one half of the cycle and to a smaller or equal increase in the value of K during the other half of the cycle. Inadequate values of K may thereby be brought up to safe values. The late John A. Roebling, M. Am. Soc. C. E., had this concept in mind when he designed the Niagara, Cincinnati, and Brooklyn bridges.

With the increase in the value of K, there is a sharp concomitant increase in the value of R, since the cable contribution to K remains unchanged. This

increase in the value of R, which will be relatively very substantial when the initial value of R is small (as it is in flexible suspension bridges), will tend to increase structural damping and thereby will raise critical velocities and reduce the amplitudes attainable.

The relative merits of different types of longitudinal diagonal stays are not discussed herein.

For maximum effectiveness, the two types or directions of longitudinal diagonal stays may be combined, so as to provide maximum resistance to both directions of displacement or swing.

If the individual stays, in either a single or double system, are given sufficient initial tension to prevent reversal of their stress in the cycle for any anticipated amplitude of oscillation, then each stay will act with full effectiveness throughout the cycle.

The augmentation of K contributed by each individual stay can be calculated for any given mode of oscillation. A convenient simplified formula is

$$\Delta K \approx \frac{3+n}{5} \frac{E_s A_s}{l_s l} S \left(\frac{a_2 - a_1}{a_m} \right)^2 \sin^2 \psi \quad \ldots\ldots\ldots\ldots (65)$$

in which a_1/a_m and a_2/a_m are the relative amplitudes at the two ends of the stay in terms of any unit amplitude at midsegment, ψ is the angle of the stay with the horizontal, and S is a multiplying factor (ranging from 1 to 2) depending upon the initial tension (and any initial sag) in the stay. The multiplier S has its minimum value of $S = 1$ if the initial tension is zero, and its maximum value of $S = 2$ if the initial tension is high enough to prevent reversal or if the amplitudes of any remaining oscillations of the stiffened structure are too small to cause reversal of the tension in the stay. (Any small initial sag in the stay will produce a slight reduction in S.)

Example 6: Increase in K by Longitudinal Diagonal Stays.—For the data and dimensions of the Tacoma main span, a single system of longitudinal diagonal stays near each end of the span, with a mean effective slope of 45° and made of wire rope strand with an aggregate cross section of $A_s = 16$ sq in. with sufficient initial tension to make $S = 2$, will produce, by Eq. 65, $\Sigma\Delta K = 270$ for $n = 2$. Thus the effective value of K will be increased from the original value of 62 to a mean augmented value of 332, and the corresponding value of R will be increased from 0.015 to 0.816. A double system of longitudinal diagonal stays, of the foregoing proportions running in both directions, will produce $\Sigma\Delta K = 540$ for $n = 2$, so that the effective value of K will be increased from 62 to 602, and the value of R will be increased from 0.015 to 0.900. This would bring K, $2K/b$, and R to relatively safe values.

Use of Transverse Diagonal Stays.—Another economical method of providing concentrated, localized resistance to torsional oscillations is the use of transverse diagonal stays (Fig. 9) located between opposite suspenders in the transverse planes near the quarter points and at other intermediate points of the span. The function of such stays is to prevent or resist out-of-phase displacement of the two sides of the span. Transverse horizontal struts between the cables may be used in conjunction with such transverse diagonal stays (see Fig. 9).

Stiffening the cross section of the suspended deck structure at the panel points, as has been suggested by some engineers, resists distortion of that cross section but does not prevent relative vertical displacement of the two sides of the undistorted cross section. In this respect a suspension bridge differs from other types. Resistance to distortion must be distinguished from resistance to torsion. Relative vertical displacement of the two sides of the section does not require distortion of the cross section but does require relative vertical displacement of the two cables, and this is resisted by transverse diagonal stays, with or without transverse struts between the cables.

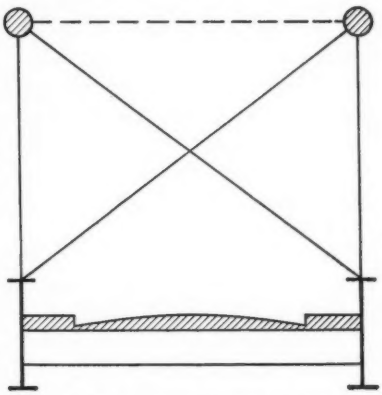

FIG. 9.—TRANSVERSE DIAGONAL STAYS TO RESIST TORSIONAL DEFORMATION

Such transverse diagonal stays and horizontal struts do not help against vertical oscillations, since they do not affect the value of K against vertical oscillations; but they do help against torsional oscillations, since they directly augment the value of K_t.

The action of transverse diagonal stays at any vertical section is effectively to resist or prevent distortion of the rectangle between cables, suspenders, and bridge floor (Fig. 9), so that torsional displacement (consisting of relative vertical displacement of the cables) then cannot take place without forcing a lateral displacement of the cables. This evokes a substantial additional force of restitution, which means a commensurate augmentation of K_t. For an adequate system of such transverse stays, with top struts included, a convenient simplified formula is

$$\Delta K_t \approx w \left[\left(\frac{4 + n^2}{5} \right) f + (4 + 2\,n^2)\, c + 5\,n^2 \frac{c^2}{f} \right] \ldots\ldots (66a)$$

in which c is the mean effective height of roadway below horizontal cable tangent. For proportioning the transverse diagonal stays, their maximum tension (per foot of span) producible by any assumed amplitude a_m is given by

$$S_t \approx 4 \frac{w}{b} \left(1 + \frac{n^2}{4} + \frac{c\,n^2}{f} \right) a_m \sec \psi \ldots\ldots\ldots\ldots (66b)$$

Without top struts, the values given by Eqs. 66 are halved.

(For the Tacoma span, Eq. 66*a* yields $\Delta K_t = 2{,}640{,}000$, corresponding to $\Delta K = 3{,}470$, and Eq. 66*b* indicates that a section of less than 1 sq in. per panel point will be adequate if no subsequent torsional amplitudes exceed 1 ft.)

Use of Damping Devices.—To supplement structural damping, artificial damping devices may be installed, for increased absorption of the energy of undulations or oscillations. Such friction damping devices have been used

against the longitudinal oscillations of the span. For greater direct effectiveness, these friction damping devices can be used in connection with longitudinal diagonal cable stays or floor stays and also in connection with transverse diagonal stays.

Use of Open-Floor Construction.—The principal aerodynamic vertical pressure forces causing vertical or torsional instability originate in the horizontal floor sections near the inside faces of the stiffening girders. By opening these horizontal sections—either by leaving open spaces or by using open-grating construction—the aerodynamic forces causing amplification of undulations or oscillations can be eliminated or reduced to negligible proportions.

Experiments indicate that the required horizontal width of such open space adjacent to the inside face of each girder is not less than one half the depth of the girder.

By eliminating the solid sidewalk or roadway over this indicated width inside of each girder, differences of pressure above and below the section are largely equalized, and the area on which such differences of pressure would act is eliminated or materially reduced. Without considering the equalization of pressures, but considering only the elimination of the critical areas on which the largest pressure differences would otherwise act, a simple calculation based on the influence areas represented in Eqs. 60 shows that two lateral vents of width $3\,b/16$ to $b/4$ will reduce aerodynamic lift by at least 60% to 75% and aerodynamic torque by at least 75% to 87%; and, in addition, by Eqs. 60, the multiplier β due to phase difference across the net effective width of section will be reduced by 40% to 60%.

The entire roadway width may be made of open-decking construction, but it appears preferable to limit the open construction to the aforementioned lateral strips. The solid middle strip of roadway contributes to aerodynamic stability by atmospheric damping action. Its weight is also desirable to increase the rigidity of the span.

Use of Outside Sidewalks.—Subject to experimental verification, another indicated method of eliminating or reducing aerodynamic instability is the use of wide horizontal fins on the outside faces of the girders. Such horizontal fins conveniently may take the form of outside sidewalks or roadways on cantilever brackets or floor beams.

The purpose of such outside horizontal fins is to reverse the aerodynamic effect otherwise produced. Downward velocity of the windward girder combined with horizontal velocity of the wind then would contribute an upward pressure resultant, opposing and damping the oscillation, instead of a downward pressure resultant, amplifying the harmonic motion.

As with the use of open construction, the negative slopes of lift and torque graphs would be reduced, eliminated, or reversed.

Very conveniently, the use of open construction in the normal sidewalk spaces and the removal of the sidewalks to outside brackets may be combined in the modification of the cross section.

Conclusions

By increasing weight, depth, rigidity, and bracing, by adding center stays, longitudinal diagonal stays, transverse diagonal stays, or other stays, and by introducing artificial damping devices, resistance to the effects of aerodynamic instability may be built up to any desired amount. These methods resist or check the effects, but do not eliminate the cause.

By modification of the cross section, as by using open spaces in the floor or by adding horizontal fins or other wind-deflecting elements to the vertical faces of the girders, the cause of aerodynamic instability may be eliminated and an aerodynamically stable section may be secured.

The one line of attack places the emphasis on providing increased resistance to a dangerous inherent characteristic; the other line of thought is devoted to avoiding or eliminating the dangerous characteristic—aerodynamic instability of the cross section.

It is more scientific to eliminate the cause than to build up the structure to resist the effect.

In conclusion, the writer asks his readers to share with him his faith and conviction that suspension bridges of all span lengths can be designed economically to any desired degree of rigidity and with assured aerodynamic stability.

APPENDIX

Notation

The following letter symbols, adopted for use in the paper, conform essentially to American Standard Letter Symbols for Mechanics, Structural Engineering and Testing Materials,[6] prepared by a Committee of the American Standards Association, with Society representation, and approved by the Association in 1932; supplemented by customary symbols used in Aerodynamics and in the Theory of Vibrations:

A_c = section of cable (square inches);
A_s = section of diagonal stay (square inches);
a = vertical amplitude at any point of span (feet);
a_m = vertical amplitude at middle of segment (feet);
a_o = limiting local vertical amplitude producing zero ΔW;
a_{om} = limiting midsegment amplitude producing zero ΔW;
a_τ = limiting midsegment amplitude reduced by structural damping;
a_1 = local amplitude at first point of attachment of a diagonal stay;
a_2 = local amplitude at second point of attachment of a diagonal stay;
b = width of section, center to center of cables (feet);
C_D = aerodynamic drag coefficient (nondimensional);
C_L = aerodynamic lift coefficient (nondimensional);
$(C_L)'$ = lift coefficient corrected for drag (nondimensional);
c = mean height of roadway below horizontal cable tangent (feet);

[6] ASA—Z10a—1932.

D = horizontal aerodynamic drag force on section (pounds per foot);
d = vertical depth of stiffening girders (feet);
E = modulus of elasticity of stiffening girders (pounds per square inch);
E_c = modulus of elasticity of cables;
E_s = modulus of elasticity of diagonal stays;
f = vertical sag of cable (feet);
f_1 = vertical sag of cable in side span;
g = gravity acceleration $\approx$ 32.2 ft per sec^2;
H = horizontal component of tension in one cable (pounds);
I = moment of inertia of section of one stiffening girder (inches^2-feet^2);
i = horizontal intercept of lift or torque graph (radians);
K = coefficient of rigidity of the span or structure (per cable) = spring constant for vertical oscillations (pounds per square foot);
K_t = spring constant of the span or structure for torsional oscillations (pounds);
K_0 = K for main span alone;
K_1 = K for side span alone;
L = vertical aerodynamic lift force on section (pounds per foot);
L' = aerodynamic lift force corrected for drag (pounds per foot);
l = length of span (feet);
l_c = length of cable (feet);
l_s = length of a diagonal stay (feet);
l_1 = length of side span (feet);
m = mass of the span per linear foot per cable = w/g;
N = natural frequency of vertical oscillations (cycles per second);
N_t = frequency of torsional oscillations (cycles per second);
n = number of segments in span l;
n_1 = number of segments in span l_1;
P = natural period of vertical oscillations (seconds) = $1/N$;
p = applied load per cable (pounds per foot);
q = coupling factor for coupled oscillations of main and side spans (nondimensional);
R = proportion of K due to stiffening girders (nondimensional);
r = polar radius of gyration of mass of the cross section (feet);
S = factor depending upon the initial tension in a stay (nondimensional);
S_t = stress in transverse diagonal stay for torsional amplitude a_m;
s = slope of lift graph = ΔC_L per radian;
s_t = slope of torque graph;
s' = slope of lift graph corrected for drag = $s + C_D$;
T = torque acting on any section of span (foot-pounds per foot);
t = time from beginning of a cycle (seconds);
u = variation factor of pressure impulse traversing the section (nondimensional);
V = horizontal velocity of wind (feet per second);
V_c = total critical wind velocity including structural damping (feet per second);

V_p = critical wind velocity due to phase difference (feet per second);
v = instantaneous vertical velocity of any point of span (feet per second);
W = energy of oscillations (foot-pounds);
w = dead load of span per cable (pounds per foot);
Δw = increment of load per cable (pounds per foot);
x = abscissa of any point of span, measured from one end (feet);
y = ordinate of any point of cable, measured from cable chord (feet);
α = angle of attack of wind, positive when upward (radians);
β = correction factor in aerodynamic amplification formulas, to correct for phase-difference effects on oscillating sections (nondimensional);
γ_1 = slope of cable chord in side spans;
δ = logarithmic increment per cycle = $\Delta a/a$ (nondimensional);
δ_s = logarithmic decrement per cycle, by structural damping (nondimensional);
δ_0 = value of δ at zero amplitude;
η = instantaneous vertical displacement of any point of span (feet);
η_w = theoretical vertical deflection of a simple beam by dead load w (feet);
θ = instantaneous angular displacement of any point of span (radians);
θ_a = angular amplitude at any point of span (radians);
θ_o = limiting local angular amplitude producing zero ΔW;
θ_{om} = limiting midsegment amplitude of torsional oscillations producing zero ΔW;
λ = negative damping coefficient = logarithmic increment per second;
ρ = air density, in units of mass per cubic foot ≈ 0.00238;
ϕ = phase angle = $2\pi N t$ or $2\pi N_t t$ (radians);
ϕ' = effective phase difference across the width of the section; and
ψ = angle of diagonal stay with horizontal.

AMERICAN SOCIETY OF CIVIL ENGINEERS

Founded November 5, 1852

PAPERS

UNUSUAL CUTOFF PROBLEMS—DAMS OF THE TENNESSEE VALLEY AUTHORITY

A SYMPOSIUM

PAGE

Deep Solution Channel, Kentucky Dam, Kentucky.
By James B. Hays, M. Am. Soc. C. E..... 1400

Flowing Water in Underground Channels, Hales Bar Dam, Tennessee.
By L. A. Schmidt, Jr., M. Am. Soc. C. E..... 1417

Note.—Written comments are invited for immediate publication; to insure publication the last discussion should be submitted by **April 1, 1944.**

DEEP SOLUTION CHANNEL, KENTUCKY DAM, KENTUCKY

By James B. Hays,[1] M. Am. Soc. C. E.

Synopsis

An unusual method of constructing a cutoff in a solution channel nearly 200 ft deep in the foundation at Kentucky Dam, together with an accurate picture of the results of grouting in the clay-filled and rock-filled channel, is described in this paper. The cutoff wall was constructed in the form of an arch dam except that it was built from the top down rather than starting from the bottom and working upward.

So little is known about grouting in clay that it is thought the results presented herein would be of interest to many engineers engaged in similar work.

Kentucky Dam, a Tennessee Valley Authority (TVA) project, is on the Tennessee River, in Kentucky, 22 miles from its confluence with the Ohio River at Paducah, and is one of the series of flood control, navigation, and power dams that will maintain a 9-ft navigation channel to Knoxville, Tenn.

The over-all length of the combined earth and concrete structure is 8,700 ft, and the maximum height of the concrete spillway section is 165 ft. The spillway section has twenty-four fixed roller gates 40 ft wide by 50 ft high, each in three sections. The normal head is 57 ft with a maximum of 73 ft. The lock chamber is 110 ft wide by 600 ft long. The power house will ultimately have five units. Turbines are of the adjustable-blade Kaplan type. A general plan of the dam is shown in Fig. 1.

The dam was constructed in three stages. The lock, built first, was completed and placed in temporary operation early in 1942. Because of the topography of the site, the lock was built in an open excavation on the east, or right, bank flood plain, surrounded by an earth-dike cofferdam to hold back flood waters. This permitted the starting of the second stage, the building of the cofferdam in the river for the power house and part of the spillway, without waiting for the completion of the lock. The third stage involves the remainder of the spillway.

Foundation drilling and exploration of several sites began in the summer of 1935, with the selection of the final site in 1937. Closer and more detailed investigations continued even after construction was started on July 1, 1939. The rock was known to be limestone of the Fort Payne formation, but very little was exposed at the site. A few outcrops occurred on the right bank above the flood plain. The overburden was deep. The shallowest depth, 20 to 30 ft,

[1] New York, N. Y.; formerly Project Mgr., South Holston and Watauga Projects, TVA, Bristol, Tenn.

to rock was in the area covered by the lock. In the river section, rock was 50 ft below the bed of the river, and, on the left bank, under the long earth-fill section, the depth was from 85 to 110 ft.

After considerable study of the cores and near-by formations, the geologists advised that most of the cavities in the foundation would probably be in the form of vertical solution channels along joints or fractures in the rock. For this reason considerable exploratory drilling was done by using 45° overlapping angle holes. This revealed many defects in the foundation that had been missed in the earlier vertical drilling. It later developed that the geologists' interpretations were generally correct, with a few exceptions.

At the time the construction department took charge, the general exploration had been nearly completed. It was necessary, however, to continue the drilling to fill in gaps and develop the conditions in more detail.

Many of the cavities or defects in the foundation were located before actual excavation had uncovered them. The drill records merely located the cavities but did not indicate their actual shape or the condition of such material as might be in them. The upper cavities were known to be generally filled with clay; those at lower elevations were often only partly filled or open.

The Fort Payne formation is a dark limestone interbedded with layers and large flat lenses of chert. The chert layers were generally from 2 in. to 6 in. thick with the limestone between varying from 4 in. to 12 in. The bedding varied from nearly flat, under a part of the lock, to a 6° dip toward the left bank. The limestone, in weathering, turned to a clay, but the chert layers remained unaltered, although generally found broken or cracked into small pieces. A large part of the area excavated to rock was covered with a thick layer of residual clay and chert varying from 8 ft to 10 ft in thickness. The clay and chert layers over solution channels had often slumped down, and the extent of this slumping generally indicated the extent of the cavity.

Several vertical solution channels in the lock had been located by the time excavation had reached full swing. The deepest and most extensive channel was found at the junction of the earth dam and the river wall of the lock just downstream from the lower lock gate. A study of the trend of the joint system in the rock, together with the earlier drilling records, indicated that this channel extended under the river and angled across the dam at about 45° to the axis and into the lower lock channel.

A line of drill holes was put down from the top of the lock cut on the side toward the river, with the idea of further developing the trend and extent of the channel. These holes were also grouted to prevent excessive leakage into the excavation. The drill records indicated layers of rock and clay with the deep cavities open or partly filled. Since the open cavities were water bearing, there was the danger that they might connect directly with the river and be a source of trouble. As a result of the grouting, there was practically no leakage through the rock or the solution channels into the lock excavation.

An intensive program of drilling was undertaken in the area of the lock foundation with holes on 20-ft centers each way to develop the extent of the solution channel (see Fig. 2). Two problems were involved: One was how the

lock-wall would be supported over the channel; the other was what treatment would be required in the channel itself to make an adequate cutoff under the dam and prevent possible serious damage in the future. This paper deals with the second problem. All holes were grouted soon after drilling was completed.

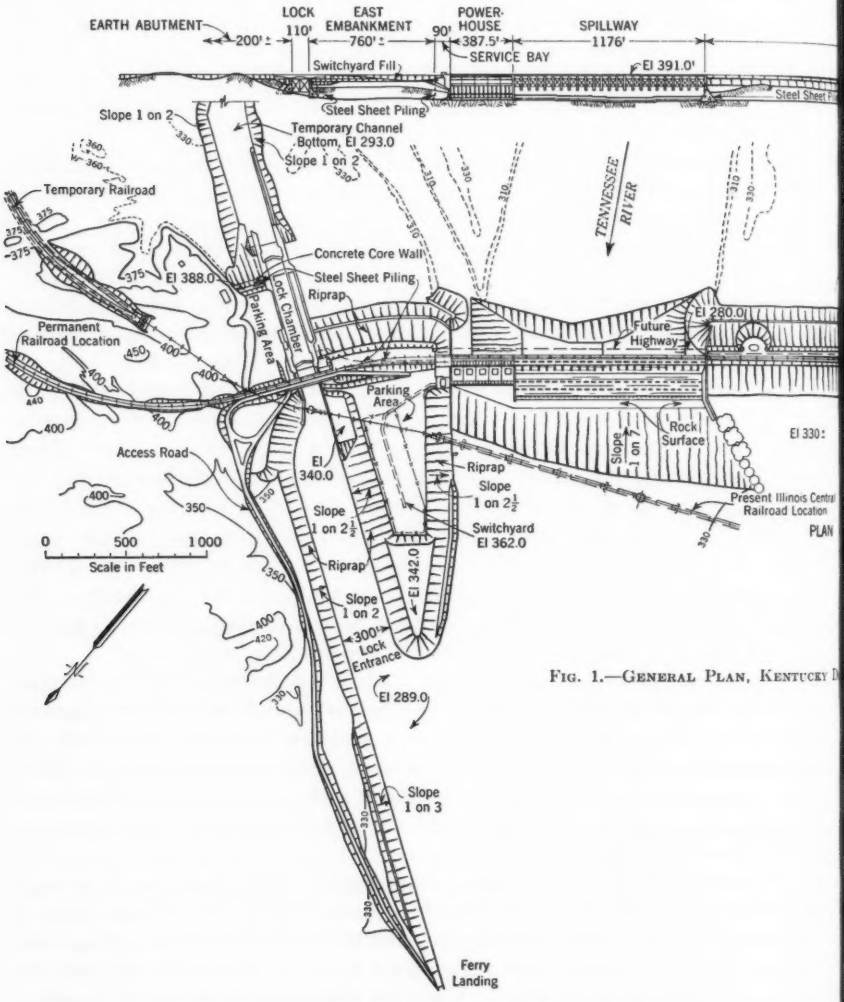

FIG. 1.—GENERAL PLAN, KENTUCKY D

These preliminary drill records (Fig. 3) indicated that there was one wide channel and a near-by smaller one probably parallel to it. The main channel at the narrowest point was approximately 70 ft wide down to a depth of 100 ft below the floor of the lock, which was at El. 289 (sea-level datum). At that point it narrowed to about 30 ft and continued another 110 ft to El. 70, with a few small cavities on one side, as shown in Fig. 3. The narrow channel was

not exposed at the rock surface under the river-wall of the lock, but there was evidence of it just downstream from the land-wall. The problem of supporting the lock-walls was solved by spanning the wide channel with deep, heavily reinforced-concrete slabs, shown in Fig. 4.

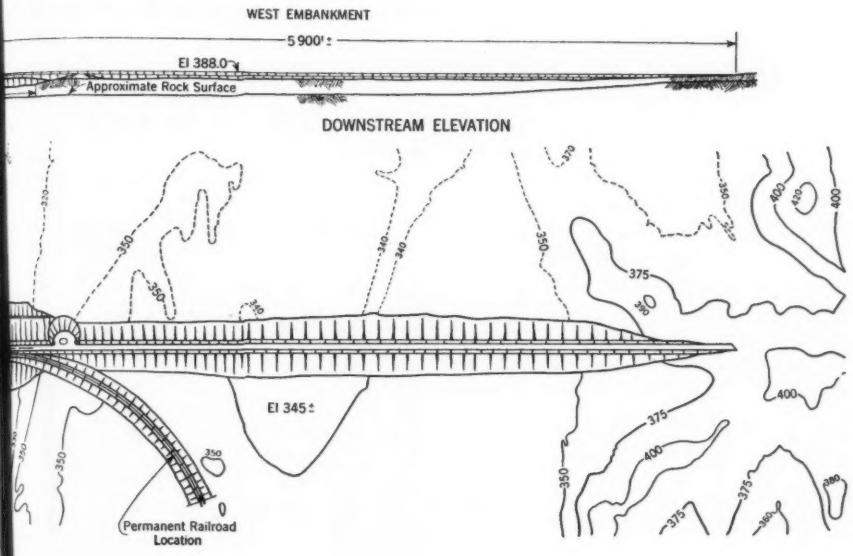

The method of making a satisfactory cutoff in the channel was discussed at considerable length. The proposal of ordinary grouting of the clay-filled channel was considered. It was felt that this would probably prove satisfactory for a time, but there would remain the uncertainty that the clay might eventually soften and be washed out by water, or pushed out by the pressure, and produce a disastrous blow.

The part of the earth dam between the power house and the lock, built on original ground, had a sheet-pile cutoff driven to rock that was originally intended to tie in to the lock-wall just downstream from the solution channel.

The final decision was to construct a definite concrete cutoff by drilling a series of holes, 36 in. and 48 in. in diameter, along a circular arc as shown in the plan, Fig. 5. These holes would be used as shafts for successively excavating small chambers and backfilling with concrete, thus creating an arch dam underground with the convex side against the water pressure. The plan view in Fig. 5 is an assumed stage in the procedure of constructing the cutoff walls. The outline of the working slab is not shown. The location was chosen to permit the underground work to proceed without delaying the construction of the lock-walls. The 48-in. holes were located over the deepest part of the solution channel since this particular drill was equipped for deep drilling. A single 48-in. hole was located to cut off the narrow channel.

The area had been grouted as well as possible. The grouting record is shown in Table 1 and Fig. 3. Previous experience had proved that it was practically impossible to drill large holes and excavate in clay-filled channels or cavities without preliminary grouting. The grout, besides filling open cavities, has a tendency to force out soft clay and to compact any that remains. On the lower two thirds of the zone, grout pressures as high as 80 to 100 lb per sq in. were used. On the upper part, pressures of from 10 to 20 lb would often blow out due to lack of sufficient cover for resistance.

TABLE 1.—BORING RECORD, WEATHERED ZONE CUTOFF WALL, EAST EMBANKMENT

Boring No. (prefix RW; see Fig. 2)	CEMENT USED (CU FT)			Refusal (see Fig. 2)	Grouting time (hr)	Date (1940)
	Stage 1	Stage 2	Stage 3			
560B–105; 45°	0	....	....	Grouted through other holes		
594B–141	460½	....	....	Ref. @ 80#–30#	32	August 6
600B–146	....	....	837	Ref. @ 60#–50#–40#	28	October 29
605B–151	96	....	....	Comp. @ 5#	1	July 19
608B–155	....	....	828½	Ref. @ 50#–40#	32	October 29
611.5B–160	....	2,765	....	Ref. @ 10#	48	September 21
619B–166	....	....	1,386	Ref. @ 40#–50#	27	October 29
626B–171	5,250	....	....	Comp. @ 0#–80#	131	August 6
629B–176	....	....	1,503	Comp. @ 5#–100#	25	November 11
631.5B–180	8,040	....	....	Ref. @ 40#	107	September 7
636.5B–185	....	....	2,210	Ref. @ 20#	19	November 10
641.5B–190	....	2,790	....	Comp. @ 0#–80#	83	September 30
645B–190; 45°	....	367	....	Ref. @ 10#	14	October 28
646.5B–195	....	....	895	Comp. @ 5#–75#	19	November 5
651.5B–200	....	1,255	....	Ref. @ 10#	32	September 20
656.5B–205	....	....	519	Ref. @ 30#	20	November 10
661.5B–210	....	4,736	....	Ref. @ 40#	58	September 30
669B–216	....	....	4¼	Ref. @ 100#	6	November 4
676B–221	584	....	....	Ref. @ 40#	8	July 19
686B–231	6	....	....	Ref. @ 100#	2	January 22
691B–236	....	10	....	Ref. @ 50#	4	October 28
696B–241	16	....	....	Ref. @ 60#	1	August 5
742B–288; 45°	....	....	....	....	....	....
701B–246	....	740	....	Ref. @ 75#–10#	16	October 28
706B–251	945	....	....	Ref. @ 60#	15	July 23
710B–255	....	20	....	Ref. @ 75#	3	October 28
714B–260	359	....	....	Ref. @ 70#	8	August 2
747B–292	....	248	....	Ref. @ 75#–10#	21	October 29
Total	15,756½	12,931	8,183¼	36,870¾ cu ft of cement		

To give the drillers a suitable place to work and to furnish the preliminary support for the first sections of concrete backfill, a thick reinforced-concrete slab was placed over the area. The surface of this slab was at El. 265. Reinforcing steel stubs were driven down into the clay, or into jackhammer holes drilled through loose rock slabs or boulders directly over the proposed concrete cutoff, to be used for anchoring the lower concrete blocks in position and prevent them from settling into the soft clay or dropping into the next excavation below. Reinforcement inserted in jackhammer holes drilled in rock was packed with clay to prevent any bond to rock that might later need to be removed. As the work progressed downward there was never any certainty that rock in the floor of a chamber would or could be allowed to remain, since any such rock might be a loose slab or boulder that would have to be removed

in the next operation. The side-walls of the channel were tested with jackhammer holes at frequent intervals.

One 48-in. and two 36-in. shot drills were set up on alternate holes. The plan, as shown in Fig. 6 (see step I), was to drill 5 ± ft below the concrete slab and excavate a chamber 6 ft wide normal to the line of the holes and half-

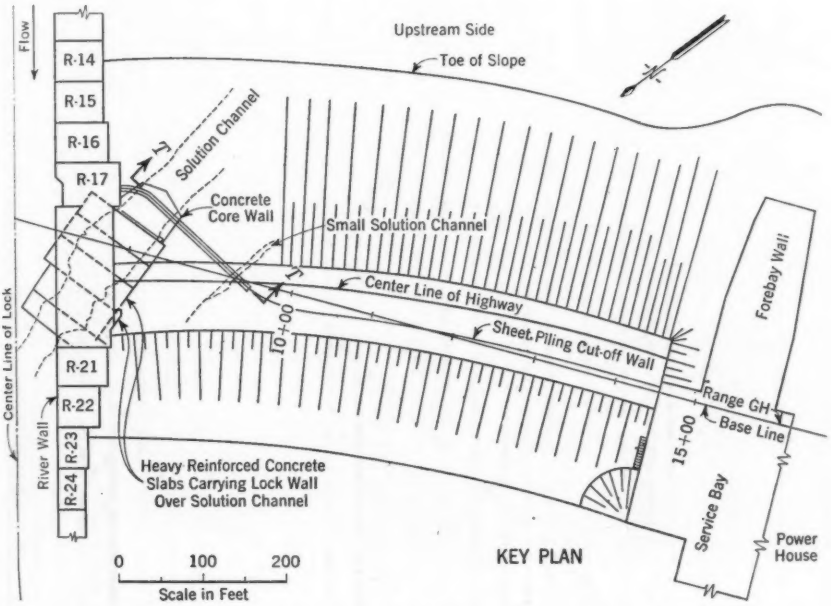

FIG. 2.—KEY PLAN OF WEATHERED ZONE CUTOFF WALL, EAST EMBANKMENT

way to the next regular hole on each side. As soon as each unit of excavation was completed, reinforcing steel stubs were driven laterally toward the two adjacent holes into the clay or into jackhammer holes drilled in boulders, and another set was driven into the floor of the chamber, lapped and tied to the steel extending down from the roof that had previously been driven into the clay below the heavy concrete mat and was exposed when the excavation was made (see dowels A, Fig. 6). The lateral steel was used to tie the blocks together and assist in arch action, since the vertical joints between blocks were quite irregular in shape. No steel was placed to come directly under the drill hole. The chamber was then filled with concrete and the drill moved to another location while the concrete hardened, to repeat the process, after which it was moved back to the first hole. The concrete that filled the first chamber was drilled through and a similar excavation was made directly under it (step II, Fig. 6). Reinforcing steel was again installed, as before, and the chamber again was filled with concrete. In filling each excavation, the concrete was placed to a depth of 2 or 3 ft in the shaft above the roof and vibrators used to force the concrete to fill the space completely.

The cycle of operations was repeated (steps III, etc.), moving the drills from one hole to another to keep up a continuous operation for the drillers and permit the concrete to harden. In some clay pockets no drilling was done, in

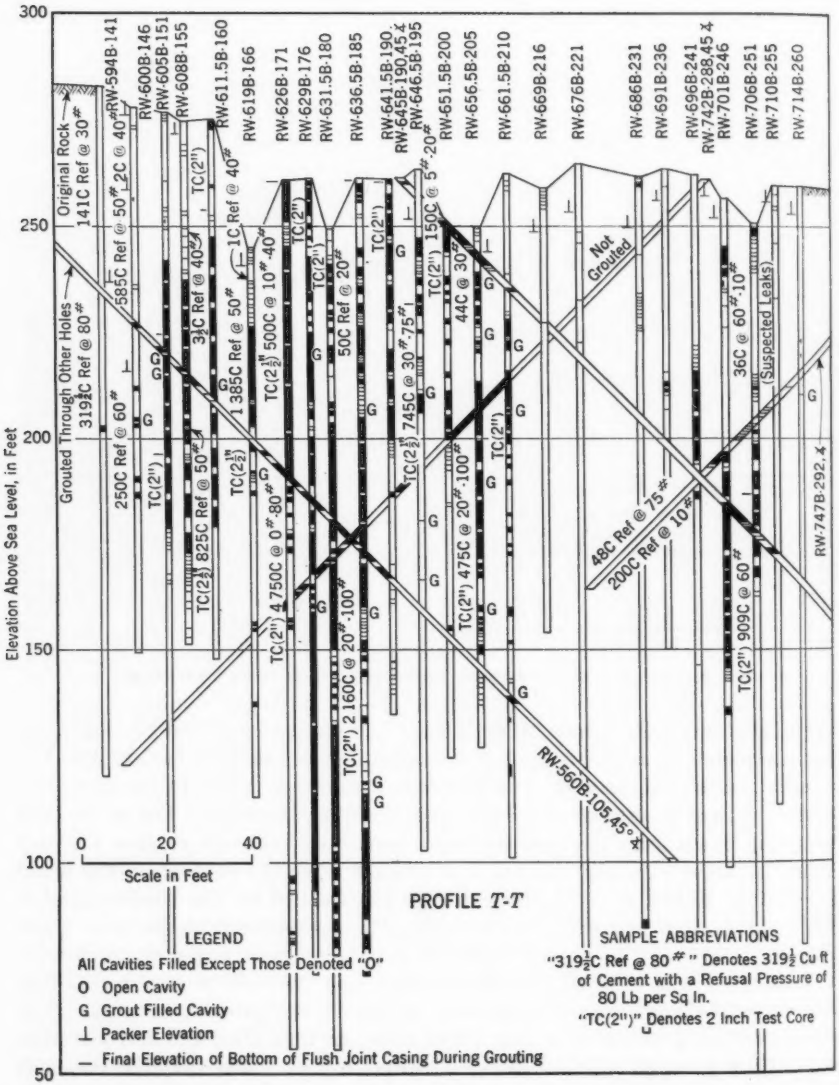

FIG. 3.—PRELIMINARY DRILL RECORDS, WEATHERED ZONE OF CUTOFF WALL, EAST EMBANKMENT

which case the drill was used only for hoisting out the muck that was excavated by hand into buckets. When contact was made with rock, a test hole was drilled by jackhammer in the center of the 36-in. or the 48-in. hole; then addi-

tional holes were drilled for dowels if the rock was found to be satisfactory. If a cavity was encountered, holes were drilled and dowels were extended into it, as before. After the first group of holes had been extended down four or five stages, the intermediate holes were started and carried down, alternating with the first set. The chambers excavated through the intermediate holes had

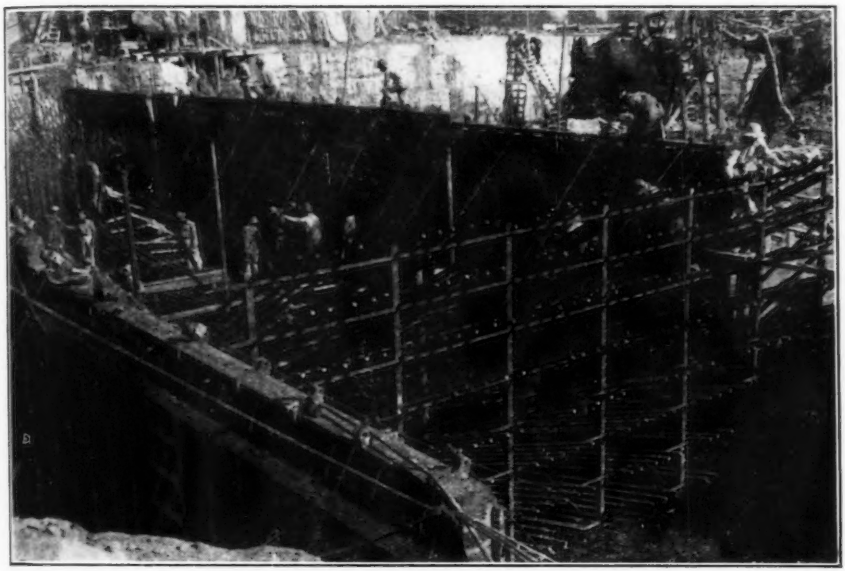

FIG. 4.—VIEW OF HEAVY REINFORCED CONCRETE SLAB

concrete on two sides, with dowels projecting from the walls as well as from the roof. Frequently these chambers were narrower than the first set, due to overbreak on the latter. In the narrow channel, the depth of excavation in each section of the hole was dependent on the conditions indicated in Figs. 7 and 8.

This series of large drill holes was started on November 16, 1940, and hole No. 6 (Fig. 8), the last one to be completed, was finished July 2, 1941. The first concrete pours were made under the slab through the large drill holes, and the drilling, mucking, and concreting proceeded in sections 5 ft to 10 ft high until the bottom was reached. To complete this cutoff required 1,763.4 lin ft of large drill holes, including holes B and C, Fig. 8.

Water leakage into the excavated chambers, which was relatively small in volume, gradually increased as the work deepened. Part of the leakage came from the drills working on other holes which usually drained into the deepest hole. Small air-driven centrifugal pumps were adequate until the head became too great. To take care of this condition, a larger chamber was opened up in hole No. 6 between El. 108 and El. 90 to be used as a relay pumping station. Hole No. 12 had followed a narrow channel and below El. 140 had been drilled deeper than the usual 6 ft before concreting and was completed earlier. In the pump room in hole No. 6 the side-walls, along the line of the cutoff, were solid

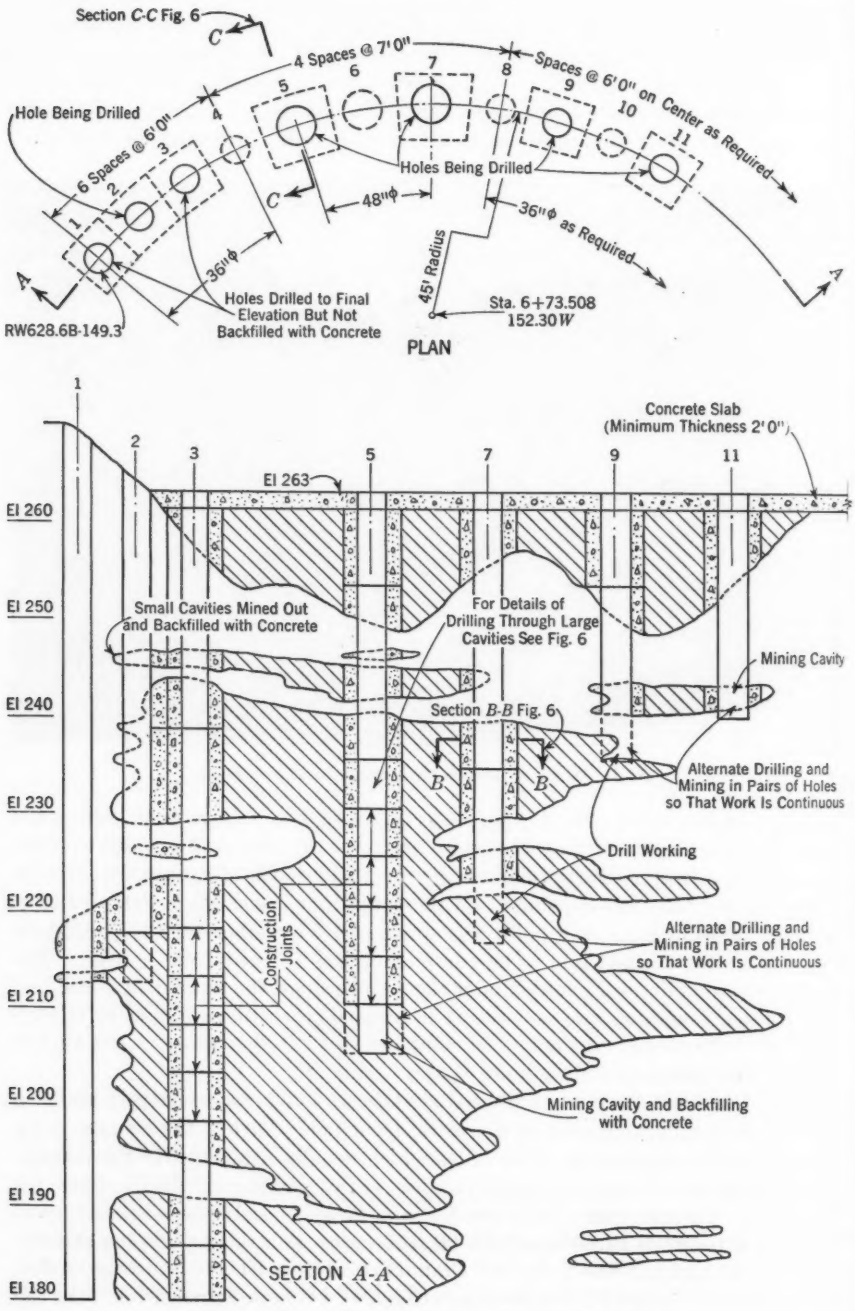

FIG. 5.—PLAN AND AXIAL SECTION SHOWING PROCEDURE

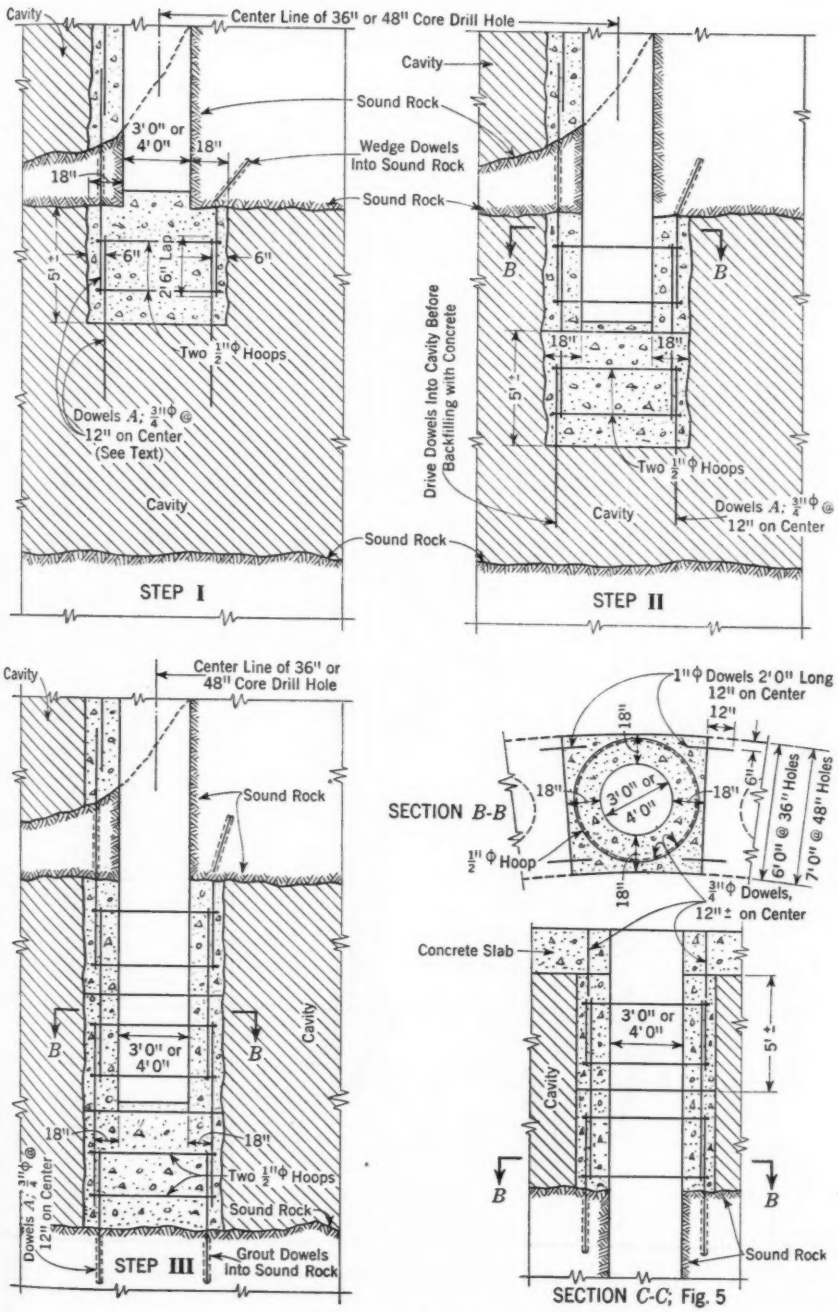
Cavity
Center Line of 36" or 48" Core Drill Hole
Sound Rock
3' 0" or 4' 0"
18"
Wedge Dowels Into Sound Rock
6"
2' 6" Lap
5' ±
Two 1" φ Hoops
Dowels A, 3/4" φ @ 12" on Center (See Text)
STEP I
Drive Dowels Into Cavity Before Backfilling with Concrete
Dowels A, 3/4" φ @ 12" on Center
STEP II
Center Line of 36" or 48" Core Drill Hole
Sound Rock
Cavity
Two 1/2" φ Hoops
Grout Dowels Into Sound Rock
STEP III
1" φ Dowels 2' 0" Long 12" on Center
SECTION B-B
1/2" φ Hoop
6' 0" @ 36" Holes
7' 0" @ 48" Holes
3/4" φ Dowels, 12" ± on Center
Concrete Slab
SECTION C-C; Fig. 5

FIG. 6.—STEPS IN THE PROCEDURE

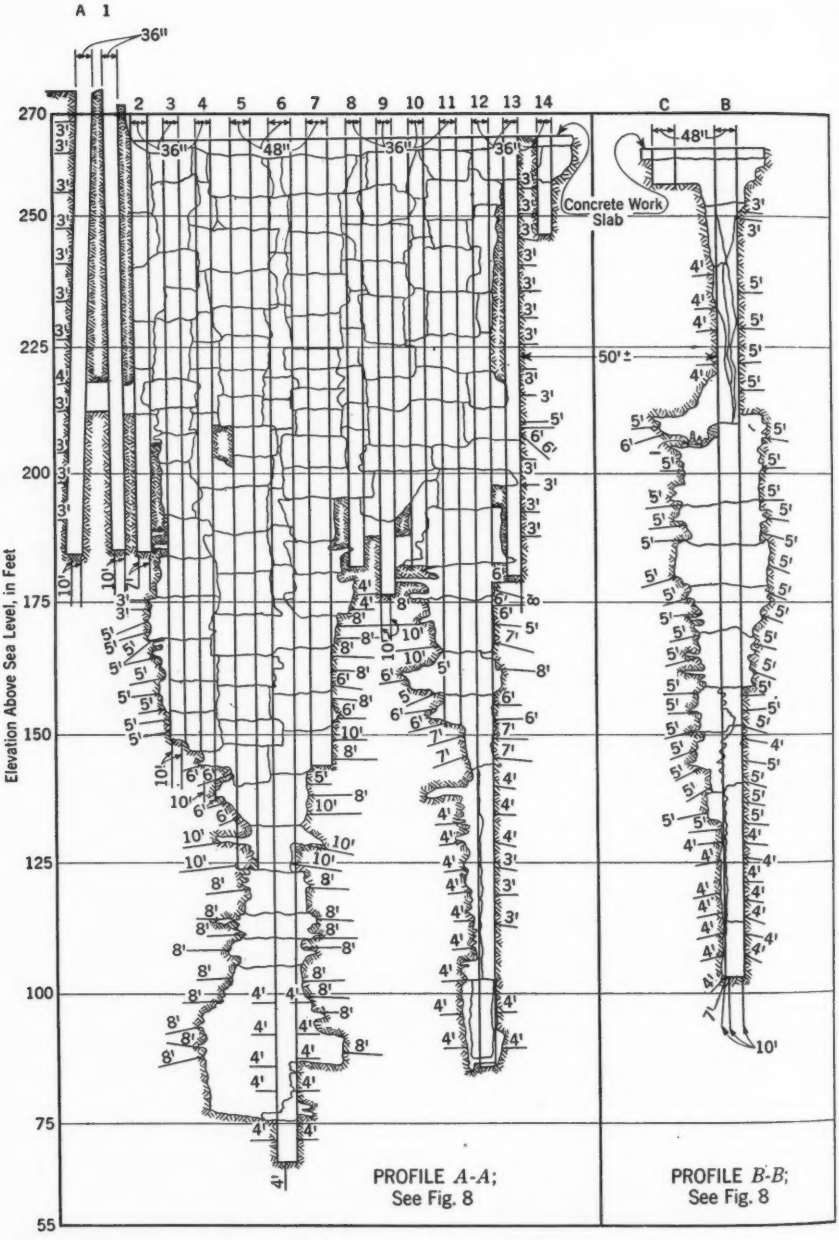

FIG. 7.—OUTLINE OF EXCAVATION, SHOWING CONCRETE POURS

rock. The upstream and downstream walls exposed grouted residual clay and were first timbered and later concreted. Test drilling with jackhammers below

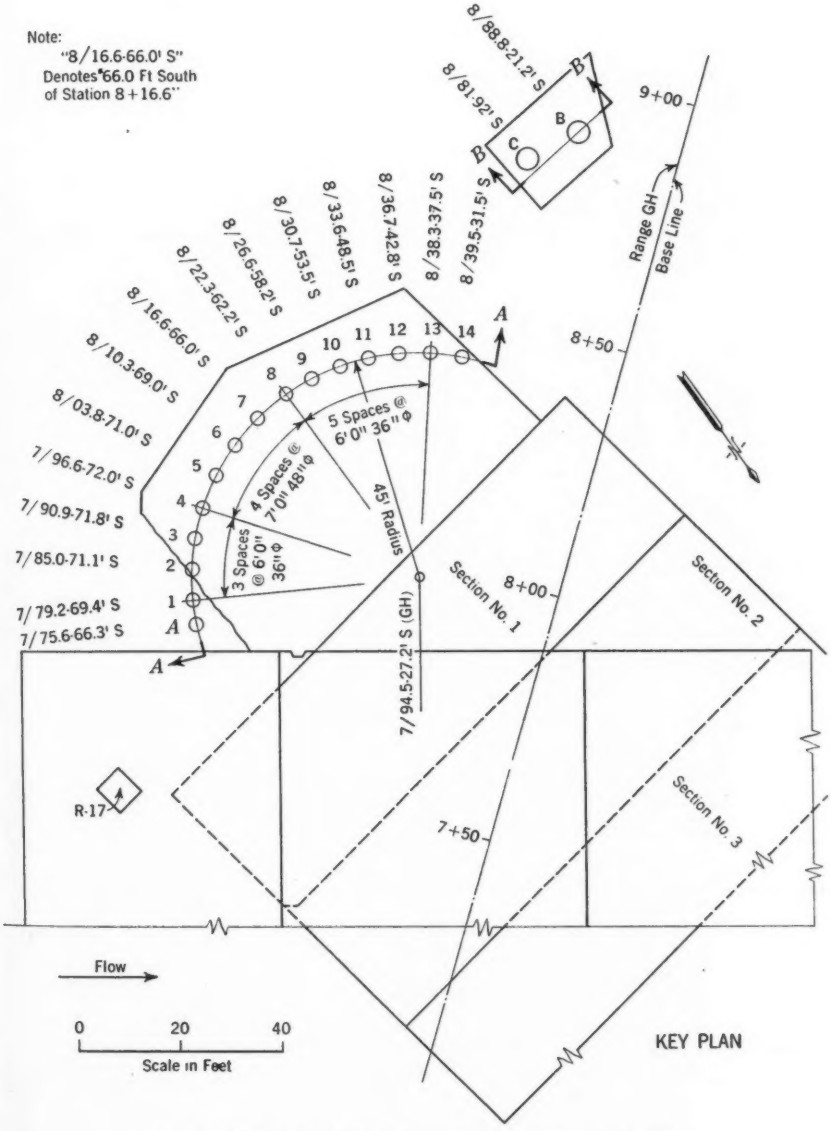

FIG. 8.—KEY PLAN SHOWING POSITION OF SECTIONS IN FIG. 7

this point indicated that the channel was narrowing. By this time the work was nearly at the level at which diamond-drill holes had indicated the existence of a channel. During the cleaning out of a narrow channel in the floor, the

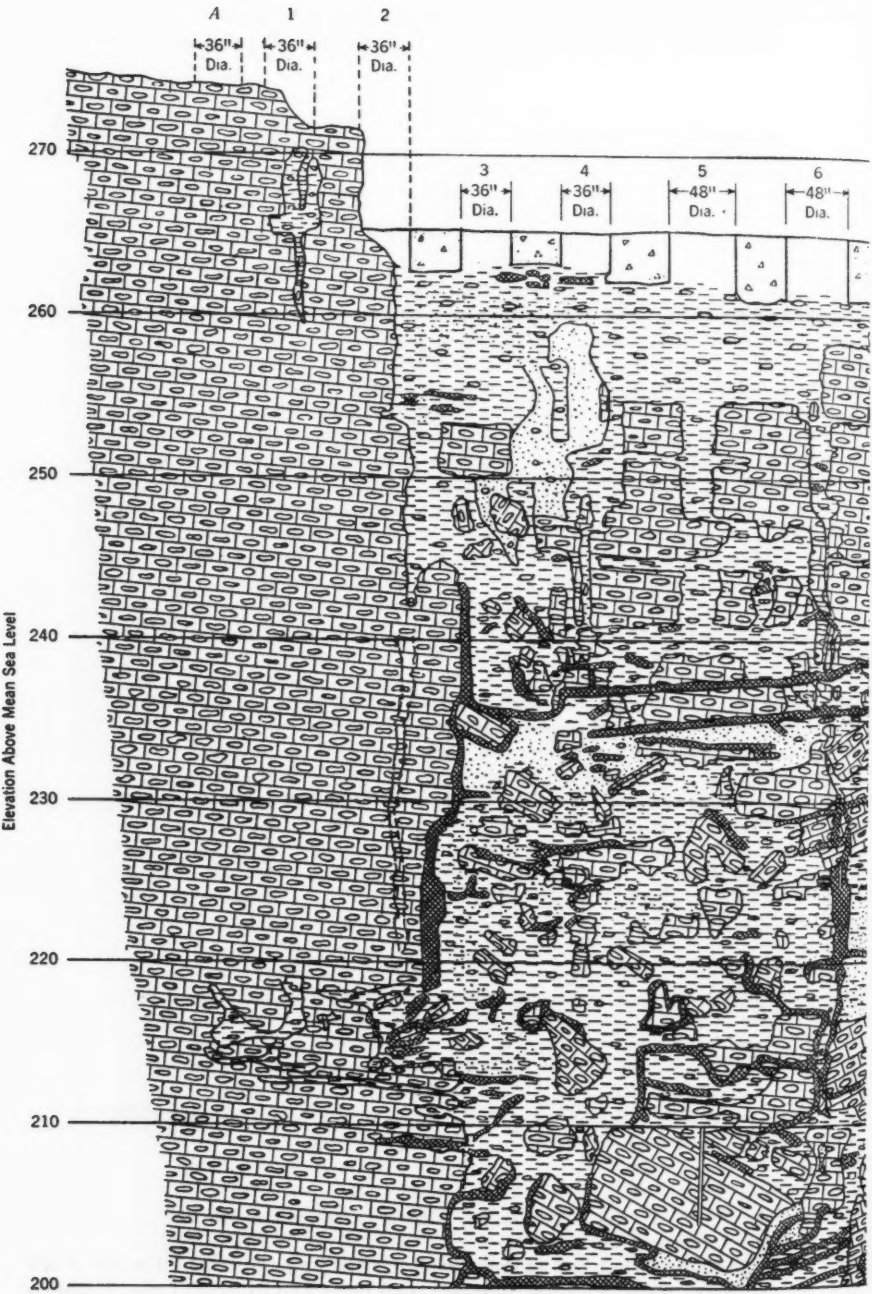

FIG. 9.—GEOLOGICAL

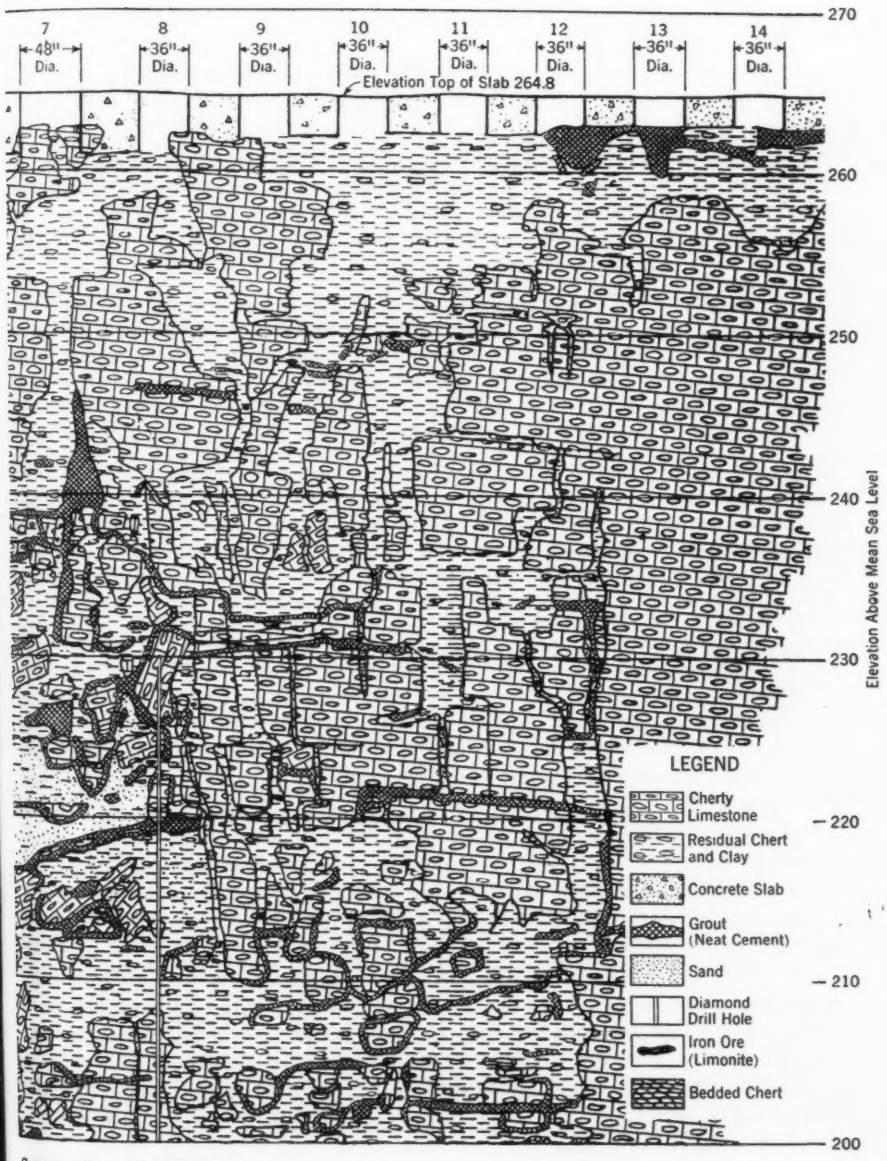

SECTION, EAST EMBANKMENT

clay began to push up from below. As the digging continued, the movement increased. Realizing that this might be dangerous, the contractor disconnected the pump and hoisted out, and the workmen then went up themselves, only a little ahead of a slowly rising column of water. The water soon flowed out of the top of the hole. The first measurement, made by pumping, gave a flow of 50 gal per min. Two hours later it had increased to 80 gal per min.

Before further work could be done on the cutoff through this hole, it was necessary to plug it and grout the lower part of the channel. To do this a 4-in. pipe was installed in the shaft, extending from the lowest point in the bottom of the 48-in. hole, at El. 87, to 3 ft above the top, at El. 268. The large chamber was filled with 3-in. crushed rock. A pump was installed with its suction inserted in the 4-in. pipe, and the water was lowered a few feet below the top of the hole to approximately El. 260. Concrete was placed over the crushed rock and well up in the 48-in. hole to seal it off, while the pump pulled the water through the 4-in. pipe.

A diamond-drill hole previously bored at approximately El. 130 between holes Nos. 4 and 5, to check and grout contact zones between blocks of concrete in the cutoff, was extended into the rock-filled chamber. Another diamond-drill hole was bored through the concrete plug to the top of the crushed rock to be used as a vent.

Grouting was started through the 4-in. pipe, from which the water had been flowing, using thick grout, 0.6 water-cement ratio by volume. In a short time the grout gate indicated no pressure. The 180-ft column of grout in the 4-in. pipe was heavier than the water pressure and created a vacuum. Eventually back pressure developed and grouting was continued until 2,297 bags of cement had been injected to a refusal pressure of 100 lb per sq in. The diamond-drill hole between holes Nos. 4 and 5 was next grouted and required 693 bags. The vent hole drilled through the concrete was deepened to El. 80 and grouted, using 3,493 bags of cement with 150-lb refusal pressure. A total of 6,483 bags of cement was used.

Drilling with the 48-in. equipment was resumed after the grout had set sufficiently. The core in the shaft had to be broken out with paving breakers, due to the 4-in. pipe which prevented breaking the core in the usual manner. The grouted broken rock below the concrete was found to be a solid mass. Jackhammer test holes indicated no pockets; hence, this material was not removed. Many of the stones were found coated with thin films of clay, but there were no continuous seams to cause leakage. The 48-in. hole was finally driven to the bottom and concreted. As a final check, diamond-drill holes were put down midway between each of the 36-in. or 48-in. holes and grouted. Fig. 7 shows the outline of each block of concrete placed in the cutoff. In the secondary channel, only one hole was drilled except where it was necessary to drill a second hole through the concrete slab at the top to fill a shallow clay-filled pocket.

The location of the sheet-pile cutoff was changed to follow directly over the underground curtain. The backfill was rolled earth and its width at this depth permitted the change.

During the process of constructing the cutoff, a detailed examination was made of the undisturbed walls and floor of each chamber just prior to backfilling

with concrete. A sketch was made of the upstream face showing the rock with its dip and strike, the residual clay, sand pockets, grout, and other rock formations. The assembly of this information to El. 200 is shown in Fig. 9. The original drawing extends downward to El. 80. There were many very thin seams and stringers of grout that were too small to indicate, and many thin seams are exaggerated in thickness. Fig. 10 is a photograph of a typical face, with arrows indicating many of the grout seams. Where diamond-drill holes were encountered, they have been shown in Fig. 9.

FIG. 10.—FACE OF EXCAVATION ON THE RIVER SIDE OF THE LINE OF CUTOFF; HOLE NO. 6 AT EL. 120

By means of this chart it was possible to develop the geology of the deep vertical solution channel, to compare the actual conditions with the original interpretations of the diamond-drill holes, and also to illustrate the results of grouting in the clay and rock-filled channel.

There is no evidence of faulting. Diamond-drill holes had been driven to 320 ft below sea level on both sides of this channel about 700 ft to the south of the cutoff. The next formation that can be identified accurately at the contact is the Chattanooga black shale at El. − 307.

The rock that was exposed in the foundation excavation had numerous vertical joints, most of which had been recemented with calcite. The genera trend of most of the weathered joints is north and south, with a secondary set at right angles. Weathered joints of all degrees of alteration have been found, and practically all of them start and develop in the same manner. Ground water readily entering the joint slowly dissolves various layers of the limestone,

but does not affect the chert layers which at first remain as rigid shelves or projections, often carrying the weight of the clay above. The residual clay at first does not completely fill the voids in the limestone. Drill holes, encountering these openings, often develop flowing water at the surface if the area has not been grouted, indicating a connection with a higher source of water. As the load on the chert, or chert and limestone, shelves becomes greater, due to the continued weathering of the lower limestone and the widening of the channels, they break down and a general slumping occurs. Strata of chert that have sagged, due to slumping, often can be traced across the weathered channel. Since the limestone is variable in its solubility, some layers dissolve more rapidly than others and many narrow seams extend outward some distance into the solid rock. These, being only partly filled, carry active waters of solution. The diamond-drill records, shown in Fig. 3, indicated open cavities near the bottom or at the sides in narrow seams with several feet of sound rock above them. No open cavities were found in the upper areas due to the slumping action in the wide part of the weathered zone, which forced clay into the horizontal lateral cavities.

A study of the effect of grout in this material is interesting. The cavities were grouted in stages, from the bottom up. Seams in massive rock were generally grouted individually. In the main body of the clay and boulders, grouting was done through the bottom of the casing which was jacked up at intervals, a foot or two at a time, until within 20 to 30 ft from the surface, where it was generally impossible to use any pressure without a blowout and no spread of grout could be obtained. It will be noted that the grout generally was found in measurable quantities adjacent to rock surfaces with main feeders often extending in a horizontal direction from one boulder to another, frequently following the layers of undissolved chert in the clay. In hole No. 6, from El. 220 to El. 225, a column of grout from 8 in. to 18 in. in diameter was found with evidence of a filled drill hole in the center. Another was found in the same hole from El. 100 to El. 108. In hole No. 7 a similar condition was found between El. 240 and El. 246.

Thin seams and isolated bulbs of grout were found in many areas. Many of the larger pieces of excavated grout were found to have pockets of clay in them. There was ample evidence that the grout had solidified the clay and packed the seams sufficiently to permit the walls to stand vertical, and without slumping, at least during the construction period.

The total work with the large drills was listed as 1,763.4 lin ft. The drills had to penetrate each section of concrete, so that the actual drilling was about twice this value. The total volume of grout used in the immediate vicinity of the cutoff was 47,198 bags before the cutoff was made, and 2,657 bags afterward. This is in addition to the amount used to stop the aforementioned sand and water flows.

Acknowledgment

T. B. Parker, M. Am. Soc. C. E., was chief engineer of the TVA, and A. L. Pauls, M. Am. Soc. C. E., is chief construction engineer. At Kentucky Dam, George P. Jessup is project manager; B. S. Philbrick, M. Am. Soc. C. E., is construction superintendent; and the writer was construction engineer, until January, 1942, when he was transferred to another project.

FLOWING WATER IN UNDERGROUND CHANNELS, HALES BAR DAM, TENNESSEE

By L. A. Schmidt, Jr.,[2] M. Am. Soc. C. E.

Synopsis

Hales Bar Dam on the Tennessee River was built by private interests (1905–1913) and is one of the classics in the annals of early dam building in the United States. Since its completion it has presented a foundation leakage problem which remained unsolved at the time the property was acquired by the Tennessee Valley Authority (TVA) in 1939. Previous efforts to correct the leakage were varied and numerous and inevitably resulted in only temporary improvement. Leakage has been progressively greater until a flow of 1,700 cu ft per sec was measured as ungainfully passing just before the present work by TVA was begun in 1940. A cutoff wall was placed in the foundation leakage area just upstream of the dam to reduce flows, and the foundation was stabilized by placing concrete, cement, and asphalt grout in the foundation under the structure. Special equipment and methods were required and devised to do this work without interrupting the hydroelectric power operations.

Among the more unique core drilling projects in the United States to date is the foundation treatment given to Hales Bar Dam on the Tennessee River, thirty-three river miles downstream from Chattanooga, Tenn. Fig. 11 is a general view of the spillway, facing upstream from the top of the south control house on the river-wall of the lock.

On heavy construction core drills are frequently used for exploration and for determining excavation requirements both as to equipment and to yardage involved. At Hales Bar core drills were used for excavation, cutting out some 35,000 lin ft of 18-in. hole and removing several thousand cubic yards of badly leaking foundation rock. This material was replaced by concrete specially placed in a predetermined pattern to effect a cutoff wall under this historical river barrier.

Stories describing many previous attempts to stop leakage at Hales Bar are legend, and the colloquial narratives are sufficiently enigmatical to intimidate engineering efforts that challenge the flow of water in the underground channels. To understand this leakage problem one must delve back to 1905–1913, the time the dam was built by private interest for hydroelectric power and for navigation improvement in the Tennessee River to Chattanooga. Even then foundation leakage into cofferdams under only nominal differential

[2] Acting Constr. Engr., TVA, Hales Bar Dam, Chattanooga, Tenn.

heads was great enough to force the constructors to build a part of the dam by the use of pneumatic caissons. After the reservoir was filled leakage in the foundation was detected from water boiling up on the downstream side of the dam.

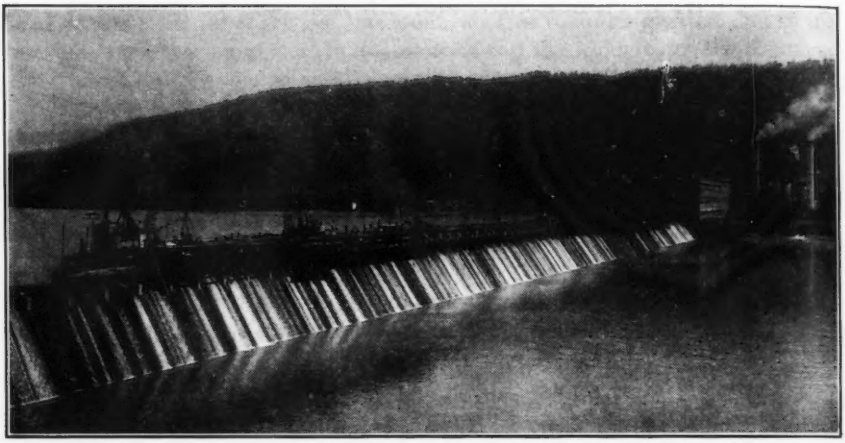

FIG. 11.—SPILLWAY OF HALES BAR DAM

The dam is built on the Mississippian limestone formations of this vicinity (see Fig. 12). Leakage at Hales Bar exists principally in the foundation under the dam. Noticeable points of suction have been found in the reservoir and the path of flow from these points to the visible boils downstream has been traced with dye. Leakage is caused by three principal foundation defects:

1. Washing out of the shales in horizontal bedding planes, causing horizontal openings (note, in Fig. 12, at El. 503.3 a piece of typical quartz with Golconda shale sticking to it was found where it had fallen from above);
2. Solution of calcites, forming vertical solution channels; and
3. Faulting.

Defect 3 probably caused very little leakage and was handled fairly easily. Defect 1 contributed considerable leakage, but when such planes were found they were readily corrected. Leakage from this cause also seemed to exist in serious quantities only in the upper foundation reaches from 2 ft to 30 ft below the foundation rock level. Defect 2 contributed greatly to leakage and through its far-reaching labyrinth of passages, some of which extend to considerable depth, large quantities of water eluded the engineer's plans and efforts to stop this waste of potential hydroelectric energy.

As early as 1915, L. C. Glenn,[3] wrote as follows:

[3] "Geology Applied to Dams and Reservoirs," by L. C. Glenn, *Proceedings*, Eng. Assn. of the South, Vol. 26.

(a) COLUMNAR SECTION IN LOOKOUT MOUNTAIN SYNCLINE

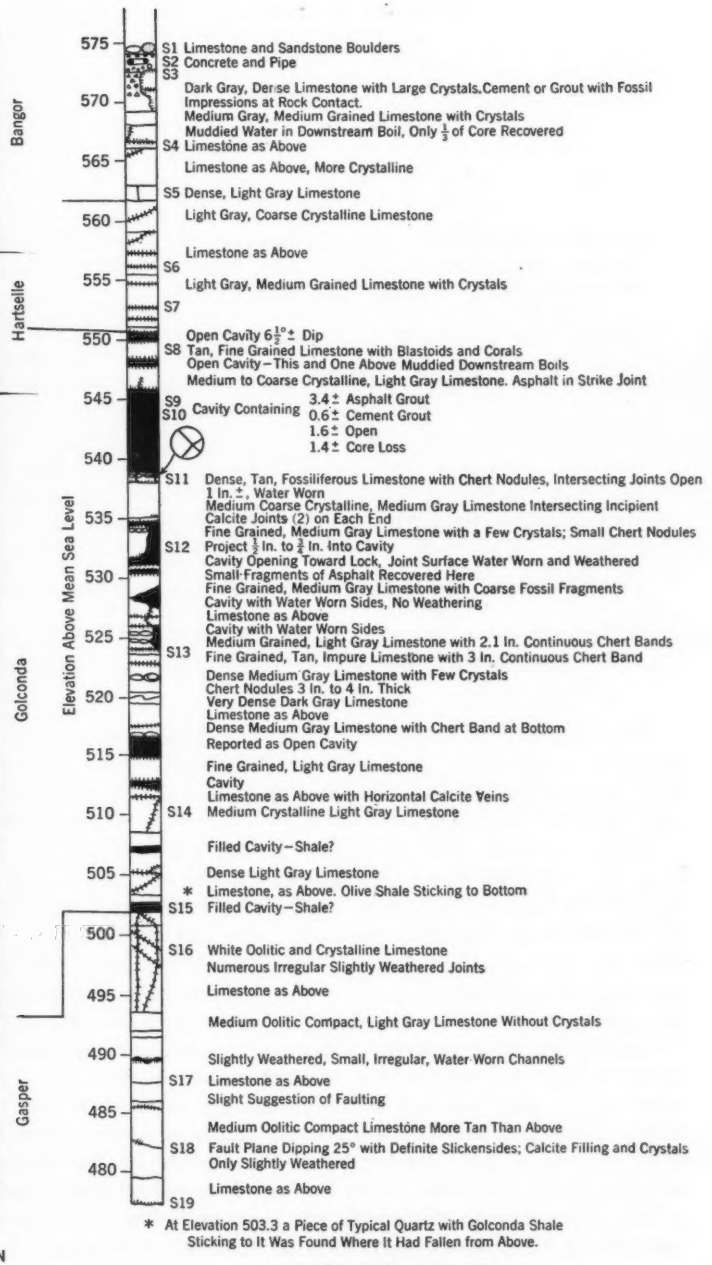
Bangor
Hartselle
Golconda
Gasper
Elevation Above Mean Sea Level
575
570
565
560
555
550
545
540
535
530
525
520
515
510
505
500
495
490
485
480
S1 Limestone and Sandstone Boulders
S2 Concrete and Pipe
S3
Dark Gray, Dense Limestone with Large Crystals. Cement or Grout with Fossil Impressions at Rock Contact.
Medium Gray, Medium Grained Limestone with Crystals
Muddied Water in Downstream Boil, Only 1/3 of Core Recovered
S4 Limestone as Above
Limestone as Above, More Crystalline
S5 Dense, Light Gray Limestone
Light Gray, Coarse Crystalline Limestone
Limestone as Above
S6
Light Gray, Medium Grained Limestone with Crystals
S7
Open Cavity 6 1/2° ± Dip
S8 Tan, Fine Grained Limestone with Blastoids and Corals
Open Cavity—This and One Above Muddied Downstream Boils
Medium to Coarse Crystalline, Light Gray Limestone. Asphalt in Strike Joint
S9
S10 Cavity Containing 3.4 ± Asphalt Grout
0.6 ± Cement Grout
1.6 ± Open
1.4 ± Core Loss
S11 Dense, Tan, Fossiliferous Limestone with Chert Nodules, Intersecting Joints Open 1 In. ±, Water Worn
Medium Coarse Crystalline, Medium Gray Limestone Intersecting Incipient Calcite Joints (2) on Each End
Fine Grained, Medium Gray Limestone with a Few Crystals; Small Chert Nodules
S12 Project 1/2 In. to 3/4 In. Into Cavity
Cavity Opening Toward Lock, Joint Surface Water Worn and Weathered
Small Fragments of Asphalt Recovered Here
Fine Grained, Medium Gray Limestone with Coarse Fossil Fragments
Cavity with Water Worn Sides, No Weathering
Limestone as Above
Cavity with Water Worn Sides
Medium Grained, Light Gray Limestone with 2.1 In. Continuous Chert Bands
S13 Fine Grained, Tan, Impure Limestone with 3 In. Continuous Chert Band
Dense Medium Gray Limestone with Few Crystals
Chert Nodules 3 In. to 4 In. Thick
Very Dense Dark Gray Limestone
Limestone as Above
Dense Medium Gray Limestone with Chert Band at Bottom
Reported as Open Cavity
Fine Grained, Light Gray Limestone
Cavity
Limestone as Above with Horizontal Calcite Veins
S14 Medium Crystalline Light Gray Limestone
Filled Cavity—Shale?
Dense Light Gray Limestone
* Limestone, as Above. Olive Shale Sticking to Bottom
S15 Filled Cavity—Shale?
S16 White Oolitic and Crystalline Limestone
Numerous Irregular Slightly Weathered Joints
Limestone as Above
Medium Oolitic Compact, Light Gray Limestone Without Crystals
Slightly Weathered, Small, Irregular, Water Worn Channels
S17 Limestone as Above
Slight Suggestion of Faulting
Medium Oolitic Compact Limestone More Tan Than Above
S18 Fault Plane Dipping 25° with Definite Slickensides; Calcite Filling and Crystals Only Slightly Weathered
Limestone as Above
S19
* At Elevation 503.3 a Piece of Typical Quartz with Golconda Shale Sticking to It Was Found Where It Had Fallen from Above.

(b) LOG OF TYPICAL DRILL HOLE, HALES BAR DAM

FIG. 12.—COMPARISON OF MISSISSIPPIAN FORMATIONS IN LOOKOUT MOUNTAIN AND AT HALES BAR DAM

"No better illustration of the serious dangers from solution channels in limestones could be given than to cite the Hale's Bar dam on the Tennessee River near Chattanooga. The Bangor limestone, very pure, highly soluble and generally noted for its caves, forms the bed rock, and extends downward for some hundreds of feet beneath the river channel. This limestone was honey-combed with intercommunicating solution channels, some of which were choked with sand, gravel and cobbles, while others carried water under pressure. Excavation was carried some distance down into this rock and the foundation was thoroughly drilled and grouted, several hundred thousand barrels of cement being pumped into these openings. This honey-combed foundation caused a delay of several years in the completion of the project and increased by five or six million dollars, or more, the cost of construction.

"The writer is by no means certain that the troubles there from leakage are ended, since geological examination shows the dam to be located on a syncline, or trough, in the Bangor limestone, and this means that the lower portion of this limestone there is the stretched member of the curved mass, and this tension, caused by the folding, undoubtedly opened joints in the lower part of the limestone and these filled with water under very considerable pressure would yield to solution more rapidly than the part up near the surface, so that the lower part is probably more open than the upper part that has been grouted, and the tendency will be, with the added head above the dam, for the water to work its way beneath the dam through these lower lying fissures and channels in constantly increasing quantities."

The reasons for correcting the leakage condition at Hales Bar were twofold:

1. To save water for power during periods of low flow; and
2. To protect the investment in this property against failure of the foundation.

The value of lost energy can be capitalized to determine a sum that may be expended economically, but economic considerations for the latter may range from the extreme of laissez-faire to that for a complete new project, in accordance with the individual opinions as to the urgency of this work.

From October 1, 1940, to October 1, 1941, there were 277 days during which river flow at Hales Bar was less than turbine capacity. Assuming that the demand for electrical energy existed during that period, a total of more than 26,500,000 kw-hr was lost. Similarly, between October 1, 1941, and October 1, 1942, the equivalent of nearly 21,000,000 kw-hr was lost. No one can gainsay but that, during these two years, the drought and then the war have demanded the conservation of every potential kilowatt-hour available.

Besides stopping leakage to increase the quantity of water available for power, it was essential that these large openings be filled to secure the bearing value of the rock foundation for permanent stability to the dam structure itself. This work was also a necessary step preparatory to raising the headwater level to El. 634, which will provide a 9-ft navigation channel to Chickamauga Dam in Tennessee, when the dam is raised after the war.

The first efforts to stop the flow in the foundation consisted of placing inert materials of many descriptions into the upstream suction inlets. These inlets were discovered when exploring for the cause of boils which appeared in the tailwater under full hydrostatic pressure as a result of filling the reservoir to

dam-crest level; but any success in this effort was short lived since flow broke out elsewhere.

In the early 1920's, corrective work was attempted by pumping more than 11,000 bbl of asphalt into the foundation by way of the newly invented hot electric wire process on which a patent was later granted. This treatment was partly effective in stopping some of the flow, but was of doubtful value for bearing purposes. Leakage increased again later to the 1940 flows, so that evidently these leaks broke out in other places, probably by additional washing of clays and shales which the asphalt could not displace or penetrate. Some credence to this theory is available from the logs of the present drill holes. Invariably open cavities either above or below, or both, were found to exist when the old asphalt was encountered. It is now believed that, if an intensive cement grouting program had followed the asphalt grouting to effect consolidation of the foundation and to confine the asphalt, the leakage problem might have been solved at that time. The years that elapsed following the completion of this work enhanced the obstacles to be overcome in effecting a barrier to this leakage so that the methods used in the decade 1920–1930 no longer were effective, at least in some areas. The predominant leakage occurred in two areas as indicated in the elevation in Fig. 13. To some extent cavitation, as shown in this figure, is hypothetical since these cavities were projected from drill logs of holes all drilled in the same vertical plane, and since much of the predication of these cavities was based on core loss, probably due to drilling through vertical seams in many cases (see Fig. 14). However, the interlocking and water-carrying connections of these cavities are well established and the openings, as they are shown, are at least representative. The general pattern of cavitation is verified by 13-in. and 3-in. holes drilled later through the dam, and downstream from the upstream face.

The approach of the TVA to the problem has been based on placing a watertight diaphragm across the valley in the bedrock below, and just upstream from the upstream face of the dam. To secure this effect, it was proposed to drill and grout the foundation wherever feasible by conventional methods. Where the openings were not groutable, special grouts were developed, and, if these failed, recourse was had to a lined cutoff trench filled with concrete to cut off the through passage of water.

Water in the reservoir stands at about El. 628.5. Overburden is at approximately El. 583, foundation rock, 573, and apparent lowest cavities 481. To maintain a full reservoir for power, which is indispensable for war industries, it was necessary to devise some means of excavating for the cutoff through 55 ft of water and for depths as great as 92 ft below that point.

The first step was to sink NX size diamond-drill holes 20 ft on centers, and approximately 125 ft in solid rock, across the entire length of the dam. These holes were water tested, air tested, and dye tested by stages, using a $1\frac{1}{2}$-in. pipe extending down the hole, and a unique quick-breaking and quick-sealing packer at the bottom. This packer was developed on other TVA work and operated so satisfactorily that its adoption at Hales Bar was a natural consequence.

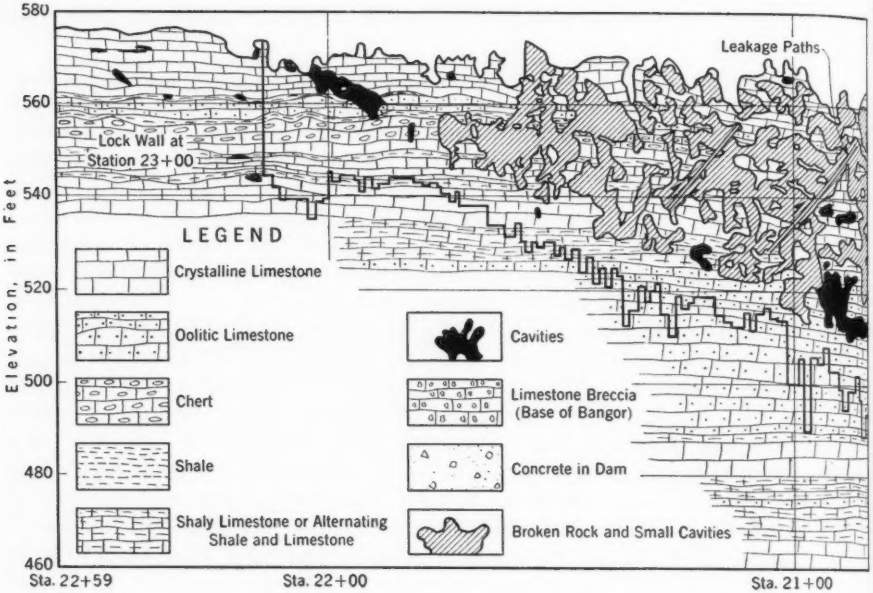

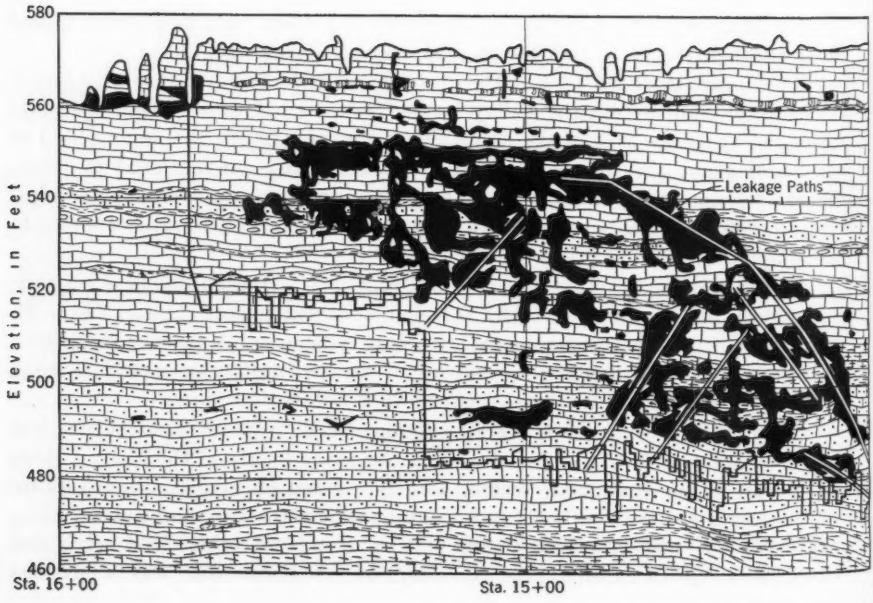

FIG. 13.—CROSS SECTION THROUGH THE FOUNDATION

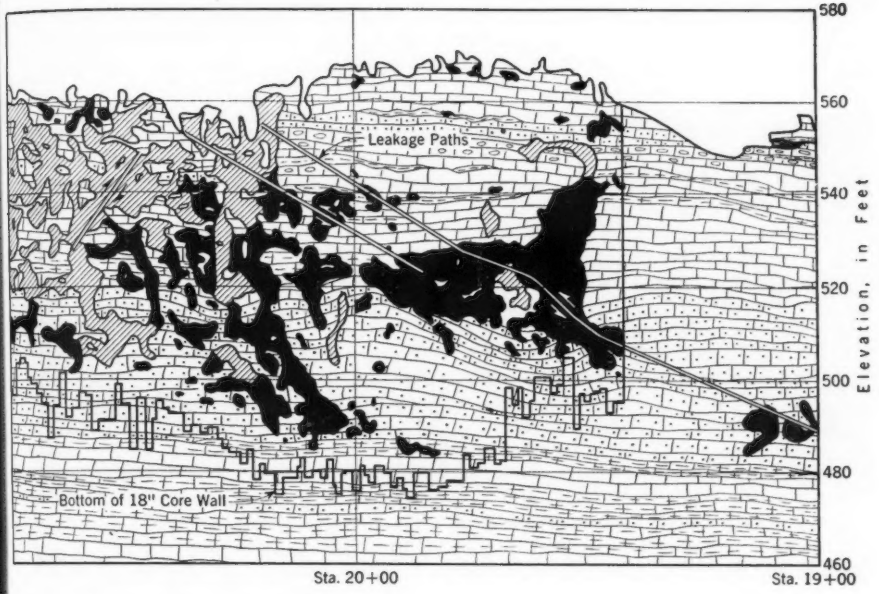

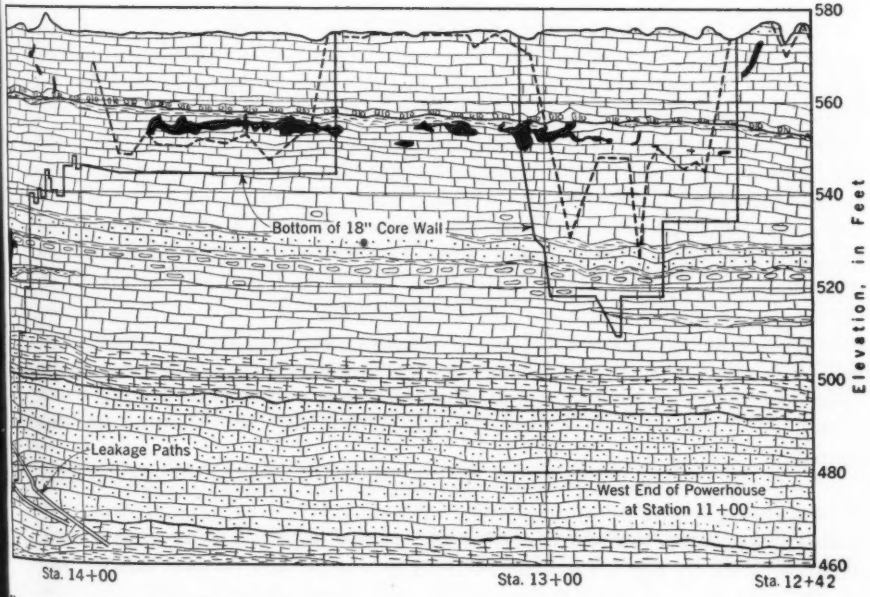

Under Hales Bar Dam, Facing Upstream

The water tests were made to determine the level to which grouting would be feasible and the type of grout to be used. Air and fluorescein dye tests established the paths of the underground connecting channels. Cavities,

FIG. 14.—TYPICAL CAVITY, AS REVEALED BY 18-IN. DRILL HOLE CORES

penetrated by holes at different levels, each connecting with different boils in the tailwater were found. The intensity of the coloring was a measure of the quantity of flow, and the travel time from the time the coloring was placed in the hole until it appeared downstream was noted carefully to establish a velocity index. Figs. 13 and 15 show the outlets and leakage paths established by these tests.

These NX holes were then grouted to as high a level as feasible under pressure varying from 30 to 70 lb per sq in., depending on the depth of rock penetrated. Grouts of consistencies varying in water-cement content from 1.0 to 0.5 were used progressively, made from neat cement, neat cement mixed with as much as 6% calcium chloride by weight of cement to accelerate the set, grouts with cottonseed hulls added, grouts "sweetened" with quick-setting property admixtures, and asphalt, depending on the characteristics of the holes. Asphalt was used only when cement grouts proved to have been lost, and then only in seams carrying water and in holes that were apart from the cutoff trench areas where it would not be feasible to extend this cutoff trench to the seam penetrated. Wherever asphalt was used it was followed immediately by cement grout for confining and consolidating the asphalt, and adjacent holes were cement grouted to assure this effect. Excellent results have been achieved by hot asphalt grouting where stoppage of flowing water is the only consideration, bituminous material being very effective for this purpose.

Wherever holes could be grout-filled to the rock surface, secondary holes were drilled midway and grouted. Additional holes at still closer spacing were drilled and grouted, as required, until the area was tight. The average volume of grout taken by the foundation per foot of hole drilled for the various hole spacings in groutable areas was as follows:

Spacing of holes (ft)	Cu ft grout per ft drilled hole
20	6.25
10	5.20
5	3.60
$2\frac{1}{2}$	1.60

Diamond-drilling speeds varied greatly due to difficulties encountered in setting the casing and other features of drilling through 60 ft of water, many

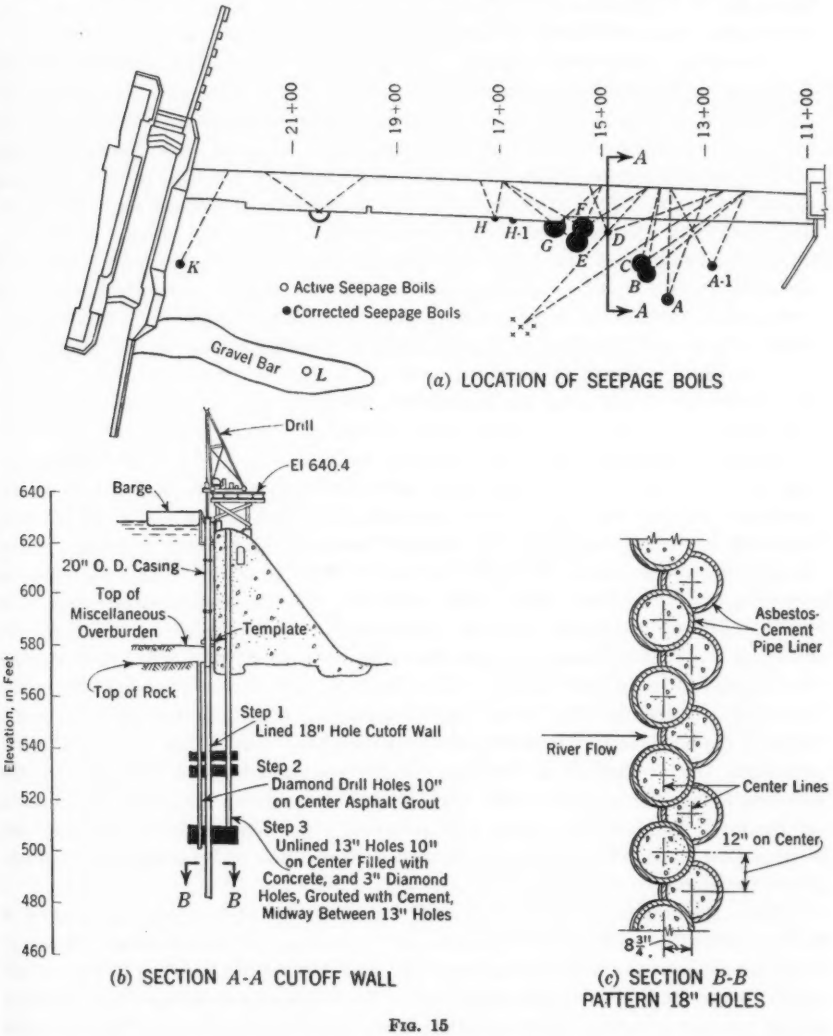

(*a*) LOCATION OF SEEPAGE BOILS

(*b*) SECTION *A-A* CUTOFF WALL

(*c*) SECTION *B-B* PATTERN 18" HOLES

FIG. 15

of which were not comparable with other jobs. In good operating, after the casing was set, 20 to 30 ft were drilled easily in one 8-hr shift. Cast-set bortz

bits were used for the most part although some work was done with tungsten-carbide-faced blank bits. The bit cost on this job was high—approximately 60¢ per foot—but it was caused by drilling in old construction territory, where it was common experience to drill through reinforcing bars, old pipe, timber, bolts, caving holes, asphalt, concrete, and many other burdensome inert materials.

The only effective and permanent cutoff across the leakage areas was felt to be a continuous concrete wall in the foundation under the dam. It was desirable to do this work without lowering the reservoir so that some novel excavating process had to be devised to accomplish this desired result.

Numerous ideas were studied. In the first experimental drilling, the plan was to core drill large diameter holes and line them with fabric and rubber bags, line-drilling the overlapping holes; but numerous defects developed which led to the evolution of the method of drilling 18-in. holes 24 in. on centers, lining them with asbestos-cement pipe, and concreting inside the asbestos-cement pipe by tremie. This step was followed by drilling intersecting holes $8\frac{3}{4}$ in. upstream and midway between the other two, again lining and concreting, using the velocity of the water to draw the liner against the previously concreted holes for a seal (see Fig. 15(*c*)). Thus a continuous cutoff, either by conventional grouting or by concrete placed into lined holes excavated by core drills, was constructed to depths required as predetermined by the cores from NX size diamond-drill holes, water and dye tests, and grouting. This excavation varied in depth from 20 to 100 ft. With this cutoff in place, the entire foundation could then be consolidated as follows (see Fig. 15(*b*)).

After completing the 18-in. drilling and concreting, diamond-drill holes were driven upstream from the new cutoff on 10-ft centers and the upstream openings were grouted by cement or asphalt to perfect the seal. These were followed wherever necessary by similar treatment at closer spacing. Later 13-in. holes were drilled through the dam, 6 ft to 10 ft on centers tapping the cavities, and these were filled with concrete. Diamond-drill holes were then drilled through the dam midway between the 13-in. holes for final cement grouting. All these holes through the dam, both 13 in. and 3 in., demonstrate the effectiveness of the cutoff. The diamond-drill holes upstream from the lined cutoff were also dye tested before asphalt grouting and these indicated a marked decrease in dye intensity and an increased travel time which, in turn, indicated the reduction of leakage, to the magnitude of a seepage, by the construction of the cutoff wall. Some asphalt grouting through the dam in particularly troublesome areas was required. In general such grouting was required for localized seepage, and it was always followed by concrete or cement grout for effective consolidation.

Since the linear feet of cutoff wall represent an undetermined number of holes, it was desirable to drill holes of as large diameter as possible. However since access into the hole to remove cores was impossible because of the underwater nature of the work, the diameter of the holes was restricted to a size that would permit breaking and removing cores by gravel-grouting the core into the core barrel. Eighteen-inch holes at depths prevailing on this job appeared to be the probable upper limit, as recommended by the drill manufacturers,

and this size was adopted. The selection of this size seems to have been well justified since no insurmountable obstacles were encountered in pulling cores although the bottom pulls in good rock were usually difficult, thus assuring contact of the cutoff trench with good foundation rock, and confirming geologists' predictions. It is believed that 20-in. or even 24-in. holes probably could have been used down to the level of good rock; but material scarcity caused by the national emergency precluded changing tools and casings to try the larger diameter.

The selection of the correct drill for such highly specialized excavation was very important. Preliminary experimental drilling was done with a 35-hp gasoline-driven 36-in. shot core drill. The results of this test indicated the desirability of having a heavier and more rugged machine, and 48-in. machines were specified for the work. These were built from standard parts to TVA specifications for a machine particularly adapted to the Hales Bar work but also one that could be used elsewhere. Nine of these drilling units were used, and were equally adaptable for the 18-in. and 13-in. drilling which was done.

Water for feeding shot to the drill bit and washing up the sludge was supplied from two 60 gal per min, 250-lb electric-driven pumps set up on the trestles at opposite ends of the drilling operations. The pumps were connected by a pipe line running along the downstream edge of the trestle, and a sufficient number of take-offs were left in this line to make quick hose connections to any drill at any time.

Air for operating the air-driven hoists, grouting, cleaning out holes, and testing was furnished from two 315 cu ft per min portable compressors permanently placed on the left bank of the river upstream from the power house. These were replaced later by one electric-driven 1,500 cu ft per min stationary compressor. Air was piped from the bank along the downstream edge of the trestle with sufficient take-offs to permit hose connections wherever desired.

Electric power was brought to the trestle from a bank of three 250-kw 44,000/2,300-v transformers in a substation on the left bank of the river, downstream from the power house. A 2,300-v bus line was suspended on cross arms over the downstream side of the trestle, to two sets of three each, 112.5-kw 2,300/440/220 v and one set of three 150-kw 2,300/440/220-v transformers; whence power was delivered to the drills in conduit to steel outlet boxes near the upstream side of the trestle and conveniently arranged so that all drills could be fed within a minimum distance. Three-conductor cable with three-pronged plugs for plugging in at these boxes made quick connections possible whenever the drills were moved.

Where there was 50 to 70 ft of water on the surface, the casing had to be at least 60 ft long and sufficiently rigid to insure that the boring itself was absolutely plumb. For this purpose 0.5-in. wall, 20-in. steel pipe (outside diameter) with cast-steel flanged couplings was selected. These three-ton casings were rotated into place, which is a most effective procedure at slow speeds. Drilling in old asphalt also slowed up the speed of rotation where horsepower was required. When the workers were drilling through cavernous areas with only one side of the bit riding on rock, high speeds and slow feeds were required but momentary horsepower was also high.

For continuous and satisfactory drilling, it was desirable, therefore, that the driving motors on the drills have multi-speed control and constant horsepower. Four-speed electric motors, of 40 hp, were specified. The efficacy of using this much horsepower has been proved in drilling holes where velocities are high. For lifting tools one 3,500-lb line-pull electric hoist and one 2,000-lb line-pull air hoist were specified. The drill derrick was designed to move back for available hook work over the hole with outside live boom equipment. The manufacturers devised a unique eccentric arrangement for this purpose and

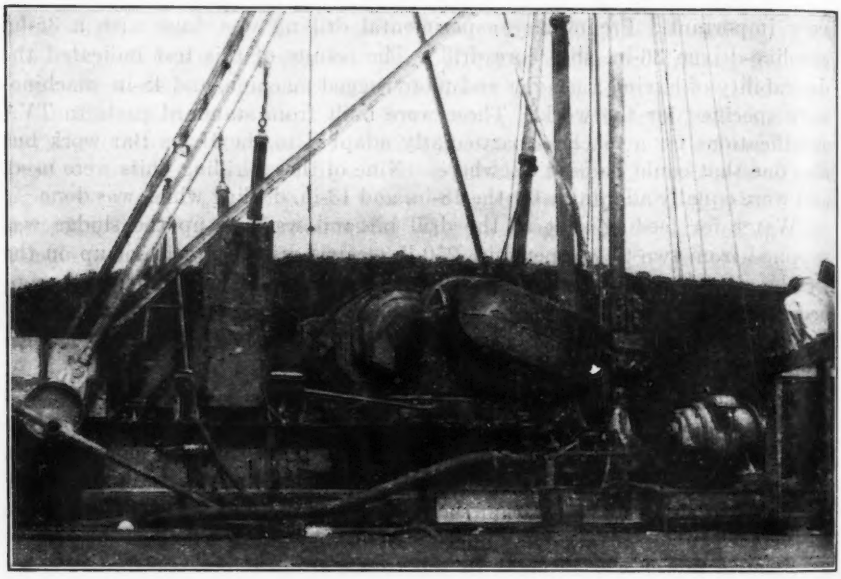

FIG. 16.—VIEW OF 48-IN. CORE DRILL

also built the five-head block sheaves and two-lead sheaves into the crown block of the derrick, resulting in a maximum available headroom and flexibility for reeving lines to the two hoists. Hoists were arranged for individual mounting, one on each side of the drill, and the operator worked up in front where he had a clear unobstructed view of operations (see Figs. 16 and 17).

Drill rods were of the 4-in. box and pin type since it would have been impossible to recover broken nuts or bolts of flanged type rods from a completely submerged hole. Oil-well type wrenches were used to break joints, the rods being supported on elevators and forks on the 20-in. casing. The cavernous condition of the foundation produced much pounding through the rods and the powerful 40-hp motors made these rods up very tight. Wrenches capable of 56,000 ft-lb of torque broke consistently, and it was necessary to specify casing tongs capable of more than 100,000 ft-lb of torque to overcome this difficulty (see Fig. 18). These tongs were activated from cables reeved through snatch blocks to air hoists, one of which was located centrally on each barge, and each hoist served several drilling units when pulling core.

For vertical holes, the drill tool was longer than 20 ft (see Fig. 19). It consisted of an open end piece on top to catch cutting sludge, a male plug designed to receive a pin type coupling from the drill rods, a core barrel, a renew-

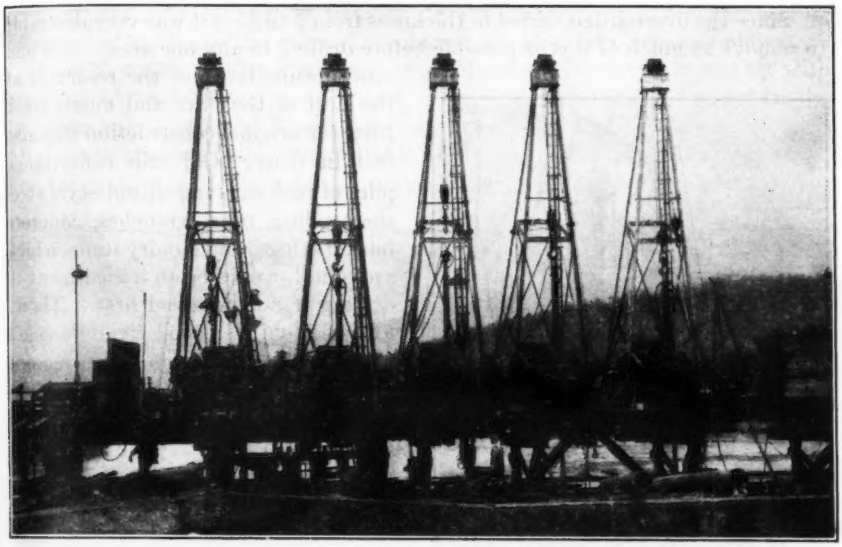

FIG. 17.—BATTERY OF 48-IN. CORE DRILLS IN OPERATION

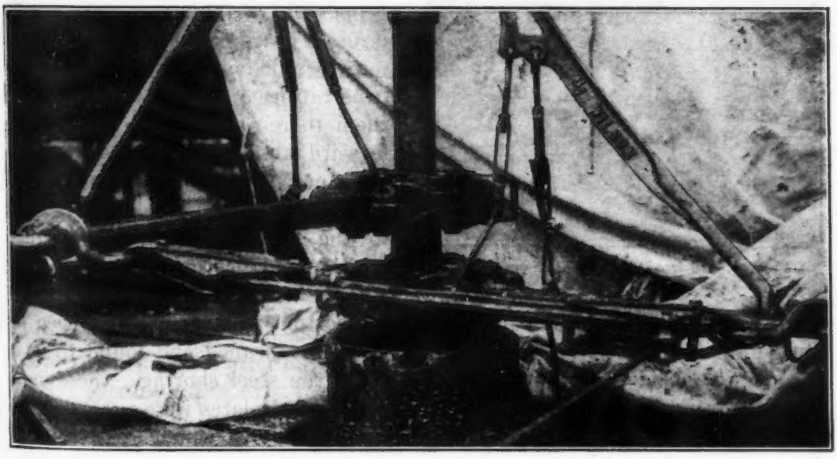

FIG. 18.—BREAKING OUT A 4.5-IN. TOOL JOINT WITH CASING TONGS

able coupling between the core barrel and bit, the point of maximum wear, and the bit. This assembly proved to be very effective and, except for the bit, was built from standard 18-in. pipe with a $\frac{1}{2}$-in. wall. The bit was intended to

be made from standard 18-in. pipe of $1\frac{1}{8}$-in. wall thickness but it was impossible to secure this type, and cast-steel bits and later even laminated bits from thinner wall pipe were used satisfactorily, although the latter did not wear as well as the solid section bits.

Since the overburden varied in thickness from 5 to 35 ft it was very desirable to remove as much of this as possible before drilling in any one area. Silt and mud accumulated in the reservoir at the heel of the dam and much trash from the original construction was also still in place. Old crib cofferdams, piles of rock excavation, old-style steel sheet piling, pipe, wrenches, concrete buckets, logs, and sundry items which are found, would be an impediment to drilling if not removed first. Therefore, a $1\frac{1}{2}$-yd clamshell digging bucket with the floating steam whirley crane was used to clean out an area 10 ft to 15 ft upstream from the upstream face of the dam before the drill operations were begun.

FIG. 19.—18-IN. DRILL TOOL ASSEMBLY

Among the many other items that needed to be removed were four old closure gates that had never been salvaged. These 19-ton gates were supposedly standing in an upright position in front of the closure blocks but it remained for an 18-in. drill penetrating one corner of one of them to reveal that they had fallen forward and were now resting flatwise in the river bed at angles from 0° to 45°. Divers were dispatched to the bottom to determine their position and location more accurately. They hooked the gates to the crane which removed them from the river bottom where they had been for almost thirty years (see Fig. 20). The steel was cleaned and found to be in surprisingly good condition, and, because of the steel shortage, these gates were disassembled and all the structural shapes and plates were reused.

Holes were alined by the template shown in Fig. 21 which was fabricated from structural steel, and suspended at the line of overburden on cables from the deck of the trestle on the dam. This template had $20\frac{1}{2}$-in. holes 24 in. on centers, with guide skirts for entering the casing. After a template had been lowered and leveled, a 20-in. flush-joint casing 60 ft long was set into one end hole by a floating whirley crane. At the opposite end of the template a flush-joint casing was set similarly into the second hole from the end. Flush-joint

casing was made up with ¼-in. square threads. A 1-in. plate, machined to take a pin type coupling, was bolted to a flange screwed to the top of the casing, and the drill rotated each of these end casings about 2 ft to 3 ft into good rock. These casings then served to hold the template in place for all intermediate drilling, and acted as guides for spacing the intersecting holes and setting adjacent templates. The steps in the use of the template were as follows:

First Template Setting, Position 1 (*Fig. 21(a)*).—The template was set with openings 1A and 2A facing upstream. The flush-joint casing was set in the template openings 1 and 2 and the casings were rotated 3 ft to 5 ft in rock. All the intermediate holes were drilled in the order shown, using flanged casings. The template was finally removed, leaving the flush-joint casings in place.

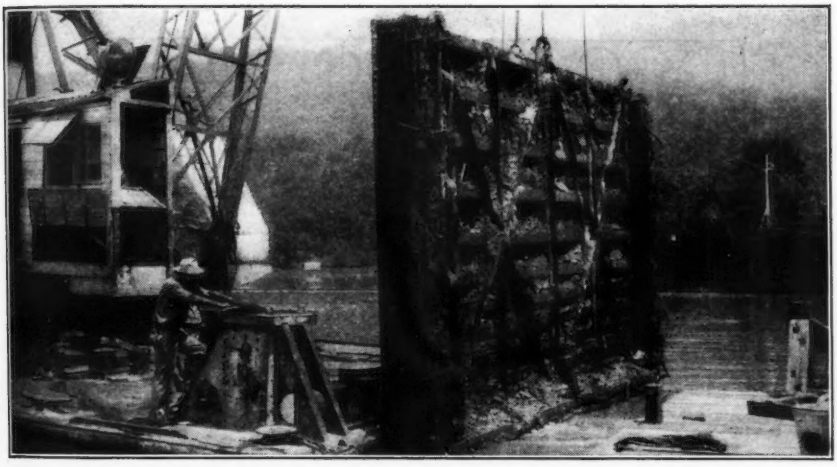

FIG. 20.—RECOVERY OF AN OLD CLOSURE GATE FROM THE RESERVOIR AT THE HEEL OF THE DAM

First Template Setting, Position 2 (*Fig. 21(b)*).—The template was then reversed by turning it end for end so that openings 1A and 2A (Fig. 21(*a*)) were placed over the flush-joint casing left in holes 2 and 1, respectively. The secondary holes were drilled in the order shown and the template was removed again, leaving all flush-joint casings in place (Fig. 21(*c*)).

Second Template Setting, Position 1 (*Figs. 21(g) and 21(h)*).—The template was moved to the left or to the right to extend the line of drill holes. As in the first setting, the template was placed with openings 1A and 2A facing upstream, the end opening being over the flush-joint casing in hole 1 when the template was moved to the left and over hole 2 if moved to the right. Flush-joint casing was set in template opening 20 and that primary hole was drilled. The intermediate primary holes were then drilled in the order shown.

Second Template Setting, Position 2 (*Figs. 21(i) and 21(j)*).—This procedure was essentially the same as Fig. 21(*b*), template opening 1A being placed over the casing in hole 1 when the move was to the left and over the casing in hole 20 when to the right. Openings 2A were placed over the flush-

joint casings in holes 20 and 2 left and right, respectively. Flush-joint casings were placed in template openings 30 and 31 and these secondary holes were drilled leaving the flush-joint casings in place temporarily. Next the flush-joint casing in holes 1 and 2 was removed. With flush-joint casings in holes 20,

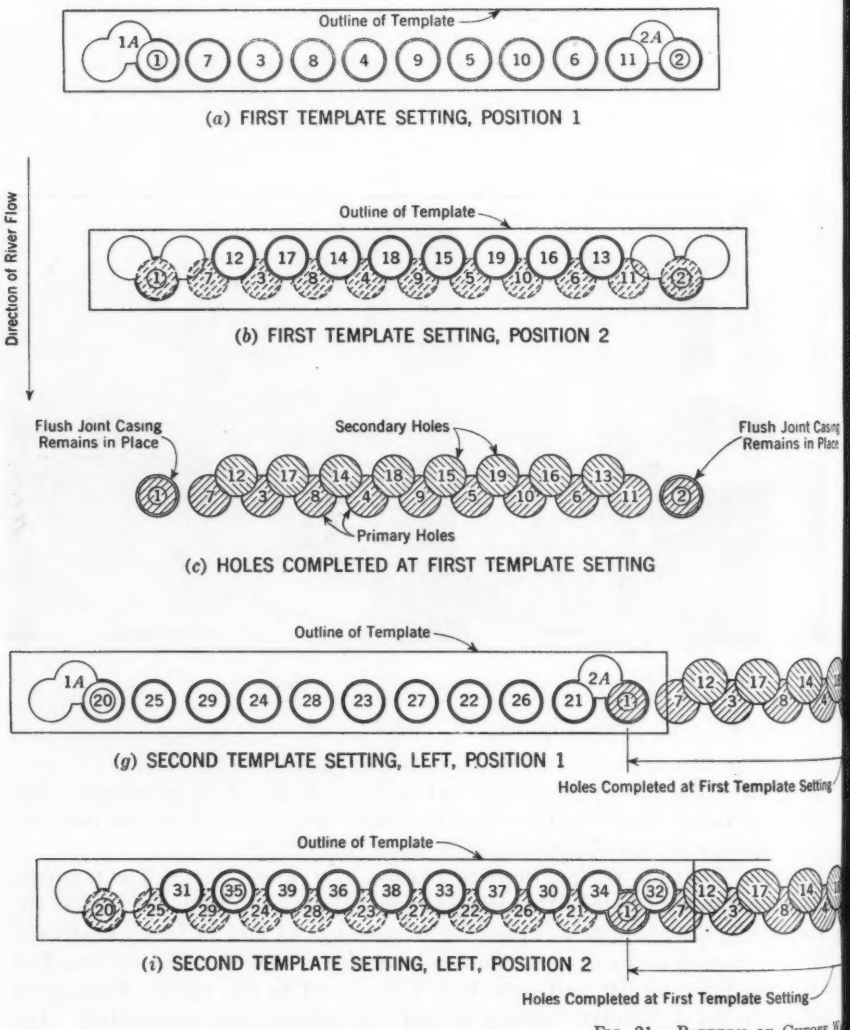
Outline of Template
1A
2A
(a) FIRST TEMPLATE SETTING, POSITION 1
Direction of River Flow
Outline of Template
(b) FIRST TEMPLATE SETTING, POSITION 2
Flush Joint Casing Remains in Place
Secondary Holes
Flush Joint Casing Remains in Place
Primary Holes
(c) HOLES COMPLETED AT FIRST TEMPLATE SETTING
Outline of Template
(g) SECOND TEMPLATE SETTING, LEFT, POSITION 1
Holes Completed at First Template Setting
Outline of Template
(i) SECOND TEMPLATE SETTING, LEFT, POSITION 2
Holes Completed at First Template Setting

FIG. 21.—PATTERN OF CUTOFF W... AND USE OF...

31, and 30, all other secondary holes were drilled, using flanged joint casing. After the drilling of secondary holes in the order shown was completed all casings except that in holes 20 were removed and the templates again were moved forward into primary position.

The flanged casings were 60 ft long and were placed by the crane in a manner similar to the flush-joint. The flanged casings were rotated to a depth of about 6 in. in solid rock. The bottom 20 ft of all casings, with which the drill tool was in contact when starting a hole, was always plumbed. For this work

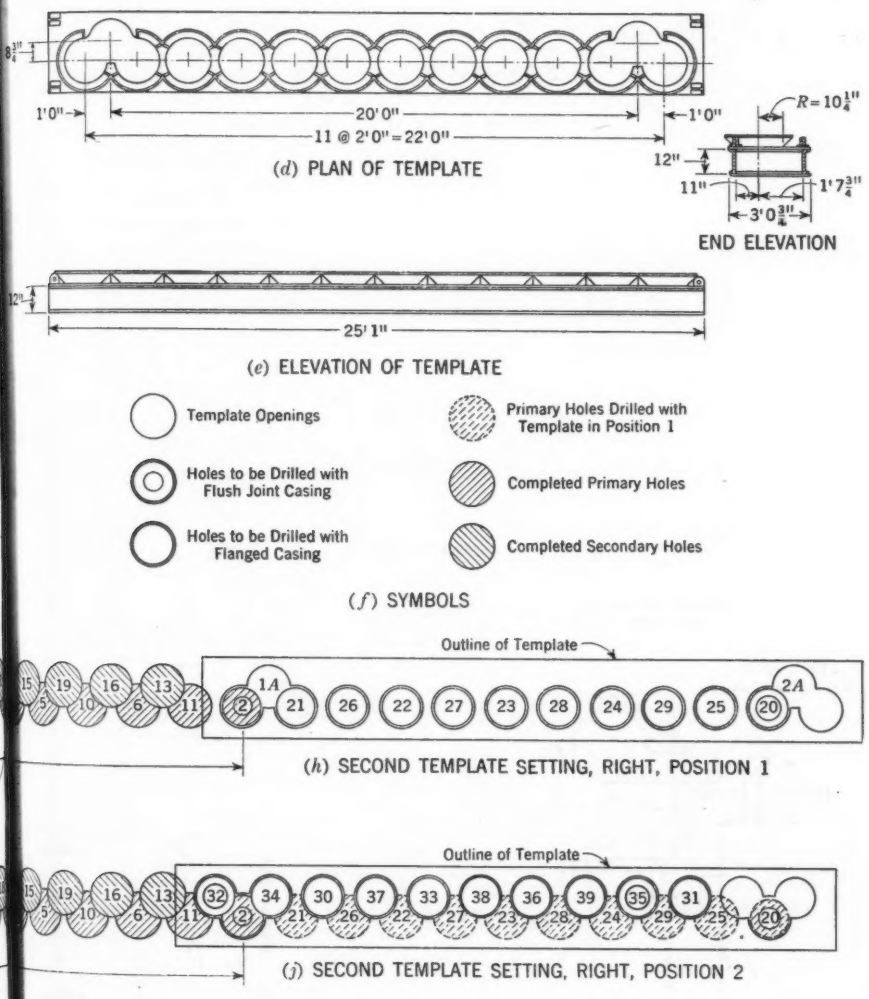

ND USE OF DRILL CASING TEMPLATE

the electric plumbing apparatus, shown in Fig. 22, was devised, consisting of a closed section of 6-in. pipe, 12 ft long, inside of which a 6-lb plumb bob was suspended on a piano wire and a ¼-in. rod. The bottom of the pipe had a flanged connection to a closed 6-in. well which was filled with oil, in which the

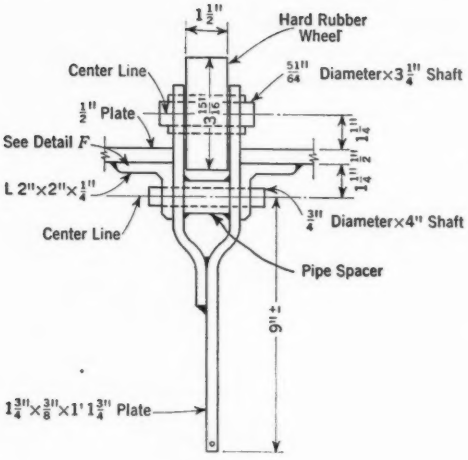

(*f*) SECTION *B-I*

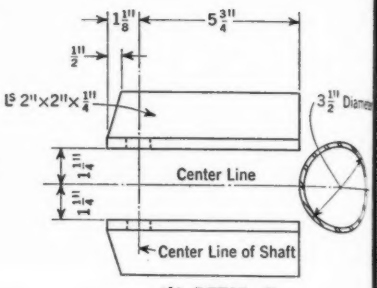

(*h*) DETAIL *F*
Two of Each Required

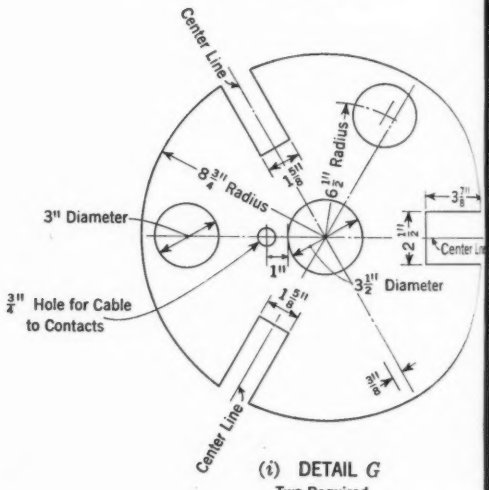

(*i*) DETAIL *G*
Two Required

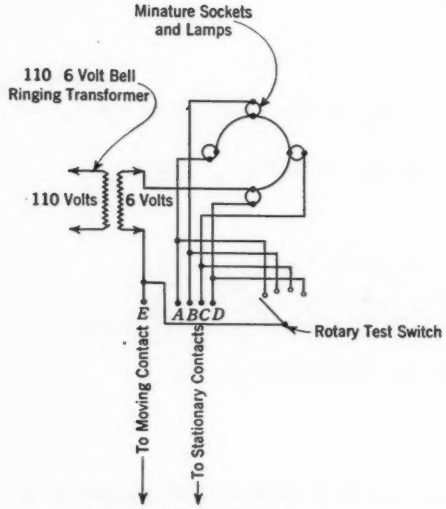

(*g*) WIRING DIAGRAM FOR CONTROL BOX

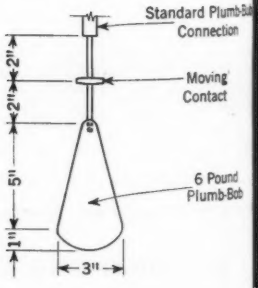

(*j*) DETAIL *H*

FIG. 22.—ELECTRIC DEVICE FO

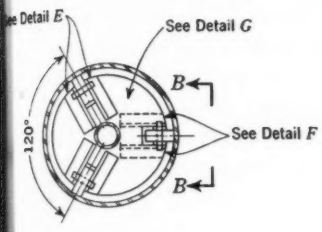

(a) SECTION A-A

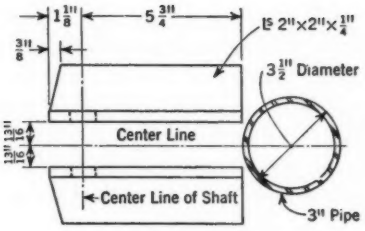

(c) DETAIL E
Four of Each Required

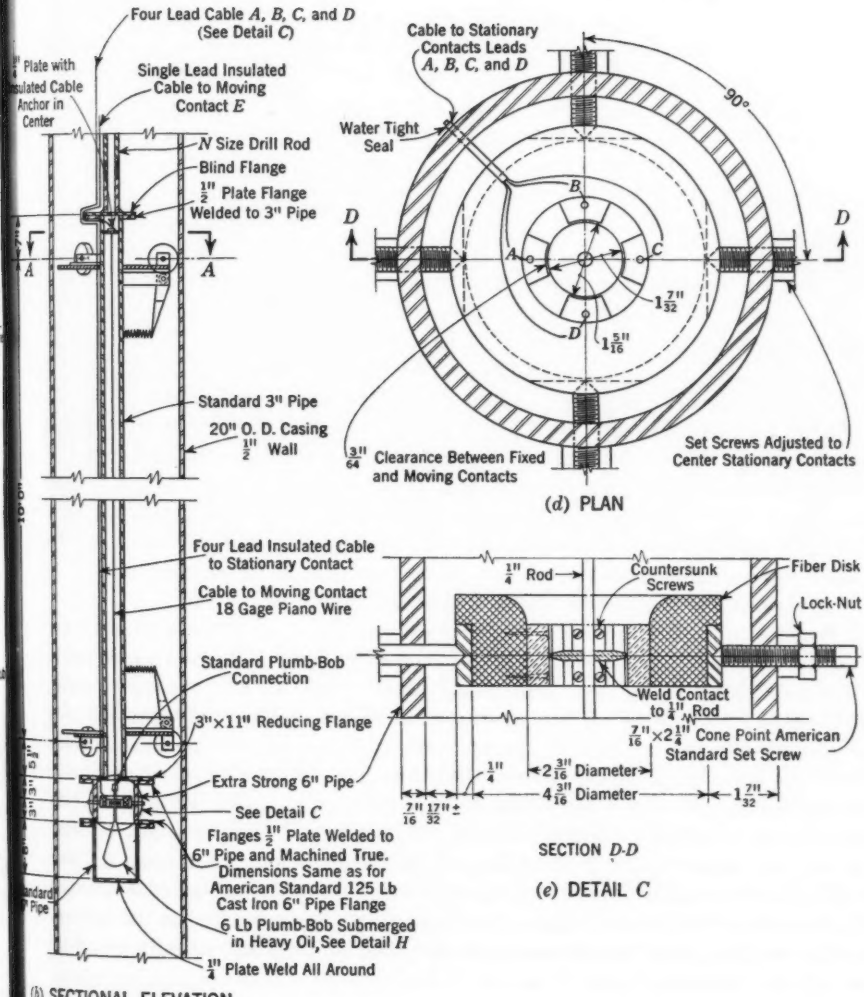
Four Lead Cable A, B, C, and D (See Detail C)
Single Lead Insulated Cable to Moving Contact E
N Size Drill Rod
Blind Flange
1/2" Plate Flange Welded to 3" Pipe
A
A
Standard 3" Pipe
20" O. D. Casing
1/2" Wall
Four Lead Insulated Cable to Stationary Contact
Cable to Moving Contact 18 Gage Piano Wire
Standard Plumb-Bob Connection
3"×11" Reducing Flange
Extra Strong 6" Pipe
See Detail C
Flanges 1/2" Plate Welded to 6" Pipe and Machined True. Dimensions Same as for American Standard 125 Lb Cast Iron 6" Pipe Flange
6 Lb Plumb-Bob Submerged in Heavy Oil, See Detail H
1/4" Plate Weld All Around
Cable to Stationary Contacts Leads A, B, C, and D
Water Tight Seal
90°
B
D
D
A
C
D
1 7/32"
1 5/16"
3/64" Clearance Between Fixed and Moving Contacts
Set Screws Adjusted to Center Stationary Contacts
1/4" Rod
Countersunk Screws
Fiber Disk
Lock-Nut
Weld Contact to 1/4" Rod
7/16"×2 1/4" Cone Point American Standard Set Screw
1/4"
2 3/16" Diameter
4 3/16" Diameter
1 7/32"
7/16" 17/32" ±

(b) SECTIONAL ELEVATION

(d) PLAN

SECTION D-D

(e) DETAIL C

plumb bob was suspended. Above the plumb bob a contactor was fastened to the ¼-in. rod, and this contactor was set at the same level as four copper contacts arranged in a circle and fastened to the inside of the 6-in. pipe. The contacts connected each to one wire of a four-conductor cable which led to the water surface where they were connected with four 6-v to 8-v lamps. The piano wire completed the circuit. A bell ringing transformer was used so that the system could be plugged into any 110-v light circuit.

The device had a set of three wheels on the outside, one of which was spring mounted both at the top and bottom. The two stationary wheels of each set were placed 120° apart on an arc of exactly 19 in., the inside diameter of the casing. The plumb-bob center was set with relation to these two wheels. The spring-mounted wheel insured that the two fixed wheels would always be in contact with the casing. It was also set at 120° with each of the other two.

This entire assembly was lowered to the bottom of the casing without pumping out. Movement of the plumb bob toward any contactor lighted the corresponding light at the surface and, by means of a jack at the center of the casing and two diagonal rods and turnbuckles, the casing could be moved in any desired direction until all lights were out, at which time the casing was plumb. These rods and jack were left in place to hold the casing during drilling, lining, and concreting. The lights were then checked by short circuiting to be sure that none had burned out. The clearance between the contacts and the contactor was $\frac{3}{64}$ in. all around.

Until a hole was 20 ft deep, a ¼-in. by 2-in. removable band in two pieces at the top of the sludge receiver was used on the cutting tool to obtain perfect vertical alinement by reducing the clearance between the drill tool and the guide casing. This band was made of two sets of two semicircular pieces of steel, the inner one projecting into the sludge collector. The inner band had four stud bolts which fastened to the sludge receiver. Therefore, the unit could be put on or taken off from any tool with a minimum of effort. Two pieces were required to form wash-out slots between the band sections.

A view of the template is shown in Fig. 23.

Studies on the drilling tool revealed that there was a point of maximum wear just above the bit; and in order to save on the other parts of the tool a renewable female coupling, 18 in. long, was placed between the bit and the core barrel. This concentrated wear on one short section of the tool, and this section was turned end for end when wear became noticeable but before the threads were worn down too far to be effective at the other end. Such a coupling was good for approximately 125 ft of drilling in this foundation. The 1¼-in. wall bits have 15 in. of wearing surface and after 35,000 ft of drilling it appeared that bit life was about 115 lin ft of drilling. The solid section bits averaged closer to 150 ft of life but the over-all average was less due to enforced use of laminated bits because of material shortages. Because they were protected at the bottom by the coupling, core barrels averaged 420 ft of drilling, and usually could be cut off and rethreaded once.

Above the core barrel a male plug was used which had a useful life of approximately 900 lin ft of drilling. When this plug was placed into the drill tool, the expensive connection between the 18-in. tool and the drill rods was reduced materially since this connection was used with various replacements of other parts of the tools; whereas, if it had been a part of the tool, the connection would have been lost each time that part wore out. Experience at Hales Bar indicated that the drill rod connecting to the male plug crystallized after

FIG. 23.—VIEW OF TEMPLATE PLACED IN SECONDARY POSITION

FIG. 24.—WELDER APPLYING ELECTRIC TUBE TUNGSTEN-CARBIDE

approximately 1,500 ft of drilling and invariably broke just above the pin type coupling. These rods were changed after 1,000 and 1,500 ft of drilling, eliminating considerable breakage at depths requiring costly "fishing" operations.

The sludge collector above the plug was made with a left-hand thread fastening to the plug. The wear on this unit was light and its life was approximately 500 lin ft. These sections were generally reclaimed from worn core barrels, which diminished somewhat the period of their useful life.

All drilling was done from a testle 11 ft above flashboard level. Three barges lined up in front of the trestle over a distance of 330 ft were used for laying out drill tools, rods, bits; removing core; and in general providing a platform and working space forward of the machines.

Where cavities were encountered which cause shot to be lost under the bits, six tungsten carbide knobs were welded to the cutting face of the bit at equally spaced interyals (see Fig. 24). This material has a Brinell hardness of 700 and generally cuts to a point at which shot can again be held under the bit after one or several applications. If a full shot ring is cut, shot can be fed under the bit about as soon as the tungsten carbide is worn smooth without removing the tools, with the advantage that the same bits may be used for either shot or this diamond substitute drilling. Tungsten carbide is made in various screen sizes for acetylene or electric application. Experiments with various available screen sizes of the tube type rods revealed that the 20-mesh to 30-mesh particles were applied easiest and cut better footage than the coarser particles in the Hales Bar foundation rock.

Since drilling at Hales Bar offered no opportunity for differentiating between work done with shot and the tungsten carbide faced bits, it is necessary to state the amount of each being used as a joint figure. Approximately 11 lb of shot and 0.12 lb of tungsten carbide were used currently per foot of 18-in. drilled hole. This value seems high but it must be remembered that shot loss in cavities was high; also, shot and the diamond substitute were used for drilling in casing, which did not contribute any 18-in. footage drilled. Comparisons between 3-in., 13-in., and 18-in. drilling indicate the use of $\frac{2}{3}$ lb of shot per inch of diameter of bit at Hales Bar.

Where large cavities occurred, the drills pounded very hard if given a slack line feed. This militated against plumb drilling and also caused repairs on the drills to run high. For such places, a turnbuckle was clamped into the hoist line, the bit was faced with extra tungsten carbide, and the drill was rotated at high speed and the drill tool fed very slowly with the turnbuckle. Although the speed of cutting was probably slower, the advantages gained by eliminating the tendency of the tool to deflect in the direction of the cavity, and by obtaining smoother operation, outweighed the disadvantage of decreased footage.

Drilling speeds varied from day to day, depending on the type of material encountered and on its state of solidity. Over-all rates for more than 35,000 ft of 18-in drilling which involved nine machines and twenty-seven different operators were: 5 in. per gross operating hour; and 6 in. per net operating hour. Thirteen-inch drilling was somewhat better, being about 9 in. and 11 in., respectively, per gross and net operating hours. The former included time for moving drills, drilling in casing, repairs, and other unavoidable delays except layoffs on account of high water—in other words, all workable shift hours. The latter is only net drilling time but includes pulling core. Monthly average rates per gross operating hour for 18-in drilling for the number of machines indicated have been as high as 7.50 in. per hr. Drilling the intersecting holes, however, reduced this rate, since the drilling was slower and more difficult. With nine drills running, 70 ft were drilled in one 8-hr shift, 199 ft in 24 consecutive shift hours, and 2,900 ft in one month of twenty-six working days.

A brief summary of the operating cost per foot for drilling 18-in. holes is as follows:

Description	Cost per foot
Labor	
Direct operations	$4.61
Repairs	0.39
Other expense	2.13
	$7.13
Drilling Tools	
Sludge collector	0.05
Plugs	0.10
Corebarrels	0.14
Couplings	0.19
Drill rods	0.14
Bits	1.07
Wrenches	0.11
	$1.80
Materials	
Lubricants	$0.16
Electricity	0.21
Air and water	0.38
Repair parts	0.28
Shot	0.42
Tungsten carbide	0.31
Sand and gravel	0.02
	$1.78
Other Costs	
Supervision	0.50
Drill depreciation	1.40
Miscellaneous	0.77
	$2.67
Totals	$13.38

It should be understood that these values do not include such job construction plant items as are customarily required in large construction work. Nor do they include such items as the trestle, templates, 20-in. casing, and other charges peculiar only to the Hales Bar project. The costs given are representative for 18-in. shot core drilling in foundation rock similar to that at Hales Bar, and, if used advisedly with due allowance for other locations and requirements, can furnish a satisfactory index of probable unit costs. It also is a satisfactory check-list of materials, equipment, and services involved in this type of operation. Application of these costs also must take into account the fact that nine drills were being used at Hales Bar, a fact which would alter labor, supervisory, and many of the other costs if less or more units are involved.

After the 18-in. hole had been drilled, in each case to a depth of 3 ft below the lowest known cavity, a $1\frac{1}{2}$-in. pipe was lowered into the hole to check the depth, thus determining if all core had been pulled. The grout pump was then hooked to this pipe and cement grout was pumped to the bottom of the hole to seal the liner. Asbestos-cement pipe, made up into one long piece from 13-ft sections, was then lowered into the hole on a 6-in. pipe screwed into a left-hand coupling which was concreted to a plug at the bottom of the asbestos-cement pipe. Sections of asbestos-cement pipe (inside diameter, 16 in.; wall thickness, $\frac{7}{8}$ in.; and lengths, 13 ft) were connected and lowered into the hole, and were supported by the 6-in. pipe on the 20-in. casing, using a fork and elevator. All these asbestos-cement pipe joints were fastened together progressively with No. 12 gage steel sheets 30 in. by 54 in., rolled to 16-in. diameter. The metal was fastened to one end of the pipe sections by six $\frac{1}{4}$-in. flat-head machine screws and nuts in the storage yard. The pipe was assembled over the hole in a vertical position, the end of the succeeding pipe being slipped over the protruding 15 in. of metal and fastened to the metal with two rows of four each,

flat-head self-tapping sheet-metal screws (see Fig. 25). Across cavernous regions, a 3-in. mesh expanded metal was placed inside the asbestos-cement pipe for reinforcing, and a $1\frac{3}{4}$-in. round bar was placed inside the 6-in. pipe to hold it in a central position so that it would not interfere with drilling the intersecting hole. When sufficient liner and reinforcement had been assembled

FIG. 25.—MAKING AN ASBESTOS-CEMENT PIPE JOINT

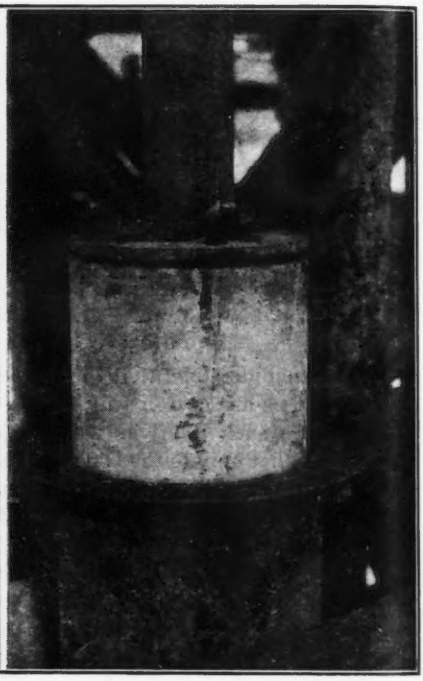

FIG. 26.—COVER OR HOLD-DOWN PLATE AT THE TOP OF THE ASBESTOS-CEMENT PIPE ASSEMBLY

to line the hole completely, a cover was placed over the top of the asbestos-cement pipe, as shown in Fig. 26. This cover had outstanding angle legs tapped for stud bolts which fastened to the outside of the 6-in. pipe. On the underside, the cover was equipped with four rollers spaced to fit the inside diameter of the liner. These permitted the 6-in. pipe to turn without disturbing the liner. This cover, therefore, held the 6-in. pipe centered and also prevented any of the asbestos-cement pipe from breaking joints. Such breaks might occur in lowering sections to the bottom due to caving rock, tightening of the hole in previously placed asphalt areas, or friction developed by the differential head against the liner. In some instances, velocities of more than 6 ft per sec, measured by lowering a current meter into the open hole, were recorded. In some cases this differential head was sufficiently high to impede the rotation of the drill tool seriously, and, in lining these holes, the liners had to be forced down, obviously necessitating the use of the cover plate.

Additional 6-in. pipe was added, permitting the assembled liner to reach bottom where it sank into the previously poured grout. The 6-in. pipe was then filled with heavy neat cement grout, and the left-hand thread at the bottom plug was unscrewed from the top. The grout dropped in the 6-in. pipe and filled the bottom of the asbestos-cement pipe until it found its level in both. Sufficient concrete to fill the liner was added through the 6-in. pipe which then acted as a tremie. The liner was overfilled by computed volume to effect a seal at the top of rock. It was important to gage this overfilling so as to be sufficient for the seal, but not so great to concrete in adjacent 20-in. holes in which other drills might still be operating. The remaining 6-in. pipe was then removed, and the 20-in. casing was pulled out and taken to the checking station where it was inspected for straightness. Small deflections were adjusted by shimming between flanges. The bottom of the casing was then prepared with a few tungsten carbide knobs and two water slots. If the casing was worn thin at the bottom it was cut off to a point where full wall thickness was available before applying the tungsten-carbide. The casing was measured and marked and set aside for placement in the next projected drill hole. One casing was always placed in front of each drill, ready for drilling. Fig. 27 shows the method of lining and concreting, and details of the joints and bottom plug. To summarize the procedure:

(1) Fill the 6-in. pipe with neat cement grout through a 1.5-in. pipe to the bottom of the hole, by means of a grout pump, using a water-cement ratio of 0.4, and remove 1½-in. pipe;

(2) Unscrew the 6-in. pipe from the left-hand cap (see Fig. 27(*k*)); the grout rises inside the asbestos-cement pipe and drops in the 6-in. pipe to the point of head equalization for grout, establishing tremie action;

(3) Fill the 6-in. pipe with 1 : 2½ : 3 concrete using quick-setting cement;

(4) Lift the 6-in. pipe and add concrete, maintaining the tremie action until the hole is full;

(5) Remove the 6-in. pipe; and

(6) Lift the 20-in. casing and thread it into the new template opening, after checking.

The 20-in. casing was handled in one piece by a floating steam whirley crane mounted on a barge. The crane had a lifting capacity of 5½ tons on a flat boom and 20 tons on a close boom. The boom was 75 ft long. The barge was equipped with one 56-ft and one 70-ft spud to reach bottom in the 50-ft to 60-ft depth of water upstream.

A small temporary plant consisting of a 10-sack concrete mixer on a barge also loaded with aggregate and cement was replaced by one of the TVA 2-yd floating concrete mixing plants, originally used during the construction of Wheeler Dam. Quick-setting cement, or standard cement with 2% calcium chloride added, was used for concrete since it was desirable to have the primary holes set up as quickly as possible so that secondary holes could be drilled. Except in a few exigencies, concrete in the primary holes was always 30 days old before secondary holes were drilled. All concrete materials except those in the mixer plant bins were normally stocked at the dock.

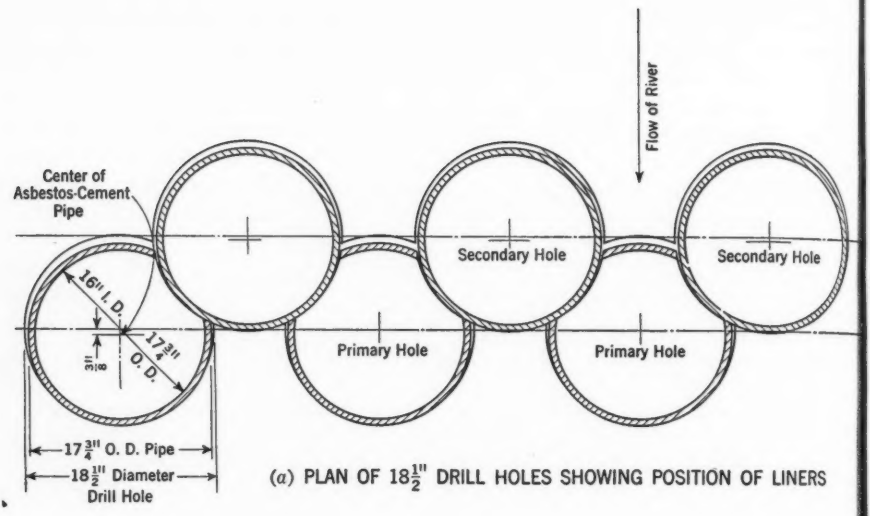

(*a*) PLAN OF 18½" DRILL HOLES SHOWING POSITION OF LINERS

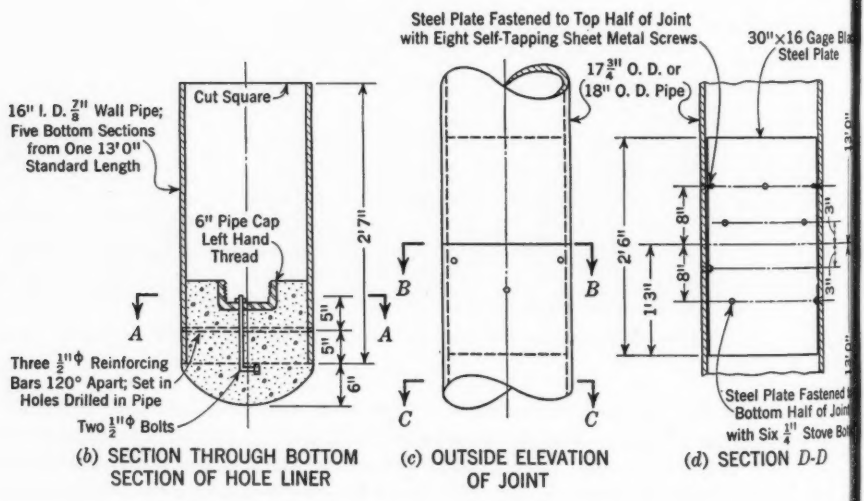

(*b*) SECTION THROUGH BOTTOM SECTION OF HOLE LINER (*c*) OUTSIDE ELEVATION OF JOINT (*d*) SECTION *D-D*

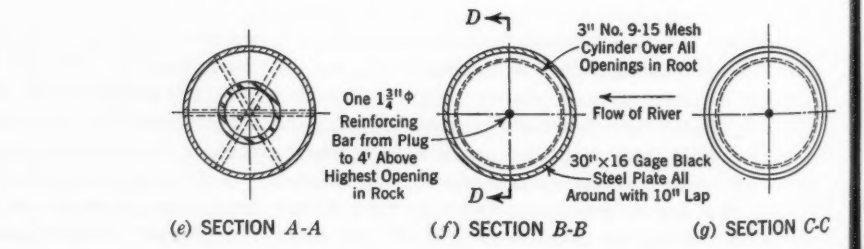
D
D
3" No. 9-15 Mesh Cylinder Over All Openings in Root
One 1 3/4"φ Reinforcing Bar from Plug to 4' Above Highest Opening in Rock
Flow of River
30"×16 Gage Black Steel Plate All Around with 10" Lap

(*e*) SECTION *A-A* (*f*) SECTION *B-B* (*g*) SECTION *C-C*

FIG. 27

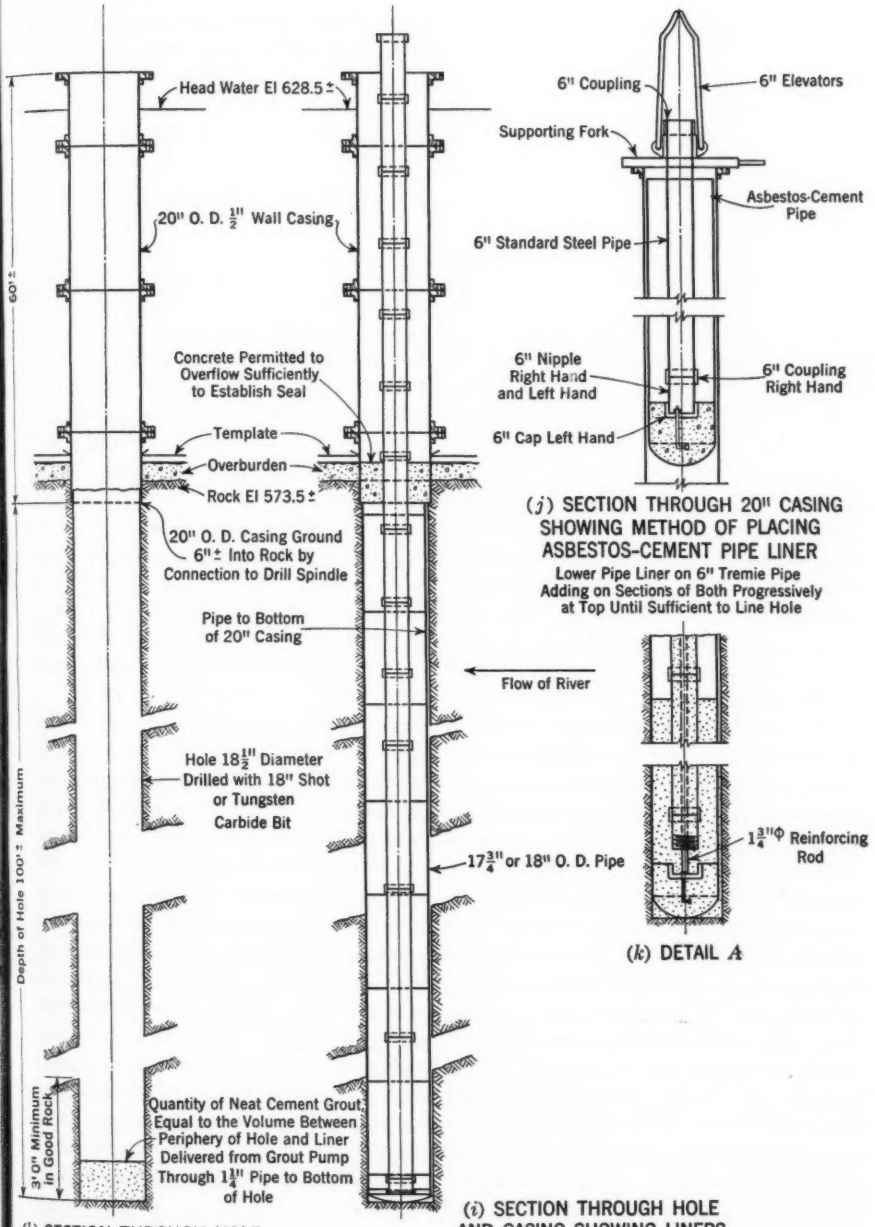
Head Water El 628.5±
20" O. D. 1/2" Wall Casing
60'±
Concrete Permitted to Overflow Sufficiently to Establish Seal
Template
Overburden
Rock El 573.5±
20" O. D. Casing Ground 6"± Into Rock by Connection to Drill Spindle
Pipe to Bottom of 20" Casing
Hole 18 1/2" Diameter Drilled with 18" Shot or Tungsten Carbide Bit
Depth of Hole 100'± Maximum
3'0" Minimum in Good Rock
Quantity of Neat Cement Grout, Equal to the Volume Between Periphery of Hole and Liner Delivered from Grout Pump Through 1 1/4" Pipe to Bottom of Hole
(h) SECTION THROUGH HOLE AND CASING READY TO RECEIVE LINERS AND CONCRETE
6" Coupling
6" Elevators
Supporting Fork
Asbestos-Cement Pipe
6" Standard Steel Pipe
6" Nipple Right Hand and Left Hand
6" Coupling Right Hand
6" Cap Left Hand
(j) SECTION THROUGH 20" CASING SHOWING METHOD OF PLACING ASBESTOS-CEMENT PIPE LINER
Lower Pipe Liner on 6" Tremie Pipe Adding on Sections of Both Progressively at Top Until Sufficient to Line Hole
Flow of River
17 3/4" or 18" O. D. Pipe
1 3/4"Φ Reinforcing Rod
(k) DETAIL A
(i) SECTION THROUGH HOLE AND CASING SHOWING LINERS AND 6" ASBESTOS-CEMENT PIPE

A 22-ft by 100-ft steel work barge, on which 20-in. casing and 6-in. pipe were stored, asbestos-cement pipe was assembled, and reinforcing mesh and rods were placed, and the TVA towboat completed the marine equipment required for this work.

Concrete was proportioned from Tennessee River gravel and sand, the nominal mix being 1 : $2\frac{1}{2}$: 3 with a water-cement ratio of 0.5. This concrete tested consistently at 4,000 lb per sq in. in 28 days and the cement factor was 1.87 bbl per yard of concrete. This is high but was believed necessary due to the underwater nature of the work.

Twenty-four hours after concrete placement, the hole was sounded to determine the effectiveness of the concrete and if it was not as high as the anticipated level, it was brought up by placing cement grout or tremie concrete, after which it was sounded again after sufficient time had elapsed to permit hardening.

On October 15, the cutoff trench had been completed; the 13-in. drilling of 7,500 ft and concrete foundation consolidation were 90% complete; diamond drilling at 49,000 ft was 90% complete; cement and asphalt grouting were approximately 90% complete. Of the fourteen original boils showing downstream from the dam, all but two have been eliminated, and these two show marked improvement as a result of the impact of the work. Most of the remaining percentage of uncompleted work as of October 15 is in contact with these, and the completed work should show the same result here as has been effected on areas completed. Fig. 13 shows the boils which have been eliminated and those on which work is still being done. Circles representing these boils indicate by their diameter the relative sizes of the visible leakage as found at the time this work was begun.

All holes were logged and plotted in order that a complete record of the entire cutoff would be available at all times. A projection of the trend of the overlap in any series of holes indicated that the failure to secure perfect overlap should not be considered an impediment to securing satisfactory results since in cases where intersections were lost the drift of the holes was not sufficient to cause any serious harm and the later upstream asphalt placement was used to correct these minor defects. This was found to be correct in principle. After the cutoff was completely in place in the worst leakage area which connected with boils G, E, and F, Fig. 15, these boils had been reduced from bubbling as much as 18 in. above tailwater surface, to flat but still visible flows, indicating an estimated 75% effectiveness. Strategically placed asphalt holes upstream from this cutoff trench eliminated the visible balance of flow. Tremie concreting under the dam through the 13-in. holes, and cement and asphalt grouting through 3-in. holes, complete the operations. Job experience also indicates that, without the cutoff trench, the asphalt seal could not have been relied upon to secure the desired results because the flows were too large. The combination use of these methods, judiciously applied, is considered effective in cutting off flows of the magnitude encountered at Hales Bar.

During the period of high water in January, 1943, just after heavy general rains over the Tennessee Valley, some interesting phenomena occurred which had not been noticed during any previous high-water periods prior to completion of some parts of the cutoff walls.

At approximately Station 12+00 and about 150 ft upstream, where suctions had previously been indicated, and at Station 16+50 just upstream from the dam, boils appeared in the swollen headwater. Some of these carried mud and others were clear, but violent upheavals were in evidence more or less at 10-sec intervals.

At Station 19+50 and approximately 225 ft upstream, air bubbles in very large quantity effervesced continuously for three or four days during high water.

In the former instance an explanation is believed to be that the channels to higher ground water, as a result of the general rains, were open, but, since the cutoff obstructed easy passage to the downstream side of the dam, the differential head produced this boiling effect in the headwater. In the latter case it seems probable that large quantities of air became trapped in openings accessible to atmosphere during the long period of dry weather and that heavy rains running off into these subterranean channels entrapped this air and, due to hydrostatic pressure, shoved it through the openings to come up in the reservoir, the normal channel under the dam having been closed off.

A repetition of high water soon after the former high flows again brought out the water boils but not the air bubbles, which lends some weight to the assumptions.

Frequent checks of concrete in the adjacent holes have indicated that it remained well in the liner. Diamond-drill holes were drilled into this concrete to ascertain its condition, and soundings were made frequently through the intersecting holes as they were being drilled.

Many improvements over the originally conceived construction methods were made in the field. Notable among these were developments of the required core drill characteristics, which were used to specify requirements in acquiring this equipment. The drill tool used was modified from the originally proposed tool to take advantage of experiences gained on the wear of this part. The substitution of $\frac{1}{2}$-in. wall casing for previously tried lighter sections, and the substitution of cast-steel instead of cast-iron flanges both on the 20-in. casing and on the 6-in. tremie pipe were important advances not originally foreseen. The development of the template and the underwater electric plumb bob stands out, perhaps, as the two most important improvements toward attaining the desired goal. The use of the tungsten carbide was essential. Not nearly enough importance can be attached to the wrenches and tongs which were acquired heavy enough to accomplish desired results after trial-and-error experiments with lighter tools. In the field of lining the holes, much work was done before the liner joints were satisfactory, and such handy adjuncts as the hold-down plate at the top of this liner were invaluable.

The original conception of a liner was that of a flexible fabric and rubber bag. In its trial stages this was found wanting. This type of liner was desirable because it filled the drilled hole completely. The very satisfactory handling of the rigid asbestos-cement liner, and the inability to secure the fabric and rubber products due to the war, precluded further experimentation with the flexible liner.

Summary

In retrospect, two improvements not evident without the experience gained on this work could have been made, and should be made if this plan is used elsewhere again:

1. After dredging upstream from the dam, a concrete block, tremied into the place of the removed overburden would have provided two advantages—
   (*a*) All casings could have been the same length; and
   (*b*) The templates could have been set directly on this block for drilling to begin.

Although it was thought that some overburden would be desirable for holding the casings in place, this was not found necessary.

2. Much importance was originally attached to overlapping of holes to secure a continuous cutoff. The amount of this overlap was determined to allow for some deflections in drilling to minimize the lack of it at lower levels. This overlapping has a definite theoretical advantage, but results at the job indicate that this is probably outweighed by practical consideration, such as:
   (*a*) Too deep overlaps cause caving of the concrete remaining in the primary holes, resulting in the necessity of drilling additional holes upstream from the secondary holes to correct this condition where it occurs. It is true that this condition obtains in only about 1% of the holes but it can be eliminated by decreasing the overlap.
   (*b*) The secondary hole does not drill as fast as the primary hole because of the overlap and consequent shot loss, particularly in holes lined with the rigid liner.
   (*c*) The time element, waiting for concrete to harden in holes adjacent to proposed intersecting holes, can be eliminated.

Therefore, to overcome these defects in application, it is felt that primary holes could have been spaced about the same, but that secondary holes should have been drilled farther upstream so that the periphery of the holes just touch instead of overlap. The disadvantage of this arrangement is that there would be slightly greater impairment of coverage of the leakage areas, but the record of overlap indicates the need for some asphalt grouting to perfect the seal anyhow, and therefore this disadvantage is outweighed by the aforementioned advantages.

Acknowledgment

The work was done by the Tennessee Valley Authority, for whom T. B. Parker, M. Am. Soc. C. E., later succeeded by C. E. Blee, M. Am. Soc. C. E., was chief engineer, and A. L. Pauls, M. Am. Soc. C. E., chief construction engineer. At the project, H. D. Towers was assistant superintendent in charge of the construction forces. He was assisted by B. W. Crowe, R. M. Winston, and L. E. Tidwell, shift foremen. A. H. Weber was in charge of engineering and inspection for the project. The writer also wishes to acknowledge the cooperation and assistance of Frank Miller and manufacturers supplying equipment and materials to the project for their part in the development of methods and specialized items required to do the work.

AMERICAN SOCIETY OF CIVIL ENGINEERS

Founded November 5, 1852

PAPERS

SHEAR EFFECT ON THE STRENGTH OF STRUTS

BY S. SERGEV,[1] ESQ.

SYNOPSIS

In studying the strength of initially straight struts, pin-supported at one end and laterally restrained at the other, loaded by a concentrated axial load at some intermediate point between the supports, it is desirable to know the effect of shearing forces on the critical load on the struts. This paper treats that problem. A general expression for buckling criteria is derived for struts of constant cross sections. A special case and an example is solved in detail comparing the strength of a latticed strut, considering shear effect, with a strut the strength of which is determined by bending considerations only.

INTRODUCTION

General.—Ordinarily, a strut is an initially straight slender member, principally subjected to axial loads. Struts may have different means of support with the loads applied anywhere along the length of the member. Slender struts fail by buckling caused by a critical load or loads on the strut. The usual method of determining critical loads on initially straight struts is to assume, at every normal cross section, the curvature to be proportional to the bending moment only. This is satisfactory for solid struts, but not for latticed struts in which shearing forces may substantially reduce the critical load. Formulas have been derived for initially straight latticed struts subjected to end loads.[2]

In practice, some struts are pin-supported at one end and laterally restrained at the other, and loaded by a single concentrated axial load applied at some intermediate point between the supports. The effect of shearing forces on the critical load has not yet been established for this case. It is desirable, therefore, to derive formulas that yield this information.

Notation.—The following letter symbols, used in this paper, conform essentially to American Standard Letter Symbols for Mechanics, Structural Engi-

NOTE.—Written comments are invited for immediate publication; to insure publication the last discussion should be submitted by **April 1, 1944.**

[1] Associate Prof., Dept. of Civ. Eng., Univ. of Washington, Seattle, Wash.

[2] "Theory of Elastic Stability," by S. Timoshenko, 1st Ed., McGraw-Hill Book Co., Inc., New York and London, 1936, pp. 139–147.

neering and Testing Materials,[3] prepared by a Committee of the American Standards Association, with Society representation, and approved by the Association in 1932:

A = cross-sectional area of a strut; also, where specially defined, A, B, C, and D are integration constants:
- A_a = area of top strut section;
- A_b = area of bottom strut section (see Fig. 1);
- A_d = area of two diagonals;
- A_p = area of two batten plates;

a = length of top strut segment (b = length of bottom segment); as a subscript, a refers to the upper strut segment;

B = integration constant (see A);

b = length of bottom strut segment (see a); as a subscript, b refers to the bottom strut segment;

C = integration constant (see A);

c = spacing of batten plates (see Fig. 2);

D = integration constant (see A);

E = Young's modulus of elasticity;

e = deflection of strut at point of load P;

G = shear modulus of elasticity;

h = length of batten plates and spacing of channels (see Fig. 2);

I_a = moment of inertia of the strut cross-sectional area about the z-axis, in the top segment equal to $u\,I_b$;

I_b = moment of inertia of the strut cross-sectional area about the z-axis, in the bottom segment;

I'_b = inertia moment of two batten plates;

I_c = moment of inertia of the cross section of a vertical channel about its own gravity axis parallel to the web;

K = beam constant for determining shear deflections;

k = a span ratio equal to $\frac{b}{L}$;

L = total length of strut equal to $a + b$;

M = bending moment about the z-axis;

m = a substitution constant (Eq. 5b); $m^2 = \frac{P}{E\,I_b}$;

n = a substitution constant; $n^2 = \frac{P}{E\,I_a} = \frac{m^2}{u}$;

P = critical load on the strut:
- P' = buckling or critical load on solid struts;

q = a substitution constant (Eq. 10e);

r = least radius of gyration with respect to the z-axis (Eq. 34a);

t = a substitution constant (Eq. 30);

u = ratio of inertia moments = $\frac{I_a}{I_b} = \frac{m^2}{n^2}$;

V = total transverse shearing force;

[3] ASA—Z10a—1932.

x = rectangular coordinate measured along the axis of the strut:
  x_a = values of x measured from the top down;
  x_b = values of x measured from the bottom upward;
y = deflection of the strut at any point x:
  y_m = deflection at x due to bending moment;
  y_v = deflection at x due to shearing force;
z = rectangular coordinate measured along the z-axis;
α = a substitution constant (see Eq. 30);
β = a substitution constant (see Eq. 32);
γ = a substitution constant for solid struts (Eq. 25);
ϕ = (see Fig. 2) angle between batten plates and diagonals;
ρ = radius of curvature; and
ψ = a substitution constant for latticed struts.

Assumptions.—All equations and formulas derived in this paper are based on the following assumptions:

1. The strut is initially straight;
2. The material composing the strut is homogeneous;
3. The weight of the strut is neglected;
4. All stresses and strains are within the limits of proportionality; that is, they conform to Hooke's law; and
5. The deflection, and hence the curvature, of the strut is small.

Except No. 5, these assumptions need no comment. To avoid repetition, and because the implications in Assumption 5 are significant, this assumption will be discussed at some length.

The deflection of a strut at the incipient buckling state is small, but for all practical purposes the strut is considered to have failed at the first indication of buckling. After buckling begins, with slight increase in the loading, the deflection increases greatly, but its relationship to the effects producing it is no longer of practical interest. Since the deflection is small within the range considered, it can be shown easily that the curvature ρ of the strut axis is approximately equal to

$$\frac{1}{\rho} = \frac{d^2y}{dx^2} \quad \ldots\ldots\ldots\ldots\ldots\ldots\ldots\ldots\ldots\ldots (1)$$

(This is the usual assumption made in all approximate computations.) The exact relationship of curvature to the bending moment M causing it is expressed by

$$\frac{1}{\rho} = \frac{M}{E\,I_b} \quad \ldots\ldots\ldots\ldots\ldots\ldots\ldots\ldots\ldots\ldots (2)$$

in which E = modulus of elasticity; and I_b = moment of inertia of the strut cross-sectional area about the z-axis, in the bottom segment. Eliminating the curvature between these two expressions:

$$\frac{d^2y}{dx^2} = \frac{M}{E\,I_b} \quad \ldots\ldots\ldots\ldots\ldots\ldots\ldots\ldots\ldots\ldots (3)$$

Eq. 3 defines a valid relationship between the deflection and bending moment

when the deflection is small relative to the span. (Another way of stating this is that, for flat curves, the rate of change of the slope at any point equals the curvature of the curve at that point, which in turn equals $\frac{M}{E I_b}$.)

Critical Load on Solid Struts

Consider a strut that is pin-supported at one end and restrained laterally at the other, and loaded by a single concentrated load at some intermediate point between the supports (see Fig. 1). The load is assumed to be symmetrically applied, thus simulating concentric load condition. The flexural rigidities of the strut in the two segments a and b are constant but unequal. Assume a solid strut for the present discussion.

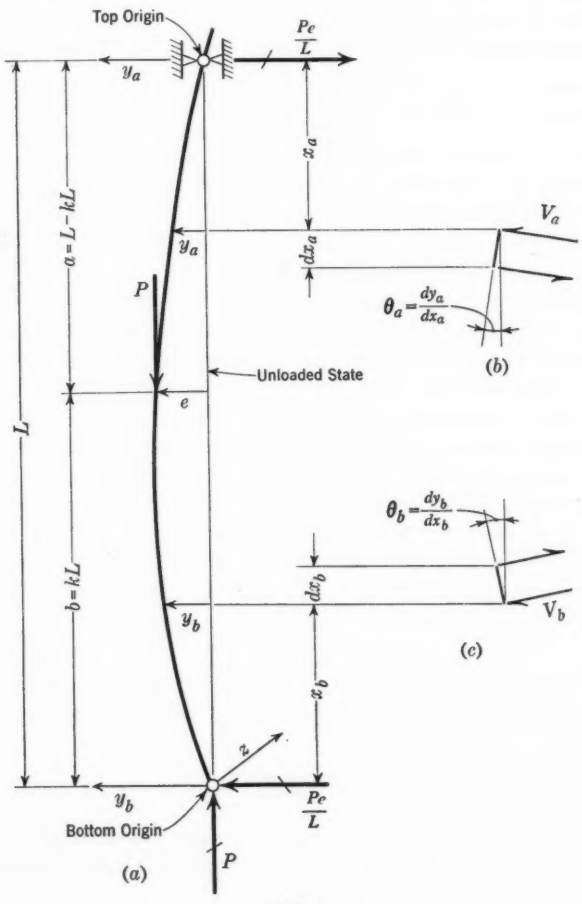

Fig. 1

Under a critical load, P, due to initial crookedness or small eccentricity, the strut axis will deflect slightly so that P will be a distance e from the initial or unloaded state of the strut. The indicated reactions are determined from the laws of equilibrium.

First consider the bottom segment b, and express the curvature of the strut axis in terms of the bending moment. The bending moment at any section distance x_b from the bottom origin is

$$M = -P y_b + \frac{P e x_b}{L} \quad \ldots\ldots (4)$$

in which the positive sign denotes compression on the side adjacent to the positive y-coordinate. The general relationship, for flat curves, between the bending moment and the deflection, y_{bm}, that it produces is

$$E I_b \frac{d^2 y_{bm}}{dx^2_b} = -P y_b + \frac{P e x_b}{L} \quad \ldots\ldots (5a)$$

Dividing Eq. 5a by $E I_b$ and using the notation $\frac{P}{E I_b} = m^2$:

$$\frac{d^2 y_{bm}}{dx^2_b} = -m^2 y_b + \frac{m^2 e x_b}{L} \quad \ldots\ldots (5b)$$

Considering the effect of shearing forces on the deflection of the strut, the total transverse shearing force is:

$$V_b = \frac{dM}{dx_b} = \frac{d}{dx_b}\left(-P y_b + \frac{P e x_b}{L}\right) = -P\left(\frac{dy}{dx}\right)_b + \frac{P e}{L} \quad \ldots\ldots (6)$$

from which

$$\left(\frac{dV}{dx}\right)_b = -P\left(\frac{d^2 y}{dx^2}\right)_b \quad \ldots\ldots (7)$$

The slope of the strut axis due to shear strain, from fundamental concepts, is equal to

$$\frac{dy_{bv}}{dx_b} = -\frac{K V_b}{A_b G} \quad \ldots\ldots (8)$$

in which the negative sign follows from Fig. 1(c) where V_b is positive and acting alone would give a negative slope. The factor K is a constant depending on the cross section of the strut. (This factor is 1.2 and 1.11 for rectangular and circular cross sections, respectively.) [4] Taking the first derivative with respect to x_b in Eq. 8, an expression is obtained for the shear curvature as a function of the total transverse shearing force:

$$\frac{d^2 y_{bv}}{dx^2_b} = -\frac{K}{A_b G}\left(\frac{dV}{dx}\right)_b \quad \ldots\ldots (9)$$

[4] "The Theory and Practice of Modern Framed Structures," by J. B. Johnson, C. W. Bryan, and F. E. Turneaure, 10th Ed., John Wiley & Sons, 1910, Vol. 2, p. 27; also "Theory of Statically Indeterminate Structures," by W. M. Fife and J. B. Wilbur, McGraw-Hill Book Co., Inc., 1st Ed., p. 27.

In Eq. 9, the expression found in Eq. 7 is substituted for $\left(\frac{dV}{dx}\right)_b$:

$$\frac{d^2y_{bv}}{dx^2_b} = \frac{K\,P}{A_b\,G}\left(\frac{d^2y}{dx^2}\right)_b \quad \ldots\ldots\ldots\ldots\ldots\ldots\ldots\ldots (10a)$$

This relationship gives the curvature of the elastic line of the strut due to shearing force. The total curvature resulting from bending moment and shearing force is the sum of the two curvatures; that is,

$$\left(\frac{d^2y}{dx^2}\right)_b = \frac{d^2y_{bm}}{dx^2_b} + \frac{d^2y_{bv}}{dx^2_b} \quad \ldots\ldots\ldots\ldots\ldots\ldots\ldots\ldots (10b)$$

If the expressions for the curvatures found in Eqs. 5*b* and 10*a* are substituted into Eq. 10*b*—

$$\left(\frac{d^2y}{dx^2}\right)_b = -\,m^2\,y_b + \frac{m^2\,e\,x_b}{L} + \frac{K\,P}{A_b\,G}\left(\frac{d^2y}{dx^2}\right)_b \quad \ldots\ldots\ldots\ldots (10c)$$

or rewriting

$$\left(\frac{d^2y}{dx^2}\right)_b\left(1 - \frac{K\,P}{A_b\,G}\right) = -\,m^2\,y_b + \frac{m^2\,e\,x_b}{L} \quad \ldots\ldots\ldots\ldots (10d)$$

Dividing each term in Eq. 10*d* by $1 - \frac{K\,P}{A_b\,G}$ and using the notation $q^2 = \frac{m^2}{1 - \frac{K\,P}{A_b\,G}}$, Eq. 10*d* may be written in the form:

$$\left(\frac{d^2y}{dx^2}\right)_b + q^2\,y_b = q^2\,\frac{e\,x_b}{L} \quad \ldots\ldots\ldots\ldots\ldots\ldots\ldots\ldots (10e)$$

The general solution of Eq. 10*e* is

$$y_b = A\,\sin q\,x_b + B\,\cos q\,x_b + \frac{e\,x_b}{L} \quad \ldots\ldots\ldots\ldots\ldots\ldots (11a)$$

The constants A and B may be determined from the boundary conditions $y_{x_b=0} = 0$ and $y_{x_b=b} = e$. The constants are found to be $B = 0$, and $A = \frac{a\,e}{L}\sin q\,b$. Substituting these into Eq. 11*a*,

$$y_b = \frac{a\,e\,\sin q\,x_b}{L\,\sin q\,b} + \frac{e\,x_b}{L} \quad \ldots\ldots\ldots\ldots\ldots\ldots\ldots\ldots (11b)$$

The slope of the elastic line of the strut, corresponding to the deflection y_b, is found by taking the first derivative with respect to x_b in Eq. 11*b*. The slope is

$$\left(\frac{dy}{dx}\right)_b = \frac{a\,e\,q\,\cos\,(q\,x_b)}{L\,\sin q\,b} + \frac{e}{L} \quad \ldots\ldots\ldots\ldots\ldots\ldots\ldots\ldots (12)$$

Consider next the deflection of the top segment. The bending moment of any distance x_a from the top origin is

$$M = -\,\frac{P\,e\,x_a}{L} \quad \ldots\ldots\ldots\ldots\ldots\ldots\ldots\ldots\ldots\ldots (13)$$

The curvature produced by this moment, using the argument discussed before, is

$$E\,I_a \frac{d^2y_{am}}{dx^2_a} = -\frac{P\,e\,x_a}{L} \quad \ldots\ldots(14)$$

Dividing both sides by $E\,I_a$ and using the notation $\frac{P}{E\,I_a} = n^2 = \frac{m^2}{u}$,

$$\frac{d^2y_{am}}{dx^2_a} = -\frac{m^2\,e\,x_a}{u\,L} \quad \ldots\ldots(15)$$

Now, considering the effect of the shearing force,

$$\frac{dM}{dx_a} = V_a = -\frac{P\,e}{L} \quad \ldots\ldots(16)$$

From the study of shear strain, as discussed before,

$$\frac{dy_{av}}{dx_a} = -\frac{K\,V_a}{A_a\,G} = \frac{K}{A_a\,G} \times \frac{P\,e}{L} \quad \ldots\ldots(17)$$

The curvature of the elastic line due to shearing force is equal to

$$\frac{d^2y_{av}}{dx^2_a} = \frac{d}{dx_a}\left(\frac{K}{A_a\,G} \times \frac{P\,e}{L}\right) \quad \ldots\ldots(18)$$

Since the term in the parentheses will be a constant at the instant buckling begins, it is seen that the curvature due to shearing forces in the top segment is zero. Consequently, the total curvature of the elastic line is that due to bending only. Hence, $\frac{d^2y_{am}}{dx^2_a} = \frac{d^2y_a}{dx^2_a}$, and from Eq. 15, integrating once—

$$\left(\frac{dy}{dx}\right)_a = -\frac{m^2\,e\,x^2_a}{2\,u\,L} + C \quad \ldots\ldots(19)$$

Integrating again,

$$y_a = -\frac{m^2\,e\,x^3_a}{6\,u\,L} + C\,x_a + D \quad \ldots\ldots(20)$$

The constants C and D may be evaluated from the following conditions:

$$(y_a)_{x_a=0} = 0; \qquad \left(\frac{dy_a}{dx_a}\right)_{x_a=a} = -\left(\frac{dy_b}{dx_b}\right)_{x_b=b} \quad \ldots\ldots(21)$$

from which $D = 0$, and

$$C = \frac{m^2\,e\,a^2}{2\,u\,L} - \frac{a\,e\,q}{L}\cot q\,b - \frac{e}{L} \quad \ldots\ldots(22)$$

Finally, substituting these values into Eq. 20:

$$y_a = -\frac{m^2\,e\,x^3_a}{6\,u\,L} - \left(\frac{m^2\,e\,a^2}{2\,u\,L} - \frac{a\,e\,q}{L}\cot q\,b - \frac{e}{L}\right) x_a \quad \ldots\ldots(23)$$

The deflection e may be eliminated from Eq. 23, using the condition that $y_a = e$ at $x_a = a$. Performing this operation and simplifying:

$$\tan q\,b = \frac{a^2\,q}{\frac{m^2\,a^3}{3\,u} - a - L} \qquad (24a)$$

If $b = k\,L$, then $a = L\,(1 - k)$, and Eq. 24*a* may be rewritten as follows:

$$\frac{\tan k\,q\,L}{q\,L} = \frac{1}{\frac{m^2\,L^2}{3\,u}(1 - k) - \frac{2 - k}{(1 - k)^2}} \qquad (24b)$$

The smallest useful roots satisfying Eq. 24*b*, using predetermined values of k and u, give the desired solution of the buckling problem under consideration. Before making specific applications of Eq. 24*b*, which, it will be remembered, was derived for solid struts, it will first be interesting to show that, with minor changes, it will apply to latticed struts.

Latticed Struts.—Eq. 24*b* applies to latticed and solid struts alike, provided the appropriate constants are used for each case. In straight solid struts loaded as shown in Fig. 1, the slope at any distance x_b from the bottom origin due to shearing force, from Eqs. 6 and 8, is

$$\left(\frac{dy}{dx}\right)_b = -\frac{K\,V_b}{A_b\,G} = -\frac{K}{A_b\,G}\left[-P\left(\frac{dy}{dx}\right)_b + \frac{P\,e}{L}\right]$$

$$= -\gamma\,P\left[\frac{e}{L} - \left(\frac{dy}{dx}\right)_b\right] \qquad (25)$$

and the resulting curvature (see Eq. 10*a*) is

$$\frac{d^2y_{bv}}{dx_b^2} = \frac{K}{A_b\,G} \times P\left(\frac{d^2y}{dx^2}\right)_b = \gamma\,P\left(\frac{d^2y}{dx^2}\right)_b \qquad (26a)$$

in which $\gamma = \dfrac{K}{A_b\,G}$. For built-up or latticed struts similarly loaded, the corresponding slope due to shearing force is

$$\frac{dy_{bv}}{dx_b} = -\psi\,V_b = -\psi\,P\left[\frac{e}{L} - \left(\frac{dy}{dx}\right)_b\right] \qquad (26b)$$

and, for the curvature,

$$\frac{d^2y_{bv}}{dx_b^2} = \psi\,P\left(\frac{d^2y}{dx^2}\right)_b \qquad (26c)$$

The constants γ and ψ may be thought of as the slope of the strut axis caused by a shearing force of unity in the solid and latticed struts, respectively. Similar logic may be applied to the top segment.

The curvature due to bending of a built-up strut is independent of the type of lattice used, the lattice bars merely serving the purpose of keeping apart the

principal longitudinal component parts of the strut. Consequently, no change in fundamental approach to curvature caused by bending need be made for latticed struts from that used for solid struts.

The foregoing demonstrates that the only difference in analysis and design of solid and latticed struts lies in the constants γ and ψ. Thus, Eq. 24*b* is valid for solid and latticed struts with the following differences: For solid struts

$$q = \frac{m}{\sqrt{1 - \frac{K P}{A_b G}}} = \frac{m}{\sqrt{1 - \gamma P}} \quad \ldots\ldots\ldots\ldots\ldots\ldots (27a)$$

and, for latticed struts,

$$q = \frac{m}{\sqrt{1 - \psi P}} \quad \ldots\ldots\ldots\ldots\ldots\ldots\ldots\ldots (27b)$$

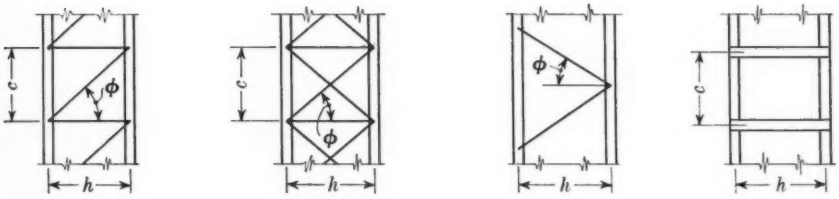

FIG. 2

The expressions for ψ for different built-up struts shown in Fig. 2 and for different types of lattice are, respectively,[5]

$$\psi_a = \frac{1}{E}\left(\frac{1}{A_d \sin\phi \cos^2\phi} + \frac{h}{c\, A_p}\right) \quad \ldots\ldots\ldots\ldots\ldots\ldots (28a)$$

$$\psi_b = \frac{1}{E}\left(\frac{1}{2\, A_d \sin\phi \cos^2\phi}\right) \quad \ldots\ldots\ldots\ldots\ldots\ldots (28b)$$

$$\psi_c = \frac{1}{E}\left(\frac{1}{A_d \sin\phi \cos^2\phi}\right) \quad \ldots\ldots\ldots\ldots\ldots\ldots (28c)$$

and

$$\psi_d = \frac{1}{E}\left(\frac{c\, h}{12\, I_p} + \frac{c^2}{24\, I_c}\right) \quad \ldots\ldots\ldots\ldots\ldots\ldots (28d)$$

in which c is the spacing of battens; h, the length of the battens between the hinges; A_p, the cross-sectional area of the two battens; A_d, the cross-sectional area of two diagonals; ϕ, the angle between batten plates and the diagonals; I_p, the moment of inertia of two batten plates about axes through the center of gravity and parallel to the z-axis; and I_c, the moment of inertia of the cross section of a vertical channel about its own gravity axis parallel to the web.

[5] "Theory of Elastic Stability," by S. Timoshenko, 1st Ed., McGraw-Hill Book Co., Inc., New York and London, 1936, pp. 141–145.

Special Application

A special application of the formulas derived will be made now for the case when $k = 0.5$, and $\frac{I_a}{I_b} = u = 1.0$. Substituting these factors into Eq. 24*b* and rearranging slightly,

$$\frac{\tan \frac{1}{2} q L}{q L} = \frac{6}{m^2 L^2 - 36} \quad \ldots\ldots (29)$$

The relationship between m and q, for solid struts, is

$$q L = \frac{m L}{\left(1 - \frac{K P}{A_b G}\right)^{0.5}} = \frac{m L}{\left(1 - \frac{K E I_b m^2 L^2}{A_b G L^2}\right)^{0.5}} = \frac{t}{(1 - \alpha t^2)^{0.5}} \quad \ldots (30)$$

in which $m^2 = \frac{P}{E I_b}$, $t = m L$; $\alpha = \frac{K E I_b}{A_b G L^2} = \frac{K E}{G \left(\frac{L}{r}\right)^2}$. Eq. 29 is now rewritten:

$$\frac{\tan \left[\frac{\frac{1}{2} t}{(1 - \alpha t^2)^{0.5}} \right]}{\frac{t}{(1 - \alpha t^2)^{0.5}}} = \frac{6}{t^2 - 36} \quad \ldots\ldots (31a)$$

The constant α in Eq. 31*a* is small, being in the order of 0.001 for $\frac{L}{r} = 50$ and $\frac{E}{G} = 2.5$. The corresponding smallest useful root satisfying Eq. 31*a* is $t = 4.3$, whereas for $\alpha = 0$, $t = 4.32$ in the writer's paper on this subject.[6] (The root is inadvertently shown as 2.2 instead of the correct root 2.16 for slenderness $\frac{b}{r}$. For slenderness $\frac{L}{r}$, the root is 2 (2.16) = 4.32.) It is thus seen that, for solid stout struts, the shear effect on the strength is small. For more slender struts, the effect of shear on the strength will be even less. Thus, it is permissible to neglect the shear effect when measuring the strength of solid struts.

Latticed Struts.—The situation is somewhat different for built-up or latticed struts, the strength of which may be significantly reduced by shearing deflections. To write the theoretical equation depicting the buckling state, use Eq. 31*a* substituting β for α:

$$\frac{\tan \left[\frac{0.5 t}{(1 - \beta t^2)^{0.5}} \right]}{\frac{t}{(1 - \beta t^2)^{0.5}}} = \frac{6}{t^2 - 36} \quad \ldots\ldots (31b)$$

in which

$$\beta = \frac{\psi E I}{L^2} = \frac{\psi E A}{\left(\frac{L}{r}\right)^2} \quad \ldots\ldots (32)$$

[6] *Bulletin No. 101*, Eng. Experiment Station, Univ. of Washington, Seattle, p. 18.

The smallest useful roots of t satisfying Eq. 31*b*, using different values of β, determine the buckling state and the critical load, P. Values of β varying from 0.0 to 0.05 were assumed and the corresponding t roots found. The results are

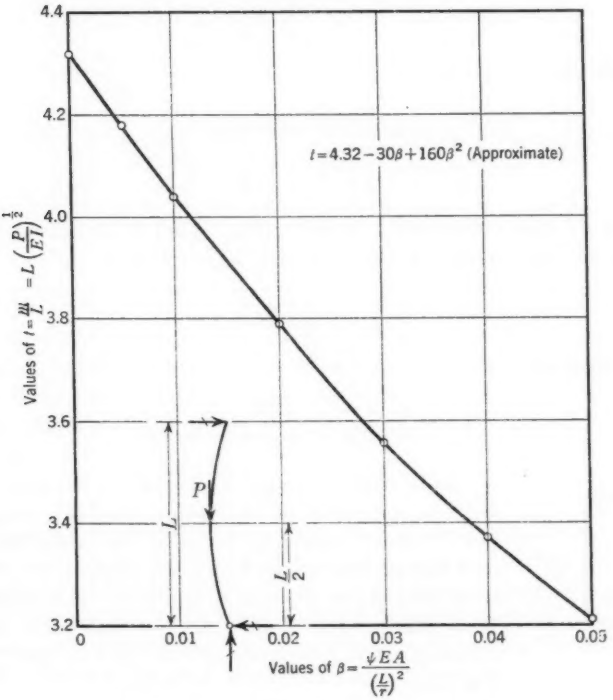

FIG. 3.—t ROOTS FOR DIFFERENT VALUES OF β

shown in Fig. 3. An approximate relationship between t and β may be expressed by the equation

$$t = 4.32 - 30\,\beta + 160\,\beta^2 \ldots\ldots\ldots\ldots\ldots\ldots (33a)$$

Having found the root t for a given value of β, the critical load on the strut may be found from the relation

$$t^2 = m^2 L^2 = \frac{P L^2}{E I} \ldots\ldots\ldots\ldots\ldots\ldots\ldots (33b)$$

Solving for P, the buckling or critical load is

$$P = \frac{t^2 E I}{L^2} = \frac{t^2 E A}{\left(\frac{L}{r}\right)^2} \ldots\ldots\ldots\ldots\ldots\ldots\ldots (34a)$$

The strength of a latticed strut may be obtained from the strength of a solid strut having the same flexural rigidity, by using a fictitious length, L_f.

This length may be determined as follows: The critical load for the solid struts is

$$P' = \frac{(4.32)^2\, E\, A}{\left(\frac{L}{r}\right)^2} \quad \ldots\ldots\ldots\ldots\ldots\ldots\ldots\ldots (34b)$$

and, for the latticed struts,

$$P = \frac{t^2\, E\, A}{\left(\frac{L}{r}\right)^2} = \frac{(4.32)^2\, E\, A}{\left(\frac{L_f}{r}\right)^2} \quad \ldots\ldots\ldots\ldots\ldots\ldots\ldots\ldots (34c)$$

The effect of shear deflections on the critical load is neglected in Eq. 34*b*. From Eq. 34*c* the required fictitious length is found to be

$$L_f = \left(\frac{4.32}{t}\right) L \quad \ldots\ldots\ldots\ldots\ldots\ldots\ldots\ldots (35a)$$

or, approximately,

$$L_f = \left(\frac{4.32}{4.32 - 30\,\beta + 160\,\beta^2}\right) L \quad \ldots\ldots\ldots\ldots\ldots\ldots (35b)$$

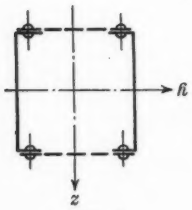

FIG. 4

Numerical Example.—Consider a straight strut (see Fig. 4) composed of two 15-in. channels weighing 35 lb per ft laced together by 2-in. by $\frac{3}{8}$-in. batten plates and lattice bars as in Fig. 2(*a*), so that $c = h = 8.5$ in., $\phi = 45°$, $A_p = A_d = 1.5$ sq in.; $A = 20.46$ sq in.; $I_y = 637$ in.^{4}, $I_z = 627$ in.^{4}, $(r_z)_{\min} = 5.5$ in., approximately, and $E = 30 \times 10^6$ lb per sq in. Then (see Eq. 32),

$$\beta = \frac{\psi\, E\, A}{\left(\frac{L}{r}\right)^2} = \frac{\psi\, E\, (20.46)}{\left(\frac{L}{r}\right)^2} \quad \ldots\ldots\ldots\ldots\ldots\ldots\ldots\ldots (36)$$

and, from Eq. 28*a*,

$$\psi_a = \frac{1}{E}\left(\frac{1}{1.5 \times 0.707 \times 0.707^2} + \frac{8.5}{8.5 \times 1.5}\right) = \frac{2.550}{E} \quad \ldots\ldots (37a)$$

Finally—

$$\beta = \frac{52.2}{\left(\frac{L}{r}\right)^2} \quad \ldots\ldots\ldots\ldots\ldots\ldots\ldots\ldots\ldots\ldots (37b)$$

By assuming different slenderness ratios, $\frac{L}{r}$, the corresponding t roots can be obtained, and subsequently the critical loads for the latticed struts, with respect to the z-axis. The critical loads on solid struts can be calculated easily. These

are listed in Table 1, Cols. 5 and 6, respectively. The ratios of the critical loads on latticed and solid struts of the same slenderness and cross-sectional areas are given in Col. 7, Table 1. The effect of shearing deflections on the critical

TABLE 1.—COMPARISON OF STRENGTH OF STRUTS

$\frac{L}{r}$	β	i	L_f	P'	P	$\frac{P}{P'}$	$\frac{P}{A}$
(1)	(2)	(3)	(4)	(5)	(6)	(7)	(8)
60	0.0145	3.92	1.1 L	0.106 E	0.0875 E	0.825	128,000 [a]
100	0.00522	4.17	1.036 L	0.0382 E	0.0356 E	0.93	52,000 [a]
120	0.00362	4.215	1.025 L	0.0265 E	0.0252 E	0.95	37,000 [a]
200	0.00131	4.28	1.01 L	0.00955 E	0.00935 E	0.98	13,700 [a]
Source	Eq. 37*b*	Fig. 3	Eq. 35*a*	Eq. 34*b*	Eq. 34*a*	....	....

[a] Pounds per square inch.

load is thus shown to be more pronounced for the stout struts than for the more slender ones. For the latticed strut of usual slenderness, a decrease in strength occurs from 5% to 10% of the strength of a strut with a solid web and equal flexural rigidity; the higher percentage pertaining to steels with a high proportional limit.

CONCLUSION

The strength of latticed struts, pin-supported at one end, laterally restrained at the other, and loaded halfway between the supports, may be substantially reduced by the shearing forces, if battens and lacing bars of small cross section are used. For the lattice systems indicated in Fig. 2, using definite batten and lacing bar sizes, the percentage reduction in strength due to shear effect can be calculated for the type of strut herein considered, by the method presented in the paper.

AMERICAN SOCIETY OF CIVIL ENGINEERS

Founded November 5, 1852

DISCUSSIONS

AERATION OF SPILLWAYS

Discussion

BY G. H. HICKOX

G. H. HICKOX,[14] M. AM. SOC. C. E.[14a]—The discussions of this paper leave very little to be added in closing.

The writer is not quite in agreement with Professor Johnson that the increase of discharge occurring with reduction of pressure beneath the nappe is caused by expanding the cross section of the nappe. The cross section may expand, but the writer prefers to attribute the increase in discharge largely to the increased velocity, which must exist because of the larger pressure difference on the lower side of the nappe.

Mr. Johnson and Messrs. Howe and Lomax remark on the lessened air requirement when air circulates beneath the nappe. The amount of air circulating depends principally on the size of the eddy in the tailwater beneath the nappe. The size of this eddy is affected by the depth of tailwater, the height of fall, and the slope of the downstream face of the spillway. In the spillways for which the experiments were made, the nappe fell on the sloping face of the spillway and no air circulated. Provision of aeration vents for the maximum air requirement will always be safe and ordinarily will not be excessively expensive.

The agreement between the writer's experiments and the independent work of Messrs. Howe and Lomax with respect to the effect of pressure reduction on discharge, as shown in Figs. 14 and 15, is very gratifying. The use of Eq. 15 will eliminate the need for Fig. 10. The data of Messrs. Rouse and Reid, cited by Mr. Stevens,[11,12,13] also show good agreement with Fig. 10.

It was not assumed, as Mr. Stevens suggests, that it is always desirable to prevent subatmospheric pressures. In the case of the dams for which the

NOTE.—This paper by G. H. Hickox, M. Am. Soc. C. E., was published in December, 1942, *Proceedings*. Discussion on this paper has appeared in *Proceedings*, as follows: March, 1943, by Joe W. Johnson, Assoc. M. Am. Soc. C. E., and May, 1943, by J. W. Howe, Assoc. M. Am. Soc. C. E., Claud C. Lomax, Jr., Jun. Am. Soc. C. E.; and June, 1943, by J. C. Stevens, M. Am. Soc. C. E.

[14] Senior Hydr. Engr., TVA, Hydraulic Laboratory, Norris, Tenn.

[14a] Received by the Secretary October 18, 1943.

[11] "Model Research on Spillway Crests," by Hunter Rouse and Lincoln Reid, *Civil Engineering*, January, 1935, p. 10.

[12] "Fluid Mechanics for Hydraulic Engineers," by Hunter Rouse, McGraw-Hill Book Co., Inc., New York, N. Y., 1st Ed., p. 316.

[13] "Model Research on Spillway Crests," by Hunter Rouse and Lincoln Reid, *Civil Engineering*, January, 1935, p. 11, Fig. 2.

studies were made, it was necessary to prevent the pressure beneath the nappe from being lowered to a point that would endanger the safety of the gate. In the case of the field tests described, the average hydrostatic head on the lower leaf was increased from a normal value of 29.5 ft to 39.2 ft. If the pressure beneath the nappe could have been reduced to the vapor pressure of the water, the average hydrostatic head on the gate would have amounted to more than 60 ft. This is twice the maximum load for which the gate was designed and does not consider any secondary effects that might be caused by vibration.

Mr. Stevens' suggestion that spillways be overloaded to increase their discharge capacity appears to have merit, if the overload condition is provided for peak discharges only and not designed for regular operation. In the present state of the knowledge of cavitation phenomena it is not safe to assume that cavitation damage will not occur, and until further knowledge of this subject is available it would seem wise not to invite it. Excessive damage should not occur during short periods of operation, however, and if the spillway face remains dry for long intervals, it would be possible to make any needed repairs. It would seem that the possibility of effecting economics by overloading spillways for short-period peak discharges could well be investigated in future designs.

The writer wishes to thank those who have contributed the valuable confirming data and the suggestions contained in their discussions.

AMERICAN SOCIETY OF CIVIL ENGINEERS

Founded November 5, 1852

DISCUSSIONS

RIVETED AND PIN-CONNECTED JOINTS OF STEEL AND ALUMINUM ALLOYS

Discussion

BY LEON S. MOISSEIFF, E. C. HARTMANN, AND R. L. MOORE

LEON S. MOISSEIFF,[19] M. AM. SOC. C. E., AND E. C. HARTMANN,[20] AND R. L. MOORE,[21] ASSOC. MEMBERS, AM. SOC. C. E.[21a]—If the sole object of this investigation had been to determine the load distribution on rivets, the arrangement of the twelve rivets in each half of the joints in three lines of four rivets or two lines of six rivets might have been a more desirable pattern, as Mr. Jones suggests. As the "Introduction" states, however, these tests were undertaken in an effort to obtain information on the strength and general behavior of large multiple-riveted joints involving different combinations of steel and aluminum alloys, as well as to obtain information on load distribution. The arrangement of the rivets in four lines of three each was chosen because it represented a more frequently used pattern of joint and appeared well suited for the over-all purposes of these tests. The results of tests of riveted joints involving combinations of steel and aluminum plates with five rivets in line on either side of the joints have been reported elsewhere.[22]

The average shear strengths of 40,600 lb per sq in. and 41,100 lb per sq in. obtained from the tests of carbon steel rivets in carbon steel plates (Tables 8 and 9(*a*)) were admittedly not as high as would be expected from conventional hot-driven rivets. These low strength values, however, may be attributed principally to the type of rivet used rather than to deficiencies in the quality of the material. Shear strengths obtained from tests of ½-in. diameter specimens machined from the rivet bar, made in a double-shear tool, averaged slightly more than 44,000 lb per sq in. It should be emphasized that the rivets used in these joints were not conventional ones, but consisted of 2½-in. lengths

NOTE.—This paper by Leon S. Moisseiff, M. Am. Soc. C. E., and E. C. Hartmann, and R. L. Moore, Assoc. Members, Am. Soc. C. E., was published in January, 1943, *Proceedings*. Discussion on this paper has appeared in *Proceedings*, as follows: April, 1943, by Jonathan Jones, M. Am. Soc. C. E.

[19] Cons. Engr., New York, N. Y. (Mr. Moisseiff died on September 3, 1943.)

[20] Research Engr., Aluminum Research Laboratories, Aluminum Co. of America, New Kensington, Pa.

[21] Research Structural Engr., Aluminum Research Laboratories, Aluminum Co. of America, New Kensington, Pa.

[21a] Received by the Secretary October 20, 1943.

[22] Discussion by H. N. Hill and Marshall Holt of paper entitled "Work of Rivets in Riveted Joints," by A. Hrennikoff, *Transactions*, Am. Soc. C. E., Vol. 99 (1934), p. 464.

of $\frac{7}{8}$-in. rod which were pressed in the $\frac{7}{8}$-in. drilled and reamed holes and then upset cold in a yoke type riveter to approximately $1\frac{5}{16}$-in. diameter at the ends. This type of rivet was selected for test purposes to permit an inspection of the plate material adjacent to the rivets, to provide additional clearance for strain readings between rivets, and to minimize the uncertain effects of friction. The writers share Mr. Jones' opinion that the results of these shear tests should not be considered as having any effect upon rivet shear allowances in specifications for carbon steel.

Mr. Jones states that Fig. 15 does not show a bearing failure for the carbon steel pin-connected joint. The writers agree that a true bearing failure, which involves a crushing of the material at the contact surfaces between pin and plates, is probably not attainable in a ductile metal any more than is a definite value of the ultimate compressive strength of such a material. Fig. 15 merely illustrates the types of failure obtained in tests in which bearing stresses were of primary importance.

An increase in the marginal distance between the pin and the edge of the plate in the bearing tests would undoubtedly have increased the ultimate bearing strength of the carbon steel joint. The increase would not be as large, however, as would be obtained in specimens having a lower ratio of pin diameter to plate thickness (D/t). The failure to develop a bearing strength in the test of the carbon steel joint comparable to strengths developed in certain tests described by Mr. Jones,[16] probably may be attributed to differences between the D/t-ratios of the specimens used. Tests to determine allowable bearing values (unenclosed bearing) for aircraft structural design, for example, have shown that, for a D/t-ratio of 8, increases in edge distance beyond approximately 2 diameters, measured from the center of the hole, result in no appreciable increase in ultimate bearing strength. For D/t-ratios of 4 or less, however, bearing strengths increase with edge distance for values of the latter ranging from 2 to 4 diameters.

[16] "Static Tests of Riveted Joints," by Jonathan Jones, *Civil Engineering*, May, 1940 (see heading "Strength of Rivets in Shear"), p. 286.

AMERICAN SOCIETY OF CIVIL ENGINEERS

Founded November 5, 1852

DISCUSSIONS

SIMPLIFIED ANALYSIS OF SKEWED REINFORCED CONCRETE FRAMES AND ARCHES

Discussion

BY BERNARD L. WEINER, AND ALFRED L. PARMÉ

BERNARD L. WEINER,[14] M. AM. SOC. C. E.[14a]—The design of any structure, including that of a skew arch, is normally divided into two parts: (1) The computation of the reactions, and (2) the design of the sections to resist the internal stresses. Although this is the usual procedure, the two steps are not as separate and distinct as they are generally assumed to be. The major part of the paper is devoted to the first step, but the second step is covered sufficiently to indicate the general method of attack. Each step will be discussed separately and in the order given.

Step I. Reactions.—The purpose of this part of the paper is to show that permissible approximations may be made in the frame constants with the result that the equations developed on the basis of the accepted theory (proved by tests) are simplified. In addition, the equations break up into groups, each of course containing fewer unknowns. That permissible approximations usually result in simplifications is, of course, obvious; nevertheless, the results are approximate and the paper has been misnamed. Neither proof nor data are given for the degree of approximation.

The author states that certain reactions are affected but slightly by the skew and can be computed from a right arch of the same square span and with the same arch constants. Once this assumption is made, the so-called "skew stresses or reactions" can be computed independently. The author states further that, for a flat-topped bridge, these properties can be proved mathematically. This has been known for some fifteen years. In fact, all that is necessary is that the members have straight center lines which are either vertical or horizontal; the individual members may have variable moments of inertia and the strict mathematical proof is still valid. The shape of such

NOTE.—This paper by Richard M. Hodges, M. Am. Soc. C. E., was published in May, 1943, *Proceedings*. Discussion on this paper has appeared in *Proceedings*, as follows: September, 1943, by Messrs. C. D. Geisler, and Arthur G. Hayden.

[14] Designer, Parsons, Brinckerhoff, Hogan & Macdonald, New York, N. Y.

[14a] Received by the Secretary September 21, 1943.

a structure is not a practical one, but, for the purpose of studying the permissible approximations, this fact is of no importance.

Many years ago the writer found that for a symmetrical structure the approximations were permissible and result in the simplifications stated. In 1931 the writer gave a complete mathematical derivation of the simplified approximate equations applying to the symmetrical rigid frame with straight center lines and with variable moments of inertia.[6] For practical structures, the approximations were shown to be negligible; influence lines obtained by the use of the approximate equations were plotted on the same chart with the corresponding curves from the more accurate analysis.[15] Two sets of curves were given—one for a 32° skew and another for a 50° skew. The square spans were 56 ft and 41 ft, respectively.

The question still remained, at that time, whether the approximate analysis was valid for unsymmetrical rigid frames and for single-span structures with sharply curved soffits. There was also no information available whether the approximations were valid for multiple-span bridges. From his own experience in the design of numerous bridges of various shapes and skews, and of one, two, and three spans, the writer has found that good approximations may be made with great reduction in the amount of numerical work involved. An experienced designer will soon find that he can make his own approximations very easily for any specific case provided he has a good basis from which to begin.

A word of caution is necessary, however. Since bridge design should be regarded as a science, an experienced and conscientious structural engineer should get a thorough understanding of the action of skew structures by completing at least one accurate analysis. He will then get the "feel" of the values involved, and will be able to find permissible approximations of his own which he can use with confidence. The design of skew bridges is not as difficult as seems to be assumed—the real difficulty, if any, is the solid geometry involved rather than the structural theory.

There is still much useful work to be done on a real and complete simplification of the skew structure. It is the writer's opinion that the governing stresses—those that exist in modified form in a right arch—may be computed in all cases by simplified equations regardless of shape and of the number of spans. The skew stresses, however, may not only be computed from approximate equations, but, since they are of lesser importance, it is the writer's belief that curves can be developed from which they could be estimated with sufficient accuracy for design purposes. The reason why this possibility suggests itself will be discussed more fully under Step II, "Stress Distribution."

The complete simplification of the skew structure is an urgent necessity, for modern highway speeds make good alinements obligatory. However, there is no excuse for distorting the alinement of a highway in order to avoid a skew bridge because the cost of even the most tedious "exact" design is less than the cost in human lives lost on sharp highway curves. As a matter of

[6] "Design of a Reinforced Concrete Skew Arch," by Bernard L. Weiner, *Transactions*, Am. Soc. C. E., Vol. 96 (1932), p. 1212.

[15] *Ibid.*, p. 1286.

fact, the difficulties which the author and others deplore are largely exaggerated. With an orderly arrangement of the equations and with a simple system of signs, the work involved is only a small part of the total man-hours necessary to prepare a complete set of plans. More time has been spent attempting to avoid work, very often, then the work itself would require. Since short cuts seem so desirable, however, they may be had practically for the asking.

Much confusion indeed has been caused by the constant search for new "methods." The writer takes issue with the author's contention that his "method" is more simple than other "methods," whether approximate or exact. All the different methods are really not different at all; it is a misuse of the English language to refer to "different methods." The differences consist of such matters as the choice of the origin of coordinates, the "basic structure" chosen for the analysis, and in some numerical short cuts which are usually present in all numerical work.

Obviously, one should choose an origin of coordinates and a basic structure which will reduce the resulting equations to the simplest form. The writer has given complete equations[6] for both the symmetrical and unsymmetrical skew arch (single span) with the origin and basic structure chosen with this idea in mind. There should be no more question about this than there is, normally, about writing $x^2 + y^2 = r^2$ rather than $(x + a)^2 + (y + b)^2 = r^2$ for the equation of the circle. Most of the variations in the different methods consist of differences as profound as that in the two equations of the circle. Furthermore, experienced designers will soon find that, when they are doing the numerical computations themselves, they can apply such arithmetic short cuts as elastic loads to the skew arch as well as to the right arch.

The writer has found from long experience in the drafting room that it is more efficient to use a formal set of equations so that the computers need do nothing more than substitute in formulas. Even the experienced designer will find that, unless a formal setup is used, he will constantly be "thinking it out," which is not only time consuming but is also a constant source of error. When deadlines have to be met and with only juniors available to do the computing, one experience will convince a supervising designer that the proper and formal setup will save him both time and grief.

Furthermore, having well setup equations, it becomes a simple matter to make the angle $\phi = 0°$ and $90°$ and thus derive approximations of his own without going through a complete derivation each time. At the same time he has the more accurate equations available for checking the results of his approximations. Although this is true (using a formal set of equations) for the single span, it is an absolute necessity for multiple spans.

The question of signs is important in all structural analysis, but it is doubly important in skew-arch work. The author does not give a formal statement as to the directions of the positive moments and thrusts. A "picture" is not sufficient, for again experience shows that there is too much room for misinterpretation. In right arches of single span, the moments and thrusts scarcely need a sign system, but even in this case there is confusion about the shears. In a multiple-span and multiple-story analysis, a sign system stated in words is

mandatory if error and confusion are to be avoided. It is equally mandatory in skew-arch work.

The writer has found that a system of signs based on the structure rather than a "space system" is very much easier to remember and to apply. In fact, it was partly because the original skew-arch theory was written on the basis of a space system that it had to be revised for efficient use in the drafting room, and this revision constitutes Part I of the writer's paper[16]—and is so stated therein. This system of signs (based on the structure) has been used by the writer for years in his subsequent work and the test in the drafting room has given the verdict. For example, in a space system, if the transverse shear, T_z or R_z, is defined as positive on the left section going away from the observer, it will reverse itself and be of opposite sense on a right section, and reverse again for a right-hand skew if the original definition is for a left-hand skew. As it happens, this shear almost always points toward the obtuse angle and, if it is defined as positive in this direction, the sign sense will not reverse either with the change in section or with the skew for the change from right to left. Such a system based on the structure is as much simpler than a space system as the ordinary convention of positive and negative moment in a horizontal beam is more simple than the clockwise and counterclockwise convention. The signs of the other forces and of the moments also are simplified similarly if the signs are based on the structure. It is a detail, but one of great importance both as a timesaver and as a way of avoiding errors. Perhaps the lack of a simple and easily applied sign system accounts for some of the confusion and difficulty which the author mentions.

The question of the assumption as to the degree of fixity of the footings is not unique with the skew arch. Actually, the footings are assumed neither fixed nor hinged; they are really designed for both conditions—for complete fixity and for free rotation about the z-axis. The theory is that, if the design is adequate for the two limits, it will also be sufficient for the actual condition of partial fixity. It was found, however, that either condition gives practically the same results except at the bottom of the "leg" or post, and even here there is sufficient dowel steel available, as a matter of practical detailing, to resist the moment produced by even full fixity. Hence, since it is simpler to design for the hinged condition and it is also slightly on the safe side for the critical crown section, the analysis is generally made on the basis of this assumption. The assumption of a virtual hinge for rotation about the z-axis is not so inconsistent therefore with fixity about the x-axis as would appear; in any case, rotation about this axis also can be taken care of easily, as the author shows. Rotation about the y-axis is hardly likely as friction and the restraint furnished by the wing walls will prevent it.

In recent years, this question of footing condition has been taken into account directly, especially where the correction is not so simple and obvious as in the single-span frame. The factor "k" or soil modulus has been introduced and thus the condition of the footing is taken into account directly in the analysis.

[16] "Design of a Reinforced Concrete Skew Arch," by Bernard L. Weiner, *Transactions*, Am. Soc. C. E., Vol. 96 (1932), p. 1214.

The writer cannot agree that unbalanced earth pressure is rarely used in practical design. Many designers have come to agree with the late William Cain, M. Am. Soc. C. E., that a structure should not be designed so as to depend for its safety on the presence of the active earth pressure. The procedure has therefore been adopted of using the balanced earth pressure only when it is of the same sign as the dead and live load moments and to omit it when of opposite sign. Unbalanced earth pressure is also used but, for this condition, the basic unit stresses are increased by 10% or 15%. This condition often governs the design of the reinforcement.

The author states that such tests as have been made were for the effect of live load in various positions and that, since the effects of these loads are small, the implication seems to be that they are of little value. The writer fails to see the point of this reasoning. The tests still prove that the computed reactions check closely with the measured reactions for loads—any loads, not necessarily live loads—applied in various ways. That more tests would be of value is no doubt true, but that still does not explain why those already made do not prove what they were intended to prove.

The writer also fails to understand the reasoning on the earth-pressure distribution. Once equivalent fluid pressure is assumed, it acts normal to the surface of the wall and that is all that there seems to be to it. It is true, of course, that the equivalent fluid pressure theory leaves much to be desired in the way of a rational theory, but this rather unfortunate situation is not unique with the skew arch; it is true of all structures subjected to earth pressure.

Step II. Stress Distribution.—Even though in practice Step I comes first, it is really, from the analytical point of view, "putting the cart before the horse." Loads acting on a structure are resisted by internal stresses and not by moments, thrusts, and shearing forces. The internal stresses are tensions (or compressions which are merely of opposite sign to tensions) and shears. The so-called bending moments, torsion moments, thrusts, etc., are merely names for the summations or resultants of the primary internal stresses. As a matter of fact, in the rigorous derivation of the beam theory by the mathematical theory of elasticity, the internal stresses are obtained first—and it is then shown that the resultants can be summarized as "bending moments," "thrusts," etc. Since, in the general case, there are stresses in all directions, the total or resultant stresses in any direction will depend on the plane of reference.

It is only in the simple beam and in certain cases of symmetry that the moments, etc., can be found directly from the loads and the geometry of the structure. Even then, the moments and forces found tell something only about the applied loads and nothing at all about the internal stresses except that they can be equated to the resultants of the unit stresses which must be found independently by more complex methods. Since the simple beam was the first and the most common structure analyzed, the fact that it is the internal stresses which are the primary factors has been overlooked, with the result that there has been much confusion of thought about the so-called stress distribution.

Since the moments and the total thrusts and shearing forces are the resultants of the internal stresses, the reference plane chosen determines the values to be obtained. Since by the ellipse of stress, tensions on one plane

correspond to shears and smaller tensions on another plane, and vice versa, the same analysis will result in different combinations of "torsion moments" and "bending moments" depending on the plane of reference. The same thing is true of the total forces.

The late George E. Beggs, M. Am. Soc. C. E., was fully aware of the confusion of thought and told the writer that he was very much in favor of discarding the use of the terms, bending moment, etc., even for the simple beam, and to refer only to couples and forces. He was encouraging his students to think along these lines.

The author gives as his reason for not using the procedure for the design of the sections, developed in the writer's paper,[6] the claim that it is too complicated. Simplification with no loss other than mere academic accuracy is not only justified, of course, but is and should be the goal of good engineering practice. It is not a question, however, of mere accuracy. The reason the writer discarded the method of design used by the author, which Mr. Hodges credits to Professor Rathbun, is that it is not correct. Two other design procedures were proposed at that time and not only did all three give results that differed radically in their numerical values, but they even differed in sign. It was for this reason that the writer undertook the study to find the principles involved.

The writer believes that the procedure developed in his paper, with the proofs given and with the qualifying considerations clearly stated, constitutes a logical design. Hindsight being better than foresight, experience has shown that some of the stress combinations derived cannot occur in a practical structure, which simply means that a few of the tabulated procedures are not used. The combinations that do occur happen also to be the most simple to compute as a study of the numerical examples will show. The writer has used the procedure for many years in the drafting room and the men have had no difficulty in following the reasoning, once they made the little effort necessary to a clear understanding.

In Step II as in Step I, much has been written and done in an apparent effort to "simplify," and the result has been confusion. Considering the fact that the design takes about only 10% of the total time necessary for the production of a complete set of plans and specifications, the writer fails to see the necessity for this constant search. Naturally, the design of a skew arch requires a little more effort for a thorough understanding than does a simple beam but the same is true of all present-day design. However that may be, there need be no mystery about the skew structures, and the work involved is nothing to worry about.

As far as the writer knows, the only tests that have been made for the purpose of studying the internal stresses were those by E. F. Gifford and were of qualitative rather than of quantitative nature. With the permission of Mr. Gifford, the writer published photographs of the models tested to destruction in his discussion of a paper by Professor Rathbun.[17] In a general way, the cracks in the models seemed to confirm the writer's stress distribution. Until

[17] "An Analysis of Multiple-Skew Arches on Elastic Piers," by J. Charles Rathbun, *Transactions*, Am. Soc. C. E., Vol. 98 (1933), p. 46, Figs. 16–25.

less crude and more complete tests are made, however, designers still will have to depend on logical reasoning for their designs.

For the sake of convenience, the reference plane, on which the total moments and thrusts of a skew arch are computed, is a radial plane parallel to the abutments. The plane chosen for the design of the sections is not the one that is most "practical" but the one on which the particular moments and forces under consideration are maximum. In other words, such recognized criteria as are furnished by the ellipse of stress must still be satisfied—regardless of the type of structure analyzed. In addition, the laws of equilibrium require that the boundary conditions be satisfied without stress on external surfaces. Neither of these conditions, among others, is fulfilled by the procedure given by the author.

To find the maximum moments producing the maximum tensions (or shears, for that matter), transformations similar to those which lead to the ellipse of stress must be made. Before this can be done, however, the moments and thrusts must be reduced to stresses (total over the thickness) per unit width. Although the author states that the width, b, does not enter into the analysis, it is only partly and approximately true; the truth is that everything is divided by b—but the structure, as the author states, is considered as a whole. Thus m/b and t/b result from the analysis, but whether or not these are stresses per unit width depends on whether the distribution is uniform or not. After the total stresses are reduced to stresses per unit width, they must be resolved to find the maximum bending moments and shearing moments ("torsion")—a procedure exactly similar to that of finding principal planes. This the author has failed to do and, however "practical" the omission may be, it is incorrect.

The author quotes Professor Rathbun incorrectly when he states that the transverse shearing force is distributed parabolically—like the shear in a rectangular beam. Professor Rathbun states quite correctly that the portion of the shear equal to the thrust multiplied by the tangent of the modified skew angle is distributed uniformly and the remainder is distributed parabolically. This procedure results from the fact that the boundary conditions must be satisfied; there would otherwise be a shear on the external face of the bridge —an impossibility, of course.

The author makes a similar statement about the shear produced by the torsion moment. In this statement, he quotes Professor Rathbun correctly, and both are in error. The reason is the same; in order to satisfy the boundary conditions for the tensions (and compressions) produced by moment, there must be shears equal to the unit tensions multiplied by the tangent of the modified skew angle. Since the resultant of the tensions is a couple, the resultant of the shears which are proportional to them must also be a couple. Therefore the terms "bending moment" and "torsion moment" are not sufficient; that is, they do not tell the whole story as far as distribution is concerned. At the boundary, the tension must be parallel to the face and the shear can be zero only on a section perpendicular to the external surface. Incidentally, the fact that this must always be true will enable the designer to eliminate some computation as soon as he gets the "feel" of the values involved. This fact may also prove to be a valuable starting point for a simplified pro-

cedure for the design of the sections. Since the design of the sections is the ultimate goal, a simplification of Step II should also simplify Step I.

St. Venant's theory of torsion and such tests that are available show that Merriman's formula is very much in error for long and narrow rectangles. Although the more exact theory of St. Venant is supposed to be quite complicated for rectangles that are nearly squares, the hyperbolic functions reach their limit very rapidly for ratios of sides greater than 3 : 1. In a bridge, the ratio is at least 10 : 1 and there is no arithmetic hardship in the use of the results derived from St. Venant's theory, as a glance at the tabulated formulas for the reduction of total stresses to stresses per unit width presented by the writer[18] will show. In any case, it is time engineers realized that their profession is a science and that, on occasion, science requires something a little more advanced that the addition of 2 + 2.

In general, whether the designer is dealing with skew arches or with any other structure, it is well for him to check the results of an analysis to see that the fundamental laws of equilibrium are satisfied; that the boundary conditions are logical; and that such accepted criteria as the ellipse of stress are also satisfied. Much grief may be avoided by this precaution.

General Remarks.—In spite of the misleading statements that have been made time and time again, the skew arch must be analyzed as a complete unit and the division by b is merely a minor arithmetic convenience which has no structural significance. The various suggestions for using longitudinal strips parallel to the face of bridge, etc., all can be shown to be in error—as often as not, on the side of danger. The "trick" of using strips and then keying and tying the laminations together results in a structure that is usually "solid" in spite of the tricks. There is no need for these subterfuges.

If a systemmatic set of equations based on a simple system of signs is used (with the origin of coordinates at the point of symmetry), even the "accurate" analysis for the reactions is not a hardship; or at least it should not be in these days when engineers are really beginning to do designing. Least difficult of all is the solution of the four simultaneous equations; for those who are worried, it can be stated that the solution can be done on one sheet of paper. However, simplifications are possible, as the writer showed many years ago, and this fact is now confirmed by the author.

As for the stress distribution, a logical design which satisfies the laws of equilibrium, and, in addition, is also consistent with such accepted criteria as the procedure by which the "ellipse of stress" leads to the conception of "principal planes" is just as simple as other "methods" and also more correct. In this phase of the problem, as in other phases, the work must be well organized —it may be said that organization is the key to true simplicity. The difficulties involved in the design of skew bridges have been largely exaggerated. Such at least has been the experience of the writer over a period of years on the design of numerous skew bridges of various shapes and of single and multiple spans. Any designer who makes the moderate effort necessary to grasp the subject need have no difficulty.

[18] "Design of a Reinforced Concrete Skew Arch," by Bernard L. Weiner, *Transactions*, Am. Soc. C. E., Vol. 96 (1932), p. 1297.

ALFRED L. PARMÉ,[19] JUN. AM. SOC. C. E.[19a]—A problem that is of vital interest to the engineering profession is treated in this paper. Unfortunately, Mr. Hodges has accepted present-day theory as adequate and has based his simplification on the existing formulas. The validity of these basic equations has not yet been completely substantiated. The writer is aware of only two quantitative experiments that have been conducted on skewed arches—one by the Bureau of Public Roads[8] and the other sponsored by the Committee on Concrete and Reinforced Concrete Arches in 1935.[10] In the former, the results obtained from tests made on concrete arches differ considerably from the values obtained by a mathematical investigation based on the method of Prof. J. Charles Rathbun,[10] M. Am. Soc. C. E. The latter series of tests, directed by the late Prof. George E. Beggs, M. Am. Soc. C. E., involved the technique of reciprocal deflections on rubber models. An apparently favorable agreement between experimental and theoretical values was obtained. However, this satisfactory trend was confined to loads at some distance from the center line of the arches. Marked deviations were noted for loads on the center line (and hence for loads symmetrical about the center line). The inconsistencies revealed by these investigations led to the careful examination (presented in this discussion) of the basic elastic equations advanced by Professor Rathbun. It will be shown that the latter contain highly questionable assumptions which militate against their usefulness.

It is not the simplification introduced by Mr. Hodges that is being questioned but the basic equations contained in the "Appendix." One difficulty with that presentation is that the equations are couched in terms not easily manipulated and having remote referents. This difficulty may be overcome by viewing the equations as extensions of the formulas derived for the analysis of curved beams. Incidentally, an excellent and lucid treatment of curved beams was presented[20] originally by A. V. Pippard and F. L. Barrow in 1926. On the basis of this mode of approach, it naturally follows that the prime difference between a two-dimensional and a three-dimensional analysis lies in the fact that displacements due to torsion are included in the latter. Thus, for the ordinary analysis of a right rigid frame:

$$\Delta = \int \frac{M\, m\, dx}{E\, I} \qquad (11a)$$

in which: Δ = the deflection at any point of the frame due to the loading on the frame; M = the bending moment at any section due to the actual loads (and reactions) acting on the frame; and m = the bending moment at any section due to the virtual or dummy load of unity (1-lb load) acting at the point whose deflection is desired, and acting in the direction of the desired deflection.

---

[19] Bronxville, N. Y.

[19a] Received by the Secretary October 1, 1943.

[8] "Progress Report on Skew Arch Tests," by G. W. Davis, *Public Roads*, Bureau of Public Roads, U.S.D.A., Vol. 6, No. 9, November, 1925, p. 185.

[10] "Concrete and Reinforced Concrete Arches," Final Rept. of the Special Committee, *Transactions*, Am. Soc. C. E., Vol. 100 (1935), pp. 1551–1573.

[20] "Stress Analysis of Bow Girders," by A. V. Pippard and F. L. Barrow, *Technical Paper No. 1*, Building Research Board, H. M. Stationery Office, 1926.

On the other hand, for a skewed frame or curved beam:

$$\Delta = \int \frac{M\,m\,dx}{E\,I} + \int \frac{T\,t\,dx}{G\,F} \quad \ldots\ldots\ldots\ldots\ldots\ldots (11b)$$

in which: T = the torsional moment acting at any section due to the actual loads (and reactions) acting on the frame; t = the torsional moment at any section due to the virtual or dummy load of unity acting at the point whose deflection is to be found and in the direction of the desired deflection; G = modulus of elasticity for concrete, in shear; and F = factor of torsion (a quantity corresponding to the moment of inertia).

It will be observed that Eq. 11*b* is a condensed statement of the relationship involved in Eq. 7*a*. Both statements (Eqs. 11*b* and 7*a*) are general and apply to any arch irrespective of its shape. To test the validity of this equation, it is best to deal directly with the simplest form of arch—namely, a straight slab clamped at each end. This selection has been made partly for the purpose of clearer exposition. However, the mathematical analysis to follow can be applied equally well to more complicated forms. In the example chosen (Fig. 7),

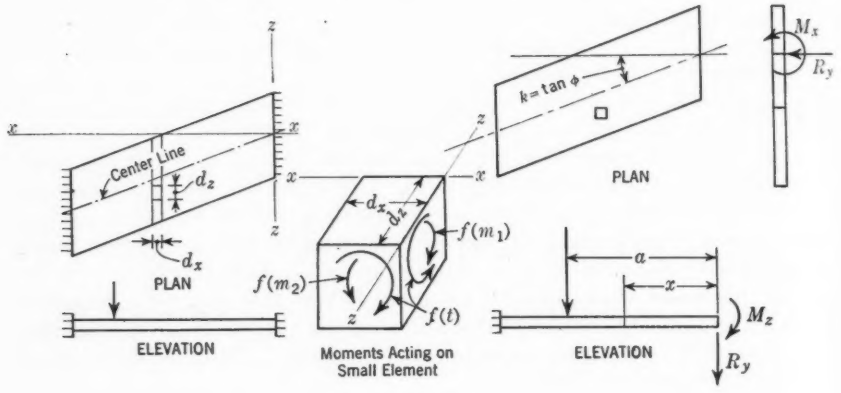

FIG. 7

the customary procedure of replacing the right support by redundant reactions has been followed. This operation transforms the slab from an indeterminate form to a determinate one. The number of equations due to displacement will be equal to the number of redundant reactions. Only the vertical displacement will be treated herein. The general equation of

$$\Delta = \int \frac{M\,m\,dx}{E\,I} + \int \frac{T\,t\,dx}{G\,F}$$

then becomes

$$\Delta = \int_a^l P\,(x-a)\,x\,\frac{dx}{E\,I} + \int_0^l [M_z\,x + R_y\,x^2]\,\frac{dx}{E\,I}$$
$$+ \int_0^l [R_y\,k^2\,x^2 + M_z\,k\,x]\,\frac{dx}{F\,G} + \int_a^l [P\,k^2\,(x-a)\,x]\,\frac{dx}{F\,G} \quad \ldots\ldots (12)$$

In this case it must be borne in mind that the moments refer to the total moment acting on a cross section of the slab.

If the problem is attacked from the strain-energy conception utilized in the analysis of thin plates, the application of a vertical load Q at N will produce bending and torsional moments on a small element. (To avoid conflict with previous notation these moments will be labeled $f(m_1)$, $f(m_2)$, and $f(t)$.) Since the internal work and external work must be equal,

$$\frac{1}{2}\left[f(m_1)\frac{\partial^2\omega}{\partial x^2} + f(m_2)\frac{\partial^2\omega}{\partial z^2} + 2f(t)\frac{\partial\omega}{\partial x\,\partial z}\right] dx\,dz = \tfrac{1}{2}(Q\,\Delta_1) \quad \ldots\ldots (13)$$

in which Δ_1 denotes the deflection of N due to the deformation of the small element; and $\frac{\partial^2\omega}{\partial x^2}$ and $\frac{\partial^2\omega}{\partial z^2}$ = angular rotation of the small element due to the load Q. Let Q now be considered a unit load; then functions $f(m_1)$, $f(m_2)$, and $f(t)$ will be the moments created by a unit load at N. Hence,

$$\left[f(m_1)\frac{\partial^2\omega}{\partial x^2} + f(m_2)\frac{\partial^2\omega}{\partial z^2} + 2f(t)\frac{\partial\omega}{\partial x\,\partial z}\right] dx\,dz = \Delta_1 \quad \ldots\ldots (14)$$

Eq. 14 expresses the relation between the deflection at N and the angular deformation at any point irrespective of the manner in which these angular deformations are produced. Now the angular deformations at any point are given by the expressions

$$\frac{\partial^2\omega}{\partial x^2} = \frac{F(M_1) + \mu\,F(M_2)}{(1-\mu^2)\,E\,I} \quad \ldots\ldots (15a)$$

$$\frac{\partial^2\omega}{\partial z^2} = \frac{F(M_2) + \mu\,F(M_1)}{(1-\mu^2)\,E\,I} \quad \ldots\ldots (15b)$$

and

$$\frac{\partial^2\omega}{\partial x\,\partial z} = \frac{F(T)}{(1+\mu)\,E\,I} \quad \ldots\ldots (15c)$$

in which $F(M_1)$, $F(M_2)$, and $F(T)$ are the moments acting on the element due to actual loads (and reactions) acting on the slab. For simplicity, assume that μ, Poisson's ratio, is equal to zero; then

$$\frac{\partial^2\omega}{\partial x^2} = \frac{F(M_1)}{E\,I} \quad \ldots\ldots (16a)$$

$$\frac{\partial^2\omega}{\partial z^2} = \frac{F(M_2)}{E\,I} \quad \ldots\ldots (16b)$$

and

$$\frac{\partial^2\omega}{\partial x\,\partial z} = \frac{F(T)}{E\,I} \quad \ldots\ldots (16c)$$

Making the proper substitution,

$$[F(M_1)\,f(m_1) + F(M_2)\,f(m_2) + 2\,F(T)\,f(t)]\frac{dx\,dz}{E\,I} = \Delta_1 \quad \ldots\ldots (17)$$

If Δ denotes the deflection of point N due to deformations in all the elements, then

$$\Delta = \int\int [f(m_1)\, F(M_1) + F(M_2)\, f(m_2) + 2\, f(t)\, F(T)] \frac{dx\, dz}{E\, I} \ldots (18a)$$

Since the designer is not interested in the effect of the transverse moment, the terms occurring because of this factor are omitted. The subscript used to differentiate the moment terms is also no longer needed. Eq. 18*a* then takes the final form

$$\Delta = \int\int [f(m)\, F(M) + 2\, f(t)\, F(T)] \frac{dx\, dz}{E\, I} \ldots\ldots\ldots (18b)$$

Eqs. 11*b* and 18*b* are two different expressions for the vertical deflection at N. The validity of the expression presented in the first part of the discussion rests on the hypothesis that a slab subject to torsion behaves like a beam. The latter has been established on a more fundamental basis. Both should yield the same result and therefore Eqs. 11*b* and 18*b* can be equated:

$$\int \frac{M\, m\, dx}{E\, I} + \int \frac{T\, t\, dx}{G\, F} = \int\int \frac{F(M)\, f(m) + 2\, F(T)\, f(t)}{E\, I}\, dz\, dx \ldots (19)$$

Recalling that M is used to designate the total moment acting on a section and that $F(M)$ expresses the moment at any point:

$$M = \int F(M)\, dz \ldots\ldots\ldots\ldots\ldots\ldots (20a)$$

and

$$m = \int f(m)\, dz \ldots\ldots\ldots\ldots\ldots\ldots (20b)$$

In a similar manner, it can be easily shown that

$$T = \int F(T)\, dz \ldots\ldots\ldots\ldots\ldots\ldots (21a)$$

and

$$t = \int f(t)\, dz \ldots\ldots\ldots\ldots\ldots\ldots (21b)$$

Therefore,

$$\int \left[\int F(M)\, dz \int f(m)\, dz\right] \frac{dx}{E\, I} + \int \left[\int F(T)\, dz \int f(t)\, dz\right] \frac{dx}{G\, F}$$
$$= \int [F(M)\, f(m) + 2\, F(T)\, f(t)] \frac{dz\, dx}{E\, I} \ldots\ldots\ldots\ldots (22)$$

Since this is an identity, each term in the expressions must correspond. Therefore:

$$\int \left[\int F(M)\, dz \int f(m)\, dz\right] \frac{dx}{E\, I} = \int\int [F(M)\, f(m)\, dz] \frac{dx}{E\, I} \ldots (23a)$$

and similarly

$$\int\left[\int F(T)\,dz\int f(t)\,dz\right]\frac{dx}{F\,G}=\int\int\frac{2\,F(T)\,f(t)\,dz\,dx}{E\,I}\ldots\ldots(23b)$$

Concentrating on only one of the terms, the integration of expression on the right side of Eqs. 23 can be performed in any order. This means, therefore, that

$$\int F(M)\,dz\int f(m)\,dz=\int F(M)\,f(m)\,dz\ldots\ldots\ldots\ldots(24)$$

Eq. 24 can be satisfied only if the variation in moment across a section is constant; but this is in sharp contradiction to established fact. As a matter of fact, the primary purpose of an analysis of skew frame is to determine just what this variation is. Therefore, the basic equations used by Mr. Hodges are incorrect because they imply an assumption that is not consistent with the physical behavior of the skewed slab.

If the variation across a section is assumed to be triangular, the moment is a linear function of z. Then, if $F(M)=K\,z$ and $f(m)=k\,z$, Eqs. 23 become:

$$\frac{12}{E\,b\,t^3}\left[\int_0^b F(M)\,dz\int_0^b f(m)\,dz\right]$$

$$=\frac{12}{E\,b\,t^3}\left[\int_0^b K\,z\,dz\int_0^b k\,z\,dz\right]=K\,k\,\frac{12\,b^3}{4\,t^3\,E}\ldots\ldots\ldots(25a)$$

and

$$\frac{12}{E\,t^3}\int_0^b F(M)\,f(m)\,dz=\frac{12}{E\,t^3}\int_0^b K\,k\,z^2=k\,K\,\frac{12\,b^3}{3\,t^3\,E}\ldots\ldots(25b)$$

A deviation of 25% is indicated in Eqs. 25. In general, $\int\frac{M\,m\,dx}{E\,I}$ is less than $\int\int F(M)\,f(m)\,\frac{dz\,dx}{E\,I}$.

It may be argued that the errors introduced apply to all terms and hence cancel. This would be true if the error in each term was a constant proportion. Such is not the case. The deviations will be more marked in terms involving the reactions than those due to loads. Therefore, the equations must lead to erroneous results. Because the final value of any reaction is the result of the difference of large numbers, it is difficult to predict in just what direction the error will lie. However, it appears that Professor Rathbun's method yields results smaller than those found experimentally.

How serious is this error? The method used to check the theory does not lend itself to an arithmetical solution. However, the results obtained experimentally and those obtained by Professor Rathbun's method can be compared, as shown in Table 12. Of all the differences to be noted between the experimental and theoretical values, the most significant is the complete lack of agreement in the values of the horizontal moment (M_y). The magnitude of

the experimental values eliminates the possibility that the deviations are just due to chance and unavoidable inaccuracies in computing and testing. It would therefore seem that the theory does not represent the elastic behavior of the skewed arches.

TABLE 12.—COMPARISON OF REACTIONS AND MOMENTS DETERMINED EXPERIMENTALLY AND THEORETICALLY

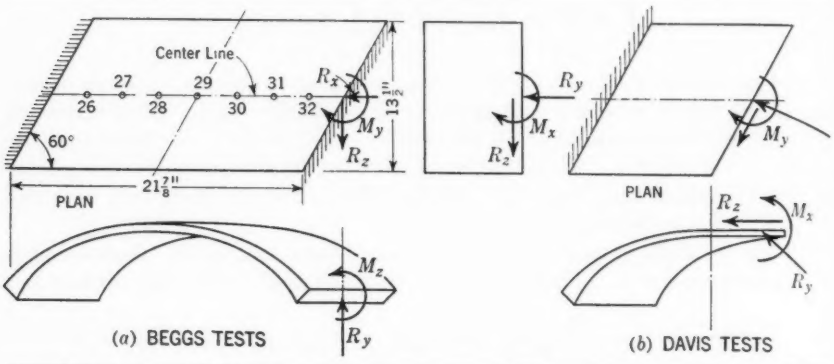

Reaction[a]	Type	(a) Beggs Tests, Arch "A"; Loads on Center Line — Distance s of Load from Reaction							(b) Davis Tests, 60° Skew Arch	
		0.90 s	0.75 s	0.64 s	0.50 s	0.36 s	0.25 s	0.10 s	Lateral restraint	Lateral displacement
R_z	Experimental	0.162	0.540	0.860	1.02	0.894	0.554	0.152	2,980	
	Theoretical	0.131	0.594	1.06	1.20	1.06	0.594	0.131	1,017	1,470
R_x	Experimental	0.002	0.046	0.192	0.27	0.188	0.036	0.026	....	....
	Theoretical	0.014	0.009	0.023	0.028	0.023	0.009	0.014	1,459	0
R_y	Experimental	0.020	0.106	0.258	0.492	0.704	0.890	0.972	2,100	
	Theoretical	0.018	0.109	0.281	0.499	0.719	0.891	0.983	2,100	2,100
M_x	Experimental	−0.010	0.32	1.14	1.56	1.14	....	0.18	83,200	
	Theoretical	0.008	0.054	0.133	0.76	0.133	0.053	0.008	9,540	53,400
M_z	Experimental	0.496	1.29	1.31	0.556	−0.575	−1.55	−1.49	....	....
	Theoretical	0.334	1.55	2.27	1.81	0.137	−1.46	−1.82	0	0
M_y	Experimental	0.088	0.096	2.44	3.02	1.80	0.46	0.050	143,100	
	Theoretical	0.016	0.110	0.244	0.39	0.73	0.40	0.31	9,432	37,080

[a] Reactions in pounds and moments in pound-inches.

In justice to the method described by Mr. Hodges it should be reemphasized that in the experiment conducted by the Committee on Concrete and Reinforced Concrete Arches much better agreement was obtained for loads near the free edges. The agreement obtained in this region does not constitute a sufficient proof of the reliability of the method however. For a theory to be tenable it must give reliable results at all points and above all for the conditions that govern the design; that is, for loads on the center line or loads symmetrical about the center line. As a matter of fact, loads symmetrical about the center line are handled as concentrated loads on the center line; that is, in the analysis

identical results are obtained for these two types of loading. In the case of rigid frame bridges of average span, the weight of the structure forms a large part of the total weight. Because of this and moreover because wheel loads will usually be near the center line, the correctness of any analysis based on Professor Rathbun's equations or similar derivations will be measured by the reliability of the theory near the center line. Since appreciable differences exist for these loads, the results obtained are highly questionable.

It has been shown theoretically that the basic equations are not valid. Furthermore, experimental values have been compared with theoretical values. Both of these facts confirm the writer's contention that at present no simple correct solution exists. However, rather than close this discussion with a negative emphasis, the writer would like to make the suggestion that some means of correcting the equations by introducing factors to account for the variation of moment across a section be introduced. The revised method should then be checked by experiment or compared with results obtained by more precise methods. At present, this problem can be most readily handled by means of finite difference equations.

AMERICAN SOCIETY OF CIVIL ENGINEERS

Founded November 5, 1852

DISCUSSIONS

PRIMARY RÔLE OF METEOROLOGY IN FLOOD FLOW ESTIMATING

Discussion

BY L. STANDISH HALL

L. STANDISH HALL,[12] M. AM. SOC. C. E.[12a]—A valuable summary of modern developments in meteorology for application to flood flow estimating is contained in this paper. In general, the rôle of meteorology as applied to flood flows is in the determination of maximum rates of precipitation. The analysis must include time-area-depth studies to cover drainage areas of various sizes, and for this purpose Table 1 contains valuable data. Having made similar studies for specific storms the writer can appreciate the time and effort necessary in the compiling of such a table.

Fig. 7 is of great interest in developing an upper limit for maximum rainfall rates. As pointed out by the author, before one can arrive at the maximum rate for a specific area the physiographic influences particular to the region in which the basin is located must be considered. As an example, on the western side of the Coast Range in the vicinity of San Francisco, Calif., a rainfall rate of 1 in. per hr can be expected once in 25 years. Whereas a rainfall rate of 2 in. per hr would occur less frequently than 100-yr intervals. This rate is materially below the world's record of between 10 and 15 in. in 1 hr, and the use of a rate in excess of 2 in. per hr for the San Francisco area would be extravagant. On many structures the use of an even smaller "design" flood would be justified when the damage caused by the rare flood would not justify the added expense of the larger structure.

Storm transposition must be used with caution in regions where orographic influences are a predominant factor. The author has not stressed this feature sufficiently. The report of the Miami Conservancy District focuses attention on this point (1*a*):[12b]

NOTE.—This paper by Merrill Bernard, M. Am. Soc. C. E., was published in January, 1943, *Proceedings*. Discussion on this paper has appeared in *Proceedings*, as follows: March, 1943, by Edgar Dow Gilman; April, 1943, by Messrs. Clarence S. Jarvis, Ivan E. Houk, W. G. Hoyt, and L. R. Beard; June, 1943, by Messrs. Robert E. Kennedy, and L. K. Sherman; and October, 1943, by Messrs. C. H. Eiffert, and Gail A. Hathaway.

[12] Hydr. Engr., East Bay Municipal Utility Dist., Oakland, Calif.

[12a] Received by the Secretary October 4, 1943.

[12b] Numerals in parentheses, thus (1*a*), refer to corresponding items in the Bibliography at the end of the paper (see Appendix 1), and at the end of discussion in this issue.

> "In beginning this investigation it was uncertain what geographic limits should be set to obtain the largest amount of useful and pertinent data. These limits at first were assumed to include the entire United States, but during the progress of the investigation it became apparent that rainfall conditions in the Western part of the country differ radically from those in the Eastern part, that by limiting the area to that east of the 103d meridian, running through Texas, Colorado, Nebraska and North and South Dakota, no applicable data would be excluded."

Under the heading, "Regions of Meteorological Homogeneity," the author has recognized the variation in rainfall intensity in California by including portions of the state within four areas (Nos. 1, 2, 3, and 7). Even with this subdivision two important areas are omitted, namely the west side of the Sierra Nevada and the east side of the Sierra Nevada. Marked variation of rainfall intensity created by the rugged topography could be cited within the boundaries of these six areas.

With reference to the contribution of snow melt to storm runoff, the author's statement, that the flood hazard increases when the snow accumulates beyond normal depth and water content, must be modified with respect to the Sierra Nevada in California. For those unacquainted with this area it should be noted that the depth of annual snowfall is not exceeded in any other part of the United States, and during the period from January to March the normal depth of snow on the ground above El. 6,000 is from 6 ft to 10 ft. Heavy snow cover over the high Sierra acts as an influence in the suppression of flood conditions.

Rainfall over the mountain areas of the Sierra is not the only element increasing floods of large magnitude in the Central Valley of California, but air temperature during the storm and the amount of snow on the ground prior to the storm are contributing factors. If cold storms have placed snow at low altitudes which is followed by a warm rain, the danger of a large flood is greatly increased. The greatest flood danger occurs when there is less than 4 ft of snow over all or a large part of the drainage area. After the snow has accumulated to a greater depth, warm rain serves only to compact the snow but does not yield much runoff. When the depth of snow is less than 4 ft, and particularly when it is less than 2 ft, a warm rain and the accompanying warm air currents can frequently melt all of the snow. Observations have been made at an elevation of approximately 4,000 ft near Calaveras Big Trees, Calaveras County, California, of a depth of 4 ft of snow being melted entirely between weekly visits during a period of high temperature and warm rains. The large flood of December, 1937, was the result of a warm rain at a time when there was less than 2 ft of snow over a large portion of the Sierra (35). The same conditions occurred in 1928 during the large flood of that year (36). Prior to the warm rain in the latter part of March, a maximum of only 4 ft of snow had been accumulated on the higher altitudes of the watersheds. This rain melted most of the snow, with the result that very large floods occurred. Prior to the flood of 1928, there was a general belief among engineers that a major flood could not occur in a year of subnormal runoff. The reports available indicate that, in the record floods of 1861–1862, there was snow at very low elevations

in the foothills prior to the storm. There were really three major floods in that year; one in December, 1861, and two in January, 1862, when warm rains melting snow augmented the runoff (37). To be sure, rains of unprecedented volume occurred at the same time. Without citing further examples, it can be stated as a result of observations of the snow-pack and meteorological conditions accompanying large floods in the Sierra that, whenever the snow is at low altitudes in the foothills and a warm rain of great intensity occurs, these are the conditions that produce the maximum flood runoff.

The procedure outlined by the author in developing the maximum possible storm for an individual basin offers a new approach to this problem of applied hydrology. With proper modifications based on the characteristics of individual basins it should yield dependable estimates of maximum flood flow. In addition to precipitation and depth of snow on the ground there are many other factors that have a very marked influence on volume of flood flow to be expected from a specific rate of precipitation. These factors for the most part are outside of the scope of the paper.

Bibliography.—

(1*a*) **"Storm Rainfall of Eastern United States,"** Miami Conservancy District, Eng. Staff, *Technical Reports*, Pt. 5, Revised Ed., Dayton, Ohio, pp. 15–16.

(35) **"Floods in the Sacramento Valley, Calif., Dec. 1937,"** by E. H. Fletcher, *Monthly Weather Review*, January, 1938, pp. 441–444.

(36) **"Floods of March 1928, in Sacramento Valley, Calif.,"** by N. R. Taylor, *ibid.*, March 1928, pp. 100–102.

(37) **Sacramento Flood-Control Project,** California State Reclamation Board, revised plans of 1925, pp. 109–115.

AMERICAN SOCIETY OF CIVIL ENGINEERS

Founded November 5, 1852

DISCUSSIONS

THE QUEENS MIDTOWN TUNNEL

Discussion

BY ORRIN L. BRODIE

ORRIN L. BRODIE,[21] M. AM. SOC. C. E.[21a]—In his several allusions to the design of the Holland Tunnel, Mr. Singstad states that in all essential respects the design for the Queens Midtown Tunnel is the same design as that for the Holland Tunnel and that extended research is no longer necessary in planning and designing tunnels for highway traffic. The length of the cast-iron ring of the latter tunnel, after two decades, could be increased to 32 in., or 2 in. over the earlier tunnel, thereby effecting considerable saving, while the number of segments (14) would remain unchanged. The initial bolt-tightening tension (25,000 lb per sq in.) is the same in the newer structure; but at the same time the author states (see heading, "Design: Lining for Shield-Driven River Tunnels") that "an allowance of about 5,000 lb per sq in. above the required bolt stress" is now made "to offset any plastic yield effect in the entire bolt assembly under sustained loading." From this statement the writer understands that 30,000 lb per sq in. is specified instead of the lower value.

Although the Holland Tunnel studies were based on a tube with an outside diameter of 29 ft, the sizes actually constructed were 29 ft 6 in. for the greater part and 30 ft 4 in. for a stretch in Jersey City in the northern tube, extending for 800 ft west of the New Jersey land shaft, to provide greater ventilation spaces and facilities for the long upgrade. This was the largest diameter shield-driven tunnel that ever had been constructed.

The author's statement that the operation of existing tunnels will continue to provide data for improvements in design is borne out in Table 1, which compares the ventilation of the Holland Tunnel with that of the Queens Tunnel.

The Holland Tunnel project presented problems unique in their time, both in design and ventilation, and called for pioneer work. It has been brought

NOTE.—This paper by Ole Singstad, M. Am. Soc. C. E., was published in March, 1943, *Proceedings*. Discussion on this paper has appeared in *Proceedings*, as follows: May, 1943, by Messrs. Thomas W. Fluhr and Howard L. King; June, 1943, by Messrs. Francis V. Wagner, William J. Wilgus, and S. A. Thoresen; and September, 1943, by Messrs. H. G. Cruthers, Leo Geenens, Charles E. Conover, Edward Levy, and Robert F. Legget.

[21] Designing Engr., Board of Water Supply, New York, N. Y. (Mr. Brodie died on October 5, 1943).

[21a] Received by the Secretary August 17, 1943.

to the writer's attention, from several sources, that the studies for the Holland Tunnel have never been published. For this reason a report in January, 1921, to Mr. Singstad (who was then engineer of designs) on the studies for design of the Holland Tunnel ring is referred to herein. (The full report has been placed on file with Mr. Singstad's records for reference in Engineering Societies Library, New York, N. Y.) The conclusions still are applicable today to its prototype, the Queens Tunnel.

Analysis of Cast-Iron Tunnel Sections, Holland Tunnel.—Subaqueous shield-tunnel practice recognizes the uncertainty of absolute values of external loading, especially at the critical times during construction. A controlling consideration is the possibility of a state of collapse during construction rather than the realization of the safe working stresses that might be employed in direct designing.

Therefore, studies that are comparative are possible and were made on different sections of cast-iron tunnels, including sections proposed for the vehicular tunnel and sections of tunnels already built and in service under similar conditions. The various results were compared rationally through the different angles of repose (Rankine's theory) assumed for the material forming the bed of the Hudson River. The investigations included angles of repose ranging from 3° to 20°, which serve as an index common to all phases of the work, and also signify different relations of horizontal thrusts to vertical loadings, exterior to the tunnel.

The resultants of the forces acting on the tunnel lining include the weight of the tunnel ring and that of interior structural features together with compressed air within the tunnel and the exterior loads. The last named are least capable of precise definition; hence, varying the exterior forces throughout a comprehensive range yields more conclusive results than if attention is confined to any one set of forces, themselves of doubtful value. These exterior forces represent active thrusts based upon Rankine's theory of earth pressure. The horizontal, abutting resistances of the surrounding material could be developed only through the deformation of the tunnel ring. This deformation develops internal stresses, all predicated on the active thrusts. Stresses due to the active thrusts of the surrounding material at a given angle of repose may be found to equal the stresses due to the abutting power of the material at some other angle of repose. Therefore, for comparative purposes it should be sufficient to base these studies on active thrusts only and thus preclude the uncertainties of speculations as to what abutting resistances might be developed at a given angle of repose. At the same time conditions are approached that are admittedly more rigorous than those for the tunnel sections in their final state of completion, since the active thrusts provide a series of horizontal and vertical loads of increasing inequality that are more nearly representative of loads encountered during construction. Thus, in these studies comparative values are emphasized rather than any consideration of the forces assumed for the exterior loading at any given angle of repose.

Conclusions were drawn from comparisons of results which indicated the more favorable of alternative designs. Local points of weakness were developed and remedial measures were devised.

The analysis comprised the determination of true equilibrium polygons for different conditions of loading from which the resultant thrusts and bending moments in the tunnel rings were determined completely. From these thrusts and moments, the stresses in the cast iron were computed directly: First, by neglecting the effects of joints and bolts locally—that is, assuming a given ring to be continuous, acting alone, and with a cross section of corresponding segment design; and, second, by means of supplementary analysis, including the effect of the joints and bolts under stress. The results were plotted as curves, in terms of the angles of repose, in both cases, and conclusions were made.

The true equilibrium polygons were determined by the method of work and the method of deflections. The advantage of the latter method is that it makes graphics unnecessary, and thereby is more precise than the natural limitations of graphical analysis. The method of work, as applied herein, consists of a graphical adaptation of the principle of least work, and, although generally satisfactory for ordinary purposes, lacks sufficient precision for low angles of repose, where percentage errors in scaling thrust eccentricities increased. Wherever both methods were used, the deflection method checked back most accurately on results found independently by employing the principle of least work.

Supplementary analysis of the action of the bolts under stress and the modifications of resulting stress in the cast iron of the segments were made. In general, the joint and bolt analysis consisted of investigations of (1) the modifications of stress sustained by the cast iron caused by the action of the bolts in the end and circumferential flanges of a segment and, through the bolts in the latter, (2) the effect of the two adjacent rings on the given ring between them. The elasticity of the bolts, the bending of the short longitudinal flanges of the tunnel ring, the transfer of compression from the joint to the body of the segment, the tendency of a joint to open, and the friction between the circumferential flanges enter this part of the investigations. These calculations of bolt and joint stresses are also dependent upon the true equilibrium polygons, determined previously.

The effect on the bending moments of the ring manifested by horizontal ties at the roof and floor of the driveway of the vehicular tunnel, 29 ft in diameter, was also approximated.

The cast-iron ring with entire internal structure, the cast-iron ring alone, and the cast-iron ring subjected to compressed air within furnished three distinct cases for investigation. The concrete lining was considered only as contributing its dead weight.

The basis of computation was 1 ft of tunnel length; 38 ft of water on 31 ft of silt were assumed to rest on the top of the tunnel ring. The weights of water and silt were assumed, respectively, at 64 lb per cu ft and 104 lb per cu ft. The air pressure, for the 29-ft tunnel, was applied at 40 lb per sq in.

As cohesion is neglected in Rankine's theory of a "granular mass," vertical forces due to tunnel ring alone, and to the overlying material, in some cases are less than the upward active pressures computed according to this theory. In such cases it appears that the structure would tend to float. For the sake

of equilibrium the vertical forces are equalized by adding the necessary difference as a uniform, overlying load, which may be considered either as due to extra fill or as a tacit recognition of the existence of cohesion in the overlying mass. During the construction of the Holland Tunnel the characteristics of the silt were found and its value in cohesive effect fully determined. The overlying depth of silt at one place, for the tunnel, showed no tendency to float

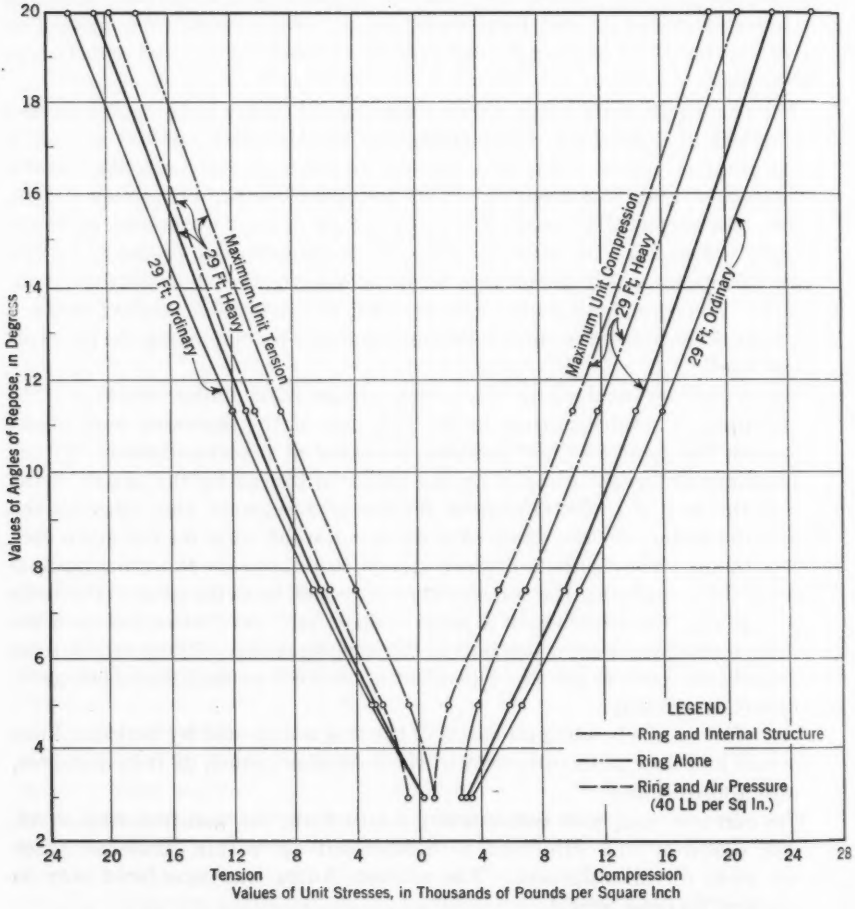

FIG. 15.—COMPARATIVE STRESSES, CAST-IRON RINGS OF THE HOLLAND TUNNEL

although its buoyancy, in terms of simple displacement of water and silt, indicated otherwise. Similarly, where the downward forces exceed the upward active pressures, the uniformly distributed difference required to balance is applied on the lower half of the structure. This additional set of forces may be considered as a partial development of the vertical abutting resistance of the material below the tunnel. In this case, the resulting upward reaction is found to lie between the values of the forces derived from the active pressures

and those that would result if the full abutting pressures could be developed, according to the theory. The assumed elastic limits were 40,000 lb per sq in. for steel bolts and 80,000 lb per sq in. for alloy ("high tensile") steel bolts. In all cases the stresses were computed for the so-called "heavy" section of segment, except for the stresses shown in Fig. 15, for the complete structure of the "ordinary" section of 29-ft tunnel. The web thickness of the heavy section

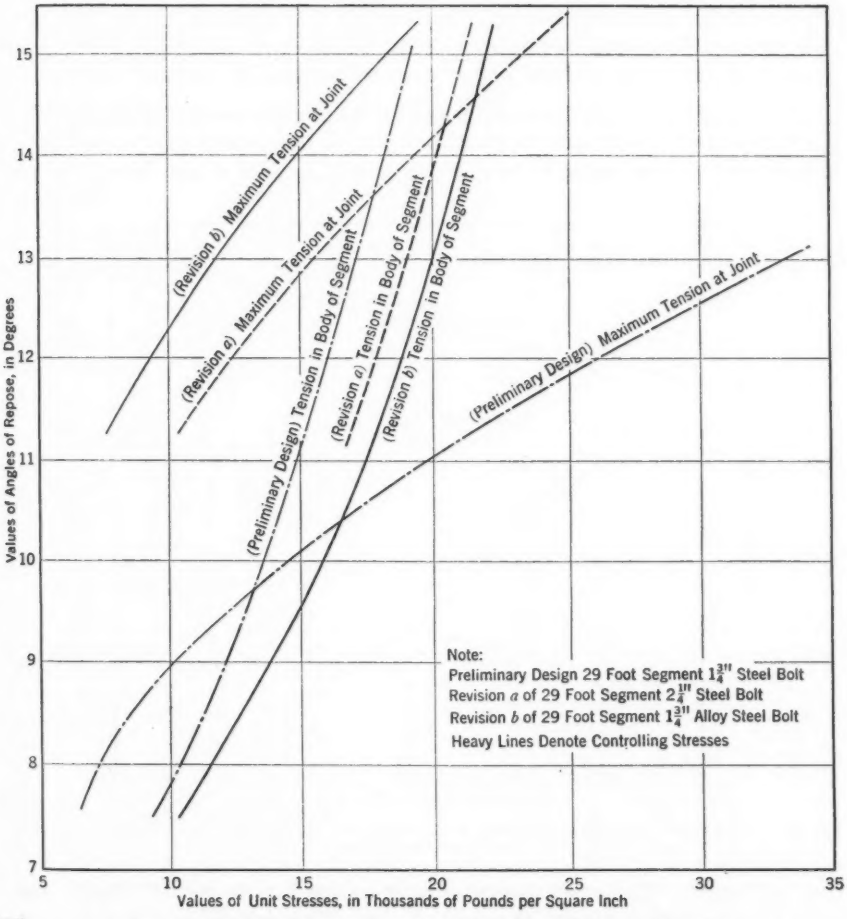

FIG. 16.—PRELIMINARY DESIGN OF CAST-IRON RINGS, HOLLAND TUNNEL

was 2 in.; that of the ordinary section, $1\frac{7}{8}$ in.; and that of the final design for the Holland Tunnel, $1\frac{5}{8}$ in. However, the extent of the web thickening for the heavy section was 7 in. back from the inside corner of the flange, instead of the 6 in. of the studied, ordinary sections. The equilibrium or funicular polygons were derived for the "ordinary" section of the 29-ft tunnel, and the stresses calculated for the "heavy" section were based on these polygons as the differ-

ence between these two sections was such as to affect inappreciably—a small fraction of 1%—the resulting bending moments and thrusts.

Discussion of Analysis.—In the following, the terms "outer," "inner," "outside," and "within" refer to directions in the circular tunnel cross section from or toward its center, respectively.

Eight features of the analysis deserve comment in so far as they apply to a similar analysis of the Queens Midtown Tunnel: (1) Application of thrust; (2) the joints; (3) location of critical stress; (4) bolt tightening; (5) location of end flange bolts; (6) the nonutility of the middle end flange bolt; (7) flange thickening at corners and the web of the section; and (8) effect of tie rods.

(1) Inspection of the funicular polygons used in the analysis indicated that the thrusts in the ring may be outside or within the neutral axis of the ring—that is, positive or negative bending moments, besides direct thrusts in the

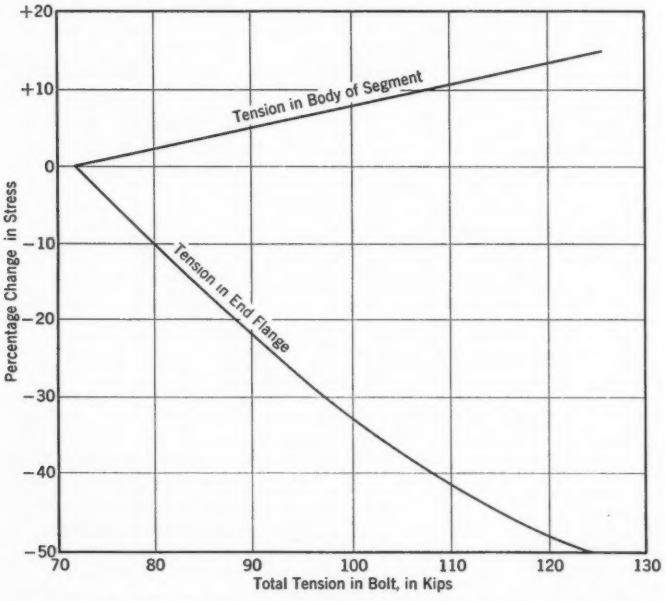

FIG. 17.—PERCENTAGE VARIATIONS IN STRESS FOR CHANGES IN TOTAL BOLT TENSION; HEAVY SECTION OF HOLLAND TUNNEL

ring may exist. Two cases thus may arise—Case I, with thrust outside, and Case II with thrust within, the neutral axis. The calculations showed that Case I resulted in maximum stresses in tension and Case II, in maximum stresses in compression; hence, Case I usually governs.

(2) The joint, as may be expected, is the weakest feature of the tunnel ring. Comparison of the stresses in the 29-ft, cast-iron-segment, heavy-section, preliminary design, with those for the same section, but with joints neglected, indicates the increase in stress due to the joints. Hence, to strengthen the ring as a whole, it is necessary to increase the strength of holding at the joints.

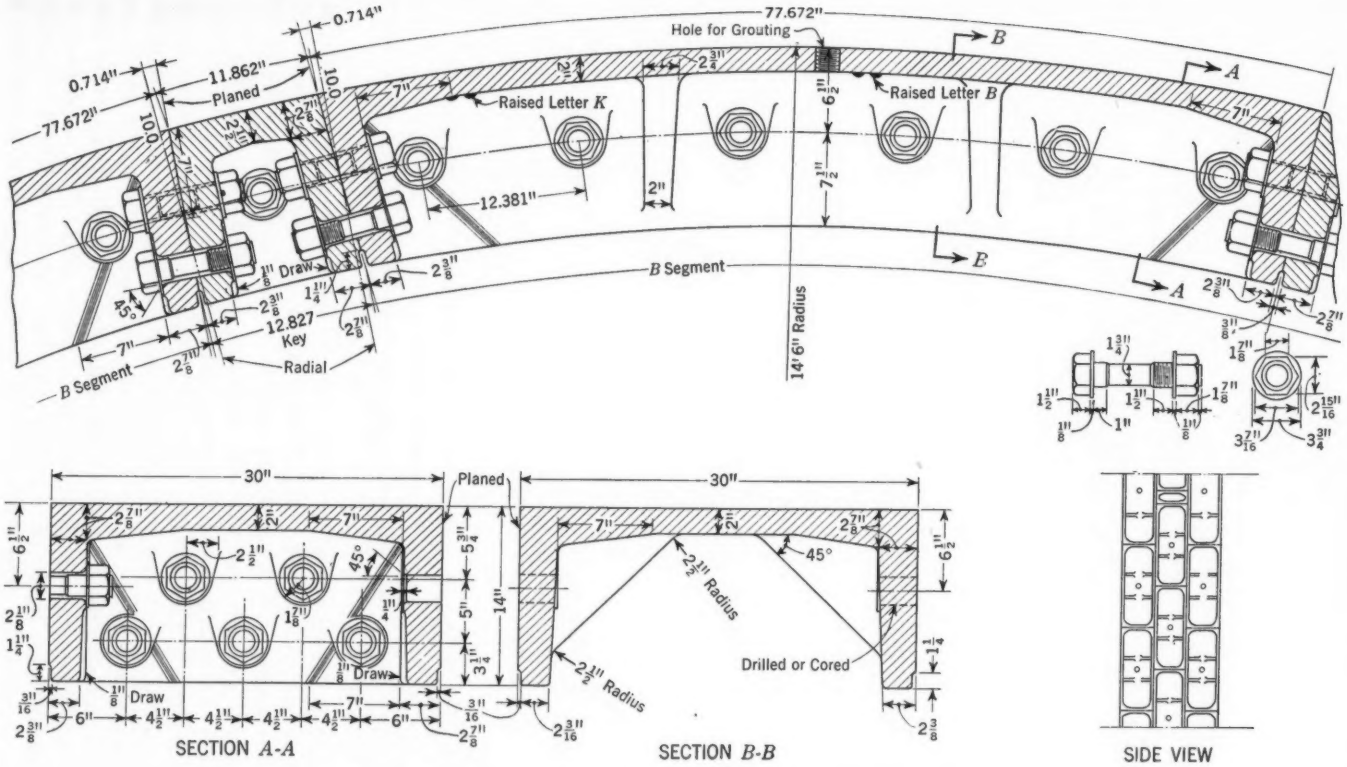

FIG. 18.—CAST-IRON DETAILS, HEAVY, 29-FT SECTIONS, HOLLAND TUNNEL

In Fig. 15, only the cast-iron segments are assumed to withstand stresses, and the effects of joints and adjacent rings are neglected. In Fig. 16, on the other hand, the effects of bolts and joints are considered. The bolts are assumed to be stressed to the elastic limit at the beginning, and the maximum tension at the joint occurs in the segment near the end flange.

(3) The critical stress in a segment is not in the joint itself, but immediately adjacent to it, at the intersection of the circumferential flange of the tunnel ring. This stress is due to the combination of the normal bending stress in the body of the segment, as this bending is modified by the circumferential bolt action, with the stress resulting from the local bending induced by the bolts of the end flange. These last bolts bind together the two successive segments of a ring at their ends.

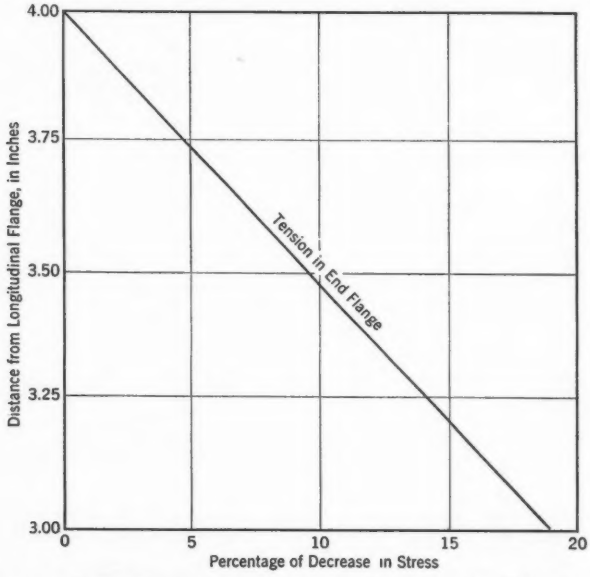

FIG. 19.—PERCENTAGE STRESS VARIATION WITH CHANGE IN BOLT POSITION (BOLTS ASSUMED STRESSED TO 40 KIPS PER SQ. IN., THE ELASTIC LIMIT, AT BEGINNING)

(4) The tighter a joint is bolted, the greater the strength of that joint, and consequently, the ring. Fig. 17 indicates that the greater the stress which the bolts can carry, as initial stress (that is, in bolting operations) the greater the strength of the ring will be. Although a small increase in tension is apparent (due mainly to the circumferential bolts) in the body of the segment, where the tensions are usually lower than at the joints, this is inconsiderable when compared with the great decrease in stress in the critical part of the segment, the end flange, where the stresses are much higher. Fig. 16 shows a similar effect obtained by utilizing the higher elastic limit of alloy steel bolts of $1\frac{3}{4}$-in. diameter, instead of that of ordinary steel. The importance of keeping all bolts tightened constantly to their utmost strength, especially during construction when the tunnel ring receives its greatest punishment, is

evident from these results alone and suggests the desirability of bolt tightening by means other than manual, if possible. Finally, the advantage of changing to the $1\frac{3}{4}$-in. alloy steel bolts is obvious. Fig. 18 shows this design.

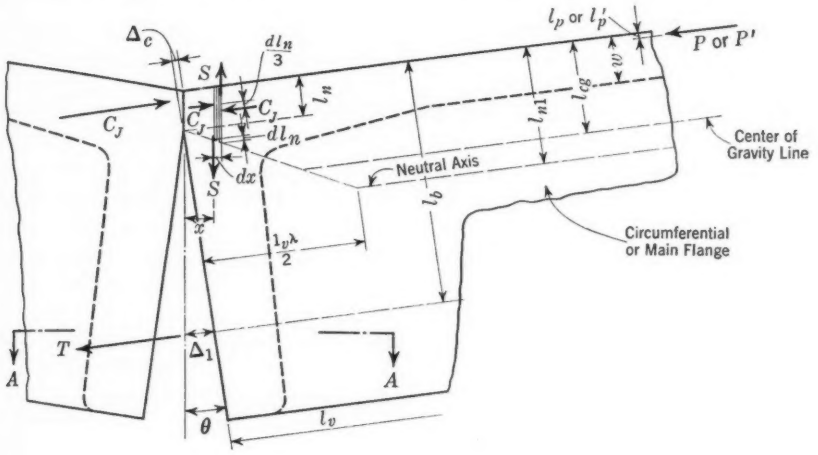

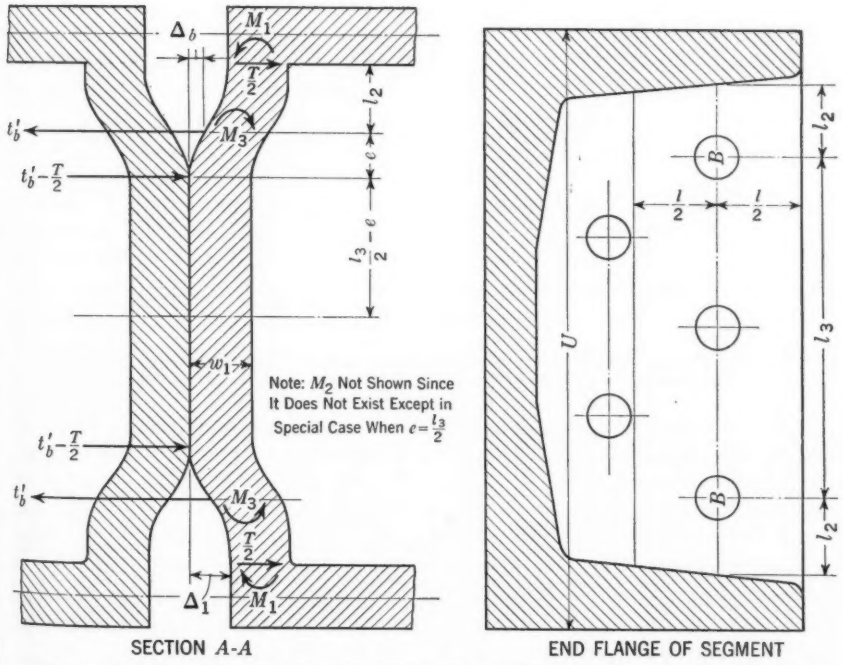

FIG. 20.—STRESS CONDITIONS WITH THE CENTER OF PRESSURE NEAR THE EXTRADOS (CASE I)

(5) The nearer the outer two bolts in the end flange of a "plate," or segment, approach the web and the nearer the two side bolts of the inner three approach

the circumferential flanges, the greater will be the reduction of local bending stresses, along with compression in the joint induced in the metal at the joint. Fig. 19 indicates the reduction in the case of the inner bolts.

(6) The middle of the three inner bolts of the end flange (Fig. 18, Section A–A) cannot act with its two adjacent bolts, for, if the elasticity of the metal of the bolts and joints is considered at all, and the elastic deformations are the essence of the studies, the action of the two inner bolts adjacent to this middle bolt puts the middle part of the end flanges of the two abutting segments meeting at this joint into compression. No possibility was found of a tension being induced in this bolt, except that caused by bolt tightening, unless the other bolts were stressed to failure, a condition that the middle bolt never could withstand. The only apparent advantage is the aid of the middle bolt in the process of tightening the remaining bolts—a practical consideration only. It is plainly easier to tighten up three bolts in line successively, back and forth, than two bolts alternately. As a factor contributing to tunnel-ring strength the value of the middle bolt is nil. This conclusion resulted from the analysis of bolt and joint stresses but may be suggested by regarding the cross section of such a segment as Section A–A of Fig. 18 along with Section A–A of Fig. 20.

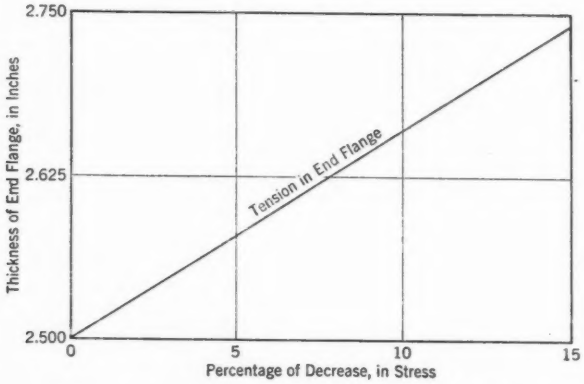

FIG. 21.—PERCENTAGE STRESS VARIATIONS WITH CHANGE IN END FLANGE THICKNESS (BOLTS ASSUMED STRESSED TO 40 KIPS PER SQ. IN., THE ELASTIC LIMIT, AT BEGINNING)

(7) To strengthen the segment locally (Conclusion 2) it was further concluded that the metal of the flanges, inside, at the corners of the segment should be thickened as shown in the side view of Fig. 18. The comparative value of this local flange thickening is brought out in Fig. 21, where the end flange is thickened $\frac{1}{4}$ in. Subsequently, when the tunnel segments were being cast, it developed that this combined thickening at the corners resulted in better castings, since the casting with more metal than heretofore cooled at the corners so that a more uniform texture of metal was indicated as observed upon castings which were purposely broken for inspection.

(8) In addition, a study of the restraining effect of transverse tie rods in the roof and floor systems indicated that they would provide for a reduction of two thirds in the values of the maximum bending moments in the ring.

AMERICAN SOCIETY OF CIVIL ENGINEERS

Founded November 5, 1852

DISCUSSIONS

SEDIMENTATION IN RESERVOIRS

Discussion

BY CARL B. BROWN, AND C. S. JARVIS

CARL B. BROWN,[8] ESQ.[8a]—The control of reservoir silting will constitute one of our most important problems of conservation in the postwar period. Construction of impounding reservoirs during the decade 1933–1943 has been a major item of public works. Reservoirs under construction in the United States in 1941 will have cost, when completed, more than $1,000,000,000, compared to a total investment in reservoir storage during the past hundred years of about $5,000,000,000, not including the dependent developments in filtration plants, power transmission lines, irrigation canals, etc. There is every reason to believe that reservoir construction will be accelerated beyond any previous levels as soon as the Nation can return to peaceful pursuits. For these reasons Mr. Witzig's paper is of timely interest.

The direct annual loss in investment from reservoir silting is not less than $10,000,000 and is more likely several times that amount. Therefore, a more widespread understanding of the silting problem is obviously needed. Control of silting begins when the dam design takes shape on the drawing board. Many reservoirs built in recent years have suffered rapid loss because their storage capacity, although adequate to meet water needs, was much too small to accommodate the sediment load of the inflowing stream—even until the project was amortized. Furthermore, the increasing knowledge of sediment-laden density currents and of other silting phenomena indicates that properly designed and operated outlets in many dams would reduce the rate of silting substantially. The design of future dams and reservoir projects should include a thorough study, so often lacking in the past, of the effects of silting. No less attention should be given to methods of conserving the reservoir storage already developed.

Of the topics which Mr. Witzig discusses, "Estimating the Rate of Reservoir Sedimentation" is, perhaps, of the most practical importance to the designing

NOTE.—This paper by Berard J. Witzig, Jun. Am. Soc. C. E., was published in June, 1943, *Proceedings*. Discussion on this paper has appeared in *Proceedings*, as follows: September, 1943, by Joe W. Johnson; and October, 1943, by Messrs. John W. Stanley, Stafford C. Happ, and Thomas H. Means.

[8] Head of Sedimentation Section, SCS, U.S.D.A., Washington, D. C.

[8a] Received by the Secretary August 27, 1943.

engineer. Unfortunately, Eq. 6 and the envelope curves shown in Fig. 3 are misleading. They imply that the annual rate of sedimentation, in acre-feet per 100 sq miles of drainage area, ΔS_R, is a function of the original storage capacity, in acre-feet per square mile, S_R, and increases with it. If this were so, the rate of sedimentation at a given site would increase indefinitely with the size of the reservoir. Obviously this is not possible since the upper limit of sedimentation depends on the amount of sediment brought in by the streams, which is independent of the size of the reservoir.

If a reservoir with $S_R = 100$ traps 90% of the incoming load and $\Delta S_R = 47$, as shown by median curve IV in Fig. 3, a reservoir at the same location with $S_R = 500$ could have a value of ΔS_R not greater than 52.2, which would represent 100% deposition of all the stream load. Curve IV would appear to indicate, however, that, where $S_R = 500$, $\Delta S_R = 175$. Actually, ΔS_R is a function of several independent or partly interdependent variables; for example:

$$\Delta S_R = f(E_n, S_R, S_h, S_c, Q_c, O_R, \cdots \text{etc.}) \quad \ldots\ldots\ldots\ldots (11)$$

in which: ΔS_R = annual rate of sedimentation; E_n = annual net watershed erosion, or sediment inflow to reservoir; S_R = reservoir storage; S_h = shape of reservoir; S_c = sediment characteristics, including textural composition and behavior under influence of dissolved load, temperature, etc., in forming density currents; Q_c = discharge characteristics of inflowing stream; and O_R = manner of operation of the reservoir. The symbols ΔS_R, E_n, and S_R are expressed in the same volume units per unit of drainage area (such as acre-feet per square mile).

The trap efficiency coefficient of a reservoir is best defined simply as the percentage of incoming sediment trapped:

$$C_T = 100 \left(\frac{\Delta S_R}{E_n} \right) \quad \ldots\ldots\ldots\ldots\ldots\ldots\ldots (12)$$

in which case C_T cannot exceed 100. From this relationship it is apparent that:

$$C_T = f\left(\frac{S_R, S_h, S_c, Q_c, O_R, \cdots \text{etc.}}{E_n} \right) \quad \ldots\ldots\ldots\ldots (13)$$

Of the factors in the numerator only S_R can be assigned a definite value from data generally available. Furthermore, few and none too reliable data have been collected on actual values of C_T as defined in Eq. 12. The data that are available to the writer have been plotted in Fig. 5.

It is apparent from general considerations that any curves defining trap efficiency must pass through the origin and approach $C_T = 100$ asymptotically. Envelope curves enclosing the data in Fig. 5 may be defined by an equation of the form:

$$C_T = 100 \left(1 - \frac{1}{1 + dS_R} \right) \quad \ldots\ldots\ldots\ldots\ldots\ldots (14)$$

The spread of the curves is due to the effect of the variables, other than S_R, on which C_T depends. Therefore, the sum of effects of these variables is ex-

pressed in the range in value of the coefficient d, from 0.046 for the lower curve to 1.00 for the upper curve. Existing information indicates that the middle curve should represent a satisfactory approximation of the average relationship of C_T and R_S for reservoirs other than those used solely for flood detention. This average, or design, curve has the equation:

$$C_T = 100 \left(1 - \frac{1}{1 + 0.1\, S_R} \right) \ldots\ldots\ldots\ldots\ldots\ldots (15)$$

Values of d tend to lie near the upper curve for: (*a*) Reservoirs in regions of smaller and more variable runoff; (*b*) reservoirs whose length and shape tend to reduce the time of flow through them; (*c*) reservoirs on watersheds which produce mainly coarse or highly coagulated sediments; and (*d*) reservoirs which

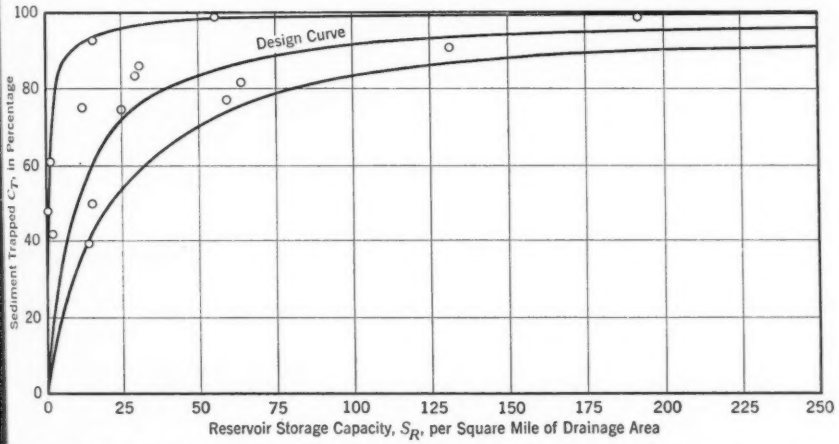

FIG. 5.—RELATION OF RESERVOIR TRAP EFFICIENCY, C_T, TO RESERVOIR STORAGE CAPACITY, S_R

are so operated as to release little water from the bottom of the dam or to hold back and store flood flows. Where $S_R > 100$, such a large proportion of the sediment is trapped that this factor generally may be ignored.

Substituting the value of C_T from Eq. 12 in Eq. 15, and transposing, it is found that, for an average reservoir:

$$\Delta S_R = \left(1 - \frac{1}{1 + 0.1\, S_R} \right) E_n \ldots\ldots\ldots\ldots\ldots\ldots (16)$$

The difference between Eq. 16 and Eq. 7 is that the latter is based on data from a paper by Messrs. Brune and Allen (4).[8b] Their letter symbol E does not denote the sediment load entering the reservoir, but is an estimate of gross erosion based on conservation surveys made by the Soil Conservation Service (SCS). These surveys are not intended to measure net watershed erosion volumetrically, but rather to show, among other things, the degree of soil loss

[8b] Numerals in parentheses, thus: (4), refer to corresponding items in the Bibliography of the paper (see Appendix II), and at the end of discussion in this issue.

from the land surface as this affects land use for agriculture and other purposes. These surveys do not ordinarily show stream-bank erosion, road erosion, or fan, colluvial, and flood-plain deposition in a form by which the quantity so eroded or deposited can be calculated. However, a rough volumetric approximation of soil loss from the land surface can be made from these surveys, and this is a fair measure of gross erosion, E_g, in most areas. The relation of E_n to E_g, as estimated from conservation surveys, varies within wide limits. Strictly, E_g should be a measure of the volume of all soil moved from place within the watershed per unit area, per unit time, regardless of where the resulting sediment is deposited. In drainage areas where sheet and gully erosion are slight and most of the sediment comes from stream-channel erosion, E_n may equal or exceed $2\,E_g$. In most watersheds, however, E_n is much less than E_g. In some of the watersheds used by Messrs. Brune and Allen, $E_n < 0.2\,E_g$. In general terms:

$$E_n = C\,E_g \ldots\ldots\ldots\ldots\ldots\ldots\ldots\ldots\ldots\ldots (17)$$

In Eq. 7, therefore, C_T is not a true "trap efficiency" coefficient for the reservoir; it is a coefficient that depends on two independent variables—the true trap efficiency of the reservoir, defined by Eq. 14, and the coefficient C in Eq. 17. The relation between gross erosion on a watershed and rate of reservoir sedimentation may be defined by

$$\Delta S_R = \left(1 - \frac{1}{1 + dS_R}\right) C\,E_g \ldots\ldots\ldots\ldots\ldots\ldots (18)$$

but careful watershed surveys will be required to determine the value of the coefficient C.

It will be apparent from this discussion that there is no simple exponential relationship, as in Eq. 7, between ΔS_R and S_R. Regional envelope curves plotted on logarithmic paper would not be straight lines, as in Fig. 3, but curved lines approaching asymptotically some limiting value of ΔS_R with increase in S_R.

Someday, perhaps, data will be sufficient to develop an equation relating ΔS_R to all of the variables on which it depends. For the present, however, it seems desirable to plot ΔS_R against some one easily determinable variable, such as size of drainage area, A_D, for each geographic region of essentially similar soils, slopes, climate, and land use. The resulting spread of data represents the influence of other variables, but the spread is not too wide to preclude use for practical design purposes. In other words, there is a limit to the range of debris production per unit of drainage area.

In Fig. 6 is shown a logarithmic plotting of ΔS_R, in acre-feet per square mile per year, against A_D in square miles. Values for all the reliable data on reservoir sedimentation and suspended loads from the Southern Piedmont and immediately adjacent parts of bordering physiographic provinces have been plotted, except that reservoirs where $S_R < 15$ have been omitted to minimize the effect of C_T, for which no corrections have been made. Suspended-load data were converted to acre-feet by assuming a specific weight of 50 lb per cu ft. Envelope curves have been drawn to bound the data, and a median curve has been drawn

"by eye." The single point outside the upper limiting curve represents Greenbelt Lake, Greenbelt, Md., where abnormal sediment production from an 0.83-sq-mile drainage area resulted from construction of a housing project (51). The envelope curves may be spread by future data, of course, but probably not much. The mean curve probably will not be changed appreciably by more data. These data appear to show that, in the Piedmont, the larger the watershed, the more limited is the range of ΔS_R, and that the mean rate decreases somewhat with size of watershed.

It should be recognized that use of the mean curve in a design problem allows no "safety factor." An erosion and sedimentation reconnaissance of the particular watershed, comparison of observed watershed characteristics with those of watersheds from which sediment data are available, careful study of the methods of water release and waste, and other factors influencing trap efficiency

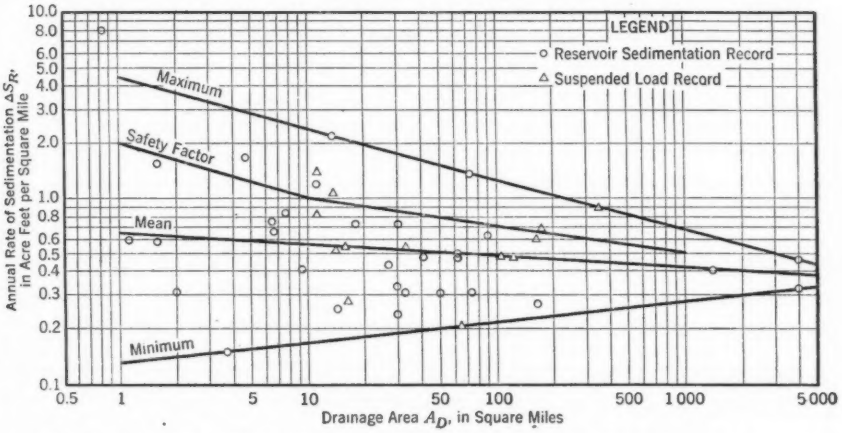

FIG. 6.—RELATION OF RATE OF SEDIMENTATION, ΔS_R, TO SIZE OF DRAINAGE AREA, A_D, IN THE SOUTHERN PIEDMONT

of the proposed reservoir should indicate whether a value above or below the mean should be chosen. Lacking such a study, the writer would recommend use of the reasonable "safety factor" curve.

Once regional charts, such as Fig. 6, are compiled, the annual rate of storage loss can be estimated by substituting values for ΔS_R in the equation:

$$\Delta S_L = 100 \left[\frac{\Delta S_R (A_D)}{S} \right] \ldots\ldots\ldots\ldots\ldots\ldots (19)$$

in which: ΔS_L = annual percentage rate of storage loss; A_D = drainage area, in square miles; ΔS_R = annual rate of sedimentation, in acre-feet per square mile of drainage area; and S = storage capacity of reservoir, in acre-feet.

Except for flood detention basins and reservoirs where $S_R < 15$, there is generally no justification, in the light of present data, to consider trap efficiency separately. Its effect is well within the spread of the envelope curves, and it is taken into account in the "safety factor" curve.

In Fig. 7 is shown the relationship of the storage-watershed ratio, S_R, to the annual silting rate ΔS_L for two regions where most data are now available. This illustration reveals the range and mean values of annual storage depletion of representative reservoirs grouped according to values of S_R.

Mr. Witzig makes the statement (see heading, "Estimating the Rate of Reservoir Sedimentation: 'Regional Indexes'") "that reservoirs surveyed thus far are more typical of severe rather than of average conditions." Actually, the reservoirs that furnished the data used in Fig. 3 are a representative cross section of important reservoirs in the regions they represent. More than 150 detailed and 250 reconnaissance reservoir surveys have been made by the SCS since 1934 for the purpose of obtaining a representative sampling of silting

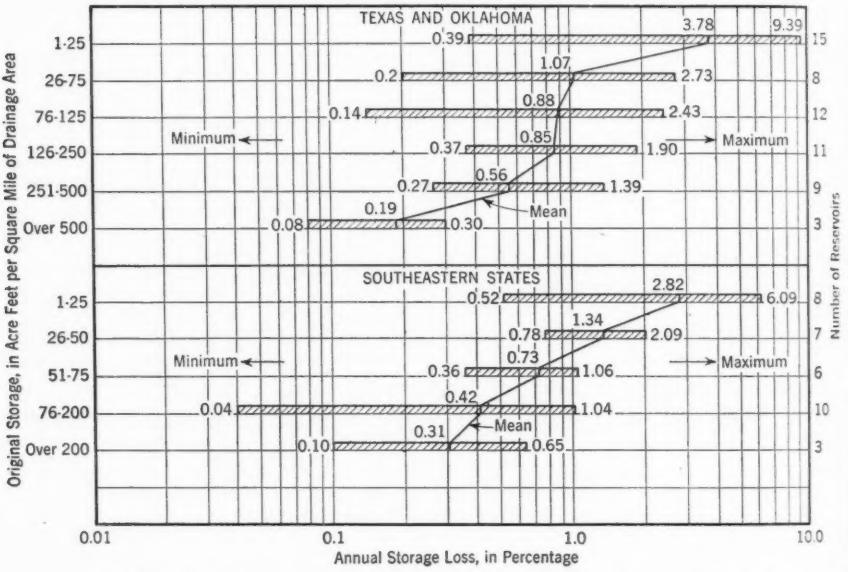

FIG. 7.—RELATION OF RESERVOIR STORAGE CAPACITY, S_R, TO RATE OF STORAGE LOSS, S_L

conditions and developing the factual basis necessary for planning silting-control measures. The average regional conditions shown are conservative because the sampling did not give sufficient weight to the hundreds of smaller reservoirs with low values of S_R that are now more than 50% filled with sediment, where it is too late or uneconomic to undertake silting-control measures. However, only a few surveys, or none, have been made in New England, the Great Lakes region, the Northern Great Plains, and certain parts of the Rocky Mountains and Great Basin. With the exception of these areas, the existing reservoir data fairly represent silting conditions in the economically important impounding reservoirs of the United States.

Many methods have been tried for the control of reservoir silting, of which Mr. Witzig describes a few. The writer (52) has classified all methods of control

into six major categories: (1) Selection of the reservoir site to avoid areas of excessive sediment production wherever possible; (2) design of the reservoir, which includes proper adjustment of capacity to watershed area and, where feasible, provision of outlets for sediment release; (3) control of sediment inflow by (*a*) settling basins, (*b*) vegetative screens, (*c*) location of reservoir off-channel, and (*d*) construction of by-pass canals and conduits; (4) control of sediment deposition by (*a*) venting density currents, and (*b*) control of waste water release; (5) removal of sediment deposits by (*a*) excavation, (*b*) dredging, (*c*) draining and flushing, (*d*) sluicing with controlled water, and (*e*) sluicing with hydraulic and mechanical agitation; and (6) watershed erosion control.

Mr. Witzig's paper is a valuable addition to the growing literature on various aspects of the problem of reservoir silting and its control. It is hoped that this paper will have the effect of stimulating interest among owners, operators, and designers of reservoirs, both in ascertaining the extent of silting in reservoirs with which they are concerned, and in studying possible methods for controlling the ill effects of this too often unrecognized menace.

C. S. JARVIS,[9] M. AM. SOC. C. E.[9a]—During more than two decades following the publication of the paper and discussions dealing with an irrigation reservoir that had lost 60.7% of its capacity in 12½ years (53), much progress has been made in the study of sedimentation phenomena and of the most promising means for their control or prevention in some degree. In spite of the notable progress accomplished by both federal and local agencies in the fields of soil conservation, channel stabilization, runoff regulation, and other activities designed to insure the utmost beneficial use of water resources along with adequate protection from the increasing flood menace, most of the required work yet lies ahead.

The paper under discussion affords a brief review of the situation and reflects diligent research and mature mental processes, along with an earnest effort to improve the outlook for the maintenance of reservoir capacities. Both Fig. 3 and Table 5 are forward steps in summarizing the findings of the Soil Conservation Service for various regions of the United States, indicating that the regional indexes are not so diverse as might have been expected in view of the wide range in climatic, rainfall, and runoff factors.

The alert irrigation farmer applying from 4 in. to 6 in. of turbid flood water on his field realizes that much fertility may be added thereby. If the thickness of the new sedimentary deposit happens to be ¼ in., he knows that from 4% to 6% by volume was carried by the irrigation lateral, in spite of all the deposits in the main canal system. Each farm is potentially a kind of hydraulic laboratory, if accurate and adequate records are kept.

Likewise with the stockwatering pond, especially if it is founded on gypsum-bearing or other highly permeable formation, the initial fillings may rapidly disappear through infiltration. The obvious corrective measure is to provide some kind of waterproof lining, such as clay or sand-clay mixture, preferably

[9] Cons. Engr., Washington, D. C.

[9a] Received by the Secretary October 25, 1943.

water-borne and deposited. Small reservoirs adequately lined in this manner have proved to be as retentive as if they had been waterproofed by much more expensive methods. Furthermore, the losses in the distribution canal system may be greatly reduced by the sedimentation processes. Where the need is great enough, it may be advisable to dump clay into a canal section for conveyance and puddling along the permeable reaches.

Wherever an irrigation supply has been deprived of its normal silt and sediment burden, either through intervening storage reservoirs or through the attainment of the ideal of effective erosion control or virtual prevention, the problem of restoring some of those elements for the aforementioned benefits is worthy of consideration. Some means of agitating the finest of the sediments within a storage reservoir, and delivering them to the irrigation canals serving lands that would be benefited by the addition of such sediment, might be devised with due regard to such regulations as the Biological Survey would necessarily impose.

In some locations, the gravel and sand deposits at the head of a reservoir might be used as a source of construction material; and the excavation resulting from such activity would serve as a trap for the next season's bed load, in the same manner as is intended for debris basins.

Now that fertile topsoil is becoming appreciated at somewhere near its true value, justifying its removal and storage in huge mounds, awaiting replacement as the final operation of some grading projects, it would appear that the finest sedimentary deposits in large storage reservoirs may have some commercial value within the range of cheap transportation, especially if waterways are available.

Bibliography.—

(4) **"A Consideration of Factors Influencing Reservoir Sedimentation in the Ohio Valley Region,"** by G. M. Brune and R. E. Allen, *Transactions*, Am. Geophysical Union, 1941, pp. 649–655.

(51) **"Advance Report on the Sedimentation Survey of Greenbelt Lake, Greenbelt, Maryland,"** by F. F. Barnes and C. B. Brown, SCS-SS-33, April, 1939, 12 pp.

(52) **"The Control of Reservoir Silting,"** by Carl B. Brown, U. S. D. A., *Miscellaneous Publication No. 521*, 1943, 166 pp.

(53) **"The Silt Problem of the Zuni Reservoir,"** by H. F. Robinson, *Transactions*, Am. Soc. C. E., Vol. LXXXIII (1919–1920), p. 868.

AMERICAN SOCIETY OF CIVIL ENGINEERS

Founded November 5, 1852

DISCUSSIONS

STRAINS, STRESSES, AND SHEAR IN ENGINEERING PROBLEMS

Discussion

BY A. A. EREMIN

A. A. EREMIN,[68] ASSOC. M. AM. SOC. C. E.[68a]—It is true, as the author states, that friction resistance at the ends of a short concrete test prism results in the appearance of an increased compressive strength in the concrete. More exact results may be obtained if the test block is made higher. Josef Fritsche[69] has shown that the compressive strength of concrete determined by a compressive test of a concrete block, with a ratio of height to width varying from 4 to 6, differs only about 20% from its true value. M. Möller[70] and later D. C. Henny,[71] M. Am. Soc. C. E., developed a method of computing the strength of concrete based on shear strength determined with a concrete test prism. The results of shear strength tests were correlated with strength tests of a concrete column and the error was found to be less than 20%.

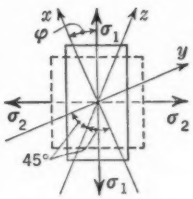

FIG. 13.—PRINCIPAL STRESSES

In the formulas for stresses and strains at an oblique section of a prism, Mr. Woodard has considered the case in which only direct stresses were applied. In practice, however, the principal stresses are generally considered along two axes. An interesting method of computing principal stresses in terms of measured strains ϵ_x, ϵ_y, and ϵ_z along three axes x, y, and z at angles of 45° was presented in 1934.[72]

NOTE.—This paper by Silas H. Woodard, M. Am. Soc. C. E., was published in February, 1943, *Proceedings*. Discussion on this paper has appeared in *Proceedings*, as follows: April, 1943, by Messrs. C. M. Goodrich, Maurice P. van Buren, Joseph A. Wise, and David B. Hall; and June, 1943, by Messrs. Roberto Contini, I. Nelidov, Bernard L. Weiner, Richard W. Albrecht, Duff A. Abrams; and September, 1943, by Messrs. C. A. P. Turner, and Mark W. Huggins.

[68] Associate Bridge Engr., Bridge Dept., Div. of Highways, State Dept. of Public Works, Sacramento, Calif.

[68a] Received by the Secretary October 18, 1943.

[69] *Beton und Eisen*, April 5, 1935, p. 113.

[70] *Ibid.*, December 20, 1930, p. 435.

[71] "Stability of Straight Concrete Gravity Dams." by D. C. Henny, *Transactions*, Am. Soc. C. E., Vol. 99 (1934), p. 1041.

[72] "La Détermination par Points, à l'Aide des Élastomètres, de la Répartition des Tensions dans les Pièces Métalliques," *Le Génie Civil*, January 13, 1934, p. 40.

In Fig. 13 the principal stresses σ_1 and σ_2 are,

$$\sigma_1 = \frac{E}{1 - \mu^2} (\epsilon_1 + \mu \epsilon_2) \ldots\ldots\ldots\ldots\ldots\ldots (32a)$$

$$\sigma_2 = \frac{E}{1 - \mu^2} (\epsilon_2 + \mu \epsilon_1) \ldots\ldots\ldots\ldots\ldots\ldots (32b)$$

and

$$\tau_{max} = \frac{\sigma_1 - \sigma_2}{2} \ldots\ldots\ldots\ldots\ldots\ldots\ldots\ldots (32c)$$

in which

$$\epsilon_1 = \frac{\epsilon_x + \epsilon_y}{2} + \frac{\epsilon_x - \epsilon_y}{2 \cos 2\phi} \ldots\ldots\ldots\ldots\ldots\ldots (33a)$$

$$\epsilon_2 = \frac{\epsilon_x + \epsilon_y}{2} - \frac{\epsilon_x - \epsilon_y}{2 \cos 2\phi} \ldots\ldots\ldots\ldots\ldots\ldots (33b)$$

and

$$\tan 2\phi = \frac{2\epsilon_z - \epsilon_x - \epsilon_y}{\epsilon_x - \epsilon_y} \ldots\ldots\ldots\ldots\ldots\ldots (33c)$$

With the known modulus of elasticity E, Poisson's ratio μ, and Eqs. 32, stresses and strains at any oblique section may be computed.

In conclusion, Mr. Woodard states that Poisson's ratio in the more accurate computations must be considered. It is to be noted that, in some cases, reliable results may be obtained only if Poisson's ratio is considered.

The term "shear stress," as used by Mr. Woodard, is a misnomer. It is true that the conception of shear stress is based on assumptions that differ from those on which direct stresses are based. However, this fact entails no difficulties in computations of structural materials energy and deformations. In the more accurate computations, important consideration should be given to the limitations resulting from the assumption of straight-line variation of stresses and strains and also the neglect of plastic flow.

AMERICAN SOCIETY OF CIVIL ENGINEERS

Founded November 5, 1852

DISCUSSIONS

A SYMMETRICALLY LOADED BASE SLAB ON AN ELASTIC FOUNDATION

Discussion

BY ALFRED L. PARMÉ

ALFRED L. PARMÉ,[12] JUN. AM. SOC. C. E.[12a]—Commendation is due Mr. Benscoter on the masterly style in which he has presented the problem of a slab on an elastic foundation. The information and ideas contained in the paper should lead to a more economical design of concrete channels and conduits and should serve to stimulate a more rational approach to the problem of designing reinforced concrete walls.

A further problem arising in the design of wide U-channels is that of determining how far the influence of the corner moments extends. For this purpose, the writer has utilized the work done by the Portland Cement Association on the design of circular tanks to develop a simple and easily applied formula. A comparison of the differential equations for circular walls and for beams on an elastic foundation reveals that both follow the same law. For an unloaded beam (see Table 1):

TABLE 1.—ANALYSIS TO DETERMINE INFLUENCE OF CORNER MOMENTS

Moment = coefficient × { edge moment / edge shear × l	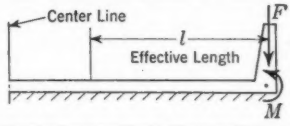									
	$0.9\,l$	$0.8\,l$	$0.7\,l$	$0.6\,l$	$0.5\,l$	$0.4\,l$	$0.3\,l$	$0.2\,l$	$0.1\,l$	$0.0\,l$
Edge moment...	−0.001	−0.043	−0.112	−0.189	−0.311	−0.464	−0.638	−0.798	−0.944	−1
Edge shear	+0.0	+0.017	+0.034	+0.060	+0.083	+0.106	+0.117	+0.109	+0.077	+0

$$\frac{d^4z}{dx^4} + \frac{4\,z}{\lambda^4} = 0 \ldots\ldots\ldots\ldots\ldots\ldots\ldots\ldots (44)$$

NOTE.—This paper by Stanley U. Benscoter, Jun. Am. Soc. C. E., was published in May, 1943, *Proceedings*. Discussion on this paper has appeared in *Proceedings*, as follows: September, 1943, by Messrs. Robert O. Jameson, and L. J. Mensch.

[12] Bronxville, N. Y.

[12a] Received by the Secretary October 4, 1943.

in which $\lambda = \sqrt[4]{\frac{4\,E\,I}{k}}$. On the other hand, for a circular tank, the equation

$$\frac{d^4z}{dx^4} + 4\,\beta^4\,z = 0 \quad \ldots\ldots\ldots\ldots\ldots\ldots\ldots\ldots (45)$$

expresses the behavior of an unloaded tank. In Eq. 45, $\beta = \sqrt[4]{\frac{3}{r^2\,t^2}}$. For $\frac{H^2}{D\,t} > 2$ the upper boundary is slightly affected by operations at the lower boundary.[13] If the relationship between the parameters is then established, a convenient way of determining the effective length of the slab will be available. Therefore, setting $\frac{l}{\lambda}$ equal to $\beta\,H$ and making the proper substitution:

$$\frac{l}{t}\sqrt[4]{\frac{3\,k\,t}{E}} = H\sqrt{\frac{3}{r^2\,t^2}} \quad \ldots\ldots\ldots\ldots\ldots\ldots\ldots\ldots (46a)$$

and therefore

$$\left(\frac{l}{t}\right)^2\sqrt{\frac{k\,t}{E}} = 2\left(\frac{H^2}{D\,t}\right) \quad \ldots\ldots\ldots\ldots\ldots\ldots\ldots\ldots (46b)$$

With $\frac{H^2}{D\,t}$ equal to 2, it follows that $\left(\frac{l}{t}\right)^2\sqrt{\frac{k\,t}{E}} = 4$; or,

$$l = t\sqrt[4]{\frac{E}{k\,t}} \quad \ldots\ldots\ldots\ldots\ldots\ldots\ldots\ldots\ldots\ldots (47)$$

To illustrate the applicability of the formula, a specific example will be computed. Assume $k = 100$ lb per cu in.; $t = 1$ ft; and $E = 3{,}000{,}000$ lb per sq in. Substituting these numerical values in Eq. 47, $l = 4 \times 1\sqrt[4]{\frac{3{,}000{,}000}{100 \times 12}} = 28.3$ ft. The value of t inside the radical must be in inches to conform with the dimensions of the other terms. The variation of the moment along the base due to an edge moment or shear is presented as an aid to detail analysis.

At this point a word of caution against the indiscriminate use of the method should be voiced. The designer should check the pressures exerted on the slab. The existence of negative pressures greater than the weight of the slab creates a condition that cannot be met in the field. Hence, it would have been desirable if the author had included the displacements due to the applied shear and moment. The inclusion of these values would immediately disclose whether the assumed conditions could be realized. In the case where the width of the channel exceeds the effective length as computed by Eq. 47, a shear greater than $\frac{2.57\,M}{l}$ will provide positive pressures throughout the slab.

[13] "Circular Concrete Tanks without Prestressing," *Concrete Information Sheet No. ST 57*, Portland Cement Assn.

AMERICAN SOCIETY OF CIVIL ENGINEERS

Founded November 5, 1852

DISCUSSIONS

CHARACTERISTICS OF HEAVY RAINFALL IN NEW MEXICO AND ARIZONA

Discussion

BY CLARENCE S. JARVIS

CLARENCE S. JARVIS,[17] M. AM. SOC. C. E.[17a]—No matter how many hours were required to assemble and analyze those hundreds of station records for the two states, comprising more than 7,000 station-years, full recompense is realized in the third from the last paragraph of the noteworthy paper under discussion. To be able to state with definite assurance that two-day rainfalls for any given recurrence interval may be taken as 10% to 20% greater than for the 24-hr record depth, or 20% to 30% greater for a three-day period, is proof of a notable achievement by the author.

The impressive array of authoritative information shown on both the relief maps and the isopluvial maps of the two states marks additional steps forward toward a firm grasp and understanding of a subject hitherto regarded as too vague and irregular for actual analysis and classification.

The writer recalls his personal observations at the Grand Canyon of the Colorado River one summer afternoon, when six or more distinct showers were in progress, moving like gray curtains against the backgrounds of intervening blue sky or red sandstone formation. Although there was no way of determining the actual intensity of each disturbance, it was noted that some of the curtains were like gauze, whereas others were nearly opaque. Presumably, other than orographic influences determined which storm centers should yield with high intensity; for all of the cloud forms were high above the canyon rims, and still higher above the areas of precipitation, which were almost invariably within the confines of the chasm.

Having been permitted to review the early draft of the paper under discussion, and having noted the distinct improvements accomplished by the author, it is the writer's pleasure to enumerate some of the distinctive modifications:

NOTE.—This paper by Luna B. Leopold, Jun. Am. Soc. C. E., was published in February, 1943, *Proceedings*. Discussion on this paper has appeared in *Proceedings*, as follows: April, 1943, by Lawrence Pratt, Assoc. M. Am. Soc. C. E.; and June, 1943, by Messrs. L. L. Harrold and A. J. Dickson, and James Girand.

[17] Hydr. Engr., With Office, Chf. of Engrs., U. S. Army, Washington, D. C.

[17a] Received by the Secretary October 18, 1943.

(1) Reduction of the number of objectives;

(2) Unification of effort toward those tangible, simple objectives;

(3) Elimination of such features as might have afforded something of a diversion without particularly strengthening the main thesis;

(4) Employment of graphical presentation at its best for the immediate purposes;

(5) According as much prominence to the deficiencies in basic hydrologic data as to the wealth of records discussed in the textual paragraphs; and

(6) Securing the most effective teamwork from both those in charge of the precipitation records, and those making the necessary transcriptions and orderly tabulations. This should amount to a guarantee as to the correctness of data used and summarized.

It is the writer's belief that the author will be able to extend the generalizations in his closure to great advantage. More of that kind of scientific contribution and discussion is needed, especially where the field has yielded so readily to a patiently conducted, yet masterly, approach.